

EFFECT OF THE COARSE FRACTIONS ON THE SHEAR STRENGTH OF COLLUVIUM

GEO REPORT No. 23

T. Y. Irfan & K. Y. Tang

**GEOTECHNICAL ENGINEERING OFFICE
CIVIL ENGINEERING DEPARTMENT
HONG KONG**

EFFECT OF THE COARSE FRACTIONS ON THE SHEAR STRENGTH OF COLLUVIUM

GEO REPORT No. 23

T.Y. Irfan & K.Y. Tang

**This report was originally produced in December 1992
as GEO Special Project Report No. SPR 15/92**

© Hong Kong Government

First published, June 1993
First Reprint, April 1995

Prepared by:

Geotechnical Engineering Office,
Civil Engineering Department,
Civil Engineering Building,
101 Princess Margaret Road,
Homantin, Kowloon,
Hong Kong.

This publication is available from:

Government Publications Centre,
Ground Floor, Low Block,
Queensway Government Offices,
66 Queensway,
Hong Kong.

Overseas orders should be placed with:

Publications (Sales) Office,
Information Services Department,
28th Floor, Siu On Centre,
188 Lockhart Road, Wan Chai,
Hong Kong.

Price in Hong Kong: HK\$126

Price overseas: US\$20 (including surface postage)

An additional bank charge of **HK\$50** or **US\$6.50** is required per cheque made in currencies other than Hong Kong dollars.

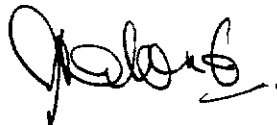
Cheques, bank drafts or money orders
must be made payable to **HONG KONG GOVERNMENT**

PREFACE

In keeping with our policy of releasing information of general technical interest, we make available some of our internal reports in a series of publications termed the GEO Report series. The reports in this series, of which this is one, are selected from a wide range of reports produced by the staff of the Office and our consultants.

Copies of GEO Reports have previously been made available free of charge in limited numbers. The demand for the reports in this series has increased greatly, necessitating new arrangements for supply. In future a charge will be made to cover the cost of printing.

The Geotechnical Engineering Office also publishes guidance documents and presents the results of research work of general interest in GEO Publications. These publications and the GEO Reports are disseminated through the Government's Information Services Department. Information on how to purchase them is given on the last page of this report.



A. W. Malone
Principal Government Geotechnical Engineer
April 1995

FOREWORD

It has long been felt that boulders and other coarse rock fragments commonly found in Hong Kong soils should increase the mass strength of the soils. There were attempts by individuals in the early 1980's to develop relations to quantify such increase. However, confidence among professionals on such relations varied.

In 1987, the Geotechnical Engineering Office (GEO) started a comprehensive study on the subject. Work along all conceivable research routes were carried out to find out the order of possible strength increase. These included literature review, field study, establishment and analysis of a theoretical slope model and a series of high quality shear tests on reconstituted samples. This report describes the work done and presents the findings of this investigation. This study was carried out and reported by Dr T.Y. Irfan and Mr K.Y. Tang. The results of the field study of colluvium are reported separately.

Dr E.W. Brand initiated the study while he was the Principal Government Geotechnical Engineer. A number of GEO staff took part in the study. Mr A.J. Cooper directed the early part of the project and reviewed the draft report. Staff of the Public Works Central Laboratory carried out the high quality laboratory tests under the direction of Mr J.M. Shen. Mr Shen also reviewed the first draft of the report and made useful suggestions especially in respect of the synthesis of research results. Most of the study was completed under the overall supervision of Dr R.P. Martin. Their contributions are gratefully acknowledged.



(Y. C. Chan)

Chief Geotechnical Engineer/Special Projects

CONTENTS

| | Page No. |
|---|-------------|
| Title Page | 1 |
| PREFACE | 3 |
| FOREWORD | 4 |
| CONTENTS | 5 |
| 1. INTRODUCTION | 9 |
| 2. OUTLINE OF THE STUDY | 10 |
| 2.1 History | 10 |
| 2.2 Study Methodology | 10 |
| 3. LITERATURE REVIEW | 11 |
| 3.1 General | 11 |
| 3.2 Experimental Studies | 11 |
| 3.2.1 Triaxial Tests on Sand-Gravel Mixtures by Holtz & Gibbs (1956) | 12 |
| 3.2.2 Triaxial Tests on Sand-Clay Mixtures by Miller & Sowers (1957) | 12 |
| 3.2.3 Triaxial Tests on Clay-Gravel Mixtures by Holtz (1960) | 13 |
| 3.2.4 Large Direct Shear Box Tests on Cobbly Soils by Patwardhan et al (1970) | 13 |
| 3.2.5 Triaxial Tests by Rico & Orozco (1975) on the Effects of Fines on the Behaviour of Crushed Gravel | 14 |
| 3.2.6 Large Diameter Triaxial Tests on Gravel-Sand-Clay Mixtures by Donaghe & Torrey (1979) | 14 |
| 3.2.7 Large Direct Shear Box Tests on Gravel-Sand Mixtures by Rathee (1981) | 14 |
| 3.2.8 Unconfined Compression Tests on Crushed Rock Aggregate-Silty Clay Mixtures by Shakoor & Cook (1990) | 15 |
| 3.2.9 Others | 15 |
| 3.2.10 Summary | 15 |

| | Page No. |
|--|-------------|
| 3.3 Analytical Strength Prediction Methods | 17 |
| 3.3.1 Dilation Model of Hencher (1983) | 17 |
| 3.3.2 Particulate Methods of Analysis by Vallejo (1979, 1989) | 17 |
| 3.4 Empirical Strength Prediction Methods | 18 |
| 4. FIELD STUDIES AND BACK ANALYSES | 18 |
| 4.1 Field Studies | 18 |
| 4.2 Slope Selection | 19 |
| 4.3 Description of Colluvium Characteristics in the Slopes | 19 |
| 4.3.1 Identification and Delineation of Colluvium Types | 19 |
| 4.3.2 Shing Mun Catchwater Slopes | 20 |
| 4.3.3 Slopes at Mount Nicholson Road and Plantation Road | 20 |
| 4.3.4 Slopes in the Mid-levels Area | 21 |
| 4.3.5 Slopes at Tsz Wan Shan Estate | 21 |
| 4.4 Back Analyses | 22 |
| 4.4.1 General | 22 |
| 4.4.2 Assumptions and Limitations of the Back Analysis Approach Used in the Study | 23 |
| 4.5 Results | 25 |
| 4.5.1 Shing Mun Catchwater Slopes | 25 |
| 4.5.2 Tsz Wan Shan Estate Slopes | 26 |
| 4.5.3 Mid-levels and the Peak Slopes | 26 |
| 4.5.4 All Data | 27 |
| 4.6 Summary | 27 |
| 4.7 CHASE-type Analysis | 28 |
| 5. LABORATORY STUDIES | 29 |
| 5.1 General | 29 |
| 5.2 Triaxial Tests Using Steel Balls (CU - BB Series) | 30 |
| 5.2.1 Test Method | 30 |
| 5.2.2 Results | 31 |
| 5.3 Triaxial Tests Using Aggregates (CU - AGG Series) | 31 |

| | Page No. |
|---|-------------|
| 5.3.1 Test Method | 31 |
| 5.3.2 Results | 32 |
| 5.4 Large Direct Shear Tests Using Aggregates (BSB Series) | 33 |
| 5.4.1 Test Method | 33 |
| 5.4.2 Results | 33 |
| 5.5 Small Direct Shear Tests Using Aggregates (NSB and NSB-D Series) | 34 |
| 5.5.1 Test Method | 34 |
| 5.5.2 Results | 34 |
| 5.6 Summary | 35 |
| 6. THEORETICAL STUDIES | 37 |
| 6.1 General | 37 |
| 6.2 Methods of Analysis and Limitations | 37 |
| 6.3 Results | 38 |
| 6.4 Summary | 40 |
| 7. DISCUSSION | 41 |
| 7.1 Effects of Coarse Fractions | 41 |
| 7.2 Proposed Analysis Models | 43 |
| 7.3 Shear Strength of the Mid-levels Colluvium | 45 |
| 7.4 Characterization and Quantification of Insitu Colluvium Properties | 45 |
| 7.5 Corestone-bearing Saprolites | 47 |
| 8. CONCLUSIONS AND RECOMMENDATIONS | 47 |
| 9. FURTHER RESEARCH NEEDS | 49 |
| 10. REFERENCES | 50 |
| LIST OF TABLES | 55 |
| LIST OF FIGURES | 73 |
| LIST OF PLATES | 155 |

| | Page No. |
|--|-------------|
| APPENDIX A : BACK ANALYSIS METHODS OF CALCULATIONS | 160 |
| APPENDIX B : DETAILED RESULTS OF BACK ANALYSES | 165 |
| APPENDIX C : SAMPLE PREPARATION TECHNIQUES | 201 |
| APPENDIX D : PROGRAM 'INCL.BAS' | 204 |
| APPENDIX E : METHOD OF CALCULATION OF MASS SHEAR STRENGTH PARAMETERS FROM THEORETICAL ANALYSIS | 219 |

1. INTRODUCTION

This document presents the results of a study carried out to quantify the effects of coarse particles of cobbles and boulders (termed as the coarse fraction) on the shear strength of colluvium in Hong Kong. The study arose from the need to investigate more accurate ways of assessing mass shear strengths in slope stability analyses for heterogeneous soils, including colluvial deposits and the corestone-bearing saprolite zones of the weathering profile. In typical stability analyses of slopes composed of heterogeneous soils in Hong Kong, the laboratory determined shear strengths, usually on small specimens, are adopted as the mass strength, except in cases where semi-empirically derived strength parameters exist (e.g. the Mid-levels area of Hong Kong Island).

The mass strength of a soil containing coarse particles depends on a number of material and mass factors specific to the fine and coarse components composing the soil and the interaction between them. In the case of corestone-bearing saprolites, the degree of weathering of the mineral constituents and the presence or absence of relict structures and their properties are also important (Irfan & Woods, 1988). The importance of some of the mass features in controlling the groundwater (e.g. localized permeable zones), which in turn affect the stability of slopes, in these materials cannot be overemphasized.

A number of studies have been carried out on colluvium in Hong Kong, but these were mainly confined to the recognition (Huntley & Randall, 1981) or the classification and age aspects (Lai & Taylor, 1983), since the early works by Berry (1957) and Berry & Ruxton (1960). A more detailed study of colluvium types and their broad engineering properties in the Mid-levels area was carried out in the early 1980s during the Mid-levels Study (GCO, 1982a). A review of published information up to late 1983 on the identification, classification and distribution aspects of colluvium can be found in Bennett (1984).

To date, no systematic study has been carried out on the strength properties of colluvium, particularly on the effects of coarse fractions, in Hong Kong. Even in the detailed Mid-levels Study, this subject was only briefly dealt with, primarily based on the results of limited laboratory tests and back analysis of a few failed and stable slopes. In the more recent Mid-levels Area Studies by GCO, Cooper (1986) gave a review of some of the previous experimental and theoretical work conducted on the factors controlling the shear strength of colluvium and similar materials. The mass strength of soils containing cobble and boulder size particles has also received very little attention elsewhere in the world.

The present study comprised a review of selective published data from similar studies, field studies, and back analyses of some stable and failed cut slopes in colluvium, laboratory triaxial and direct shear tests and the establishment and analysis of an appropriate theoretical slope model. A series of laboratory experiments were conducted on compacted soil specimens containing steel balls and rock materials (aggregates) as the coarse fraction in a fine-grained soil matrix. Back analyses were carried out on a number of existing cut slopes in order to directly assess the effects of cobble and boulder size particles on the insitu strength of natural colluvium deposits. Different levels of field characterization were adopted in the field study to identify and quantify the material and mass properties that are likely to control the insitu shear behaviour of colluvium. This was done in order to provide a realistic and comparative framework for the assessment of shear strengths determined from the laboratory experiments

and the numerical analyses. A theoretical slope model was established to provide a direct quantitative assessment of the role of coarse particles on slope stability. Comprehensive analyses were conducted to examine the effects of variables such as particle size, shape and spacing, as well as matrix strength and slope height.

Although included in the original project brief, the effects of corestones on the mass strength of saprolitic soils were not studied in any detail. However, the applicability of the study results to these soils are briefly discussed in the report.

The results of the field characterization of colluvium in Hong Kong are presented in a separate document (Irfan & Tang, 1992).

2. OUTLINE OF THE STUDY

2.1 History

The project COL 3: Boulder Content, was included in the GEO R & D framework set up in 1983/84 under Theme 152: Geology and Engineering Properties of Colluvium, in the Area of Properties of Materials. A draft project brief was prepared in 1986 upon upgrading of the project to Category B in 1986. The project was upgraded to Category A in late 1987 when the 1987/88 R & D Programme (Massey & Martin, 1987) was accepted by GEO Mancom. The project was commenced in December 1987 by the Special Projects Division.

2.2 Study Methodology

Three separate research items were proposed for the very ambitious original project brief. These were :

- (a) Back analysis of failed and stable slopes in colluvium and corestone-bearing saprolites (based on detailed site characterization of at least 50 slopes with coarse fraction contents of over 30%).
- (b) Desk studies of hypothetical slopes involving analyses of potential failure surfaces constrained by varying proportions and arrangements of coarse particles.
- (c) Direct shear box tests in the laboratory of remoulded soils with varying grain size mixtures, grain shapes and densities.

The work outlined in the original project brief required a substantial amount of time to be spent on fieldwork and theoretical stability analyses. It was considered that, with present resources and commitments of the Special Projects Division, it was not possible to complete the project within a reasonable time scale. Instead, a reduced-scale project under the following four main lines of research was adopted for the current study in May 1989 :

- (a) Literature review of experimental work and strength

prediction methods (both analytical and empirical) in colluvium and other heterogeneous materials.

- (b) Back analyses of a few existing slopes in colluvium using the data obtained from detailed field characterization, in order to determine the field (insitu) strength of colluvium.
- (c) Limited laboratory direct shear and triaxial tests on compacted soils containing coarse particles.
- (d) Establishment (from the field studies) and analysis of an appropriate theoretical slope model to provide a direct quantitative assessment of the role of coarse particles on slope stability.

3. LITERATURE REVIEW

3.1 General

A review of published literature revealed that, although bouldery colluvium deposits are widespread in Hong Kong and elsewhere, very little work, experimental or otherwise, has been carried out on their strength properties. This is also true for corestone-bearing saprolites. This stems mainly from the fact that tests cannot sensibly be carried out on samples which are large enough to be truly representative of the soil mass. Another factor is that these soils are heterogeneous and are hence difficult to characterize.

In view of the lack of experimental results on natural colluvium deposits and saprolites, other methods of assessing their mass strengths have been attempted, particularly in Hong Kong. These can be grouped under the following headings :

- (a) Experimental studies on reconstituted soil materials containing coarse particles.
- (b) Analytical strength prediction methods.
- (c) Empirical strength prediction methods.

3.2 Experimental Studies

The small amount of published literature on the effects of coarse particles nearly all relates to compacted fills, especially in connection with the stability studies of road embankments and earth dams (for example, see, Maclean & Williams, 1948; Holtz & Gibbs, 1956; Huang et al 1957; Holtz & Ellis, 1961; Patwardhan et al 1970; Katti et al 1973; Rico & Orozco, 1975; Jain & Gupta, 1975; Donaghe & Torrey, 1979; Rathee, 1981; Shakoor & Cook, 1990). A summary of some of the selected experimental work is given in Table 3.1. A brief review of relevant experimental work with the main conclusions drawn from each study is given below.

3.2.1 Triaxial Tests on Sand-Gravel Mixtures by Holtz & Gibbs (1956)

One of the earliest and most comprehensive studies on the effects of coarse particles was carried out by Holtz & Gibbs (1956). They studied the effects of density, proportion of coarse fraction, gradation, maximum particle size, and particle shape on the shear resistance of gravel-sand mixtures. A total of 183 consolidated drained triaxial tests were carried out on up to 9 inch (230 mm) diameter remoulded specimens using sand as the matrix material and gravel size fragments (up to 76.8 mm) as the coarse fraction. The gravel contents tested were 20%, 35%, 50% and 65% (by weight). The specimens in each test series were compacted to the same relative density of either 50% or 70%. The main conclusions drawn from the study by Holtz or Gibbs (1956) were :

- (a) The shear strength of gravelly sand increased with increasing gravel content of up to 50% to 60%.
- (b) The shear strength did not increase, or even became less, beyond a gravel content of 50% to 60%.
- (c) Increasing the maximum size of the gravel particles from 19.2 mm (3/4 in.) to 76.8 mm (3 in.) had no significant effect on the shear strength. (This conclusion was based on a few tests only).
- (d) The shape of the gravel particles had a significant effect on the shear strength. Angular, quarry-crushed particles gave higher shear strengths than the subrounded to subangular river gravels.

A summary of selected test results from Holtz & Gibbs (1956), normalized with respect to the shear strength of the matrix material, is given in Figure 3.1.

3.2.2 Triaxial Tests on Sand-Clay Mixtures by Miller & Sowers (1957)

Miller & Sowers (1957) investigated the effects of varying the proportions of coarse-grained and fine-grained soils on the strength of the resulting mix, in connection with road pavement design. They carried out unconsolidated undrained triaxial tests on reconstituted soil specimens prepared from a river sand and an inorganic sandy clay (decomposed gneiss). Various mixtures of soils were made ranging from 100% sand and fine gravel (as aggregate) to 100% clay (binder). The specimens were compacted to their maximum dry densities at their optimum moisture contents. Pore pressures were not measured during the tests. The test results summarized in Figure 3.2 showed that there was no apparent change in the angle of internal friction (or the shearing resistance) while the cohesion decreased gradually up to an aggregate content of about 67%. A sharp change occurred in the soil behaviour for aggregate contents between 67% and 74%, with the friction angle rapidly increasing and the cohesion rapidly decreasing. Beyond 74% aggregate content, the friction angle rose gradually to that of the 100% aggregate-only specimen. An examination of their test results showed that the matrix densities of the specimens decreased with increasing aggregate content (Figure 3.2).

Miller & Sowers (1957) explained the pattern of increase in the friction angle of the composite soil by considering the possible grain structures for different aggregate contents and the degree of compaction of the matrix material. One of the more important conclusions that can be derived from the test results is that at somewhere between 67% and 74% aggregate content, the strength of the composite soil starts to be dominated by the granular skeleton rather than the clayey matrix.

3.2.3 Triaxial Tests on Clay-Gravel Mixtures by Holtz (1960)

Subsequent to Holtz & Gibbs (1956), Holtz carried out a companion study using clay as the matrix material by means of unconsolidated undrained triaxial testing (Holtz, 1960; Holtz & Ellis, 1961). Pore water pressures were measured in the tests, but an examination of Holtz's test data indicates that the specimens were not fully saturated. The specimens were compacted to 95% of their standard compaction maximum dry density, determined individually for each gravel content. The gravel content varied between 0% and 65% (by weight). The main conclusions from this study, summarised in Figure 3.3, were :

- (a) The change in shear strength was not significant for gravel-bearing clayey soils below a gravel content of about 35% (by weight).
- (b) Shear strength increased sharply with gravel content above a value somewhere between 35% and 50%.

A comparison of the test results on clayey soils with sandy soils (Holtz & Gibbs, 1956) indicated that the clayey gravel soils had lower frictional strength than the sandy gravel soils for equal gravel contents (not shown in Figure 3.3).

The above results show that the shear strength of a gravelly clay soil is controlled by the properties of the clayey matrix up to a gravel content of about 35%. Above this value, interference from the coarse particles results in a relatively large increase in the effective angle of shearing resistance, (ϕ') of the composite soil, with a corresponding reduction in the cohesion value.

3.2.4 Large Direct Shear Box Tests on Cobbly Soils by Patwardhan et al (1970)

Patwardhan et al (1970) carried out a series of direct shear tests on cobble-clay mixtures using a 910 mm x 910 mm (3 ft x 3 ft) box. The average size of the cobbles was 150 mm and the cobble content varied between 0% and 100%. The tests were carried out without normal load being applied. The specimens were prepared at an initial void ratio of 0.7 or 0.8 and were saturated prior to shearing. The results are plotted in Figure 3.4. The limited data showed a gradual increase in the shear strength of the cobbly soil with increase in the cobble content up to about 40%, followed by a sharper increase beyond this value.

3.2.5 Triaxial Tests by Rico & Orozco (1975) on the Effects of Fines on the Behaviour of Crushed Gravel

Rico & Orozco (1975) studied the effects of fines on the mechanical behaviour of a gravelly crushed rock material used as road base. Three types of fines of different proportions varying from 0% to 20% were added to a sandy gravel material (crushed aggregate) of mixed granitic and volcanic rock origin. The fines used were: a CL-ML material, a commercial kaolinite and a bentonite. The specimens were prepared by dynamic compaction at their optimum water contents and undrained triaxial tests were carried out. Typical results are given in Figure 3.5. In general, the undrained strength increased with increase in the fines content up to about 5% to 10% depending on the type of matrix material, but then it decreased sharply to a value below that of the aggregate - only soil.

3.2.6 Large Diameter Triaxial Tests on Gravel-Sand-Clay Mixtures by Donaghe & Torrey (1979)

Donaghe & Torrey (1979) carried out consolidated undrained triaxial tests with pore water pressure measurements on large diameter (381 mm) specimens of gravel-sand-clay mixtures. The specimens were compacted to 95% of their standard compaction maximum dry densities. The three gradings tested contained 20%, 40% and 60% gravel of 4 mm to 76 mm size in sand-clay mixtures. Three tests were also carried out on 'scalped and replaced' gradings using smaller 152 mm diameter specimens. The maximum particle size was 19 mm for the smaller specimens. Selected relevant test results, normalized with respect to the matrix strengths of the specimens, are replotted in Figure 3.6. The results showed that the effective shear strength of the gravelly soil increased, in general, with increasing gravel content and particle size. The increase occurred in spite of a decrease in the dry density of the sand-clay matrix. The matrix densities were lower for the specimens with smaller gravel-size particles.

3.2.7 Large Direct Shear Box Tests on Gravel-Sand Mixtures by Rathee (1981)

Rathee (1981) carried out direct shear tests on sand-gravel mixtures, in order to investigate the effects of ratio of specimen size to maximum particle size, relative density, gravel content and maximum grain size on the shear strength of granular materials to be used in dams. The tests were conducted in a large (300 mm) direct shear box under low confining pressures of below 200 kPa. The specimens containing 10%, 30%, 50% and 100% gravel (a maximum size of 50 mm) were compacted at 25% and 75% relative densities. The shear strength of the sandy matrix material was not determined. The results from the tests carried out on the specimens with similar relative densities, indicated that :

- (a) the angle of internal friction of the sand-gravel mixtures increased with (i) increasing gravel content, (ii) increasing maximum particle size, and (iii) increasing relative density (Figure 3.7), and
- (b) the minimum ratio of specimen size to maximum particle size, without affecting the shear strength, was about 10 to 12

for the sand-gravel mixtures. This value increased up to 20 for uniform gravels.

3.2.8 Unconfined Compression Tests on Crushed Rock Aggregate-Silty Clay Mixtures by Shakoor & Cook (1990)

A number of unconfined compressive tests were carried out by Shakoor & Cook (1990) on specimens of silty clay containing varying proportions of aggregate as the coarse fraction in their study of the compaction characteristics of clay-stone mixtures. The specimens were compacted to a minimum of 95% maximum dry density. Three size gradations of a limestone aggregate (2 mm - 4.75 mm, 4.75 mm - 12.5 mm and 12.5 mm - 18.75 mm) were used. The test results showed that the unconfined compressive strength of the soil-aggregate mix generally decreased with increasing gravel content and gravel size (Figure 3.8). The decrease in strength was explained as mainly due to the lack of confining pressure resulting in no appreciable increase in friction. Also, the decrease in strength could be partly due to decrease in the dry density of the matrix with increasing stone content. No appreciable effect of stone shape on the strength was observed.

3.2.9 Others

A number of other researchers carried out experimental work on the effects of clay/silt contents on the shear strength of sandy soils. For example, Kurata & Fujishita (1960) conducted direct shear tests on sand mixed with various proportions of silt and clay (Figure 3.9). Loose soil mixtures were placed in a shear box and consolidated under a selected normal stress. Generally, no change in the shear strength was observed for clay/silt contents of up to 60% by weight.

Ting et al (1982) carried out a series of consolidation and triaxial tests on a reconstituted soil with a view to determine whether the soil behaves as a 'cohesive' or 'cohesionless' material at a given coarse fraction content. The specimens were prepared by mixing various proportions of coarse fraction and fine fraction separated from a residual granitic soil. They found that the behaviour of the composite soil was dominated by the fine fraction and was cohesive up to about 60% sand content. In undrained triaxial shear tests, the composite soils were found to exhibit cohesionless behaviour at a higher sand content than for the drained tests.

3.2.10 Summary

In the majority of the experimental studies reviewed in the study, the laboratory specimens were prepared either by the same compaction effort or at the same relative density. As a consequence, the matrix density varied from one specimen to the other in each test series, generally decreasing with increasing coarse fraction content. Only Patwardhan et al (1970) conducted tests on specimens with identical matrix densities. Their results indicated that the shear strength of a cobbly soil increased, first slowly, then rapidly with increasing cobble content. The critical content for a sharper change in the shear strength was about 30%

to 40%.

A similar pattern of increase was also apparent in the test results by Holtz & Gibbs (1956) and Rathee (1981), where the relative densities of the gravel-sand mixtures were kept constant. The drained shear strength of the granular soil was found to increase with increasing gravel content of at least up to about 50%. In these tests, the matrix density generally decreased with increasing gravel content. In contrast, in the studies where gravel/sand size particles were mixed with silt/clay materials, conflicting patterns of shear strength increases were reported. For example, Holtz & Ellis (1961) found no change in the effective shear strength up to a gravel content of 35%. However, a significant strength increase was obtained by Donaghe & Torrey (1979) at 20% gravel content for a sand-clay soil. Both studies were carried out using undrained triaxial tests with pore water pressure measurements.

A similar conflicting pattern is apparent in the undrained behaviour of heterogeneous soils. For example, Shakoor & Cook (1990) reported a decrease in the unconfined compressive strength of a gravelly (crushed rock) clay as the coarse fraction content increased. The results from Miller & Sowers (1957) showed an increase in the undrained strength of a gravelly sand up to about 25% clay content. After that, it decreased rapidly to a minimum value at about 35% and remained unchanged with increasing clay content. This initial increase in the undrained shear strength was also reported by Rico & Orozco (1975) who added various types of clay material to a sandy gravel soil. In terms of the undrained strength parameters, Miller & Sowers (1957) demonstrated that the cohesion value decreased while the internal friction angle increased with increasing proportion of aggregate, particularly beyond 65% sand content.

Although very limited, the results from previous experimental studies allow us to assess, at least preliminarily, the effects of increasing coarse fraction content on the shear strength when the matrix density is constant. The results, which are normalized with respect to the strength of matrix materials, are plotted in Figure 3.10. It is apparent from this figure that the effective shear strength increases with increasing coarse fraction content of at least up to 50%, irrespective of the type of test and matrix material. This conclusion could also explain some of the contrasting patterns observed in the undrained behaviour of the soils with silt/clay components in some of the above studies. In these, laboratory tests were conducted on the specimens prepared at similar compaction efforts. As such, the density or compactness of the matrix should vary with the coarse fraction content. Data from Miller & Sowers (1957), Donaghe & Torrey (1979) and Shakoor & Cook (1990) suggest a decrease in the matrix densities of the test specimens with increasing coarse fraction content. In undrained tests, decreasing matrix density would result in a reduction of the strength component due to the matrix material, while increasing coarse fraction content would lead to an increase in shear strength due to interference (dilation) from the coarse particles.

A marked change in the strength behaviour of heterogeneous materials appear to occur somewhere between about 60% and 80% coarse particle contents (Holtz & Gibbs, 1956; Holtz & Ellis, 1961; Miller & Sowers 1957; Kurata & Fujishita, 1960 and Ting et al, 1982). This probably corresponds to transition from a matrix-dominated to a granular-skeleton dominated soil structure.

3.3 Analytical Strength Prediction Methods

3.3.1 Dilation Model of Hencher (1983)

In an internal GCO report on the Chai Wan Road Landslide, Hencher (1983) proposed the following formula to calculate the shear strength of bouldery colluvium :

$$\tau = \sigma' \tan(\phi' + i_m + i_f) \dots \dots \dots (3.1)$$

where τ is the shear strength, σ' is the normal effective stress, ϕ' is the internal friction angle for the matrix (corrected for dilation), i_m is the stress dependent dilation angle for the matrix and i_f is the dilation angle for the overall shear plane, taking account of boulder interference.

The values of ϕ' and i_m were obtained from the direct shear test results. The value of i_f was taken to be the averaged value of deviations of slip surfaces from the main direction of failure. For the failed slope considered in the report, a total friction angle of over 90 degrees was obtained for a boulder content of 50%. It was acknowledged that the method gave an estimate of the upper-bound shear strength for the bouldery colluvium.

Cooper (1986) commented that this method of calculation was not appropriate for the bouldery colluvium, since it was doubtful that the matrix dilation and the dilation of the soil mass arising from the presence of boulders were directly additive. In addition, this method is likely to give consistently high i_f values as the value of i_f is taken to be equal to the average of the deviation angles of the local shear planes from the overall shear plane. Use of the minimum deviation angle as the dilation angle would have been more appropriate.

3.3.2 Particulate Methods of Analysis by Vallejo (1979, 1989)

Vallejo (1979, 1989) argued that the rigid-homogeneous-continuous approach of Skempton & DeLory (1957) proposed for the analyses of infinite slopes cannot be applied to mudflows and debris flows consisting of mixtures of clay or rock lumps in a soft mud matrix. Instead, he developed a particulate method of analysis to study the stability of soil masses that have a particulate and deformable structure. Based on the experimental work on two-phased systems such as sand-clay and gravel-clay mixtures by Kurata & Fujishita (1960), Rico & Orozco (1975) and others, he concluded that for values of volumetric grain concentration ratio, C , greater than 0.8, the shear strength of the soil mixture will be governed by the frictional shear resistance between the large particles. When the grain concentration ratio has values between 0.8 and 0.55, the shear strength of the soil mixture will be dictated in part by the frictional resistance between the large particles and in part by the shear strength of the clayey matrix, represented by the following simplified formula:

$$s = C\sigma' \tan \phi' + [1-C]c_u \dots \dots \dots (3.2)$$

where ϕ' is the effective angle of internal friction between the large particles and c_u is the undrained shear strength of the matrix (mud). If the value of the grain concentration ratio is below 0.55, the shear strength of the soil mixture will be dictated solely by the shear strength of the matrix. A graphical representation of Vallejo's shear resistance relationship with grain

concentration ratio is given in Figure 3.11.

3.4 Empirical Strength Prediction Methods

In the lack of experimental and theoretical data on the mass shear strength of colluvium, a number of empirical strength prediction methods have been used in Hong Kong since the early 1980s to account for the effects of coarse particles, particularly the boulders. For example, in the Mid-levels Study (GCO, 1981a) a number of stable and failed cut slopes were back-analysed in an attempt to compare the mass shear strength of the bouldery colluvium with the shear strengths measured in the laboratory tests on the matrix materials. In all the cases, it was assumed that the factor of safety was unity under the critical pore pressure conditions, which meant that the back-analysed mass shear strength was a lower-bound value. The results obtained from the back analyses are given in Figure 3.12 for the slopes in the Mid-levels area. It is apparent that the deduced minimum shear strengths are generally appreciably higher than the effective strengths obtained from laboratory specimens. Based on the back analysis, the parameters $c' = 10$ kPa and $\phi' = 41^\circ$ were recommended for colluvium when the boulder content exceeded 50%. The shear strength parameters for the overall colluvium matrix were determined as $c' = 5$ kPa and $\phi' = 35^\circ$ (Figure 3.13), based on a number of triaxial test results on specimens from three colluvium classes present in the Mid-levels area (GCO, 1981b). No discernible differences in the matrix shear strengths of different colluvium classes were observed in the test results, all lying within the same scatter.

Hencher & Martin (1982), apparently based on the results of the work carried out by GCO (1981b) and Holtz (1960), proposed a relative increase of about 4.0% in shear strength for every 10% increase in the volumetric content of coarse particles when the total cobble and boulder content exceeded 30%. They used the following empirical formula to calculate a 'layer strength' for the overall colluvium :

$$\text{Layer Strength (LS)} = S (1 + 3/700 \times (C-30)) \dots \dots \dots (3.3)$$

where S is the shear strength index of the fine fraction (matrix) and C is the coarse fraction content. The shear strength index was defined by an empirical formula which incorporated the hand penetrometer and Schmidt hammer values determined on the matrix material.

Cooper (1986), using the empirical shear strength criterion of Barton & Kjaernsli (1981) developed for rock fill and rock joints, proposed values of $c' = 10$ kPa and $\phi' = 45^\circ$ for the shear strength of colluvium when the boulder content exceeded 50%.

4. FIELD STUDIES AND BACK ANALYSES

4.1 Field Studies

Back analyses were carried out on a limited number of cut slopes in order to directly assess the effects of cobbles and boulders on the mass (field) shear strength of colluvium. An engineering geological characterization of each slope site was undertaken in terms of the material and slope properties given in Table 4.1. This was done in order to collect quantitative data, as far as possible, for a meaningful correlation of the back-calculated mass

strengths with the colluvium properties at each site. The field study also provided typical properties of the colluvial slopes in Hong Kong for the establishment of an appropriate theoretical slope model (Section 6).

In the engineering geological characterization of colluvium, the emphasis was placed on the soil properties which were considered to have significant effects on the mass shear strength. These included size, surface nature and weathering grades of both cobble and boulder size particles, and density or consistency (i.e. strength) and grain size of the matrix material, as well as their volume proportions and the overall degree of weathering of the deposit (Table 4.1). Different levels of characterization were applied to the slopes depending on the presence of reliable data, availability of the slope to detailed mapping at the time of the study, ease of access and the nature of the deposits. These are explained in a separate report by Irfan & Tang (1992). A brief description of general slope and colluvium characteristics of the sites is given in Section 4.3.

4.2 Slope Selection

Prior to the selection of slopes for the field study, many areas in Hong Kong, which are known to have cut slopes in reasonably thick colluvium deposits, were visited (e.g. the Mid-levels and the Tai Tam Catchwater areas on Hong Kong Island, the Shing Mun Catchwater slopes and Kowloon foothills, various CHASE slopes). Also, a small number of cut slopes in corestone-bearing saprolites were inspected. Due to time and financial constraints, only the colluvial slopes on which some data were available (e.g. CHASE data, GCO Stage 2/3 Study report) or where sufficient information could be readily obtained, for example, by the use of chunam strips, were chosen. The majority of these slopes had either failed previously or were found 'unstable' by the conventional stability analyses (Table 4.2).

4.3 Description of Colluvium Characteristics in the Slopes

4.3.1 Identification and Delineation of Colluvium Types

The identification and delineation of colluvium types (layers) in each slope were based on one or more of the following quantitative or qualitative criteria (see, Irfan & Tang, 1992 for details) :

- (a) The volumetric contents of cobbles and boulders (quantitative).
- (b) The degree of insitu weathering (descriptive).
- (c) The density or consistency of the matrix (semi-quantitative).
- (d) The degree of cementation (descriptive).
- (e) The size, shape and surface characteristics of cobbles and boulders (descriptive).

- (f) The colour and nature of the matrix (descriptive).

In general, more than one colluvium layer was identified in each slope, with each layer having broadly distinctive matrix and coarse fraction properties related mainly, but not necessarily, to the age of the deposit and the insitu weathering state. In some instances, further subdivision into a number of sublayers was possible based on the proportion of cobbles and boulders or any of the properties listed above. Generally, the older layers have much denser (stronger) matrix, and may also show a weak cementation by the iron-oxides and hydroxides.

4.3.2 Shing Mun Catchwater Slopes

Six of the eight slopes studied along the Shing Mun Catchwater, Ch 4000 to Ch 6200 (Figure 4.1), had either failed in the past or was subjected to the LPM works in the late 1980s (Table 4.2). The original cutting gradients of these slopes were estimated to be 65° to 72° from the measurements made on their unfailed portions (see cross-sections in Appendix B). Up to four colluvium layers or sublayers were identified in each slope.

The coarse fraction content in the colluvium layers varied from 0% to 60% (by volume) in most slopes, with the cobble size fragments forming the bulk of the coarse fraction. The older the layer was the more weathered were the boulders and particularly the cobbles. However, some younger layers also contained coarse particles showing advanced weathering. The matrix was generally loose (if sandy) to soft (if clayey) in the topmost layer. In general, the matrix strengths were higher in the deeper layers, particularly when the layer had undergone insitu weathering. However, this was not the case in one of the slopes, and all four layers appeared to have been deposited one after the other, within a short period of time. A typical slope from this area is shown in Plate 4.1.

4.3.3 Slopes at Mount Nicholson Road and Plantation Road

Five layers of colluvium were identified in the cut slope at the junction of Mount Nicholson Road and Stubbs Road (Figure 4.2, Plate 4.2). The slope had a gradient of 60° prior to a failure sometime between 1967 and 1976. There was a very rapid lateral change in the boulder content of the uppermost layer, which increased to almost 100% in the central portion of the slope. While the first four layers contained volcanic rock fragments, the lowermost layer was predominantly composed of granitic material, with few large boulders of granite showing thick weathered rinds.

The slope at Plantation Road, at a gradient of 53°, consists of two colluvium layers. The upper layer was poor in cobbles and boulders (less than 20% by volume), but the lower layer (divided into two sublayers) had a very high coarse fraction content of 70% to 80%, which mainly consisted of boulder size rock fragments. Although the fragments were mostly moderately to highly decomposed, the degree of weathering of the lower layer itself was insignificant.

4.3.4 Slopes in the Mid-levels Area

Detailed field characterization was carried out on two slopes selected in the Mid-levels area (Figure 4.2).

Three distinct colluvium layers and a number of sublayers were identified in the slope behind the Chater Hall service reservoir. The Mid-levels study (GCO, 1982a) identified two colluvium layers (Classes 2 and 3 of the Mid-levels Study) at this locality. The colluvium in the slope occurs as a V-shaped valley infill with a maximum thickness of 18 m (Plate 4.3). The lowermost layer, which showed the highest degree of insitu weathering, was thin and contained decomposed granitic cobbles and occasional boulders. The middle layer, 4 m to 15 m thick, which also showed some degree of insitu weathering, was divided into a number of sublayers based mainly on the weathering characteristics of the coarse fractions and the stiffness of the matrix. The coarse fraction content of volcanic rock origin varied from 20% to 90% in this layer. The relative matrix strength varied from generally soft (if clayey) or loose (if sandy, gravelly) in the topmost layer to very stiff or very dense (weakly cemented) in the lower layers. In general, the matrix was composed of clayey sandy silt with some gravel, but showed variation from layer to layer.

Four distinct colluvium layers with a number of sublayers were identified in the slope behind Fairmont Gardens (Plate 4.4). The colluvium thickness was very variable in the slope area. The upper three layers were very coarse in nature with the coarse fraction content in excess of 50%. Some of the boulders in the lower layers were very large having diameters up to 7 m. In some places, the colluvium was boulder-supported with little or no fine matrix material between the boulders or the cobbles. The lowermost layer was thin, less than 0.5 m, and intensely weathered. The layer could be easily confused with the underlying residual granitic soil were it not for the presence of occasional decomposed volcanic gravels.

4.3.5 Slopes at Tsz Wan Shan Estate

Five cut slopes behind the Tsz Wan Shan estate, Kowloon (Figure 4.3, Table 4.2) were selected because of the known presence of thick colluvium in the slopes. No field study was carried out, but the slope geometries and colluvium properties used in the back analyses were derived from the existing site investigation reports (SWKP 1975, 1976, 1979) and the CHASE data sheets. However, the information was not sufficiently detailed to make an accurate characterization of the colluvium types present in the slopes. Due to difficulty in recognising the boundaries between various layers from the borehole data, the colluvium on the site was described as one unit by SWKP (1979). The coarse fraction content of mixed rock origin varied between 50% and 80% according to the CHASE data sheets. The cobbles and boulders were mostly moderately decomposed with some slightly, highly and completely decomposed. The proportions of the completely decomposed cobbles and boulders were not given in the CHASE sheets. The colluvium thickness varied from 13 m to over 20 m.

4.4 Back Analyses

4.4.1 General

In this study, a number of simplifying assumptions were made in carrying out the back analysis, restrained by the limitations of the field investigation and the data availability and quality. These are explained in the proceeding section. It should be pointed out that the back analysis approach adopted here was primarily for the purpose of assessing the pattern of change in the shear strength of insitu colluvium, with increasing coarse fraction content. Accurate determination of the shear strength parameters is not possible with the quality of the data collected.

A total of eighteen representative sections on fifteen slopes were selected for back analysis. For each section, average shear and normal stresses acting along a number of assumed potential failure surfaces were calculated by means of the Morgenstern and Price (1965) method of analysis. The method of calculation is described in Appendix A. An enveloping curve drawn to these average stresses represents the most critical average stress conditions in that section of the slope (Kenney, 1967). The critical stress envelopes were fitted in this study by means of the least squares method of analysis, for easy manipulation of the data. The results of the back analyses are summarised as Figures and Tables in Appendix B.

The data obtained from the back analyses were assessed under three slope groupings based on location. These are : the Shing Mun Catchwater slopes, the Tsz Wan Shan Estate slopes and the Mid-levels and Peak Areas slopes. For each group, four types of plots were produced.

- (a) a plot of average shear stress versus average normal stress along each potential slip surface analysed; drawn for (i) boulder content, and (ii) coarse fraction content,
- (b) a plot of the best-fit shear strength envelopes for each colluvium layer or layer combination (if more than one layer exist in the slope) calculated from (a) at a low stress level of $\sigma' < 50$ kPa,
- (c) a plot of back-calculated c' against ϕ' for each colluvium layer or layer combinations, determined from (a), and
- (d) a plot of minimum shear stress (at a low stress of $\sigma' = 30$ kPa) versus coarse fraction or boulder contents determined from (a) for each colluvium layer or layer combinations.

The above plots were also produced for all slope areas combined in order to obtain a global picture for the effects of coarse particles on the shear strength of Hong Kong colluvium. The effect of the matrix strength on the mass shear strength was also assessed indirectly from the results. A relative scale of matrix strength used in the study is given in Table 4.3. The relative matrix strengths were assessed by using a hand penetrometer or a geological hammer in the field.

4.4.2 Assumptions and Limitations of the Back Analysis Approach Used in the Study

The back analysis of any case history involves a series of assumptions and procedures, each of which is a potential source of errors according to Leroueil & Tavenas (1981). They emphasized that back analysis cannot be used to determine reliable numerical values of soil parameters whenever some of the key input data to the back analysis have to be assumed. In most instances, the geometry and the geological model of a failed slope can be determined with some degree of accuracy. However, the exact pore pressures developed at the time of failures are generally unknown and must therefore be assumed. A small error on the position of water table can result in a high error on the calculation of effective cohesion (see, Leroueil & Tavenas, 1981). In many cases in Hong Kong, the groundwater pressures are extremely transient and the degree of uncertainty that exists over this can make back analysis very unreliable as a test of real values of shear strength at failure (Hencher et al, 1984; Brand, 1985).

The assumptions made in the back analysis carried out for this study and the quality of the input data used for the analysis are briefly discussed below :

(a) Failure conditions and methods of analysis

It was assumed that the soil stress conditions can be modelled by the Morgenstern & Price (1965) method of analysis (see Appendix A). It was also assumed in the analysis that the limiting conditions of failure applied to the slopes. For slopes which have been stable, assuming failure or near-failure conditions is a very conservative approach. For the slopes which were modified as a result of LPM works or had failed in the past, the back analyses were carried out on the pre-LPM or pre-failure profiles. For the failed slopes, the existing slope profiles were not analysed because of doubts that they represented the actual failure surfaces.

(b) Suction effects and groundwater

No suction was assumed to exist in the slopes. This is probably the case for thin colluvium deposits with vegetated surfaces where the suction would drop to almost zero during a heavy rainfall. However, this assumption would most probably be not exactly true for thick deposits or for slopes effectively sealed against infiltration (see GCO, 1984).

No positive pore pressures arising either from a permanent base water table or intermittent perched water table(s) were assumed to occur in the slopes. No signs of permanent perched tables were observed in many slopes during the field study carried out in the wet season of 1989, except some slopes at Tsz Wan Shan Estate, where seepages were evident even in the dry season of 1989. However, intermittent

perched water tables can form very quickly and rise up to almost ground surface in colluvium slopes during heavy rainfall, particularly when the deposit is thin.

(c) Three-dimensional effects

Three-dimensional slope effects were not taken into account in the analysis. The above assumptions (a), (b) and (c) taken together should therefore give a lower-bound back-calculated mass shear strength in most cases.

(d) Geological model

In many cases, the simplified geological models used in the analysis were based on the data obtained from narrow chunam or vegetation strips (usually one) excavated on each slope. In a few cases, this was supplemented by available ground investigation and other data (e.g. the CHASE study). However, the quality of colluvium descriptions in many boreholes and other investigation logs examined during the study was found to be poor. Layer boundaries were drawn generally parallel to the existing ground surface.

(e) Layer properties

Volumetric cobble and boulder contents assigned to each layer were those determined in the field from limited observations, or those derived from available data. In the case of Tsz Wan Shan Estate slopes, the data quality was poor and very generalised.

In cases where the coarse fraction content of a layer was determined solely from the chunam strips, either visually estimated or measured areal proportions of the boulders and cobbles were adopted as their relevant volumetric contents. In a slope with a random distribution of coarse particles it can be shown that the average areal proportion of particles per unit slope area is equal to their average volumetric proportions per unit volume.

(f) Analysis of multi-layers

It is not possible to back analyse multi-layered slopes unless the shear strength parameters of all layers but one or the locations of the potential failure surfaces are known. In this study, the multi-layered slopes were analysed as if they consisted of one layer.

In assigning a coarse fraction content to a failure surface which is contained in more than one layer, an averaging process based on the relative lengths of that surface in each layer was used. The values so calculated were rounded off to the nearest 10%.

(g) Slope profile

The slope profiles used for the back analyses of the existing stable slopes were generally derived from the detailed survey plans. In the absence of survey plans, simple tape and compass surveys were carried out by the authors. The data quality is therefore considered generally good for these profiles. The slopes which had failed in the past and where no detailed plans existed, pre-failure surfaces were reconstructed from the measurements made either on the unfailed slope portions or on other soil slopes in the vicinity of each site. The quality of the data in these cases is assessed as fair.

4.5 Results

4.5.1 Shing Mun Catchwater Slopes

The slope geometries used for the back analysis of the Shing Mun Catchwater sites were mostly those of the pre-failure surfaces reconstructed from the measurements made on unfailed slope portions or other soil slopes in the vicinity (Figures B1 to B8 in Appendix B). The geological data used in the analysis was based on the data collected from the chunam or vegetation strips excavated on the slopes. Therefore, the overall quality of the slope and material data is generally poor.

The average stresses calculated from the back analysis are tabulated in Table B.1. The results are plotted in various forms, as outlined in Section 4.4.1. Only selective results are given in Figures 4.4 to 4.7. The remaining plots can be found in Figures B.9 to B.12 in Appendix B. The least-square shear strength envelopes, within the normal stress range of 0 to 50 kPa, show that individual layers or layer combinations with 20% coarse fraction content fall in a broad band and those with, for example, 50% or more fall either within this band or below it (Figure 4.5).

Figure 4.6 shows that the majority of the back-calculated 'minimum' shear strength parameters fall between $c' = 5$ kPa to 10 kPa and $\phi' = 28^\circ$ to 38° . No clear relationship is apparent between the coarse fraction content and the shear strength parameters. Also, Figure 4.7 indicates no practical increase in the back-calculated shear strength with increasing coarse fraction content. Similarly, no clear trends are obtained when only the boulder contents are considered (Figures B.9 to B.12).

The results of the back analyses, taken overall, indicate no regular pattern of increase in the mass shear strength of colluvium with increasing coarse fraction content for the Shing

Mun Catchwater slopes. However, the results should be viewed in the light of various simplifying assumptions made for the analyses and the generally poor quality of the data that was obtained for these slopes.

4.5.2 Tsz Wan Shan Estate Slopes

The slope geometries analysed (Figures B13 to B17 in Appendix B) were those of the pre-LPM surfaces except for one slope where the original cutting profile was used. The geological models were derived from the consultants' reports (SWKP, 1980a, b, c & d). The coarse fraction content assigned to each slope was based on the information given in the CHASE data sheets. The boulder contents in the slopes were not determined by the CHASE Study.

The average stresses calculated from the back analysis are tabulated in Table B.2. The results are plotted in various forms in Figures 4.8 to 4.11. The shear strength envelope of the non-bouldery colluvium determined from the laboratory triaxial tests (SWKP, 1979) is also plotted in these figures for comparison. The matrix strength of the overall colluvium layer in each slope was described as 'very dense' in the CHASE data sheets. A plot of back-calculated c' against ϕ' in Figure 4.10 shows that the mass shear strength parameters for the colluvium at Tsz Wan Shan are $c' = 2$ kPa to 8 kPa and $\phi' = 33^\circ$ to 36° for a coarse fraction content of 50% to 60%. The colluvium containing 80% coarse fraction has a back-analysed mass strength defined by $c' = 10$ kPa and $\phi' = 45^\circ$.

The results of the back analysis for the Tsz Wan Shan slopes indicate a rapid increase in the mass strength of colluvium above 50% coarse fraction content (Figures 4.9 and 4.11). The relationship for lower contents is not known since no slopes with less than 50% boulder and cobble contents were available for analysis from this site. Nevertheless, if the back-calculated shear strength parameters are compared with those determined in the laboratory on non-bouldery colluvium (i.e. $c' = 7$ kPa and $\phi' = 36^\circ$), it can be deduced that the coarse fraction content becomes significant only when it is at or above 60%. It should be pointed out that the accuracy of the geological data used in the analysis of Tsz Wan Shan slopes, particularly the coarse fraction contents, is considered to be low.

4.5.3 Mid-levels and the Peak Slopes

The slope geometries used in the back analysis (Figures B18 to B22 in Appendix B) were those of the existing surfaces with the exception of the slope at Mount Nicholson Road, for which the pre-failure profile was extracted from the CHASE study on the slope. The geological models were based on field mapping and available borehole data. The quality of the geological data used in the back analyses is considered fair to good for the four slopes on Hong Kong Island, bearing in mind the limitations of the field characterization as outlined in Irfan & Tang (1992).

The average stresses calculated from the back analysis are tabulated in Tables B.3 and B.4. Selective results are given in Figures 4.12 to 4.16, with the remaining results plotted in Figures B.23 to B.25 in Appendix B. The shear strength envelopes recommended by GCO

(1981b) and Cooper (1986) for the Mid-levels colluvium are also shown on these graphs for comparison. All the least-square shear strength envelopes in Figure 4.13 fall below those recommended for the bouldery colluvium in the Mid-levels area (for a boulder content of over 50%).

There is no obvious pattern of increase in the mass shear strength with increasing total coarse fraction in Figure 4.13 nor in c' versus ϕ' plot in Figure 4.14. However, a broad pattern emerges when the averaged matrix densities of the colluvium layers are taken into account. The data points have been grouped under three broad matrix strength classes separated by approximate hand-drawn class boundaries in Figure 4.14. Individual colluvium layers or layer combinations with the highest matrix strengths have the highest combination of c' - ϕ' values.

Figures 4.15 and 4.16 show that the 'minimum' shear strength increases broadly with increasing coarse fraction content, particularly with the boulder content, within each matrix density class. In these figures, the shear strength parameters recommended by GCO (1981b) and Cooper (1986) for the bouldery colluvium plot at the uppermost range of values.

4.5.4 All Data

Selective results of the back analyses on all slopes are given in Figures 4.17 to 4.19, with the remaining results plotted in Figures B.26 to B.28 in Appendix B. The plot of c' versus ϕ' in Figure 4.17 shows no regular pattern of shear strength increase with coarse fraction content. The relationships observed between the matrix strength classes and the c' - ϕ' combination of values in the Mid-levels slopes are also not apparent when all the data points are considered. However, the colluvium layers having low matrix strength generally fall in the lower range of c' - ϕ' values. Inconsistency in assessing the matrix strength in the field and over-generalization of the input data used in the back analyses might have affected the results. The majority of the colluvium layers and layer combination have back-analysed 'minimum' shear strengths within the range represented by $c' = 5$ kPa to 12 kPa for $\phi' = 27^\circ$ to 42° .

Some general trends are apparent when the matrix strengths of the colluvium layers are taken into account (Figures 4.18 and 4.19). The main conclusion that can be derived from these two figures is that the matrix strength plays a significant part in controlling the shear strength of insitu colluvium. While the average increase in shear strength is about 2 kPa to 2.5 kPa for every 10% increase in boulder or coarse fraction content, this value can be up as much as 15 kPa to 20 kPa for the colluvium with low and high matrix strengths at the same coarse fraction content.

4.6 Summary

A limited amount of back analyses were carried out on fifteen cut slopes in colluvium, in various parts of Hong Kong. Bearing in mind the limitations of the study explained in Section 4.4.2, a number of general conclusions can be derived from the results. These are summarised below.

The average shear strength parameters calculated from the back analyses show a wide scatter of values for a given coarse fraction content. This suggests that factors other than the coarse fraction content affect the stability of slopes in colluvium. This may also be, in part, due to the slopes selected for back analyses not being at their limiting conditions of failure as assumed. The main fact emerging from the back analyses is that the matrix strength plays a significant role in controlling the mass strength of colluvium in Hong Kong, particularly in the older deposits. Owing to greater overburden pressures and a lower time period for effecting diagenetic changes, the older and more deeply buried deposits are likely to be more completely lithified (hence stronger) than the more recent near-surface deposits.

As pointed out previously, the accuracy of the input data is the most important factor in a back analysis. For example, good relationships were obtained between the shear strength parameters, the matrix strength classes and the coarse fraction contents for the Mid-levels and the Peak slopes, where the quality of the data collected was considered high within the limitations of the study. The results of the back analyses on Tsz Wan Shan slopes indicate a different pattern of shear strength increase than the general pattern shown by the other two areas (Figure 4.18). The characteristics of the colluvium layers present in the Tsz Wan Shan slopes were based on the existing information which was very generalized and crude in comparison to the data collected by the authors for other slope areas.

The following range of mass shear strength parameters were obtained for the overall colluvium from the least-square curve fitting analyses for normal stresses below 50 kPa : $c' = 5$ to 12 kPa for $\phi' = 27^\circ$ to 42° . The higher values belong to the colluvium having high to very high matrix strengths. The shear strength parameters ($c' = 10$ kPa, $\phi' = 40^\circ$) recommended by GCO (1981b) for the bouldery colluvium en-masse in the Mid-levels area for a boulder content of over 50% fall in the uppermost range of values, whereas those ($c' = 10$ kPa, $\phi' = 45^\circ$) recommended by Cooper (1986) are on the very high side of the values. It should be pointed out that these two references did not make any distinction in the applicability of their recommended strength values to different colluvium types with different matrix strengths.

4.7 CHASE-type Analysis

The CHASE Study concluded that the stability of Hong Kong soil slopes cannot be predicted on the basis of a few easily measurable parameters (Brand & Hudson, 1982). Nevertheless, the study established some simple semi-empirical relationships between some selected parameters for slopes in saprolitic and residual soils when the rock type was taken into account. Two such relationships were established between the slope height and the slope angle and between the slope height and the discriminant function value for both stable granitic and volcanic soil slopes (GCO, 1982b). The discriminant function value is a function of slope height, catchment area, natural slope angle and average shear strength of material. No such relationships were found for slopes in colluvium deposits, one reason being the limited data.

A limited CHASE-type analysis was carried out in this study to determine whether such semi-empirical relationships can be derived for the colluvial slopes, by using a more comprehensive database. A total of forty cut slopes, including twenty-two slopes studied by the CHASE and Mid-levels Studies, were analysed (Table 4.4).

The slope height versus slope angle graph is shown in Figure 4.20 for the slopes included in this study. The colluvial slopes studied by the CHASE and the Mid-levels Studies are included in Figure 4.21 for a more comprehensive assessment of the empirical relationship between the slope height, the slope angle and the coarse fraction content. The coarse fraction contents and the matrix strengths shown in the figures are the average values for the overall colluvium layer in each slope. The CHASE lower-bound curve for failed granite soil slopes is also plotted in these two figures for comparison.

The data are too limited and also too scattered to draw any conclusions between the coarse fraction content and the slope height/angle (Figure 4.20). One conclusion that can be reached is that the granite lower-bound curve may also apply to the failed colluvium slopes. However, if post-failure configurations of all slopes are considered, some of the slopes plot to the left of this lower-bound curve (Figure 4.21). If these slopes are assumed to have reached their stable equilibrium conditions after failure, then the lower-bound curve for granitic slopes cannot be applied to the slopes in colluvium.

5. LABORATORY STUDIES

5.1 General

As reviewed in Section 3.2, the published experimental work on the shear strength of cobbly and bouldery soils is very limited. Although a broad pattern of shear strength increase with increasing coarse fraction content was apparent from some of the published relevant test results, these were too little to gain a full understanding of the shear behaviour of heterogeneous soils.

Therefore, a laboratory study was undertaken to investigate more fully the effects of coarse fraction on the shear strength of colluvium and similar materials by using reconstituted soils containing large particles in a fine grained matrix.

The soil specimens were formed by mixing various proportions of crushed rock aggregates (the coarse fraction) with a fine-grained soil (the colluvium matrix). A small number of tests were carried out on specimens containing steel balls. The specimens were compacted to the same matrix density for each series of tests. In total, five series of tests using different types of testing techniques, test conditions and coarse particles were carried out. A summary of the testing programme is given in Table 5.1.

A completely decomposed granitic soil from Mount Butler quarry in Hong Kong Island was used as the matrix material. Particle size distribution of this material, a gravelly silty sand, is given in Figure 5.1. The decomposed granite was sieved to produce two types of test samples having maximum grain sizes of 2 mm and 1.18 mm. This was done in order to achieve a more uniform soil sample in terms of grading, and also to widen the size difference between the matrix material and the two selected coarse fraction sizes. The final soil matrix chosen was therefore a silty sand with a clay content of less than about 3%. Natural soil material was not used, since it was considered that it would be difficult to achieve specimen uniformity and hence repeatability in the test results due to variability of colluvium.

Three types of materials were used as the coarse fraction : single size steel balls

(12.7 mm diameter), 20-28 mm size rock aggregates and 5-6.3 mm size rock aggregates. The crushed rock aggregates were obtained from Mount Butler quarry. The study was aimed primarily at investigating the effects of increasing coarse fraction content on the shear strength of the soil mixtures.

In the case of aggregates, the size difference between the particles was kept to a minimum by using two consecutive British Standard sieves. Very flaky and elongated pieces were removed in order to obtain grains with similar shapes having a maximum-to-minimum dimension ratio of less than 4.0. This figure was based on average boulder dimensions in the slope behind Fairmont Gardens, Mid-levels. Weathered (discoloured) pieces were removed to minimize particle crushing during specimen compaction and testing. The elongation index (which indicates the amount of aggregate particles having the greatest dimension greater than 1.8 times their mean dimension) and the flakiness index (which indicates the amount of aggregate particles having the smallest dimension less than 0.6 times their mean dimension) of the coarse aggregate sample (20-28 mm size) are given in Table 5.2. These indices are not applicable to the material passing 6.35 mm sieve.

In selecting the particle size, the following two conflicting requirements were considered, in addition to the limitations imposed by the available equipment in the Public Works Central Laboratory :

- (a) the maximum particle size in relation to the specimen thickness, and
- (b) the modelling requirements.

It is specified in many laboratory standards (e.g. ASTM, 1990) and guide books (e.g. GCO, 1984) that the minimum sample size (thickness or diameter) should not be less than six times the maximum grain diameter. This is considered necessary to eliminate the size effects in shear strength testing. For the direct shear test, ASTM (1990) also specifies that the specimen diameter (or width) should be at least twice the thickness. In accordance with these requirements, the maximum particle size for 100 mm x 100 mm wide x 44 mm deep box is about 7 mm, and for a 300 mm x 300 mm wide x 148 mm deep box it is about 25 mm. For 100 mm and 76 mm diameter triaxial samples, the maximum grain sizes are about 16 mm and 13 mm respectively. On the other hand, for modelling purposes it is necessary that the particles are as large as possible in order to constitute realistic laboratory models of natural colluvium materials containing cobble and boulder size rock fragments.

The sizes of the aggregates and steel balls used in the laboratory tests were generally within the range specified in (a) (Table 5.1).

5.2 Triaxial Tests Using Steel Balls (CU - BB Series)

5.2.1 Test Method

A number of triaxial tests were carried out on compacted soil specimens containing steel balls. The main reason for using uniform-sized balls was to isolate the effects of increasing coarse fraction content from other variables.

The matrix material and the steel balls were placed in layers in a 100 mm-diameter mould and were compacted under static compression. The initial matrix dry density was kept constant at 1.70 Mg/m^3 (corresponding to an initial void ratio, e_i , of 0.55). However, at 45%, the specimens could only be compacted to a lower matrix density of about 1.60 Mg/m^3 ($e_i = 0.63$). The details of sample preparation are given in Appendix C.

Multi-stage consolidated undrained tests were carried out on the specimens containing 0%, 15%, 30% and 45% steel balls (by volume). Three tests were conducted at each coarse fraction content on the specimens consolidated under 30 kPa, 65 kPa and 100 kPa confining pressures. The back-pressure saturation technique was used to achieve complete saturation of the specimens.

5.2.2 Results

The detailed results of the triaxial testing programme are given in Soil Testing Report No. 392 prepared by the Materials Division. A summary of the test results is given in Table 5.4. A p' - q plot of the failure stresses is shown in Figure 5.2. Only the first stage test results are considered in this study.

The failure stresses, expressed as $\max(\delta_1/\delta_3)$, all fall within a very narrow band, with the exception of one result on the specimen containing 45% steel balls. The shear strength envelope of the matrix material is shown in the figure for comparison. Figure 5.2 shows that there is practically no change in shear strength with increasing ball content. This result is rather unexpected as some increase in strength, particularly at high coarse fraction contents, should have occurred. One possible explanation is that the shear planes formed in the specimens did not intersect any steel balls along their paths. Alternatively, it might be possible that the amount of interlocking of the spherical-shaped grains was negligible to result in a significant change in strength. Also, the smoothness of the steel balls will reduce any increase in strength because of the presence of a much lower friction between the soil and the steel than between the soil grains. Another possible explanation could be that very few steel balls had direct surface-to-surface contacts during shear, even at 45% coarse fraction content, due to the presence of soil coating around the particles. This was observed to be the case when the specimens were split and examined after testing. It is also possible that the matrix was already so dense ($\phi' = 46^\circ$, see Figure 5.2) that its dilatancy masked the effect of increasing coarse fraction content.

The stress paths of the specimens sheared at 30 kPa and 100 kPa confining pressures are given in Figures 5.3 and 5.4. The stress paths and the pore water versus axial strain graphs (Soil Testing Report No. 392) indicate that all specimens dilated when sheared.

5.3 Triaxial Tests Using Aggregates (CU - AGG Series)

5.3.1 Test Method

Single and multi-stage consolidated undrained triaxial tests were carried out on soil specimens containing 10%, 25% and 40% (by volume) 5-6.3 mm size crushed rock aggregates embedded in a silty sand matrix with nominal grain size of 1.18 mm. The initial dry density

of the matrix was selected as 1.35 Mg/m^3 after some compaction trials in the laboratory. Lai & Taylor (1984) reported a matrix dry density of about 1.35 Mg/m^3 for the youngest colluvium in the Mid-levels area. The specimens were prepared by the static compression method described in Appendix C. Initially, it was planned to test specimens containing 60% aggregates. However, this was not possible due to excessive particle crushing during sample preparation. Three specimens were tested at each coarse fraction content after consolidating them under confining pressures of 30 kPa, 65 kPa and 100 kPa, (Table 5.1).

5.3.2 Results

The detailed results are given in Soil Testing Report No. 437. A summary of the test results is given in Table 5.5. Only the first stage test results are considered here. A p' - q plot of the failure stresses is shown in Figure 5.5. The shear strength parameters calculated by the least-squares method are given in Table 5.6 for various coarse fraction contents, and the corresponding shear strength envelopes are drawn in Figure 5.6. Failure stresses of the specimens comprising 0% and 10% particles fall practically along the same least-square line in Figure 5.5.

The stress paths of the specimens are plotted in Figures 5.7 to 5.9 for different stress levels. The shear strength envelope of the matrix material is also shown in the figures for comparison. The following conclusions can be drawn from the results :

- (a) No practical increase occurs in the shear strength up to an aggregate (coarse fraction) content of about 10%. Beyond this value, the shear strength increases first slowly, then rapidly with increasing aggregate content.
- (b) A coarse fraction content of about 25% appears to be the critical value above which the shear strength increases more rapidly. This value appears to correspond to a change in the soil behaviour as observed in the specimen stress paths.
- (c) Above 25%, the soil shows dilatant behaviour. Below this value, the soil behaviour is similar to that of the matrix material. The soil behaviour at this value depends on the confining stress level.

A quantitative assessment of particle crushing was made by measuring the change in weight of aggregate retained on 5 mm sieve. The results show that the higher the coarse fraction content, the higher was the aggregate crushing (Table 5.5). A significant amount of particle crushing was experienced in the specimens containing 40% aggregates. Some crushing also occurred during sample preparation.

5.4 Large Direct Shear Tests Using Aggregates (BSB Series)

5.4.1 Test Method

A limited number of direct shear tests were carried out using a large direct shear box (300 mm x 300 mm x 148 mm deep), as only one set of equipment was available and it took about 1 week to complete one test. The aggregate size used was 20-28 mm crushed granite, giving a box size/maximum particle size ratio of about 5.3 (Table 5.3).

The test specimens were prepared at an initial matrix dry density of about 1.60 Mg/m^3 . The details of sample preparation are given in Appendix C. The proportion of aggregates used were 10%, 20%, 30% and 40% by volume. Only one test at each coarse fraction content was carried out. The specimens were soaked for at least 2 days under a normal stress of 5 kPa. It was not possible to prepare the specimen containing 40% aggregates at a matrix density of 1.60 Mg/m^3 . The final density achieved for this specimen was 1.52 Mg/m^3 . All specimens were consolidated and sheared under a normal stress of about 35 kPa.

Anomalous results were obtained for the two specimens comprising matrix material and 10% aggregates. This was attributed to incomplete saturation of the large specimens at low coarse fraction contents. Therefore, two additional specimens were prepared and these were soaked for longer periods (7 days) before testing.

5.4.2 Results

The detailed results are given in Soil Testing Report Nos. 403 and 435. A summary of the test results is tabulated in Table 5.7. Shear stress versus horizontal displacement and vertical displacement versus horizontal displacement plots of the test results are presented in Figure 5.10.

Some anomalous results are apparent in Table 5.7 and Figure 5.11. The strength of the specimen containing no aggregates (soaked for 2 days) is higher than those with 10% and 30% aggregates. Even after 7 days of soaking, its strength is still higher than the specimens with 10% aggregates and only slightly smaller than the specimens with 20% and 30% aggregates. Also, at 10% aggregate content, the specimen which was soaked for 7 days showed a slight increase in strength instead of a decrease, in comparison with the specimen soaked for 2 days. A similar anomaly is also apparent in the stress-displacement behaviour of the specimens containing 10% aggregates (Figure 5.10). In contrast to all other specimens which show a sharp peak at about 3 mm to 6 mm horizontal displacement and a strong dilatant behaviour, these specimens show very broad peaks at larger displacements and a compressive behaviour.

This anomalous behaviour cannot be attributed to variation in the matrix density as all but one specimens were compacted and consolidated to very similar densities of 1.58 Mg/m^3 to 1.62 Mg/m^3 (void ratios of 0.62 to 0.65), with the specimens containing 10% aggregates being the densest (Table 5.7). No further explanation can be given at this stage as the number of tests were very limited.

It is difficult to assess the change in strength with increase in coarse fraction content because of the anomalous test results from the large shear box tests. However, it can be

inferred from the limited test results that the increase in shear strength is small from 20% to 30% coarse fraction content (about 4%), but it becomes very significant from 30% to 40% (about 55%). Table 5.7 shows that a significant amount of particle crushing took place at aggregate contents of 30% and over (about 10% by weight).

5.5 Small Direct Shear Tests Using Aggregates (NSB and NSB-D Series)

5.5.1 Test Method

Two series of direct shear tests were carried out on specimens containing 5-6.3 mm size crushed granite aggregates, using 100 mm x 100 mm shear boxes. The maximum grain size of the matrix material was 1.18 mm and the initial matrix density was 1.35 Mg/m³. The proportion of aggregates used were 10%, 20%, 30% and 40%. The details of specimen preparation are given in Appendix C.

In the first series of tests (NSB-series), four specimens (soaked overnight) were tested at each coarse fraction content under normal stresses of 15 kPa, 30 kPa, 60 kPa and 120 kPa (Table 5.1). In the second series (NSB-D series), only a limited amount of tests were carried out using dry specimens containing no aggregates and 40% aggregates. Quantitative assessment of particle crushing was also made for selected specimens.

5.5.2 Results

The detailed results are given in Soil Testing Report No. 403. A summary of the test results is given in Table 5.8. Plots of failure stress versus normal stress are shown in Figure 5.12. Figures 5.13 to 5.15 display shear stress versus horizontal displacement and vertical displacement versus horizontal displacement relationships for selected specimens.

The least-square lines are fitted to the data points in Figure 5.12 in order to determine the mean shear strength envelopes at different coarse fraction contents. Figure 5.16 shows the effects of increasing coarse fraction content on the mean shear strength envelope at various normal stress levels.

Figures 5.13 to 5.15 show that as the coarse fraction content increases from 10% to 20%, the soil behaviour changes from the one having no peaks in the stress-displacement curves at 10% to the one having broad peaks at 20%. The soil also becomes more dilatant showing only a small initial compression at 20%. At about 30%, the soil behaviour changes from being initially compressive followed by dilatant behaviour to all dilatant behaviour, even at high stress levels. The shear stress-displacement curves start to show sharp peaking followed by a drop at later stages of shearing.

The results of the direct shear tests carried out on oven-dry specimens are shown in Figure 5.17. The test results on the soaked specimens at the same coarse fraction contents are also shown in the figure for comparison. The least-square lines drawn through the data points show that the increase in shear strength with increasing coarse fraction content is greater for dry specimens than the soaked specimens.

The following conclusions can be drawn from the results of the direct shear tests on small specimens :

- (a) Shear strength increases sharply as the coarse fraction content increases from 0% to 40%.
- (b) The increase in shear strength is stress dependent, smaller for higher normal stresses at the same coarse fraction content (Figure 5.16).
- (c) A coarse fraction content of about 20% appears to be the critical value at which the soil behaviour changes from being compressive to mildly dilative to strongly dilative.

5.6 Summary

Limited direct shear and triaxial test results show that the shear strength of a soil containing large non-spherical particles generally increases with increasing coarse fraction content, within the range considered in this study. However, the pattern of increase in the shear strength is not uniform. It depends on many factors such as the test type (triaxial or direct shear), the specimen size, the moisture content and the shape of the coarse particles, as well as the applied stress level. Other factors such as the size and strength of the particles and the matrix properties may also be important, but these were not researched in any detail in the laboratory study.

The test results indicate that the increase in shear strength with increasing coarse fraction content generally follows a broad pattern as illustrated in Figure 5.18. This pattern of increase in the shear strength of soil containing coarse particles can be explained as follows :

- (a) At very low coarse fraction contents of below about 10%, the effect of coarse particles on the shear strength is very small or negligible. The soil behaviour is entirely controlled by the fine-grained matrix. The large particles are usually not in contact with each other or with the plane of shearing. This results in a negligible increase in the frictional component of the shear strength arising from the interlocking and overriding of the large particles.
- (b) The pattern of change in the shear strength is different for the direct shear and triaxial tests as the coarse fraction content increases from 10% to 30%. As expected, the results are very much stress dependent; larger increases are obtained at lower normal stresses arising from more freedom for the specimen to dilate during shear.

The matrix still appears to be the dominant component in

controlling the shear behaviour, but the coarse particles also play an increasing role.

Lower shear strength increases were obtained from the triaxial tests in this study. This can be explained as follows : In triaxial tests, not many coarse particles may fall along the induced shear surface, which generally follows the weakest path (i.e. through the weaker matrix material). The contribution to the shear strength resulting from grain interlocking is therefore small. In direct shear tests, where the orientation of the induced shear surface is pre-determined by the testing arrangement, more coarse particles are likely to fall along the failure path. Therefore, in the latter tests, a considerable shear resistance is mobilised due to interlocking (i.e. dilating) effects of the large grains.

- (c) As the coarse fraction content increases beyond 30%, the shear strength increases more rapidly. The coarse fraction becomes increasingly dominant in controlling the soil behaviour. A major portion of the shear resistance is derived from the frictional forces arising from grain interlocking and to a lesser degree from the matrix strength.

High particle crushing observed during both types of tests indicate that a significant number of large grains come into contact with each other during shearing at 40% coarse fraction content. Again, large increases in the shear strength were recorded from the tests carried out in the small direct shear box in comparison to those recorded from the triaxial or the large shear box tests.

The laboratory test results in this study on specimens with a silty sand matrix are in striking contrast to the theoretical considerations by Vallejo (1989) on mudflow deposits containing large fragments. He stipulated that the soil strength is dominated by the fine-grained muddy matrix alone up to a coarse fraction content of 55%. The limited results by Patwardhan et al (1970) are in broad agreement with this study as far as the coarse fraction contents are considered. Their direct shear test results showed that the coarse fraction starts having a strong influence from about 30%-40% (see Figure 3.4).

The increase in shear strength beyond a coarse fraction content of 40% was not researched here. Based on the test results carried out by others, it is expected that the shear strength would continue to increase with increasing proportion of coarse particles and approach to that of a material containing all rock fragments (i.e. a rockfill).

No practical strength increase was apparent in the triaxial test results on soil specimens containing steel balls, even at a coarse fraction content of 40%. This is attributed to the spherical shapes and smooth surfaces of the steel balls.

6. THEORETICAL STUDIES

6.1 General

A theoretical slope model was established from the results of the field studies to provide a direct quantitative assessment of the role of coarse fractions on slope stability. The results were used to assess indirectly the individual effects of a number of variables on the mass shear strength of heterogeneous soils, particularly the colluvium. The variables examined included particle size, shape, spacing and dry density as well as matrix strength.

6.2 Methods of Analysis and Limitations

The geometry of potential failure surfaces in soil slopes containing coarse rigid particles (i.e. cobbles and boulders) will be dependent on the distribution and geometry of the coarse particles, particularly when the intact strengths of these particles are significantly higher than that of the matrix. The presence of regular-spaced particles will cause the lengthening (unevenness) of the potential failure surfaces. The effect of the unevenness on the factor of safety can be assessed using the limit equilibrium method of analysis.

In this study, the Morgenstern & Price (1965) method of analysis was used to compute the factors of safety. In the analysis, it was assumed that the slope portion above the potential failure surface comprised only the matrix material. Analyses were carried out for different shaped failure surfaces which might result from the presence of different contents, shapes, sizes and spacings of coarse particles.

The configuration of the theoretical slope model is given in Figure 6.1, which also shows the notations used in this section. The slope angle was kept constant at 59° , which is fairly typical for many soil cut slopes formed before 1980s. An upper slope angle of 20° was selected, which is again typical of many natural slopes above the cut slopes in colluvium. A slope height of 10 m was based on the practical limitations of the GSLPC computer program (Leung et al, 1986) with respect to the range of particle dimensions selected for the analysis.

The dimensional properties of boulder-size particles used in the model were based on the measurements made in the colluvial slope behind Fairmont Gardens, Mid-levels (Irfan & Tang, 1992). The mean length (l) of all boulders present in the excavated slope portion was 1.6 m and their mean height/length (h/l) ratio was about 1/2. It was observed during the field study that the orientation of the basal surfaces of boulder size fragments was not random. In this respect, a mean dip angle of 24° was determined from the stereplot analysis. These figures were adopted as the reference values for the theoretical slope and detailed analyses were carried out for a range of coarse fraction contents of up to 55%. A matrix strength represented by $c' = 5$ kPa and $\phi' = 35^\circ$ was adopted as the reference value. A mass unit weight of 18 kN/m^3 was used for the soil composing the slope. Table 6.1 gives a summary of various parameters used in the theoretical analysis.

For simplicity, a uniform distribution of coarse particles in a layered rectangular array format (Figure 6.1) was assumed in the analysis. The actual distribution and shapes of boulders in a real colluvium slope are unlikely to be uniform (Section 4). However, such analyses should provide a relative and comparative assessment of the effects of each variable

on the factor of safety for a range of coarse fraction contents. Nevertheless, the results should be viewed with respect to somewhat idealized nature of the boulder shapes, sizes and spacings adopted for the theoretical analysis.

Combinations of shear strength parameters adopted in the sensitivity analysis for the strength of the matrix material (Table 6.1) cover the range of $c'-\phi'$ values commonly used in analysing colluvial slopes in Hong Kong. The mass density of the soil at different boulder contents was calculated by assuming a matrix density of 1.5 Mg/m^3 and a particle density of 2.55 Mg/m^3 (i.e. the average density of a slightly to moderately decomposed igneous rock).

Initially, stability analyses were carried out on hand-drawn failure surfaces. It was subsequently observed that the location of the critical potential failure surface in a slope with regularly-spaced coarse particles coincided approximately with that of the same slope without coarse particles (Figure 6.2). A computer program named 'INCL.BAS' was then written to generate slip surfaces automatically (Appendix D). In program-generated slip surfaces, the position of each failure surface was fixed in a way that it touched the opposing corners of the adjacent particles (Figure 6.2). The critical failure surfaces created by the program coincided exactly with the hand-drawn surfaces using the same criterion when the coarse fraction contents were 30% or more. At 20% coarse fraction content, the calculated factors of safety were found to be very similar for the smoother hand-drawn and the zig-zag shaped computer-generated curves (Table 6.2). This finding confirmed that the computer program written for the generation of potential failure surfaces was appropriate for the type of stability analyses undertaken in this study. The program was used to generate the potential failure surfaces when the coarse fraction content was 30% or more.

6.3 Results

Selected results of the theoretical analyses are given in Figures 6.4 to 6.19.

Figure 6.4 illustrates the effects of increasing coarse fraction content on the factor of safety of the theoretical slope. There is a slight increase in the factor of safety when the coarse fraction content increases from 10% to 30%. This is followed by a rapid increase above 30%. The effect of the matrix strength on the factor of safety is shown in Figure 6.5. The pattern of increase is similar to that observed in Figure 6.4. The same results are presented in Figure 6.6 using a normalized factor of safety, FOS_n , which is defined as "the ratio of the factor of safety of a slope with coarse particles to the factor of safety of the same slope without". Despite the differences in the matrix strengths, all data points fall within a narrow band. The normalized factor of safety is therefore a convenient way of expressing the results of the theoretical analyses within the coarse fraction range considered in this study.

The effect of the particle spacing ratio, ST/SL , on the normalized factor of safety is shown in Figure 6.7. The minimum FOS_n occurs when $ST/SL = 1.0$, i.e. when the particles are uniformly-spaced. The same figure also shows variation in FOS_n with coarse fraction content at $ST/SL = 1.0$.

The effect of the particle size (constant shape) on FOS_n is shown in Figure 6.8. The FOS_n appears to be slightly higher for a slope containing larger particles when the coarse

fraction content is greater than 20%. At 50%, the FOS_n drops rapidly for both sizes (not shown in the figure). A possible cause for this unreal effect is that parts of the computer-drawn potential failure surfaces are vertical or inclined forward for the assumed regular pattern of particle distribution in the slope (Figure 6.9). It is possible that the Morgenstern & Price method used in the analysis may not be appropriate for analysing such situations. However, this topic is not researched any further here.

The effect of the height/length (h/l) ratio (i.e. the particle elongation ratio) on FOS_n is shown in Figure 6.10, for a coarse fraction content of 40%. The FOS_n increases from 1.25 to 1.65 as the h/l ratio increases from a reference value of 0.5 to 1.5. The rate of increase in FOS_n is greater when the h/l ratio exceeds 1.0. The values calculated for 30% to 45% in Figure 6.10 indicate that the effect of h/l ratio can be as significant as the coarse fraction content itself. Individual effects of the particle length and the particle height on FOS_n are shown in Figures 6.11 and 6.12 respectively. The size effects are summarized together in one graph in Figure 6.13. This plot shows that the FOS_n has a minimum value at a particle elongation ratio of about 0.4.

The effect of the particle shape on FOS_n (constant area) is shown in Figure 6.14. The curve for a circular shape gives a lower factor of safety than a rectangular shape, at the same coarse fraction content. For the reference slope, the FOS_n is lower for particles with circular sections (i.e. spherical or cylindrical shapes) than those with square sections (i.e. cubic or prism shapes) at the same coarse fraction content.

A limited number of analyses were carried out on a slope of 15 m height. The results plotted in Figure 6.15 show that the normalized factors of safety for 10 m and 15 m high slopes are practically the same. This suggests that FOS_n is virtually independent of the slope height (i.e. the colluvium thickness), within the usual range of thicknesses of colluvium deposits found in Hong Kong slopes.

Until now, all analyses were carried out using a constant unit weight of 18 kN/m^3 for the soil mass composing the theoretical slope. As the proportion of coarse particles increases in a soil, the overall density also increases. Figure 6.16 shows the combined effects of increasing mass density and coarse fraction content on FOS_n . The decrease in FOS_n is very small, about 1.5% for every 10% increase in coarse fraction content or for every 7% increase in mass density. The increasing particle density decreases the normalized factor of safety of the hypothetical slope to a value below unity for coarse fraction contents of up to about 25%.

The mass shear strength parameters, c_{mass}' and ϕ_{mass}' , were back calculated for different coarse fraction contents from the results of the theoretical slope analyses, using the method given in Appendix E. The results are shown in Figure 6.17 for different matrix strengths. Because of the combined effects of c' and ϕ' parameters on the shear strength, it is not easy to assess the pattern of change in mass strength from this figure. However, it can be seen that at a low matrix cohesion value of 5 kPa, ϕ_{mass}' increases sharply with increasing coarse fraction content, while c_{mass}' remains almost the same, except for a small drop below 20%. This indicates that the increase in the mass shear strength is dominated by the ϕ' -component (i.e. the interlocking effect). This effect can be better seen in Figure 6.18 where the change in ϕ_{mass}' , $\Delta\phi'$, has been plotted against the coarse fraction content. In Figure 6.19, the difference in the mass cohesion value, c_{mass}' , is plotted against $\Delta\phi_{\text{mass}}'$. This figure also

highlights that it is the frictional numerical component of the mass strength which is most affected by the increasing coarse fraction content.

In order to assess directly the effects of increasing coarse fraction content on the mass shear strength, the back-calculated strengths are plotted against their respective coarse fraction contents in Figure 6.20. A normal stress of 20 kPa was used in back calculating mass shear strengths from the usual Mohr-Coulomb formula. This value corresponds to the average stress acting along a potential failure surface in a 10 m to 15 m high slope. It should be noted that all curves presented in Figures 6.17 to 6.20 are for a specific particle spacing of $ST/SL = 1.0$, and particle dimensions of $h = 0.8$ m and $l = 1.6$ m.

6.4 Summary

Theoretical studies showed that the factor of safety of a slope comprising regularly spaced boulder-size particles in a fine soil matrix is a function of a number of variables. Some of the more important variables are listed below in order of decreasing significance, as found from the theoretical slope model analyses :

- (a) shear strength of the finer grained matrix
- (b) coarse fraction content
- (c) shape of the coarse particles
- (d) particle elongation ratio (height/length)
- (e) size of the coarse particles
- (f) spacing between the coarse particles
- (g) dry density of the coarse particles

The order was determined by comparing the magnitude of change in FOS_n due to a particular variable at 40% coarse fraction content with that due to 10% increase in coarse fraction content. A schematic summary of the effects of various variables on shear strength is given in Figure 6.21.

When only the effects of coarse fraction content is considered (Figure 6.4), the following pattern of change is observed in the factor of safety (and consequently in the mass shear strength) :

There is no change in the factor of safety for up to a coarse fraction content of 10%. This is followed by a small increase between 10% and 30%, and a much larger and almost constant increase beyond 30%. Consequently, a similar pattern of change can be seen in the mass shear strength back-calculated from the numerical analysis at a specific normal stress (Figure 6.20). The rate of change beyond 50% to 55% coarse fraction content is not known due to the limitations of the analysis technique used for the theoretical slope model.

The presence of uniformly-spaced coarse particles causes the lengthening and unevenness of the potential failure surfaces in a slope and this results in a computation of higher factors of safety and mass shear strengths. The increase in the mass shear strength can

hence be expressed mostly in terms of an increase in the mass frictional angle of shearing resistance. With this in mind, the following explanation can be suggested for the observed pattern of change in the factor of safety :

- (a) At very low coarse fraction contents of less than 10%, the locations and shapes of the potential failure surfaces are unlikely to be influenced by the presence of coarse particles. However, the soil density increases with increasing coarse fraction content and this results in a reduction of the overall factor of safety to a value below that of the same slope without coarse particles. The most adverse situation occurs when there is a local concentration of boulders near the slope surface in a colluvium slope. This situation will lead to an increase in the destabilizing force due to increasing weight while not affecting the shapes of the potential failure surfaces.
- (b) As the coarse fraction content increases from 10% to 30%, the shapes and locations of the failure surfaces are increasingly affected by the presence of the coarse particles. However, the increase in the overall factor of safety is very small due to the adverse effects of increasing soil mass density.
- (c) Beyond 30%, the shapes and locations of failure surfaces are increasingly dominated by the coarse particles.

7. DISCUSSION

7.1 Effects of Coarse Fractions

The laboratory studies on soil-aggregate mixtures indicated negligible increases in the shear strength below 10% and a small increase between 10% and 30% coarse fraction contents. The threshold value appears to be at about 30% for a sharper increase in the shear strength. The results of the direct shear tests are in broad agreement with the limited tests carried out by Patwardhan et al (1970), who used a very large shear box. The general pattern of increase observed in the laboratory studies is similar to the broad pattern derived from a review of previous relevant but limited experimental work carried out by others. This is in spite of using a different approach in the laboratory study where the soil-aggregate mixtures were prepared and tested at similar matrix densities. In comparison, the previous laboratory studies were carried out on heterogeneous soil materials mostly prepared under similar compaction efforts.

A similar pattern of change was also apparent in the shear strengths back-calculated from a comprehensive analysis carried out on a theoretical slope model. The approach adopted in the theoretical studies, where a limit equilibrium method of analysis was used to calculate the factor of safety, ignored any interaction between the coarse fraction and the soil matrix. This is different from the composite material approach adopted in the experimental studies. The threshold value for a sharper increase in the shear strength was also found to be

at about 20% to 30% coarse fraction content, depending upon the characteristics of the coarse particles and the matrix strength (see, for example, Figures 6.20 and 6.21)

Due to the limitations of the numerical method of analysis used for the theoretical slope, the rate of change in the shear strength beyond about 55% coarse fraction content is not known. Similarly, specimens containing more than 40% coarse particles were not tested in the laboratory due to difficulty in sample preparation. However, it is not unreasonable to expect that the mass strength will keep on increasing beyond 50% to 55% coarse fraction content and at some high value it will approach to that of a soil comprising entirely coarse particles. This threshold value where the soil behaviour will be entirely controlled by the coarse particles is probably at about 80% based on Vallejo (1989).

Different patterns of shear strength increases were obtained from the triaxial and direct shear tests. Smaller strength increases were from the back-pressure saturated triaxial test specimens. This is attributed to the different stress conditions and modes of failure imposed on the specimens by the two different testing techniques.

The back analyses of a limited number of colluvial slopes indicated that the matrix strength is an important factor in controlling the mass shear strength of colluvium in Hong Kong.

The theoretical analyses showed that the factor of safety (and subsequently the mass shear strength) is strongly influenced by the dimensional characteristics of the coarse particles, as well as the matrix strength and the coarse fraction content, with the particle spacing and density being less important. At a particular coarse fraction content, uniformly-spaced spherical-shaped particles gave the lowest shear strength.

Other factors may also affect the change in the mass shear strength. The effects of the particle strength and the grain size and density of the matrix were not researched in the experimental and the theoretical studies. In natural colluvium deposits which usually contain a mixture of weaker more decomposed boulders and cobbles as well as the strong fresher ones, crushing of weaker particles is likely to occur during shearing. In addition, rotation and translation of the particles, particularly in colluvium layers with loose matrix, are likely to take place during failure. The spatial arrangement of the cobbles and boulders in natural colluvium slopes are far from the uniform distribution assumed in the study. The material used as the matrix in the laboratory tests was a silty sand, whereas the matrix of the natural deposits has a much wider particle size distribution ranging from gravelly silty sand to gravelly silty clay.

In summary, the increase in mass shear strength is negligible for coarse fraction contents of up to about 20%. This is followed by a small increase between about 20% and 30%. Beyond 30%, the increase is much more rapid and almost linear with the coarse fraction content. The mass strength is also strongly influenced by the matrix properties and the shape and size characteristics of both boulder and cobble size fragments and their arrangements in the soil. As the coarse fraction content increases, the component of the strength due to the matrix properties decreases and at some high value (80% ?), the coarse fraction characteristics entirely control the mass shear strength. The effects of various variables on the mass shear strength are illustrated schematically in Figure 7.1.

7.2 Proposed Analysis Models

The failure mechanism of a soil mass containing rigid coarse particles can be visualized as shearing occurring along an irregular surface defined by the characteristics of the coarse particles, particularly their shapes, sizes and spacings. The increase due to dilation of the soil mass during shearing along such an irregular surface can be expressed by an increase in the frictional component of the mass shear strength, i.e as an increase in the angle of internal friction of the matrix material. The theoretical slope analyses showed that the mass friction angle, ϕ_{mass}' , increases sharply (and almost linearly) with increasing coarse fraction content beyond a critical value, while the mass cohesion parameter, c_{mass}' , changes very little.

Both the laboratory studies and the theoretical slope analyses showed that increase in the mass shear strength is appreciable only when the coarse content reaches a critical value, C_c . The increase below this value is very small or negligible. By conservatively ignoring the small increase, the mass shear strength of soil with a small amount of coarse particles can be expressed by the following formula :

$$\tau_{\text{mass}} = \tau_{\text{mass}}^0 = c_{\text{mass}}^0 + \sigma_n' \tan \phi_{\text{mass}}^0 \dots \dots \dots (7.1)$$

for a coarse fraction content $< C_c$

where c_{mass}^0 = mass cohesion parameter of the soil without coarse particles,

ϕ_{mass}^0 = mass friction angle of the soil without coarse particles, and

C_c = a critical coarse fraction content at which the mass strength starts to increase sharply, usually a value between 20% and 30%.

The value of C_c depends on a number of variables, including the properties of the matrix, and the size, shape and spacings of the coarse particles, etc.

The rate of increase in the mass friction angle is almost constant above the critical coarse fraction content, but it is also strongly dependent upon the shapes and sizes of the particles and their distribution in the soil. Following from the above argument, the mass shear strength of a heterogeneous soil containing cobble and boulder size rock fragments can be represented by the following general formula :

$$\tau_{\text{mass}} = c_{\text{mass}}^0 + \sigma_n' \tan [\Delta\phi + \phi_{\text{mass}}^0] \dots \dots \dots (7.2)$$

for a coarse fraction content $\geq C_c$

where $\Delta\phi$ = increase in the mass friction angle resulting from increase in coarse fraction content and is equal to :

$$\Delta\phi = (C_n - C_c)\alpha \dots \dots \dots (7.3)$$

where α = a site (material) specific constant which depends on the shape and size properties of the coarse particles, their spacings, etc., and

C_n = coarse fraction content of the soil (in percent)

The applicability of this formula above a coarse fraction content of about 60% is not known.

In Figure 7.2, the results of selected laboratory tests and theoretical slope model analyses (Figure 6.19) are plotted in the form of $\Delta\phi'$ versus coarse fraction content. The friction angles from the laboratory results were calculated by assuming that c_{mass}^0 was equal to c_{matrix} determined on laboratory specimens. Also plotted on the figure is the triaxial test data from Holtz & Gibbs (1956). Only the test results on the samples having similar matrix density are included and a particle density of 2.65 Mg/m³ is used in converting weight proportions of the coarse fractions to their respective volume proportions. The increase in the mass friction angle in all cases can be approximated by the proposed relationships in equations 7.1 and 7.2 as given in Figure 7.3. The corresponding values of C_c and α calculated from Figure 7.3 are given in Table 7.1. The rate of increase in the mass friction angle is generally greater in the direct shear tests than in the triaxial tests. The critical coarse fraction contents vary between 0.23 and 0.45. These values are for specific coarse fraction characteristics, slope heights, etc used in each study. Full range of values of C_c and α for different slope and material characteristics have not been determined.

In Figure 7.3, a lower-bound curve is drawn to the study results and other data given in Figure 7.2. No increase in the mass friction angle is assumed to occur below a coarse fraction content of 25%, based on the results of this study. Also, since the increase above about 50% to 60% coarse fraction content is not known with any accuracy, it is conservatively assumed that no further increase in the mass friction angle occurs above 60%. The friction angle increases by about 4° for every 10% increase in coarse fraction content between these two threshold values.

It is considered that the chart given in Figure 7.3 can be used to estimate conservatively the increase in the mass friction angle of a natural colluvial deposit when the coarse fraction content is between 25% and 60%. Below a coarse fraction content of 25%, the mass friction angle can be taken equal to that of the matrix material. It is to be noted that, in layered colluvium deposits, each layer is likely to have a different shear strength depending on its coarse fraction and matrix properties.

An alternative method which can also be used to incorporate the effects of coarse particles in practical slope designs in colluvial deposits is the normalized factor of safety approach. The normalized factor of safety of a slope containing coarse particles is, for all practical purposes, independent of the matrix strength and the slope height (see Figures 6.6 and 6.15). This suggests that a colluvial slope can first be evaluated in terms of its factor of safety (FOS_{matrix}) by using the matrix strength determined in the laboratory, for the appropriate normal stress range. Then, a correction factor (β) can be applied to obtain the factor of safety of the slope with coarse particles ($FOS_{coarse\ fraction}$) :

$$FOS_{coarse\ fraction} = \beta FOS_{matrix} \quad (7.4)$$

where the factor β depends on the coarse fraction content as well as on the characteristics of the coarse fraction. This approach can be used to assess the stability of two slopes having the same coarse fraction contents and properties but different matrix strengths.

7.3 Shear Strength of the Mid-levels Colluvium

The Mid-levels Study (GCO, 1981b) and Cooper (1986) recommended a mass shear strength represented by $c' = 10$ kPa for $\phi' = 41^\circ$ and $c' = 10$ kPa for $\phi' = 45^\circ$, respectively, for the colluvium deposits in the Mid-levels area when the boulder content exceeded 50%. The shear strength parameters (usually $c' = 5$ kPa for $\phi' = 35^\circ$) derived from the tests carried out on the fine matrix material were applied to the colluvium containing less than 50% boulders.

A comparison of the factors of safety calculated by using these two sets of 'mass' strength parameters with those calculated from the theoretical analysis is given in Table 7.2 for 10 m and 15 m high slopes. The average coarse fraction properties used for calculating the factor of safety of the theoretical Mid-levels slope were the same as those adopted in Section 6 (Figure 6.18). The factors of safety calculated by the equations 7.1 and 7.2, using the lower-bound curve in Figure 7.3, are also shown in Table 7.2. It was assumed that the matrix strength of the colluvium is represented by $c' = 5$ kPa and $\phi' = 35^\circ$.

For a coarse fraction content of 50%, the factors of safety calculated from the theoretical model are marginally above the values calculated using the parameters proposed by GCO (1981b), but lower than those based on Cooper (1986). The proposed shear strength formula gave the lowest factors of safety (Table 7.2). This is not surprising since the relationship suggested for calculating the increase in $\Delta\phi'$ is a lower-bound solution.

At 40% and 30%, the factors of safety calculated from the parameters recommended by GCO (1981b) are about 16% lower than those calculated from the proposed relationship.

In the above calculations, it was assumed that the colluvium deposit consisted of one layer. In fact, the colluvium in Hong Kong usually consists of a number of layers. The matrix strength and the coarse fraction content of each layer would need to be determined separately for a more accurate assessment of the mass shear strength of the overall colluvium in each slope. Although the Mid-levels Study found no significant differences in the matrix strength of different classes of colluvium present in the Mid-levels area, this study (see also, Irfan & Tang, 1992) revealed that significant differences can occur in terms of matrix strength, particularly if the deposits are of different ages and weathered to different degrees.

7.4 Characterization and Quantification of Insitu Colluvium Properties

In many slopes in Hong Kong, colluvium occurs as a layered deposit, with each layer having broadly distinctive matrix and coarse fraction properties related mainly, but not necessarily, to its relative age and insitu weathering state. The deeper layers have much denser (stronger) matrix and contain more intensely decomposed boulders and cobbles.

Distinguishing colluvium from other types of soil is not generally difficult, particularly in surface exposures. However, in some cases, the definition of the boundary between the base of colluvium and the underlying weathered rock, may not be so obvious in borehole cores and small excavations. This is particularly so if the colluvium layer has undergone extensive insitu weathering since its deposition and was derived from the same rock type as the

underlying saprolitic or residual soil.

The majority of the colluvium characteristics which affect the shear strength can only be described semi-quantitatively using the recommended terminology given in GCO (1988) for the coarse-grained soils. Additional properties can be described using the terms adopted in Irfan & Tang (1992). However, it is very difficult, if not impossible, to determine a numerical value for each property that can be applied to the layers in stability analysis of such a variable material.

The coarse fraction content of a colluvium layer can be estimated to the nearest 5% to 10% from an inspection of surface vegetation or chunam strippings. However, considerable care and judgement should be exercised in applying the coarse fraction content or any other property so determined to the whole layer(s) in a stability assessment of a colluvial slope. In addition, this is a subjective assessment and is prone to operator error. Inspection of borehole cores and core photographs would be useful in supplementing the information gained from surface strippings. Usually, many boreholes would be required for a reasonably accurate determination of the boulder/cobble contents in a very variable deposit. In general, it is not possible to determine the size and shape properties of boulders and their spatial arrangement from small size rotary boring techniques usually adopted for colluvium in Hong Kong. Also, the weaker highly decomposed cobbles and boulders would not normally be recovered by the conventional double-tube rotary drilling, resulting in an underestimation of the coarse fraction content.

The properties of the matrix materials are easier to determine in comparison to those of the coarse fragments. The index and shear strength properties of the matrix can be determined accurately by usual laboratory techniques, particularly when it does not contain a significant proportion of gravel size fragments.

In the field, the relative strength of the colluvium matrix can be assessed by the use of a hand penetrometer (if fine-grained) or by other probing techniques (if coarse-grained). It should be emphasised that the matrix characteristics can also be variable throughout the deposit.

For slope stability analyses purposes, the positions of layer boundaries (if more than one layer exists in the slope) would need to be known. However, this is not easy from the results of surface mapping using strips, trial pits or trenches. Detailed borehole logs would be required, in order to delineate the exact positions of various layers in a slope. The groundwater behaviour of each layer or layers would also need to be determined for an accurate determination of the mass shear strength of insitu colluvium. Hydrogeological aspects of the colluvium in Hong Kong were not included in this study.

Assessment of the preferred orientation of the coarse fragments, which is one of the factors affecting the mass shear strength of colluvium, would be very difficult from the inspection of surface strippings or trial pits. A full assessment of preferred orientation can only be made if the slope is undergoing large scale excavation works. Statistical analysis may need to be applied to the data in order to determine the direction and dip of the preferred orientation.

Identification and description of colluvium in Hong Kong and quantification of its properties for slope stability purposes are further discussed in Irfan & Tang (1992).

7.5 Corestone-bearing Saprolites

The theoretical study used in Section 6 would be particularly applicable to saprolites containing uniformly-spaced and sized corestones but without any adverse relict points. The corestones, particularly in widely-jointed coarse-grained rocks, tend to be distributed in a regular pattern due to weathering effects being primarily controlled by more or less regularly-spaced joints. However, it is expected that, even in the saprolites which contain the most favourable joint orientation for stability (i.e. vertical and horizontal joint sets), some structure control would still occur as the relict joints have lower shear strengths than the intact soil material (Irfan & Woods, 1988).

The upper limit of corestone content where the theoretical model (and equation 7.2) would not be applicable is not known with any accuracy. For example, a jointed weathered rock mass containing 60% corestones (i.e. a moderately weathered rock mass) would not be behaving in the same way as a transported soil containing 60% boulders in a fine-grained soil matrix (e.g. colluvium). The behaviour of the former would be controlled by the discontinuities and the shear strength of such a rock mass can probably be determined by the rock mechanics methods of analysis such as the empirical strength criterion of Hoek & Brown (1980). There is however a lack of experimental data on the applicability of these methods of analysis to the moderately and highly weathered rock masses. From field evidence, it is considered that the theoretical approach adopted in this study would only be applicable up to a corestone content of about 30%-35%, i.e. somewhere in the highly weathered rock mass, assuming no discontinuity control is operative. Usually, in a weathered rock mass containing over 30%-35% corestones, the decomposed material in between the corestones is not entirely composed of weak soil (i.e. completely decomposed rock) but also less weathered stronger rock material.

8. CONCLUSIONS AND RECOMMENDATIONS

- (a) It is concluded that the effects of increasing coarse fraction content on the mass shear strength of colluvium and similar heterogeneous soils are complex. The study showed that the major factors affecting the mass shear strength of a soil containing coarse particles are the strength of the matrix material, the coarse fraction content and the shape of the coarse particles. Other significant factors are the particle size, elongation ratio, density and spacing and the effective normal stress.
- (b) The back analysis of existing cut slopes in colluvium indicated that the cobble-size particles also influence the insitu strength. However, it is emphasized that quantification of many of the colluvium properties is almost impossible

because of great variability and inhomogeneity shown by these deposits in Hong Kong. Therefore, an accurate assessment of the effects of various factors on the mass shear strength of natural colluvium deposits was not possible in the numerical methods used in this study.

- (c) The following broad pattern of increase in shear strength with increasing coarse fraction content was obtained from the results of laboratory tests and theoretical slope analysis :
 - (i) No practical increase in the shear strength occurs up to a coarse fraction content of about 20%. At such low contents, the contribution to the mass shear strength resulting from grain interlocking or dilatancy is small during shearing and the strength is dominated by the matrix properties.
 - (ii) There is a small increase in the shear strength between about 20% and 30% coarse fraction contents.
 - (iii) The shear strength starts to increase sharply beyond about 30% coarse fraction content, mainly due to the increased contribution from the interlocking effect of the coarse particles during shearing.
- (d) The above conclusion is in contrast to previous studies by GCO (1981b) and Cooper (1986) which concluded that the effects of coarse particles on the mass shear strength of colluvium were negligible below a 'boulder' content of 50%.
- (e) Normalized factor of safety approach using a hypothetical slope model has been found to be a useful method in assessing the effects of various material and slope variables on the mass shear strength of soils containing coarse particles.
- (f) The increase in the mass shear strength resulting from increasing coarse fraction content can be expressed as an increase in the friction angle component. In this respect, a generalized shear strength formula has been proposed to incorporate the effects of increasing coarse fraction content on the mass shear strength of heterogeneous soils.
- (g) Based on the results of this study and other available relevant studies, a conservative method of calculating the minimum increase in the mass friction angle has been recommended for colluvium and similar deposits when the coarse fraction

content exceeds 25%. The mass friction angle of a particular colluvium layer can be calculated either from the chart given in Figure 7.3 or by adding 4° to the matrix friction angle for every 10% increase in the coarse fraction content.

- (h) It is cautioned that the mass shear strengths determined from the above approach should not be used for stability analysis of cut slopes if persistent weak layers (i.e. clay seams) of unfavourable orientation exist in a colluvium layer or along the boundaries between the layers.
- (i) Usually, more than one layer of colluvium exists in Hong Kong slopes, with each layer having broadly distinctive matrix and coarse fraction properties, related mainly, but not necessarily, to its age and weathering state. For a more realistic slope stability analysis, average properties of each layer of colluvium at a particular site would need to be determined by means of detailed site mapping and other investigation techniques. In calculating a coarse fraction content for each layer, the completely decomposed rock fragments should not be included. The methods of field characterization adopted in Irfan & Tang (1992) can be used for the characterization and quantification of various colluvium properties.
- (j) No field studies were carried out on the corestone-bearing saprolitic soils. However, the applicability of the results of this study to corestone-bearing saprolite is doubtful, particularly beyond a corestone content of about 30% to 35%. This is because of the special soil-mass conditions produced by the weathering process and the presence of relict discontinuities. Even in the saprolite containing the most favourable relict joint orientations for stability, some structure control would still be expected due to generally lower shear strengths present along the relict joints.

9. FURTHER RESEARCH NEEDS

A more comprehensive study might lead to a better assessment of the mass shear strength of colluvium. This study could include the following :

- (a) field studies on a large number of slopes in order to give a better assessment of insitu colluvium properties,
- (b) back analysis of a large number of slopes with more accurate field data so that the effects of various field factors on the mass strength of colluvium can be better determined,

- (c) more systematic laboratory testing, especially on the effects of matrix density and grading, and particle surface roughness, size and shape, and
- (d) use of numerical techniques or approaches other than those adopted in this study.

However, in view of difficulty of characterizing and quantifying various properties, coupled with great inhomogeneity and heterogeneity of the natural colluvium deposits in Hong Kong and the staff resources required for such a detailed project, this is not recommended at this stage.

10. REFERENCES

- ASTM (1990). Standard method for direct shear test of soils under consolidated drained conditions (ASTM D 3080 - 72), 1990 Annual Book of ASTM Standards, Volume 04.08, Soil and Rock; Dimension Stone; Geosynthetics. American Society For Testing and Materials, pp 385-387.
- Barton, N. & Kjaernsli, B. (1981). Shear strength of rockfill. Journal of the Geotechnical Engineering Division, American Society of Civil Engineers, vol. 107, No GT7, pp 873-891.
- Bennett, J.D. (1984). Review of Superficial Deposits and Weathering in Hong Kong. Geotechnical Control Office, Hong Kong, 51 p, (GCO Publication No. 4/84).
- Berry, L. (1957). Superficial deposits of the Hong Kong harbour area. Hong Kong University Engineering Journal, vol. 21, pp 38-50.
- Berry, L. & Ruxton, B.P. (1960). The evolution of Hong Kong Harbour basin. Zeitschrift fur Geomorphologie, vol. 4, no. 2, pp 97-115 (plus 7 plates).
- Brand, E.W. (1985). Predicting the performance of residual soil slopes. (Theme Lecture). Proceeding of the Eleventh International Conference on Soil Mechanics and Foundation Engineering, San Francisco, vol. 5, pp 2541-2578.
- Brand, E.W. & Hudson, R.R. (1982). CHASE - An empirical approach to the design of cut slopes in Hong Kong soils. Proceedings of the Seventh Southeast Asian Geotechnical Conference, Hong Kong, vol. 1, pp 1-16.
- Cooper, A.J. (1986). Mid-levels Area Study, Areas 1 & 8. Geotechnical Control Office, Hong Kong, Mid-levels Report No. MLR 5/86, 159 p, plus 17 drawings, (unpublished).
- Donaghe, R.T. & Torrey, V.H. (1979). Scalping and replacement effects on strength parameters of earth-rock mixtures. Proceedings of the Seventh European Conference on Soil Mechanics and Foundation Engineering, Brighton, England, vol. 2, pp 29-34.

- Geotechnical Control Office (1981a). Mid-levels Study : Case Histories Subject Report, Glenealy, Seymour and Central Areas. Geotechnical Control Office. 265 p plus 54 drawings, (unpublished).
- Geotechnical Control Office (1981b). Mid-levels Study: Soil Properties Subject Report. Geotechnical Control Office, 59 p plus 80 drawings, (unpublished).
- Geotechnical Control Office (1982a). Mid-levels Study: Report on Geology, Hydrology and Soil Properties. Geotechnical Control Office, Hong Kong, 2 vols, 266 p. plus 54 drawings.
- Geotechnical Control Office (1982b). CHASE: Cutslopes in Hong Kong Assessment of Stability by Empiricism, GCO Report No. 5/82, Geotechnical Control Office, 3 volumes plus 7 Appendices, 562 p., (unpublished).
- Geotechnical Control Office (1984). Geotechnical Manual for Slopes. (Second edition). Geotechnical Control Office, Hong Kong, 295 p.
- Hencher, S.R. & Martin, R.P. (1982). The description and classification of weathered rocks in Hong Kong for engineering purposes. Proceedings of the Seventh Southeast Asian Geotechnical Conference, Hong Kong, vol. 1, pp 125-142.
- Hencher, S.R. (1983). Landslide Studies, 1982. Case Study no. 1 Chai Wan Road. Geotechnical Control Office, Hong Kong, Special Project Report No. SPR 2/83, 34 p plus 3 drawings, (unpublished).
- Hencher, S.R., Massey, J.B. & Brand, E.W. (1984). Application of back analysis to some Hong Kong landslides. Proceedings of the Fourth International Symposium on Landslides, Toronto, vol. 1, pp 631-638.
- Holtz, W.G. & Gibbs, H.J. (1956). Triaxial shear tests on pervious gravelly soils. Journal of the Soil Mechanics and Foundations Division, American Society of Civil Engineers, vol. 82, No. SM1, pp 1-22.
- Holtz, W.G. (1960). Discussion to session "Testing Equipment, Techniques, and Errors". Proceedings of the American Society of Civil Engineers Research Conference on Shear Strength of Cohesive Soils, Boulder, Colorado, pp 997-1002.
- Holtz, W.G. & Ellis, W. (1961). Triaxial shear characteristics of clayey gravel soils. Proceedings of the Fifth International Conference of Soil Mechanics and Foundation Engineering, Paris, vol. 1, pp 143-149.
- Hoek, E. & Brown, E.T. (1980). Empirical strength criterion for rock masses. Journal of Geotechnical Engineering, American Society of Civil Engineers, vol. 106, pp 1013-1035.
- Huang, E.Y., Squier, L.R. & Triffo, R.P. (1963). Effect of geometric characteristics of soil-aggregate mixtures. Highway Research Board Record, No. 22, pp 38-47.

- Huntley, S.L. & Randall, P.A. (1981). Recognition of colluvium in Hong Kong. Hong Kong Engineer, vol. 9, No. 12, pp 13-18.
- Irfan, T.Y. and Tang K.Y. (1992). An Engineering Geological Characterization of Colluvium in Hong Kong. Geotechnical Engineering Office, Hong Kong, Technical Note No. TN 4/92, 128 p, (unpublished).
- Irfan, T.Y. & Woods, N.W. (1988). The influence of relict discontinuities on slope stability in saprolitic soils. Proceedings of the Second International Conference on Geomechanics in Tropical Soils, Singapore, vol. 1, pp 267-276.
- Jain, S.P. & Gupta, R.C. (1975). A large shear box for tests on river bed material. Indian Geotechnical Journal, vol. 5, No. 2, pp 98-113.
- Katti, R.K., Kulkarni, S.K., Divshikar, D.G. and Chavan, C.P. (1973). Report on evaluation of shear parameters of spoil material from Hidkal dam project. Indian Institute of Technology, Soil Eng. Rep. 46, 16 p.
- Kenney, T.C. (1967). Slide behaviour and shear resistance of a quick clay determined from a study of the landslide at Selnes, Norway. Proceedings of the Geotechnical Conference, Oslo, vol.1, pp. 57-64.
- Kurata, S. & Fujishita, T. (1960). Research on the engineering properties of sand-clay mixtures. Proceedings of the First Asian Regional Conference on Soil Mechanics and Foundation Engineering, New Delhi, India, vol. 1, pp 1-12.
- Lai, K.W. & Taylor, B.W. (1983). The classification of colluvium in Hong Kong. Proceedings of the Meeting on Geology of Surficial Deposits in Hong Kong, Hong Kong, pp 75-85. (Published as Geological Society of Hong Kong, Bulletin no. 1, edited by W.W.S. Yim, 1984).
- Leroueil, S. & Tavenas, F. (1981). Pitfalls of back-analyses. Proceedings of the Tenth International Conference on Soil Mechanics and Foundation Engineering, Stockholm, vol. 1. pp 185-190.
- Leung, Y.C., Lam, H.F. & Cooper, A.J. (1989). User Manual for GCO Program 'GSLPC'. Geotechnical Control Office, Computer Manual CM 1/89, 88 p, (unpublished).
- Maclean, D.J. & Williams, F.H.P. (1948). Research on soil compaction at the Road Research Laboratory of Great Britain. Proceedings of the Second International Conference of Soil Mechanics and Foundation Engineering, Rotterdam, vol 4, pp 247-256.
- Massey, J.B. & Martin, R.P. (1987). GCO R & D Programme, Special Projects Division 1987/88. Geotechnical Control Office, Administrative Report No. AR 3/87. 63p. (unpublished).
- Miller, E.A. & Sowers, G.F. (1957). The strength characteristics of soil-aggregate mixtures. Highway Research Board Bulletin, No. 183, pp 16-23.

- Morgenstern, N.R. & Price, V.E. (1965). The analysis of the stability of general slip surfaces. Geotechnique, vol. 15, pp 79-93.
- Patwardhan, A.S., Rao, J.S. & Gaidhane, R.B. (1970). Interlocking effects and shearing resistance of boulders and large size particles in a matrix of fines on the basis of large scale direct shear tests. Proceedings of the Second Southeast Asian Conference on Soil Mechanics, Singapore, pp 265-273.
- Rathee, R.K. (1981). Shear strength of granular soils and its prediction by modelling techniques. Journal of the Institution of Engineers, India, vol. 62, No. 22, pp 64-70.
- Rico, A. & Orozco, J.M. (1975). Effect of fines on the mechanical behaviour of granular roadbase materials. Proceedings of the Fifth Panamerican Conference on Soil Mechanics and Foundation Engineering, Buenos Aires, vol. 1, pp 31-41.
- Shakoor, A. & Cook, B.D. (1990). The effect of stone content, size, and shape on the engineering properties of a compacted silty clay. Bulletin of the Association of Engineering Geologists, Vol. XXVII, No. 2, pp 245-253.
- Skempton, A.W. and DeLory, F.A. (1975). Stability of natural slopes in London Clay. Proceedings of the Fourth International Conference on Soil Mechanics and Foundation Engineering, London, vol. 2, pp.378-381.
- SWKP (1975). Slope Stability & Other Safety Investigations Report on Area 29 - Tsz Wan Shan Estate, Scott Wilson Kirkpatrick & Partners, March, 1975.
- SWKP (1976). Slope Stability & Other Safety Investigations Report on Area 29 - Tsz Wan Shan Addendum, Scott Wilson Kirkpatrick & Partners, October 1976.
- SWKP (1979). Tsz Wan Shan Estate Remedial Works to Slopes on Northern Boundary Geotechnical Submission: vol. 2, Scott Wilson Kirkpatrick & Partners.
- SWKP (1980a). Hong Kong Housing Authority Tsz Wan Shan Estate Remedial Works to Slopes on Northern Boundary Geotechnical Submission, vol. 4, Slope 11NE-A/CR10 and C11, Scott Wilson Kirkpatrick & Partners.
- SWKP (1980b). Hong Kong Housing Authority Tsz Wan Shan Estate Remedial Works to Slopes on Northern Boundary Geotechnical Submission, vol. 5, Slope 11NE-A/C9, Parts 1-3, Scott Wilson Kirkpatrick & Partners.
- SWKP (1980c). Hong Kong Housing Authority Tsz Wan Shan Estate Remedial Works to Slopes on Northern Boundary Geotechnical Submission, vol. 6, Slope 11NE-A/C6, Parts 1-3, Scott Wilson Kirkpatrick & Partners.
- SWKP (1980d). Hong Kong Housing Authority Tsz Wan Shan Estate Remedial Works to Slopes on Northern Boundary Geotechnical Submission, vol. 5, Slope 11NE-A/C8, Parts 1-3, Scott Wilson Kirkpatrick & Partners.

- Ting, W.H., Mun, K.P. & Toh, C.T. (1982). Characteristics of a composite residual granite soil. Proceedings of the Seventh Southeast Asian Geotechnical Conference, Hong Kong, vol. 1, pp 879-887.
- Vallejo, L.E. (1979). An explanation for mudflows. Geotechnique, vol. 29, pp 351-354.
- Vallejo, L.E. (1989). An extension of the particulate model of stability analysis for mudflows. Soils and Foundations, Japanese Society of Soil Mechanics and Foundation Engineering, vol. 29, No. 3, pp 1-13.

LIST OF TABLES

| Table No. | | Page No. |
|-----------|---|----------|
| 3.1 | Summary of Previous Experimental Work on Heterogeneous Soils | 57 |
| 4.1 | List of Slope and Material Attributes Described for Each Slope (Applicable to both Weathered Rock and Colluvium) | 58 |
| 4.2 | Summary of Site and Material Characteristics of Colluvium Slopes Included in Back Analyses | 59 |
| 4.3 | A Relative Scale of Strength for Describing Colluvium Matrix | 61 |
| 4.4 | Summary of Slope Data Used in Empirical Analyses of Colluvium Slopes | 62 |
| 5.1 | Summary of Laboratory Testing Programme | 63 |
| 5.2 | Shape Characteristics for 20-28 mm Size Aggregates Used in 300 mm Direct Shear Box Tests | 64 |
| 5.3 | Dimensions of Test Specimens and Maximum Particle Sizes Used in Laboratory Tests | 64 |
| 5.4 | Results of Triaxial Tests on Specimens Containing Steel Ball | 65 |
| 5.5 | Results of Triaxial Tests on Specimens Containing Crushed Rock Aggregates | 66 |
| 5.6 | Shear Strength Parameters Calculated from the Results of Triaxial Tests on Specimens Containing Aggregates | 67 |
| 5.7 | Results of Direct Shear Tests on Specimens Containing Aggregates (300 mm Box) | 67 |
| 5.8 | Results of Direct Shear Tests on Specimens Containing Aggregates (100 mm Box) | 68 |
| 6.1 | Slope and Material Variables Used in Theoretical Slope Model Analyses | 69 |
| 6.2 | Comparison of Factors of Safety for Computer-generated (by the Program INCL) and Manually-drawn Potential Failure Surfaces (at 20% Coarse Fraction Content) | 70 |

| Table No. | | Page No. |
|--------------|--|-------------|
| 7.1 | Critical Coarse Fraction Contents for Rapid Increase in Shear Strength of a Heterogeneous Soil Determined from Various Study Results | 71 |
| 7.2 | Comparison of Factors of Safety for a Theoretical Slope Model in Colluvium in the Mid-levels Area | 72 |

Table 3.1 - Summary of Previous Experimental Work on Heterogeneous Soils

| Reference | Test | Densification Effort | Matrix Material | Coarse Fraction | Remarks |
|--|---------------------------------|---|---|--|---|
| Holtz & Gibbs (1956) | Triaxial (CD) | Same relative density | Sandy fine gravel; $D_{50} = 1.6$ mm; $D_{60}/D_{10} = 5$ | Varying amounts of gravel (4.8 - 76.8 mm); subangular to subrounded | Results of samples having maximum particle size larger than 38 mm are to be ignored because of the sample size effect |
| Miller & Sowers (1957) | Triaxial (UU) | Maximum compaction dry density | Silty sandy clay; $D_{50} = 0.04$ mm; $D_{60}/D_{10} = 133$ | | |
| Kurata & Fujishita (1960) | Direct Shear Test | Same consolidation pressure on loose samples | Clay & Silt, less than 0.05 mm | Sand | |
| Holtz & Ellis (1961) | Triaxial Sealed (UU) | 95 % of standard compaction maximum dry density | Clayey silty sand | Single grade of gravel (4.8 - 76.8 mm); $D_{50} = 30$ mm; subangular to subrounded | The samples were not fully saturated prior to shearing; test results could have been affected by sample size as $D_{sample}/d_{max. particle size} = 3$ |
| Patwardhan et al (1970) | Large Scale Direct Shear Test | Details not given | LI-ML clay | 150 mm size cobbles; subangular | Test details not given |
| Rico & Orozco (1975) | Triaxial (UU) | Dynamic compaction at optimum water content | 1) CL-ML 2) Kaolinite 3) Bentonite | Sandy gravel | |
| Donaghe & Torrey (1979) | Triaxial (CU) | 95 % of standard compaction maximum dry density | Sand & Clay (plastic fines < 25 %) | Gravel of : 1) 5-19 mm; $D_{50} = 9$ mm; 2) 5-76 mm; $D_{50} = 40$ mm; | |
| Rathee (1981) | Direct Shear Test | Same relative density | Fine to medium sand; $D_{50} = 0.2$ mm; $D_{60}/D_{10} = 2$ | Rounded to subrounded gravel; different sizes (max 50 mm) | No test result on 0% gravel content |
| Ting et al (1982) | Triaxial (CU & CD) | Consolidation | Silt & Clay | Sand | Test specimens prepared from coarse and fine fractions separated from a residual granitic soil |
| Shakoor & Cook (1990) | Triaxial Unconfined Compression | Maximum compaction dry density | Silty clay (CL) | Gravel of : 1) 2 - 4.75 mm 2) 4.75 - 12.5 mm 3) 12.5 - 18.75 mm | |
| Note : D_{50} : The sieve size allowing 50% of the material to pass. | | | | | |

Table 4.1 - List of Slope and Material Attributes Described for Each Slope
(Applicable to both Weathered Rock and Colluvium)

| SLOPE ATTRIBUTES | | | | | |
|--|--|---|--|---|--|
| General | Surface Cover | Landform | Geometry | Hydrology/ Groundwater | Geology |
| Slope No Location Coordinates Inspection date Weather Inspected by Slope Age | Type of Cover (on slope) - Chunam - Stone pitching - Spray concrete - Grass - Shrubs - Trees - Others Type of Cover (above slope) Percentage of Cover Surface Drains - Crest - Berms - Cross-slope | Terrain Type - Side Slope - Hill Crest - Ridge - Footslope - etc. | Plan Shape - Straight - Convex - Concave Slope Height (max.) Gradient (ave.) Length Orientation Toe Width Natural Slope Gradient Retaining Structures Cross-section | Seepage Height (max.) Seepage Height (obs.) Upslope Catchment area Slope Catchment Area Standardized Catchment | No. of Layers Soil Type - Colluvium - Insitu Weathered Rock |
| MATERIAL ATTRIBUTES (for each layer) | | | | INSTABILITY | PREVIOUS STUDIES |
| Layer Properties | Fine Fraction (Matrix) | Coarse Fraction | | | |
| Soil Type - Colluvium - Completely Weathered Rock ¹⁰ - Highly Weathered Rock Thickness of Layer Nature of Boundary Orientation of Boundary Percentage of Coarse Fraction Insitu Weathering ¹¹ | Field Strength - Consistency ¹ - Density Hand Penetrometer Strength ² Colour ³ Grain size ⁴ Particle Size Distribution ⁵ Other geological information (e.g. Discontinuities) (Decomposition state of feldspars) ⁶ (Weathering state of material around corestones) ⁷ | Rock Type Grading and Percentage for - 60-200 mm size - 200-600 mm size - 600-2000 mm size > 2000 mm size Angularity ⁸ Shape ⁹ Nature of surface - Broken - Joint Plane - Smooth Surface Roughness - rough - very rough Rim Thickness Decomposition Grade - core - rim Joint spacing | | Evidence of Instability - Observed - by API Location Date Causes (if known or assessed) (Discontinuity Control) - wholly - partially | Summary of Investigation |
| Notes : | | | | | |
| obs Observed at the time of inspection | | (6) Based on Irfan (1988) Table III | | | |
| () To be described only for insitu weathered rock layer | | (7) See Table 4 in GCO (1988) | | | |
| (1) See Table 4.3 | | (8) See Table 14 in GCO (1988) | | | |
| (2) Two measurements at 0.5 m interval | | (9) See Table 5 Irfan & K Tang (1992) | | | |
| (3) See Table 3 in GCO (1988) | | (10) Mass weathering grade of rock (BSI, 1981) | | | |
| (4) See Table 11 in GCO (1988) | | (11) Mass weathering grade of soil (BSI, 1981) | | | |
| (5) If determined in laboratory | | | | | |

Table 4.2 - Summary of Site and Material Characteristics of Colluvium Slopes Included in Back Analyses (Sheet 1 of 2)

| Location | Shing Mun Catchwater | | | | | | | |
|--|----------------------|---------------------|---------|----------------|-------------|---------------------|------------------|---------------|
| Slope Reference No. | Ch 4050 | Ch 4215 | Ch 4305 | Ch 4415 | Ch 5315 | Ch 5400 | Ch 5845 | Ch 6135 |
| Instability | Yes | Yes | Yes | Yes | No | Yes | Yes(?) | No (?) |
| Chunam on existing slope face | No | Yes | No | No | No | Yes | Yes | Yes |
| Chunam behind present slope face | No | No | No | No | No | No | No | No |
| No. of colluvium layers | 2 | 2 | 1 | 2 | 2 | 4 | 2 | 3 |
| Range of coarse fraction contents in layers (%) | 5 to 15 | 15 to 20 | 25 | 60 | 10 to 20 | 10 to 60 | 40 to 70 | 0 to 80 |
| Range of matrix strengths in layers | Stiff to very stiff | Stiff to very stiff | Stiff | Loose to dense | Stiff/dense | Firm to stiff/dense | Stiff/very dense | Firm to stiff |
| Original cut slope gradient used for back analysis | 70° | 65° | 65° | 65° | 72° | 65° | 65° | 65° |

Table 4.2 - Summary of Site and Material Characteristics of Colluvium Slopes Included in Back Analyses (Sheet 2 of 2)

| Location | Mt. Nicholson Road | Plantation Road | Tsz Wan Shan Estate | | | | Chater Hall |
|--|---------------------|-----------------|---------------------|------------|------------|------------|---------------------|
| Slope Reference | 11SW-D/C340 | 11SW-D/C471 | 11NE-A/C6 | 11NE-A/C8 | 11NE-A/C9 | 11NE-A/C11 | 11SW-A/C36 |
| Instability | Yes | No | No | Yes | Yes | Yes | No |
| Chunam on existing slope face | Yes | Yes | Yes | Yes | Yes | Yes | Yes |
| Chunam behind present slope face | No | No | No | No | No | No | No |
| No. of colluvium layers | 5 | 3 | 1 | 1 | 1 | 2 | 3 to 4 |
| Range of coarse fraction contents in layers (%) | 10 to 80 | 20 to 80 | 60 | 50 | 60 | 0 to 80 | 20 to 80 |
| Range of matrix strengths in layers | Soft to stiff/dense | Soft to firm | Very dense | Very dense | Very dense | Very dense | Loose to very dense |
| Original cut slope gradient used for back analysis | 60° | 55° | 55° | 43° | 43° | 65° | 60° |

Table 4.3 - A Relative Scale of Strength for Describing Colluvium Matrix

| Strength Term | Consistency (Silty, Clayey) | Density (Sandy, Gravelly) |
|---|--------------------------------|------------------------------|
| Low | Soft | Loose |
| Medium | Firm | Medium dense |
| High | Stiff | Dense |
| Very high | Very stiff | Very dense |
| Note : For equivalent quantitative scales of strength in terms of undrained shear strength or SPT N-Values see Table 12 of GCO (1988) | | |

Table 4.4 - Summary of Slope Data Used in Empirical Analyses of Colluvium Slopes

| Location | Before Failure | | After Failure | | Assessed Matrix Strength | Remarks |
|--------------------------------|------------------|--------------------|------------------|--------------------|--------------------------|------------------|
| | Slope Height (m) | Slope Angle (deg.) | Slope Height (m) | Slope Angle (deg.) | | |
| Shing Mun CH4050 | 6.0 | 70 | 7.0 | 53 | Medium | COL 3 Study |
| Shing Mun CH4215 | 7.8 | 65 | 5.5 | 72 | High | COL 3 Study |
| Shing Mun CH4305 | 2.0 | 65 | 2.9 | 44 | Low | COL 3 Study |
| Shing Mun CH4415 | 6.6 | 65 | 11.0 | 48 | High | COL 3 Study |
| Shing Mun CH5315 | 7.0 | 72 | - | - | Medium | COL 3 Study |
| Shing Mun CH5400 | 13.2 | 65 | 13.0 | 54 | Medium | COL 3 Study |
| Shing Mun CH5845 | 6.0 | 65 | 6.8 | 52 | High | COL 3 Study |
| Shing Mun CH6135 | 5.3 | 65 | 7.9 | 41 | Medium | COL 3 Study |
| Mount Nicholson Road | 12.0 | 60 | 14.5 | 52 | Medium | COL 3 Study |
| Plantation Road | 10.0 | 52 | - | - | Low | COL 3 Study |
| Chater Hall CS2 | 12.5 | 57 | - | - | High | COL 3 Study |
| Chater Hall CS3 | 25.5 | 56 | - | - | High | COL 3 Study |
| Chater Hall CS4 | 25.0 | 56 | - | - | Medium | COL 3 Study |
| Fairmont Gardens Section 1-1 | 13.0 | 48 | 15.5 | 37 | High | COL 3 Study |
| Fairmont Gardens Section 2-2 | 14.0 | 51 | 16.0 | 40 | High | COL 3 Study |
| Tse Wan Shan 11NE-A/C6 (CH80) | 15.4 | 57 | - | - | High | COL 3 Study |
| Tse Wan Shan 11NE-A/C6 (CHB96) | 16.2 | 52 | - | - | High | COL 3 Study |
| Tse Wan Shan 11NE-A/C8 | 26.5 | 40 | 25.5 | 41 | High | COL 3 Study |
| Tse Wan Shan 11NE-A/C9 | 26.2 | 43 | - | - | High | COL 3 Study |
| Tse Wan Shan 11NE-A/C11 | 26.0 | 63 | 27.0 | 47 | High | COL 3 Study |
| Slope at rear of Chater Hall | 17.0 | 69 | - | - | - | Mid-Levels Study |
| Panorama | 20.0 | 56 | - | - | - | Mid-Levels Study |
| Realty Gardens | 16.0 | 50 | - | - | - | Mid-Levels Study |
| Slip No.3 | 4.5 | 45 | 2.5 | 37 | - | Mid-Levels Study |
| Slip No.7 | 25.5 | 50 | 20.0 | 45 | - | Mid-Levels Study |
| Slip No. 8 | 11.7 | 46 | 6.6 | 33 | - | Mid-Levels Study |
| Failure 5 | 26.6 | 44 | 19.4 | 40 | - | Mid-Levels Study |
| Failure 4 | 31.5 | 42 | 26 | 41 | - | Mid-Levels Study |
| Failure 1 | 33.6 | 35 | 25.4 | 32 | - | Mid-Levels Study |
| Slope No.57 | 2.8 | 62 | - | - | High | CHASE Study |
| Slope No.82 | 6.0 | 52 | - | - | High | CHASE Study |
| Slope No.82 | 11.7 | 56 | - | - | High | CHASE Study |
| Slope No.83 | 6.5 | 30 | - | - | High | CHASE Study |
| Slope No.89 | 6.0 | 39 | - | - | High | CHASE Study |
| Slope No.89 | 14.8 | 40 | - | - | High | CHASE Study |
| Slope No.91 | 10.5 | 39 | - | - | High | CHASE Study |
| Slope No.100 | 6.0 | 60 | 6.0 | 64 | Very High | CHASE Study |
| Slope No.101 | 9.2 | 56 | - | - | High | CHASE Study |
| Slope No.115 | 6.1 | 70 | - | - | High | CHASE Study |
| Slope No.136 | 20.8 | 43 | - | - | High | CHASE Study |
| Slope No.137 | 14.5 | 43 | 16.4 | 35 | High | CHASE Study |

Table 5.1 - Summary of Laboratory Testing Programme

| Test Series | Test Type | Wetting Process | Matrix Maximum Particle Size (mm) | Matrix Dry Density (Mg/m ³) | Coarse Fraction Type (Size) | Confining Pressure σ_c or σ_a (kPa) | Coarse Fraction by Volume (%) |
|-------------|--|-------------------------|--------------------------------------|--|-----------------------------|--|----------------------------------|
| CU-BB | Multi-stage CU triaxial tests (100 mm diameter) | Back pressure saturated | 2 | 1.7 1.6 | Steel balls (12.7 mm) | 30, 65, 100 | 0, 15, 30, 45 |
| CU-AGG | Multi-stage CU and single stage CU triaxial tests (76 mm diameter) | Back pressure saturated | 1.18 | 1.35 | Aggregates (5 - 6.3 mm) | 30, 65, 100 | 0, 10, 25, 40 |
| BSB | Direct shear tests (300 mm box) | Soaked for 2-7 days | 2 | 1.6 1.5 | Aggregates (20 - 28 mm) | 30 | 0, 10, 20, 30, 40 |
| NSB | Direct shear tests (100 mm box) | Soaked overnight | 1.18 | 1.35 | Aggregates (5 - 6.3 mm) | 15, 30, 60, 120 | 0, 10, 20, 30, 40 |
| NSB-D | Direct shear tests (100 mm box) | Oven-dried | 1.18 | 1.35 | Aggregates (5 - 6.3 mm) | 15, 30, 60, 120 | 0, 40 |

Table 5.2 - Shape Characteristics for 20-28 mm Size Aggregates
Used in 300 mm Direct Shear Box Tests

| Shape Index | Before Laboratory Testing | After Laboratory Testing |
|---|---------------------------------|--------------------------------|
| Elongation Index (%) | 16 | 6 |
| Flakiness Index (%) | 2 | 1 |
| Note : The shape indices were determined in accordance with BS 812:Section 105.1:1985 and BS 812:Part 1:1975. | | |

Table 5.3 - Dimensions of Test Specimens and Maximum Particle Sizes
Used in Laboratory Tests

| Test Series | Test Type | Minimum Specimen Size D_{min} (mm) | Specimen Width L (mm) | Maximum Particle Size d_{max} (mm) | $\frac{D_{min}}{d_{max}}$ | $\frac{L}{d_{max}}$ |
|-------------|-----------------|--|--------------------------------|--|---------------------------|---------------------|
| CU-BB | Triaxial | 100 | - | 12.7 | 7.9 | - |
| CU-AGG | Triaxial | 76 | - | 6.3 | 12.1 | - |
| BSB | Direct Shear | 148 | 300 | 28 | 5.3 | 11 |
| NSB | Direct Shear | 38.5 | 100 | 6.3 | 6.1 | 15.8 |
| NSB-D | Direct Shear | 38.5 | 100 | 6.3 | 6.1 | 15.8 |

Table 5.4 - Results of Triaxial Tests on Specimens Containing Steel Balls

| Test No. | Steel Ball Content by Volume (%) | Test Stage | Matrix Properties | | | Consolidation Pressure σ_c (kPa) | p' (kPa) | q (kPa) |
|----------|----------------------------------|------------|--------------------------|---|----------------------------------|---|------------|-----------|
| | | | Initial Void Ratio e_i | Initial Dry Density γ_i (Mg/m ³) | Void Ratio Before Shearing e_s | | | |
| CU-BB-1 | 0 | 1 | 0.556 | 1.68 | 0.575 | 30 | 149.8 | 113.4 |
| | | 2 | | | 0.566 | 65 | 279.0 | 200.0 |
| | | 3 | | | 0.559 | 100 | 436.1 | 297.4 |
| CU-BB-2 | 0 | 1 | 0.556 | 1.68 | 0.581 | 65 | 255.2 | 187.1 |
| | | 2 | | | 0.564 | 100 | 397.5 | 277.5 |
| | | 3 | | | 0.558 | 140 | 552.3 | 371.9 |
| CU-BB-3 | 0 | 1 | 0.550 | 1.69 | 0.563 | 100 | 312.4 | 223.6 |
| | | 2 | | | 0.555 | 140 | 522.3 | 355.8 |
| | | 3 | | | 0.550 | 200 | 660.8 | 438.7 |
| CU-BB-4 | 15 (14.7) (14.8) (14.8) | 1 | 0.554 | 1.69 | 0.592 | 30 | 143.9 | 109.0 |
| | | 2 | | | 0.582 | 65 | 300.2 | 214.8 |
| | | 3 | | | 0.577 | 100 | 429.6 | 295.3 |
| CU-BB-5 | 15 (14.8) (14.9) (14.9) | 1 | 0.549 | 1.69 | 0.570 | 65 | 245.6 | 178.3 |
| | | 2 | | | 0.561 | 100 | 449.2 | 302.3 |
| | | 3 | | | 0.557 | 140 | 565.5 | 375.6 |
| CU-BB-6 | 15 (14.7) (14.8) (14.8) | 1 | 0.548 | 1.69 | 0.588 | 100 | 255.8 | 182.0 |
| | | 2 | | | 0.576 | 140 | 422.4 | 295.6 |
| | | 3 | | | 0.569 | 180 | 640.7 | 413.4 |
| CU-BB-7 | 30 (29.6) (29.7) (28.8) | 1 | 0.548 | 1.69 | 0.581 | 30 | 168.1 | 122.3 |
| | | 2 | | | 0.573 | 65 | 304.6 | 213.4 |
| | | 3 | | | 0.568 | 100 | 426.9 | 289.6 |
| CU-BB-8 | 30 (29.3) (29.5) (29.6) | 1 | 0.552 | 1.69 | 0.603 | 65 | 200.9 | 143.4 |
| | | 2 | | | 0.590 | 100 | 387.2 | 263.1 |
| | | 3 | | | 0.584 | 140 | 522.2 | 344.8 |
| CU-BB-9 | 30 (29.9) (30.0) (30.0) | 1 | 0.541 | 1.70 | 0.550 | 100 | 323.0 | 226.5 |
| | | 2 | | | 0.543 | 140 | 518.5 | 346.6 |
| | | 3 | | | 0.539 | 165 | 654.5 | 426.4 |
| CU-BB-10 | 45 (43.9) (44.0) (44.0) | 1 | 0.631 | 1.61 | 0.628 | 30 | 167.3 | 123.4 |
| | | 2 | | | 0.620 | 65 | 385.6 | 266.6 |
| | | 3 | | | 0.615 | 100 | 504.7 | 339.8 |
| CU-BB-11 | 45 (44.1) (44.2) (44.3) | 1 | 0.631 | 1.61 | 0.614 | 65 | 306.0 | 217.3 |
| | | 2 | | | 0.607 | 100 | 474.8 | 324.4 |
| | | 3 | | | 0.603 | 140 | 587.3 | 392.0 |
| CU-BB-12 | 45 (43.5) (43.6) (43.7) | 1 | 0.594 | 1.64 | 0.622 | 100 | 337.1 | 221.2 |
| | | 2 | | | 0.615 | 140 | 466.2 | 297.2 |
| | | 3 | | | 0.610 | 180 | 577.0 | 360.4 |

Note : (14.7) True Volumetric Content of aggregate in test specimen.

Table 5.5 - Results of Triaxial Tests on Specimens Containing Crushed Rock Aggregates

| Test No. | Aggregate Content by Volume (%) | Test Stage | Matrix Properties | | | Consolidation Pressure σ_c (kPa) | p' (kPa) | q (kPa) | Particle Crushing ¹ (%) |
|---|---------------------------------|------------|--------------------------|---|----------------------------------|---|----------|---------|------------------------------------|
| | | | Initial Void Ratio e_i | Initial Dry Density γ_i (Mg/m ³) | Void Ratio Before Shearing e_s | | | | |
| CU-AGG-0%-30 | 0 | 1 | 0.955 | 1.33 | 0.983 | 30 | 48.3 | 28.6 | - |
| | 0 | 2 | - | - | 0.958 | 65 | 64.8 | 35.5 | - |
| | 0 | 3 | - | - | 0.918 | 100 | 89.6 | 49.4 | - |
| CU-AGG-0%-65 | 0 | 1 | 0.953 | 1.33 | 0.944 | 64 | 53.3 | 31.8 | - |
| CU-AGG-0%-100 | 0 | 1 | 0.951 | 1.33 | 0.950 | 100 | 70.8 | 43.7 | - |
| CU-AGG-10%-30 | 10 (9.9) (10.0) (10.1) | 1 | 0.954 | 1.33 | 0.953 | 30 | 54.7 | 30.6 | - |
| | | 2 | 0.954 | - | 0.932 | 65 | 78.8 | 43.3 | - |
| | | 3 | 0.954 | - | 0.899 | 100 | 88.6 | 49.6 | 1.2 |
| CU-AGG-10%-65 | 10 (9.9) | 1 | - | 1.33 | 0.946 | 65 | 61.7 | 37.3 | 0.5 |
| CU-AGG-10%-100 | 10 (10.0) | 1 | - | 1.33 | 0.919 | 100 | 66.1 | 39.9 | 1.5 |
| CU-AGG-25%-30 | 25 (24.5) (24.5) (24.9) | 1 | 0.960 | 1.33 | 0.981 | 30 | 66.8 | 47.1 | - |
| | | 2 | - | - | 0.966 | 65 | 122.9 | 75.8 | - |
| | | 3 | - | - | 0.941 | 100 | 145.3 | 90.5 | 2.5 |
| CU-AGG-25%-65 | 25 (24.8) | 1 | 0.960 | 1.33 | 0.946 | 65 | 117.7 | 72.1 | 1.6 |
| CU-AGG-25%-100 | 25 (24.6) | 1 | 0.960 | 1.33 | 0.970 | 100 | 140.7 | 85.0 | 2.2 |
| CU-AGG-40%-30 | 40 (8.8) (39.1) (39.2) | 1 | 0.969 | 1.32 | 1.025 | 30 | 106.6 | 76.5 | - |
| | | 2 | - | - | 1.003 | 65 | 228.9 | 149.4 | - |
| | | 3 | - | - | 0.988 | 100 | 300.6 | 191.8 | 9.5 |
| CU-AGG-40%-65 | 40 (39.2) | 1 | 0.969 | 1.32 | 0.993 | 65 | 193.9 | 134.9 | 10.8 |
| CU-AGG-40%-100 | 40 (39.2) | 1 | 0.969 | 1.32 | 0.994 | 100 | 218.9 | 149.3 | 5.8 |
| Legend : (9.9) True volumetric percentage of aggregate in soil specimen | | | | | | | | | |
| Note : (1) Particle crushing is defined as: | | | | | | | | | |
| $\frac{\text{Change in weight of (5 - 6.3 mm) size aggregate after test}}{\text{Weight of (5 - 6.3 mm) size aggregate before test}} \times 100\%$ | | | | | | | | | |

Table 5.6 - Shear Strength Parameters Calculated from the Results of Triaxial Tests on Specimens Containing Aggregates

| Aggregate Content by Volume | c' (kPa) | ϕ' (deg) |
|-----------------------------------|---------------|------------------|
| 0% | 0.0 | 37.1 |
| 9.9% | 1.0 | 36.2 |
| 24.6% | 16.0 | 30.6 |
| 39.1% | 9.3 | 40.8 |

Note : $c' - \phi'$ values calculated by the least-squares method.

Table 5.7 - Results of Direct Shear Tests on Specimens Containing
Aggregates (300 mm Box)

| Test No. | Wetting Condition (soaking time) | Aggregate Content by Volume (%) | Consolidation | | Normal Stress σ_{xx} (kPa) | Shear Stress τ_{xy} (kPa) | Particle Crushing (%) |
|----------|-------------------------------------|---|--|--------------------------------|---|--|------------------------------|
| | | | Matrix Dry Density γ_i (Mg/m ³) | Matrix Void Ratio e_i | | | |
| BSB-0% | 2 days | 0 | 1.58 | 0.647 | 36.1 | 50.8 | - |
| BSB-10% | 2 days | 10 (10.1) | 1.62 | 0.604 | 30.9 | 24.8 | 0.5 |
| BSB-20% | 2 days | 20 (19.9) | 1.59 | 0.633 | 33.1 | 41.8 | 2.2 |
| BSB-30% | 2 days | 30 (29.9) | 1.60 | 0.629 | 33.8 | 43.4 | 11.1 |
| BSB-40% | 2 days | 40 (38.8) | 1.52 | 0.710 | 37.8 | 67.5 | 9.2 |
| BSB-0% | 7 days | 0 (0.0) | 1.59 | 0.634 | 35.3 | 41.6 | - |
| BSB-10% | 7 days | 19 (10.0) | 1.61 | 0.619 | 35.9 | 31.5 | - |

Note : (10.1) True volumetric content of aggregate in specimen.

Table 5.8 - Results of Direct Shear Tests on Specimens Containing Aggregates (100 mm Box)

| Test No. | Wetting Condition | Aggregate Content by Volume (%) | Consolidation | | Normal Stress σ_{xx} (kPa) | Shear Stress τ_{xy} (kPa) | Particle Crushing (%) |
|------------|-------------------|---------------------------------|---|-------------------------|-----------------------------------|--------------------------------|-----------------------|
| | | | Matrix Dry Density, γ_1 (Mg/m ³) | Matrix Void Ratio e_1 | | | |
| | | | | | | | |
| NSB-0%-1 | Soaked | 0 | 1.35 | 0.923 | 15.6 | 15.1 | - |
| NSB-0%-2 | Soaked | 0 | 1.40 | 0.859 | 33.3 | 32.2 | - |
| NSB-0%-3 | Soaked | 0 | 1.36 | 0.909 | 64.3 | 54.3 | - |
| NSB-0%-4 | Soaked | 0 | 1.38 | 0.891 | 135.7 | 104.2 | - |
| NSB-10%-1 | Soaked | 10 (10.1) | 1.37 | 0.899 | 15.8 | 22.1 | - |
| NSB-10%-2 | Soaked | 10 (10.2) | 1.38 | 0.887 | 32.5 | 35.3 | - |
| NSB-10%-3 | Soaked | 10 (10.2) | 1.38 | 0.886 | 64.4 | 58.5 | - |
| NSB-10%-4 | Soaked | 10 (10.5) | 1.42 | 0.827 | 130.8 | 124.3 | 3.2 |
| NSB-20%-1 | Soaked | 20 (20.1) | 1.36 | 0.911 | 15.6 | 23.5 | - |
| NSB-20%-2 | Soaked | 20 (20.3) | 1.38 | 0.886 | 32.1 | 46.5 | - |
| NSB-20%-3 | Soaked | 20 (20.3) | 1.37 | 0.892 | 63.9 | 78.0 | - |
| NSB-20%-4 | Soaked | 20 (20.8) | 1.42 | 0.833 | 130.9 | 162.3 | 3.6 |
| NSB-30%-1 | Soaked | 30 (30.0) | 1.35 | 0.926 | 15.8 | 28.0 | - |
| NSB-30%-2 | Soaked | 30 (30.0) | 1.35 | 0.926 | 31.3 | 56.2 | - |
| NSB-30%-3 | Soaked | 30 (30.1) | 1.36 | 0.926 | 63.2 | 80.8 | - |
| NSB-30%-4 | Soaked | 30 (30.5) | 1.38 | 0.926 | 126.6 | 153.4 | 7.8 |
| NSB-40%-1 | Soaked | 40 (41.1) | 1.38 | 0.879 | 15.3 | 31.6 | - |
| NSB-40%-2 | Soaked | 40 (40.9) | 1.37 | 0.894 | 30.6 | 64.9 | - |
| NSB-40%-3 | Soaked | 40 (40.9) | 1.37 | 0.900 | 62.1 | 106.5 | - |
| NSB-40%-4 | Soaked | 40 (41.1) | 1.40 | 0.860 | 124.0 | 190.1 | 12.0 |
| NSB-0%-1D | Dry | 0 | 1.36 | 0.916 | 15.3 | 22.3 | - |
| NSB-0%-2D | Dry | 0 | 1.38 | 0.890 | 30.6 | 37.6 | - |
| NSB-0%-3D | Dry | 0 | 1.36 | 0.908 | 61.7 | 73.4 | - |
| NSB-0%-4D | Dry | 0 | 1.37 | 0.903 | 126.5 | 122.7 | - |
| NSB-40%-1D | Dry | 40 (40.2) | 1.36 | 0.908 | 15.2 | 51.0 | - |
| NSB-40%-2D | Dry | 40 (40.3) | 1.37 | 0.901 | 30.6 | 84.6 | - |
| NSB-40%-3D | Dry | 40 (40.2) | 1.36 | 0.912 | 61.4 | 132.3 | - |
| NSB-40%-4D | Dry | 40 (40.7) | 1.39 | 0.870 | 124.0 | 257.0 | 10.5 |

Note : (10.1) True volumetric content of aggregate in specimens.

Table 6.1 - Slope and Material Variables Used in Theoretical Slope Model Analyses

| Factor | Particle Dimension Height x Length (m x m) | Particle Spacing Ratio ST/SL | Coarse Fraction Content by volume (%) | Matrix Shear Strength | | Slope Height (m) | Unit Weight (kN/m³) |
|--|--|---------------------------------|---|--------------------------|----------------------------|-------------------------|----------------------------|
| | | | | c' (kPa) | φ' (deg.) | | |
| <u>I. Interlocking Mechanism</u> | | | | | | | |
| Volumetric Content of Coarse Particles | 0.8 x 1.6 | 1 | 0, 10, 20, 30, 40, 45, 50, 55 | 5 | 35 | 10 | 18 |
| Shear Strength of Matrix | 0.8 x 1.6 | 1 | 0, 10, 20, 30, 40, 45, 50, 55 | 5 5 10 10 10 | 39 41 35 41 45 | 10 | 18 |
| Spacing between Particles | 0.8 x 1.6 | 2,1.5, 1.33, 0.75, 0.67 | 40 | 5 | 35 | 10 | 18 |
| Size of Particles (shape constant) | 1.6 x 1.6 | 1 | 0, 10, 20, 30, 40, 45, 50 | 5 | 35 | 10 | 18 |
| | 0.8 x 0.8 | 1 | 0, 10, 20, 30, 40, 45, 50 | 5 | 35 | 10 | 18 |
| Height/Length Ratio of Particles (area constant) | 1.6 x 0.8 1.39 x 0.92 1.13 x 1.13 0.92 x 1.39 | 1 | 40 | 5 | 35 | 10 | 18 |
| Length of Particles | 0.8 x 2.4 0.8 x 1.2 0.8 x 0.8 | 1 | 40 | 5 | 35 | 10 | 18 |
| Height of Particles | 1.6 x 1.6 1.2 x 1.6 0.4 x 1.6 | 1 | 40 | 5 | 35 | 10 | 18 |
| Shape of Particles | Circular (1.6) | 1 | 0, 10, 20, 30, 40, 45, 50 | 5 | 35 | 10 | 18 |
| | Square (1.42 x 1.42) | 1 | 30, 40, 45, 50 | 5 | 35 | 10 | 18 |
| | Rectangular (0.8 x 1.6) | 1 | 30, 40, 45, 50 | 5 | 35 | 10 | 18 |
| Slope Height | 0.8 x 1.6 | 1 | 30, 40, 45, 50 | 5 | 35 | 10 | 18 |
| | 0.8 x 1.6 | 1 | 30, 40, 45, 50, 55 | 5 | 35 | 10 | 18 |
| <u>II. Mass Density</u> | | | | | | | |
| Mass Density | | | 10, 20, 30, 40, 50, 60 | 5 | 35 | 10 | - |

Table 6.2 - Comparison of Factors of Safety for Computer-generated (by the Program INCL) and Manually-drawn Potential Failure Surfaces (at 20% Coarse Fraction Content)

| Minimum Factor of Safety | | |
|--|-------------------------------|--------------------------------------|
| Particle Dimensions, Height x Length (m x m) | Hand-drawn failure surface | Program-generated failure surface |
| 0.8 x 1.6 | 0.88 | 0.89 |
| 0.8 x 0.8 | 0.94 | 0.92 |
| 1.6 x 1.6 | 0.91 | 0.94 |

Table 7.1 - Critical Coarse Fraction Contents for Rapid Increase in Shear Strength of a Heterogeneous Soil Determined from Various Study Results

| Source | Critical Coarse Fraction Content C_c (%) by Volume | Rate of Change in $\Delta\phi'$ α (°) |
|---|---|---|
| Theoretical Model (Figure 6.19) | 16 | 0.45 |
| Soil-Aggregate Test - Direct Shear Tests (NSB series) | 0 | 0.45 |
| - Triaxial Tests (CU-AGG series) | 22 | 0.38 |
| Holtz & Gibbs (1956) (Triaxial Tests) | 0 | 0.23 |
| Proposed Relationship (Figure 7.3) | 25 | 0.40 |

Table 7.2 - Comparison of Factors of Safety for a Theoretical Slope Model in Colluvium in the Mid-levels Area

| Coarse Fraction Content by Volume (%) | Source | Mass Shear Strength Parameters | | Slope Height ² | |
|--|---|--------------------------------|------------------------------|---------------------------|-----------------------|
| | | c'_{mass} (kPa) | ϕ'_{mass} (deg.) | 15 m Factor of Safety | 10 m Factor of Safety |
| 50 | Theoretical Model ¹ (Figure 6.18) | - | - | 1.11 | 1.22 |
| | GCO (1981B) | 10 | 41 | 1.08 | 1.23 |
| | Cooper (1986) | 10 | 45 | 1.19 | 1.33 |
| | Proposed Relationship ¹ (Figure 7.3) | 5 | 45 | 0.98 | 1.10 |
| 40 | Theoretical Model ¹ (Figure 6.18) | - | - | 0.94 | 1.05 |
| | GCO (1981b) | 5 | 35 | 0.76 | 0.85 |
| | Cooper (1986) | 5 | 35 | 0.76 | 0.85 |
| | Proposed Relationship ¹ (Figure 7.3) | 5 | 41 | 0.89 | 0.99 |
| 30 | Theoretical Model ¹ (Figure 6.18) | - | - | 0.84 | 0.92 |
| | GCO (1981b) ³ | 5 | 35 | 0.76 | 0.85 |
| | Cooper (1986) ³ | 5 | 35 | 0.76 | 0.85 |
| | Proposed Relationship ¹ (Figure 7.3) | 5 | 37 | 0.80 | 0.90 |
| <p>Notes : (1) Matrix shear strength parameters used are $c' = 5$ kPa and $\phi' = 35^\circ$. (2) Cut slope gradient = 59° and upper slope gradient = 20°, one colluvium layer. (3) The mass shear strength is equal to matrix shear strength below boulder contents of less than 50%.</p> | | | | | |

LIST OF FIGURES

| Figure No. | | Page No. |
|------------|---|----------|
| 3.1 | Selected Normalized Triaxial Test Results Showing the Effects of Gravel Content on Shear Strength of Sandy Soils (after Holtz & Gibbs, 1956) | 79 |
| 3.2 | Triaxial Test Results from Miller & Sowers (1957) Showing the Effects of Sand Content on Shear Strength of Soil-Aggregate Mixtures | 80 |
| 3.3 | Triaxial Test Results Showing the Effects of Gravel Content on Shear Strength of Clayey Soils (after Holtz & Gibbs, 1960) | 81 |
| 3.4 | Results of Large Direct Shear Box Tests Showing Variation of Shear Strength with Cobble Content (after Patwardhan et al, 1970) | 82 |
| 3.5 | Typical Triaxial Test Results from Rico & Orozco (1975) Showing the Effects of Fines on Shear Strength of a Gravelly Road Base | 83 |
| 3.6 | Summary of Normalized Triaxial Test Results Showing the Effects of Gravel Content on Shear Strength of Gravel-Sand-Clay Mixtures (after Donaghe & Torrey, 1979) | 84 |
| 3.7 | Large Direct Shear Test Results from Rathee (1981) Showing the Effects of Gravel Content on Internal Friction Angle | 85 |
| 3.8 | Selected Triaxial Test Results from Shakoor & Cook (1990) Showing the Effects of Coarse Fraction (Gravel) Content on Unconfined Compressive Strength of Soil-Aggregate Mixtures | 86 |
| 3.9 | Direct Shear Test Results from Kurata & Fujishita (1960) Showing the Effects of Clay Content on Shear Strength of Sand-Clay Mixtures | 87 |
| 3.10 | Summary of Selected Previous Test Results Showing the Effects of Coarse Fraction Content on Normalized Shear Strength | 88 |
| 3.11 | Graphical Representation of Shear Strength - Coarse Fraction Content Relationship of Mudflows (After Vallejo, 1989) | 89 |
| 3.12 | 'Minimum' Mass Shear Strength of Bouldery Colluvium Deduced from Back-analyses of Cut Slopes in the Mid-levels Area (GCO, 1981a) | 90 |

| Figure No. | | Page No. |
|------------|---|----------|
| 3.13 | Shear Strength of Colluvium Matrix in the Mid-levels Area (GCO, 1981b) | 91 |
| 4.1 | Location Map of Slopes Studied along the Shing Mun Catchwater | 92 |
| 4.2 | Location Map of Slopes Studied on Hong Kong Island | 93 |
| 4.3 | Location Map of Slopes Studied at Tsz Wan Shan | 94 |
| 4.4 | Back-analysed Average Shear and Normal Stresses along Potential Failure Surfaces, Shing Mun Catchwater Slopes | 95 |
| 4.5 | Back-calculated Least-squares Shear Strength Envelopes for Various Coarse Fraction Contents, Shing Mun Catchwater Slopes | 96 |
| 4.6 | Plot of Back-calculated c' versus ϕ' for Various Coarse Fraction Contents, Shing Mun Catchwater Slopes ($\sigma_n' \leq 50$ kPa) | 97 |
| 4.7 | Variation of Back-calculated Shear Stress at $\sigma_n' = 30$ kPa with Coarse Fraction Content, Shing Mun Catchwater Slopes | 98 |
| 4.8 | Back-analysed Average Shear and Normal Stresses along Potential Failure Surfaces, Tsz Wan Shan Estate Slopes | 99 |
| 4.9 | Back-calculated Least-Squares Shear Strength Envelopes for Various Coarse Fraction Contents, Tsz Wan Shan Estate Slopes | 100 |
| 4.10 | Plot of Back-calculated c' versus ϕ' for Various Coarse Fraction Contents, Tsz Wan Shan Estate Slopes ($\sigma_n' \leq 50$ kPa) | 101 |
| 4.11 | Variation of Back-calculated 'Minimum' Shear Stress at $\sigma_n' = 30$ kPa with Coarse Fraction Content, Tsz Wan Shan Estate Slopes | 102 |
| 4.12 | Back-analysed Average Shear and Normal Stresses along Potential Failure Surfaces, Mid-levels and Peak Slopes | 103 |
| 4.13 | Back-calculated Least-Squares Shear Strength Envelopes for Various Coarse Fraction Contents, Mid-levels and Peak Slopes | 104 |
| 4.14 | Plot of Back-calculated c' versus ϕ' for Various Total Coarse Fraction Contents, Mid-levels and Peak Slopes ($\sigma_n' \leq 50$ kPa) | 105 |

| Figure No. | | Page No. |
|------------|--|----------|
| 4.15 | Variation of Back-calculated 'Minimum' Shear Stress at $\sigma_n' = 30$ kPa with Coarse Fraction Content, Mid-Levels and Peak Slopes | 106 |
| 4.16 | Variation of Back-calculated Shear Stress at $\sigma_n' = 30$ kPa with Boulder Content, Mid-Levels and Peak Slopes | 107 |
| 4.17 | Plot of Back-calculated c' versus ϕ' for Various Coarse Fraction Contents, All Slopes ($\sigma_n' \leq 50$ kPa) | 108 |
| 4.18 | Variation of Back-calculated 'Minimum' Shear Stress at $\sigma_n' = 30$ kPa with Coarse Fraction Content, All Slopes | 109 |
| 4.19 | Variation of Back-calculated Shear Stress at $\sigma_n' = 30$ kPa with Boulder Content, All Slopes | 110 |
| 4.20 | Slope Height versus Slope Angle for Selected Colluvium Slopes in Hong Kong | 111 |
| 4.21 | Slope Height versus Slope Angle for Colluvium Slopes in Hong Kong | 112 |
| 5.1 | Particle Size Distribution of Completely Decomposed Granite Used as Matrix Material in Laboratory Tests | 113 |
| 5.2 | p' - q Plot of Triaxial Test Results on Soil Specimens Containing Steel Balls | 114 |
| 5.3 | Selected Stress Paths of Triaxial Tests Carried Out on Soil Specimens Containing Steel Balls ($\sigma_c' = 30$ kPa) | 115 |
| 5.4 | Selected Stress Paths of Triaxial Tests Carried Out on Soil Specimens Containing Steel Balls ($\sigma_c' = 100$ kPa) | 116 |
| 5.5 | p' - q Plot of Triaxial Test Results on Soil Specimens Containing Aggregates | 117 |
| 5.6 | Results of Triaxial Tests on Soil Specimens Containing Aggregates Showing Variation of Shear Strength with Coarse Fraction Content | 118 |
| 5.7 | Selected Stress Paths of Triaxial Tests Carried Out on Soil Specimens Containing Aggregates ($\sigma_c' = 30$ kPa) | 119 |

| Figure No. | | Page No. |
|------------|--|----------|
| 5.8 | Selected Stress Paths of Triaxial Tests Carried Out on Soil Specimens Containing Aggregates ($\sigma'_c = 65$ kPa) | 120 |
| 5.9 | Selected Stress Paths of Triaxial Tests Carried Out on Soil Specimens Containing Aggregates ($\sigma'_c = 100$ kPa) | 121 |
| 5.10 | Typical Shear Stress versus Horizontal Displacement Curves for Soil Specimens Containing Aggregates, Tested in 300 mm Shear Box | 122 |
| 5.11 | Results of Direct Shear Tests Carried Out on Soil Specimens Containing Aggregates Showing Variation of Shear Strength with Coarse Fraction Content (300 mm Shear Box) | 123 |
| 5.12 | Results of Direct Shear Tests Carried Out on Soil Specimens Containing Aggregates Showing Variation of Shear Strength with Coarse Fraction Content (100 mm Shear Box) | 124 |
| 5.13 | Typical Shear Stress versus Horizontal Displacement Curves for Soil Specimens Containing Aggregates, Tested in 100 mm Direct Shear Box ($\sigma_n = 30$ kPa) | 125 |
| 5.14 | Typical Shear Stress versus Horizontal Displacement Curves for Soil Specimens Containing Aggregates, Tested in 100 mm Direct Shear Box ($\sigma_n = 60$ kPa) | 126 |
| 5.15 | Typical Shear Stress versus Horizontal Displacement Curves for Soil Specimens Containing Aggregates, Tested in 100 mm Direct Shear Box ($\sigma_n = 120$ kPa) | 127 |
| 5.16 | Summary Results of Direct Shear Tests Carried Out on Soil Specimens Containing Aggregates Showing the Effects of Coarse Fraction Content on Normalized Shear Strength (100 mm Shear Box) | 128 |
| 5.17 | Results of Direct Shear Tests Carried Out on Soil Specimens Containing Aggregates Showing the Effects of Moisture Content on Shear Strength | 129 |
| 5.18 | Schematic Summary of Laboratory Test Results Showing Variation of Shear Strength with Coarse Fraction Content | 130 |
| 6.1 | Theoretical Slope Model Adopted to Analyse the Effects of Coarse Fractions on Slope Stability | 131 |

| Figure No. | | Page No. |
|------------|--|----------|
| 6.2 | Locations of Typical Potential Failure Surfaces in the Theoretical Slope Model | 132 |
| 6.3 | Hand-drawn Potential Failure Surfaces in the Theoretical Slope Model with a Coarse Fraction Content of 20% | 133 |
| 6.4 | Results of Theoretical Slope Model Analysis Showing the Effects of Coarse Fraction Content on Factor of Safety | 134 |
| 6.5 | Results of Theoretical Slope Model Analysis Showing the Effects of Matrix Strength and Coarse Fraction Content on Factor of Safety | 135 |
| 6.6 | Results of Theoretical Slope Model Analysis Showing the Effects of Coarse Fraction Content on Normalized Factor of Safety for Different Matrix Strengths | 136 |
| 6.7 | Results of Theoretical Slope Model Analysis Showing the Effects of Particle Spacing and Coarse Fraction Content on Normalized Factor of Safety | 137 |
| 6.8 | Results of Theoretical Slope Model Analysis Showing the Effects of Particle Size (Constant Shape) on Normalized Factor of Safety | 138 |
| 6.9 | Potential Failure Surface with Vertical-to Forward-Inclined Portions in the Theoretical Slope Model | 139 |
| 6.10 | Results of Theoretical Slope Model Analysis Showing the Effects of Particle Elongation Ratio (Constant Area) on Normalized Factor of Safety | 140 |
| 6.11 | Results of Theoretical Slope Model Analysis Showing the Effects of Particle Length on Normalized Factor of Safety | 141 |
| 6.12 | Results of Theoretical Slope Model Analysis Showing the Effects of Particle Height on Normalized Factor of Safety | 142 |
| 6.13 | Summary of Theoretical Slope Model Analysis Showing the Effects of Particle Elongation Ratio on Normalized Factor of Safety | 143 |
| 6.14 | Summary of Theoretical Slope Model Analysis Showing the Effects of Particle Shape (Constant Area) on Normalized Factor of Safety | 144 |
| 6.15 | Summary of Theoretical Slope Model Analysis Showing the Effects of Slope Height on Normalized Factor of Safety | 145 |

| Figure No. | | Page No. |
|------------|---|----------|
| 6.16 | Results of Theoretical Slope Model Analysis Showing Combined Effects of Increasing Coarse Fraction Content and Mass Density on Normalized Factor of Safety | 146 |
| 6.17 | Summary Results of Theoretical Slope Model Analysis Showing the Effects of Coarse Fraction Content on Back-calculated Mass Cohesion and Mass Friction Angle for Different Matrix Strengths | 147 |
| 6.18 | Summary Results of Theoretical Slope Model Analysis Showing the Effects of Coarse Fraction Content Expressed as Increases in Mass Friction Angle | 148 |
| 6.19 | Summary Results of Theoretical Slope Model Analysis Showing the Relationship between Mass Friction Angle, Mass Cohesion and Coarse Fraction Content | 149 |
| 6.20 | Summary Results of Theoretical Slope Model Analysis Showing the Effects of Coarse Fraction and Matrix Strength on Back-calculated Mass Shear Strength | 150 |
| 6.21 | Schematic Diagram Summarizing the Results of Theoretical Slope Model Analysis on the Effects of Coarse Fraction Properties on Normalized Factor of Safety | 151 |
| 7.1 | Schematic Diagram Showing the Results of Laboratory Tests, Back Analysis and Theoretical Slope Model Analysis on the Effects of Coarse Fraction and Matrix Strength on Mass Shear Strength of Colluvium | 152 |
| 7.2 | Comparison of Results of Laboratory Study and Theoretical Slope Model Analysis and the Relationship Between Increase in Mass Shear Strength and Coarse Fraction Content | 153 |
| 7.3 | Summary of the Hong Kong Study and the Recommendation for Mass Strength Increases For Slope Analysis in Colluvium | 154 |

Consolidated Drained Triaxial Tests

Matrix : Sandy Fine Gravel

Coarse Fraction : Gravel

| Symbol | Relative Density (%) | Maximum Particle Size (mm) |
|--------|----------------------|----------------------------|
| △ | 50 | 19.2 |
| □ | 70 | 38.4 |
| × | 70 | 38.4 |

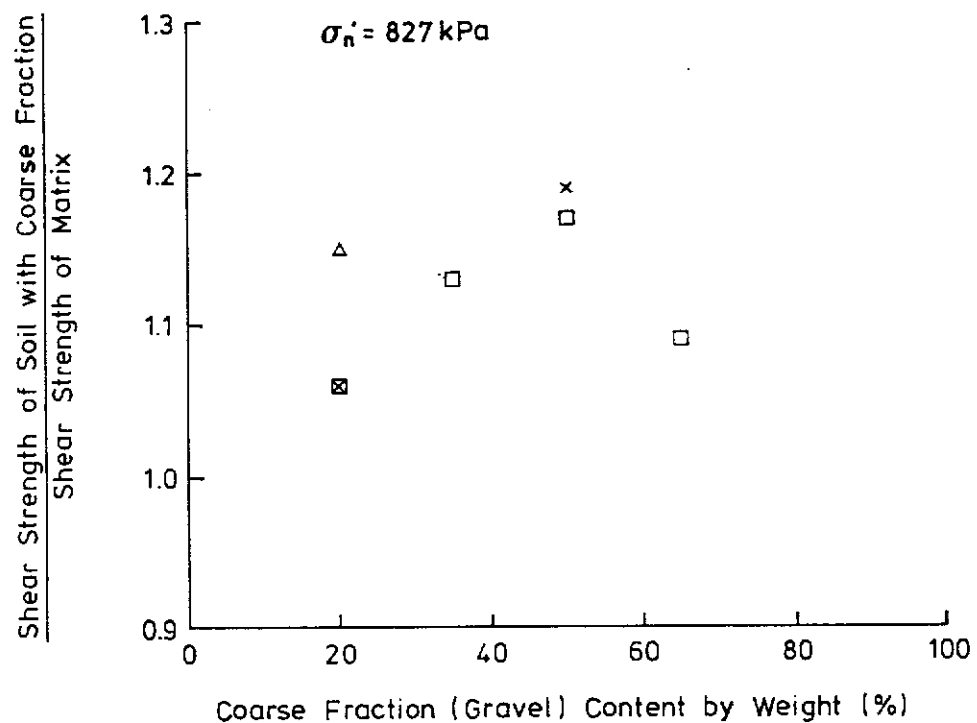


Figure 3.1 - Selected Normalized Triaxial Test Results Showing the Effects of Gravel Content on Shear Strength of Sandy Soils (after Holtz & Gibbs, 1956)

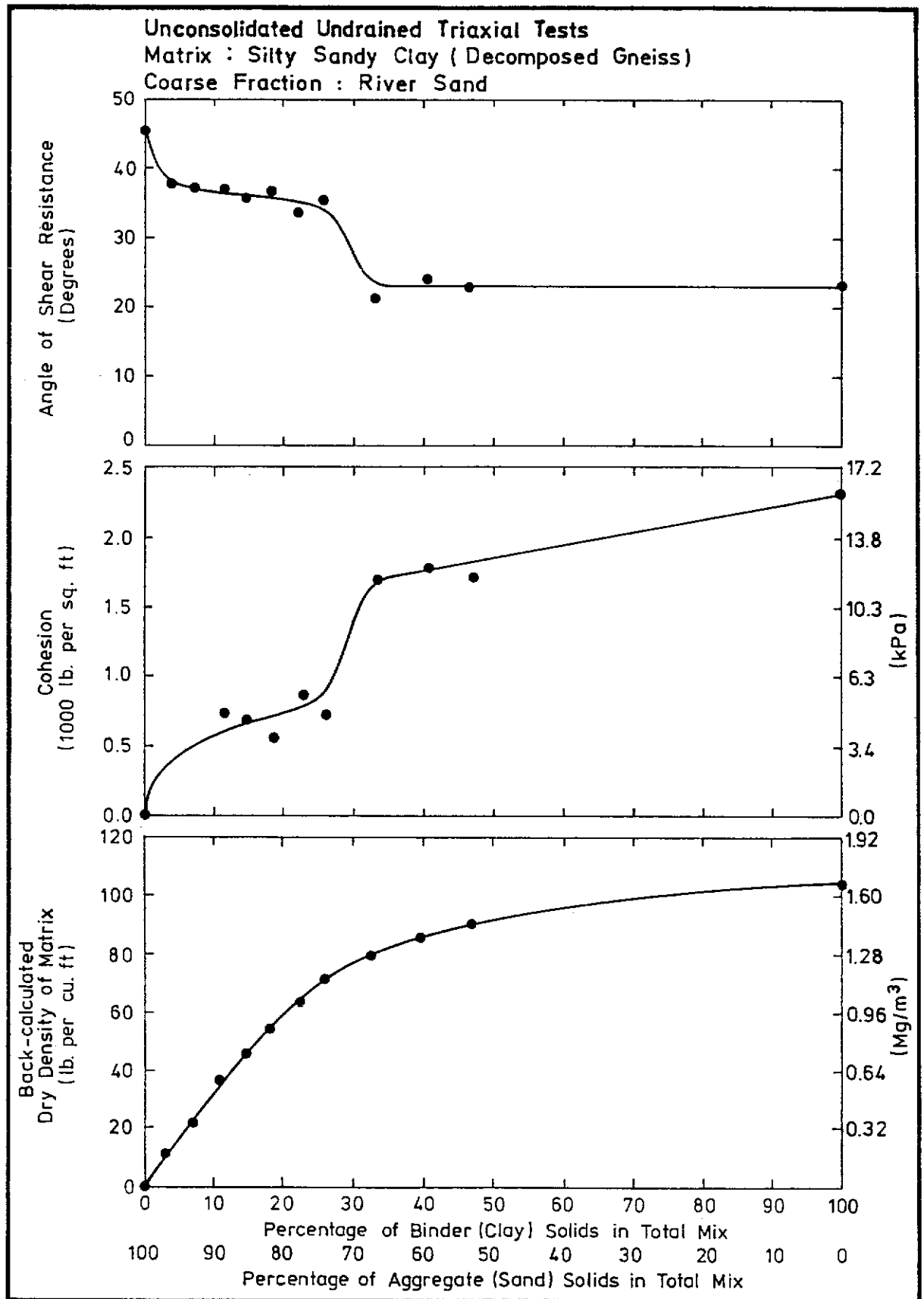


Figure 3.2 - Triaxial Test Results from Miller & Sowers (1957) Showing the Effects of Sand Content on Shear Strength of Soil-Aggregate Mixtures

Unconsolidated Undrained Triaxial Tests

Matrix : Clayey Silty Sand

Coarse Fraction : Gravel

| Shear Strength Envelope | Percentage of Gravel by Weight | ϕ' (deg) | c' (kPa) |
|-------------------------|--------------------------------|---------------|------------|
| ----- | 0 | 24 | 60 |
| - - - - - | 20 | 26 | 48 |
| — · — · — | 35 | 25 | 57 |
| ----- | 50 | 32 | 31 |
| ————— | 65 | 34 | 34 |

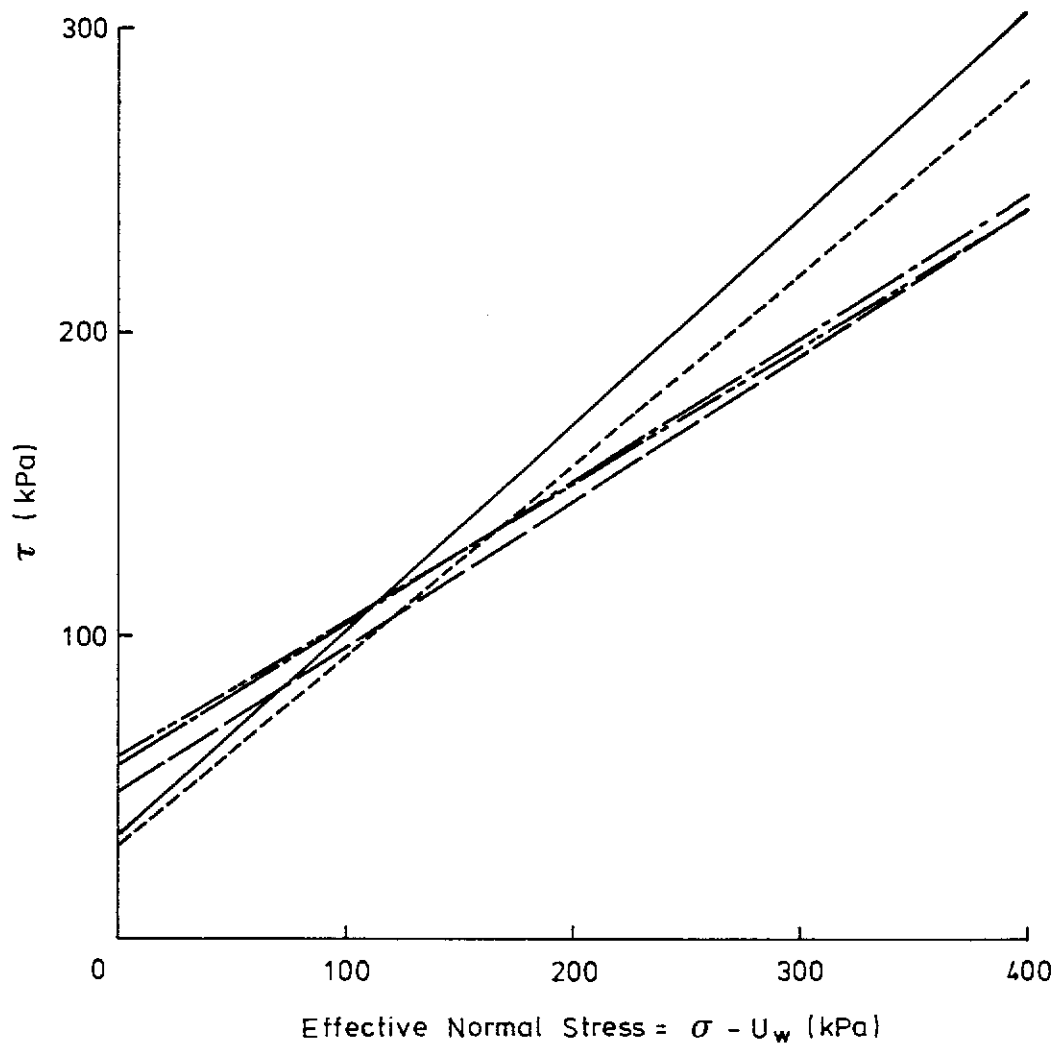


Figure 3.3 - Triaxial Test Results Showing the Effects of Gravel Content on Shear Strength of Clayey Soils (after Holtz & Gibbs, 1960)

Direct Shear Tests (without Normal Load) Using 0.91×0.91m Box
Matrix : Clay
Coarse Fraction : Cobbles (150mm)

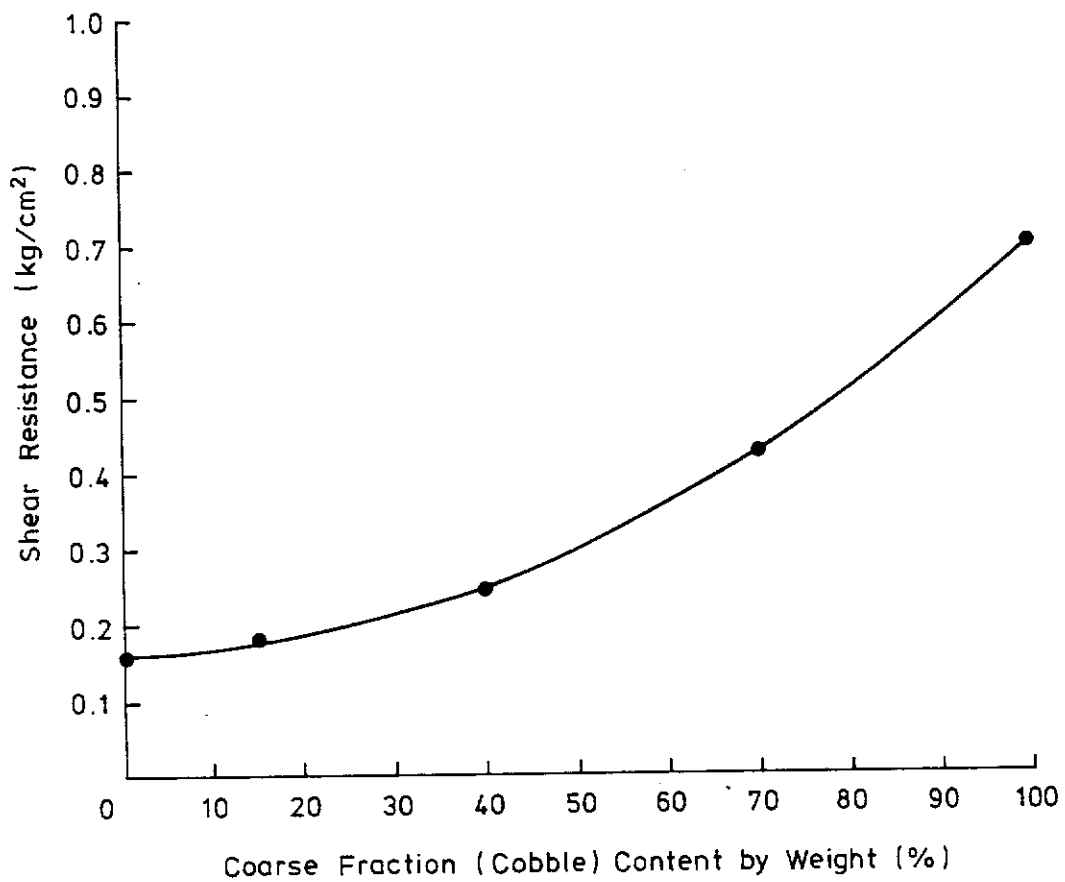
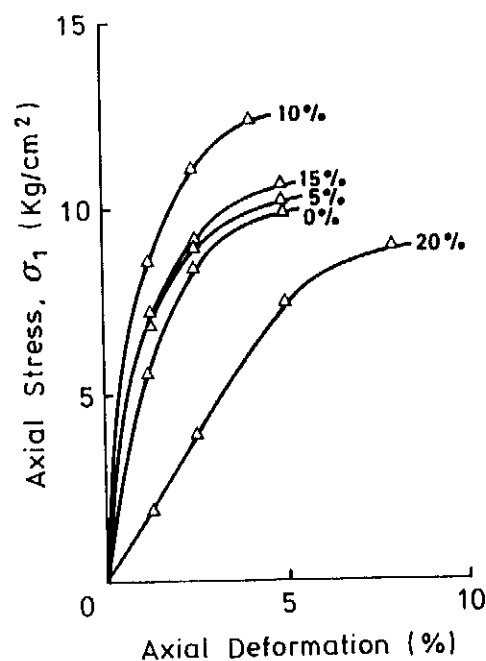


Figure 3.4 - Results of Large Direct Shear Box Tests Showing Variation of Shear Strength with Cobble Content (after Patwardhan et al, 1970)

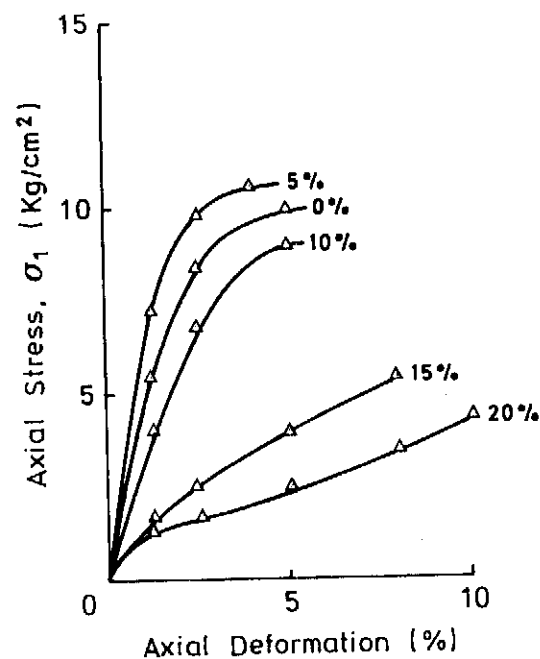
Consolidated Undrained Triaxial Tests
Coarse Fraction : Sandy Gravel (Crushed Aggregate)

Matrix : CL-ML



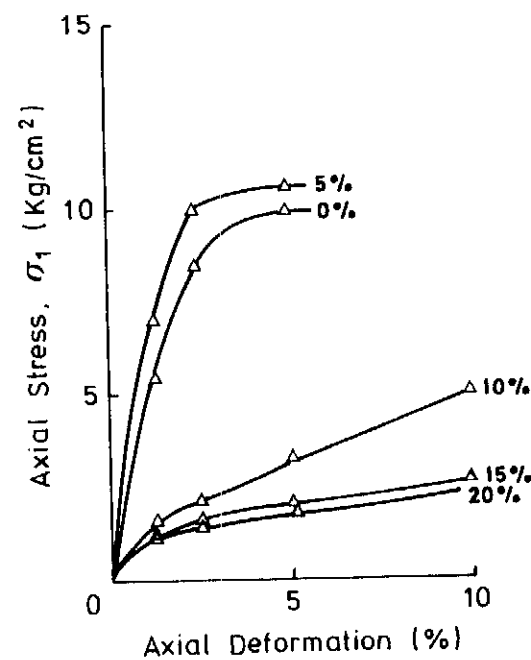
(a) Sandy Gravel and CL-ML

Matrix : Kaolinite



(b) Sandy Gravel and Kaolinite

Matrix : Bentonite



(c) Sandy Gravel and Bentonite

Note : Percentage of fines given in the figures is by weight.

Figure 3.5 - Typical Triaxial Test Results from Rico & Orozco (1975) Showing the Effects of Fines on Shear Strength of a Gravelly Road Base

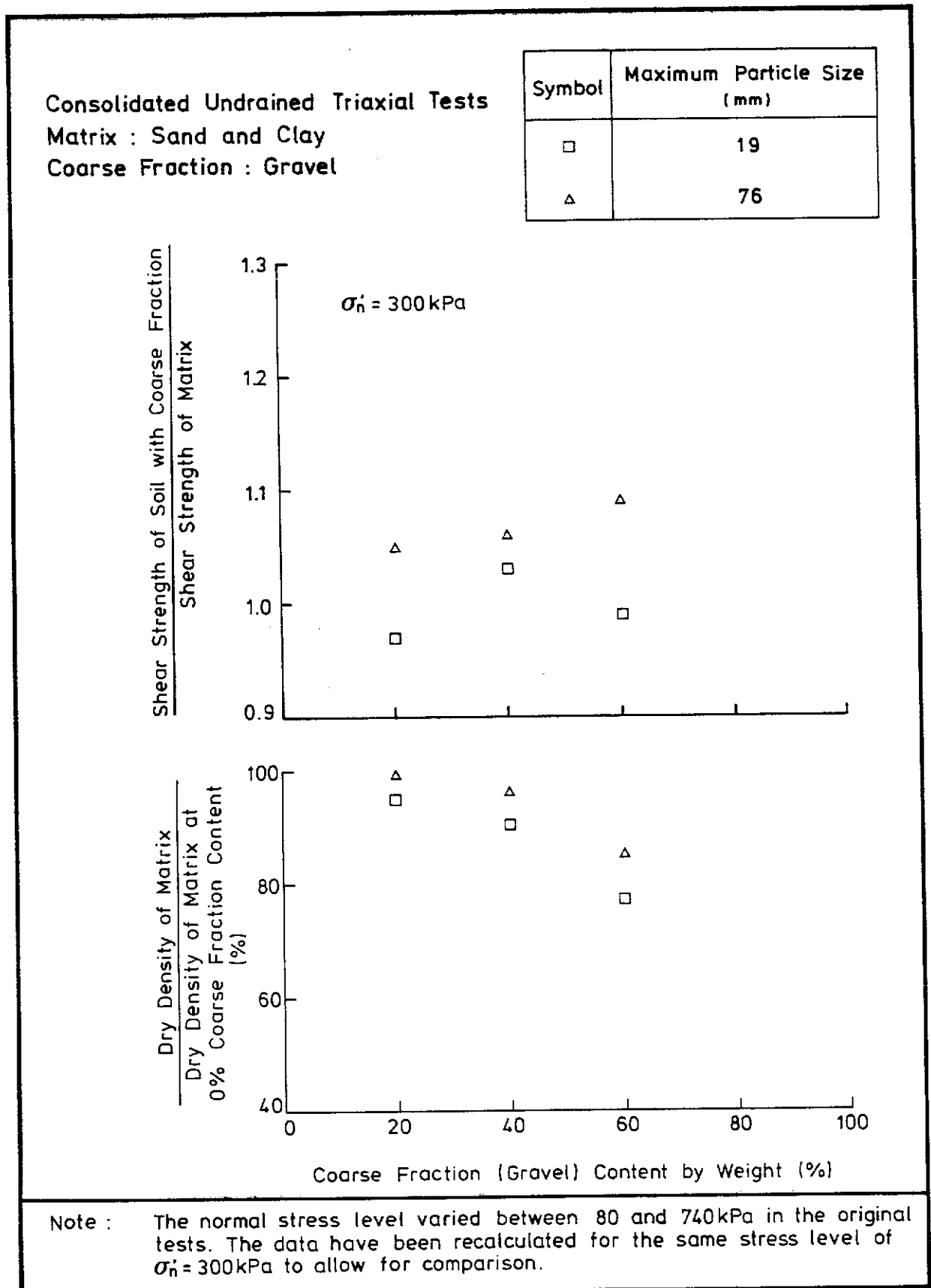


Figure 3.6 - Summary of Normalized Triaxial Test Results Showing the Effects of Gravel Content on Shear Strength of Gravel-Sand-Clay Mixtures (after Donaghe & Torrey, 1979)

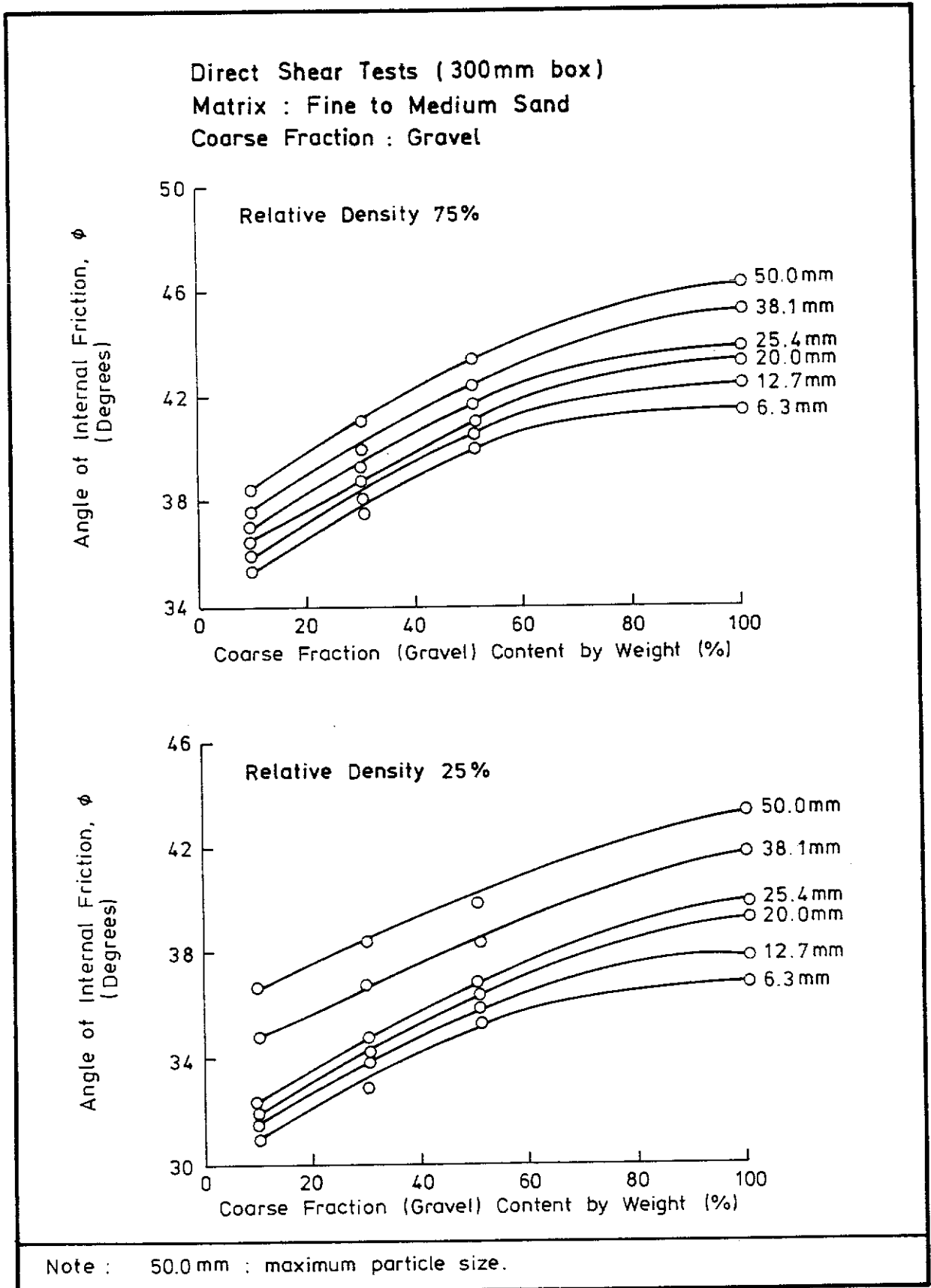


Figure 3.7 - Large Direct Shear Test Results from Rathee (1981) Showing the Effects of Gravel Content on Internal Friction Angle

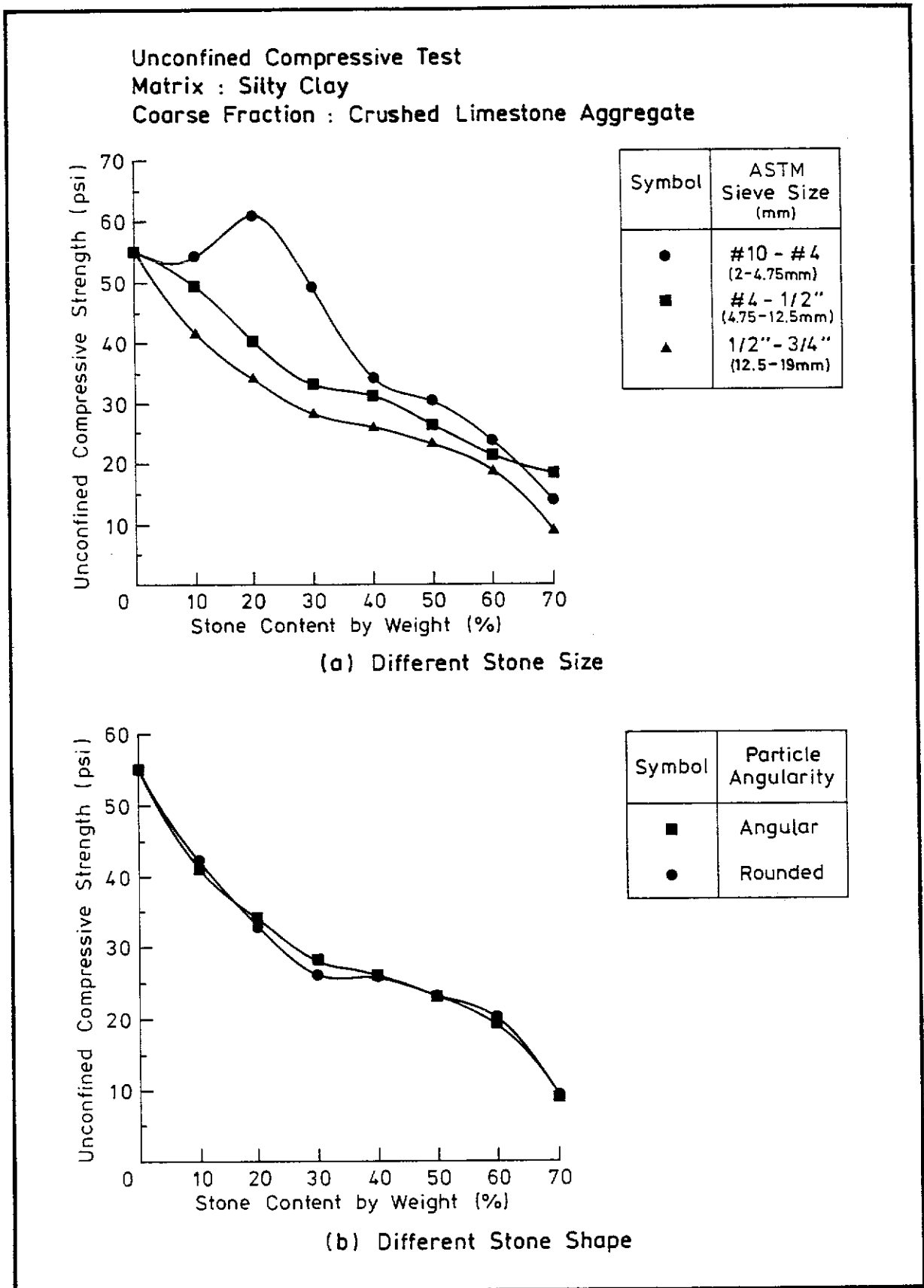


Figure 3.8 - Selected Triaxial Test Results from Shakoor & Cook (1990) Showing the Effects of Coarse Fraction (Gravel) Content on Unconfined Compressive Strength of Soil-Aggregate Mixtures

Direct Shear Test
Matrix : Clay/Silt less than 0.05mm
Coarse Fraction : Sand

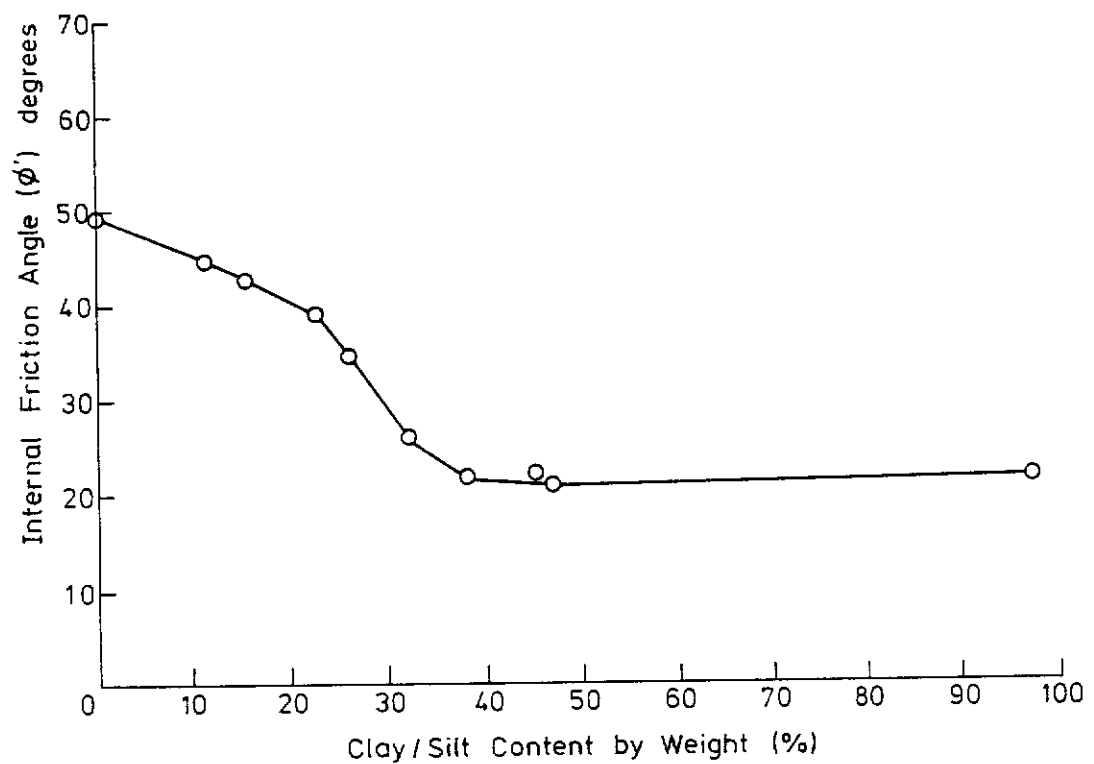


Figure 3.9 - Direct Shear Test Results from Kurata & Fujishita (1960) Showing the Effects of Clay Content on Shear Strength of Sand-Clay Mixtures

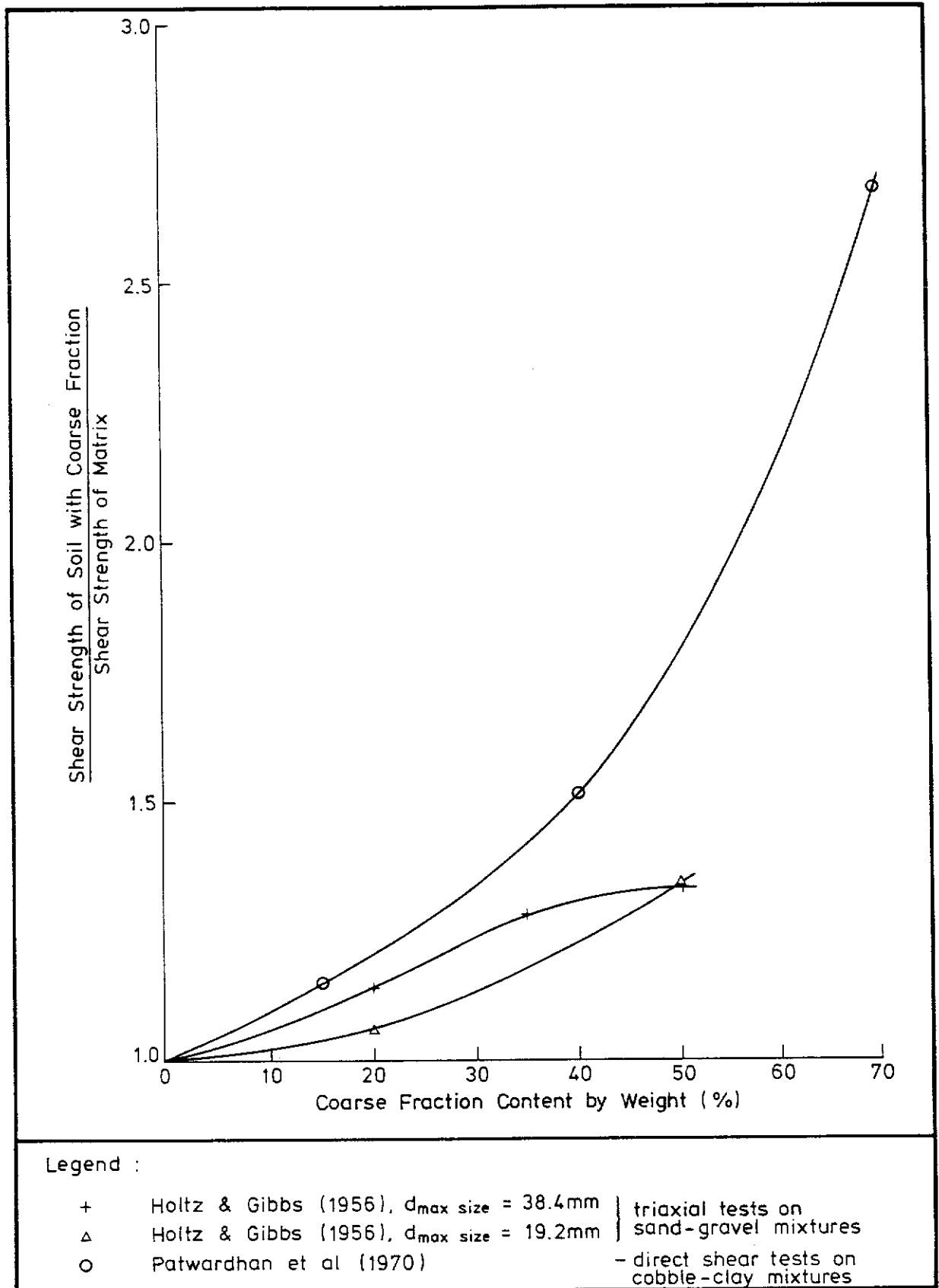


Figure 3.10 - Summary of Selected Previous Test Results Showing the Effects of Coarse Fraction Content on Normalized Shear Strength

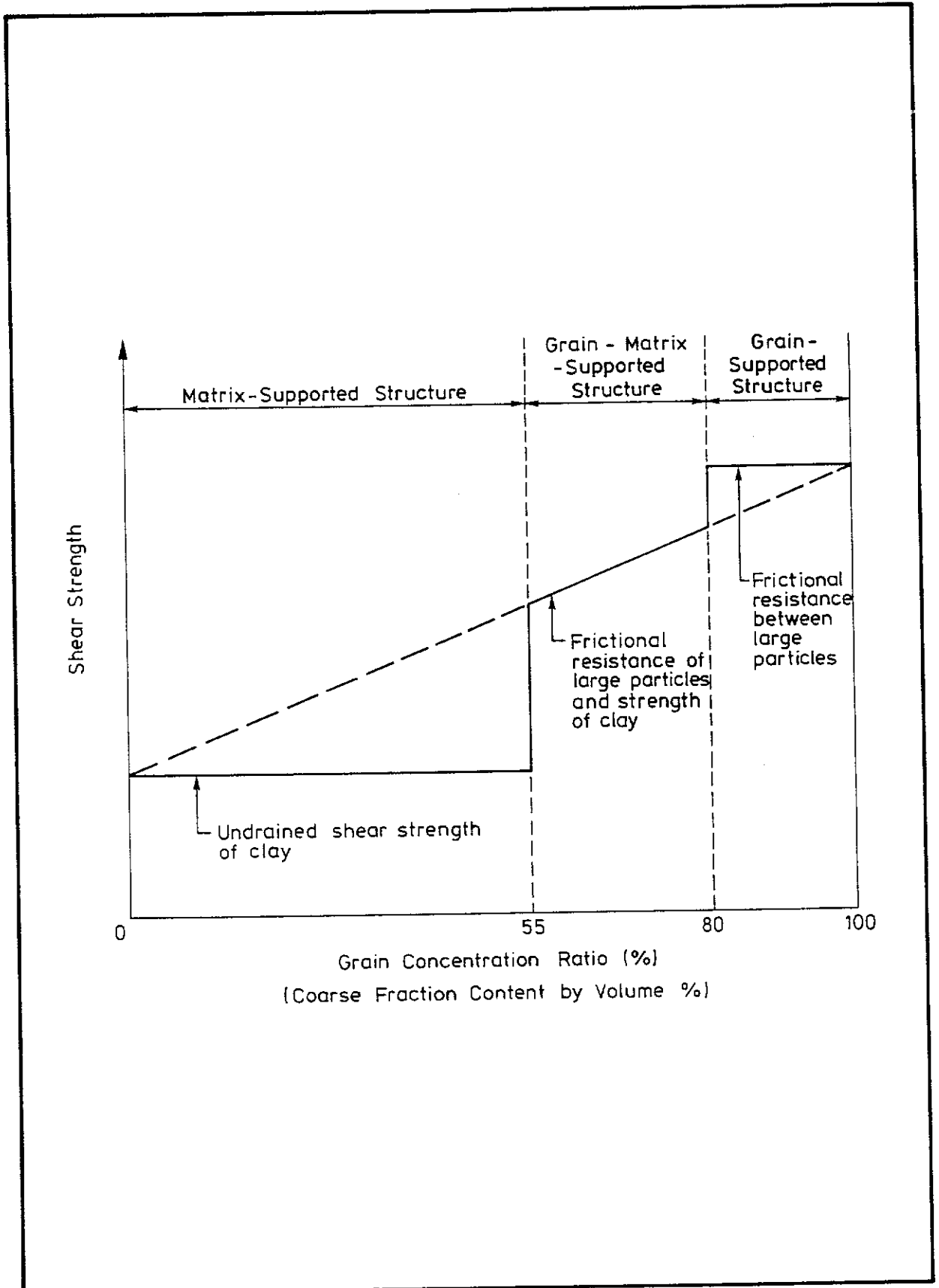


Figure 3.11 - Graphical Representation of Shear Strength - Coarse Fraction Content Relationship of Mudflows (After Vallejo, 1989)

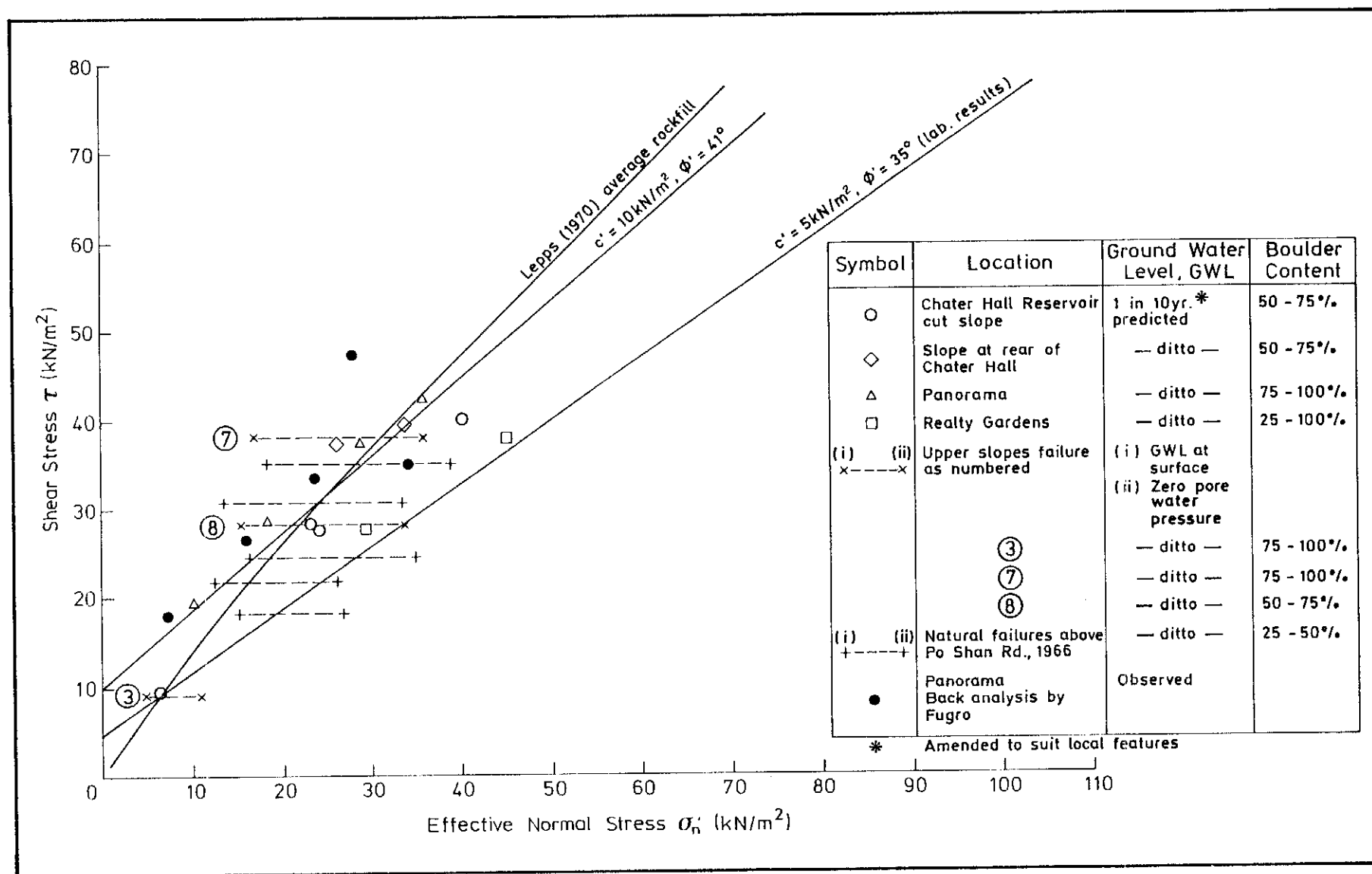


Figure 3.12 - 'Minimum' Mass Shear Strength of Bouldery Colluvium Deduced from Back-analyses of Cut Slopes in the Mid-levels Area (GCO, 1981a)

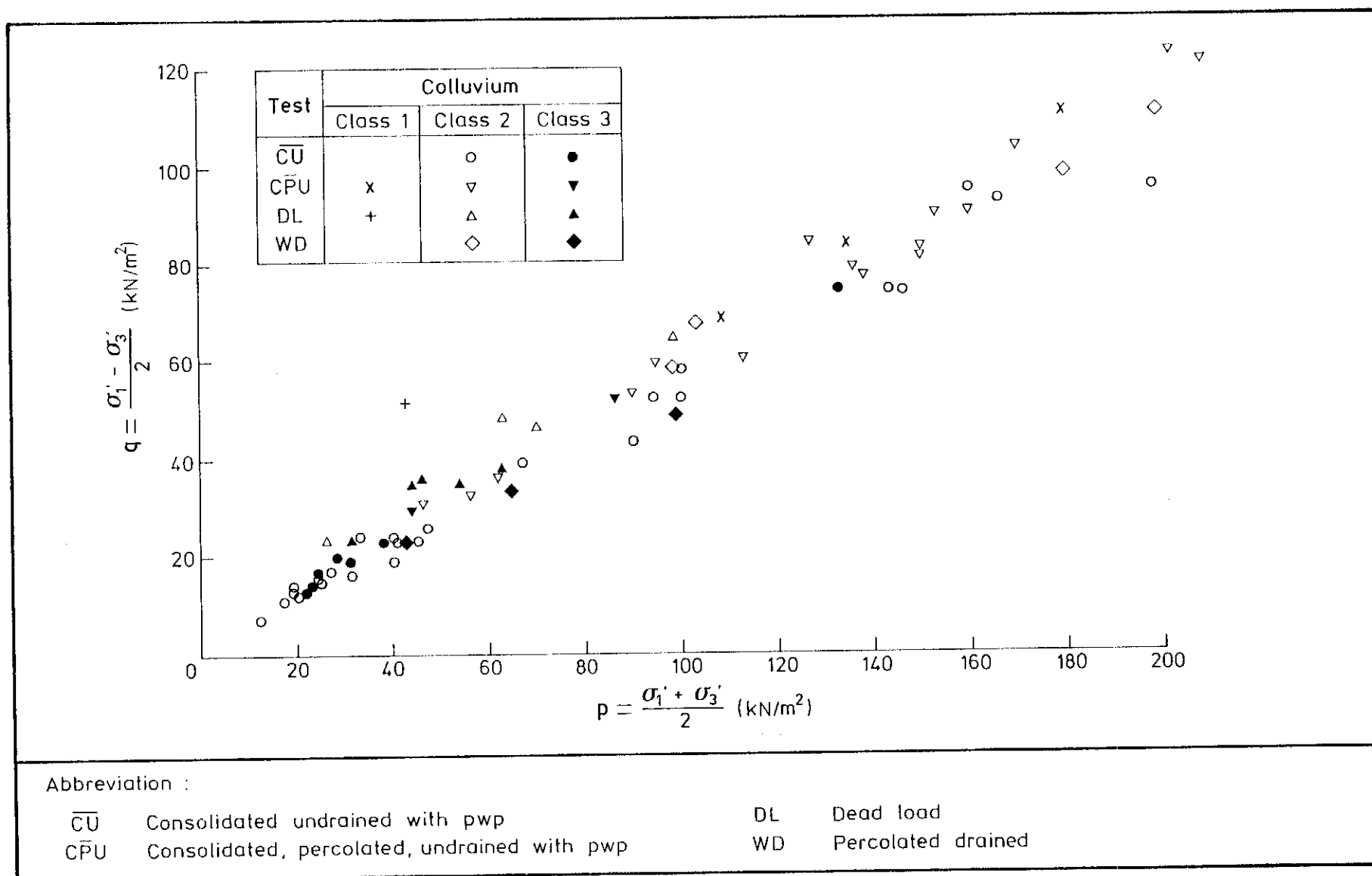


Figure 3.13 - Shear Strength of Colluvium Matrix in the Mid-levels Area (GCO, 1981b)

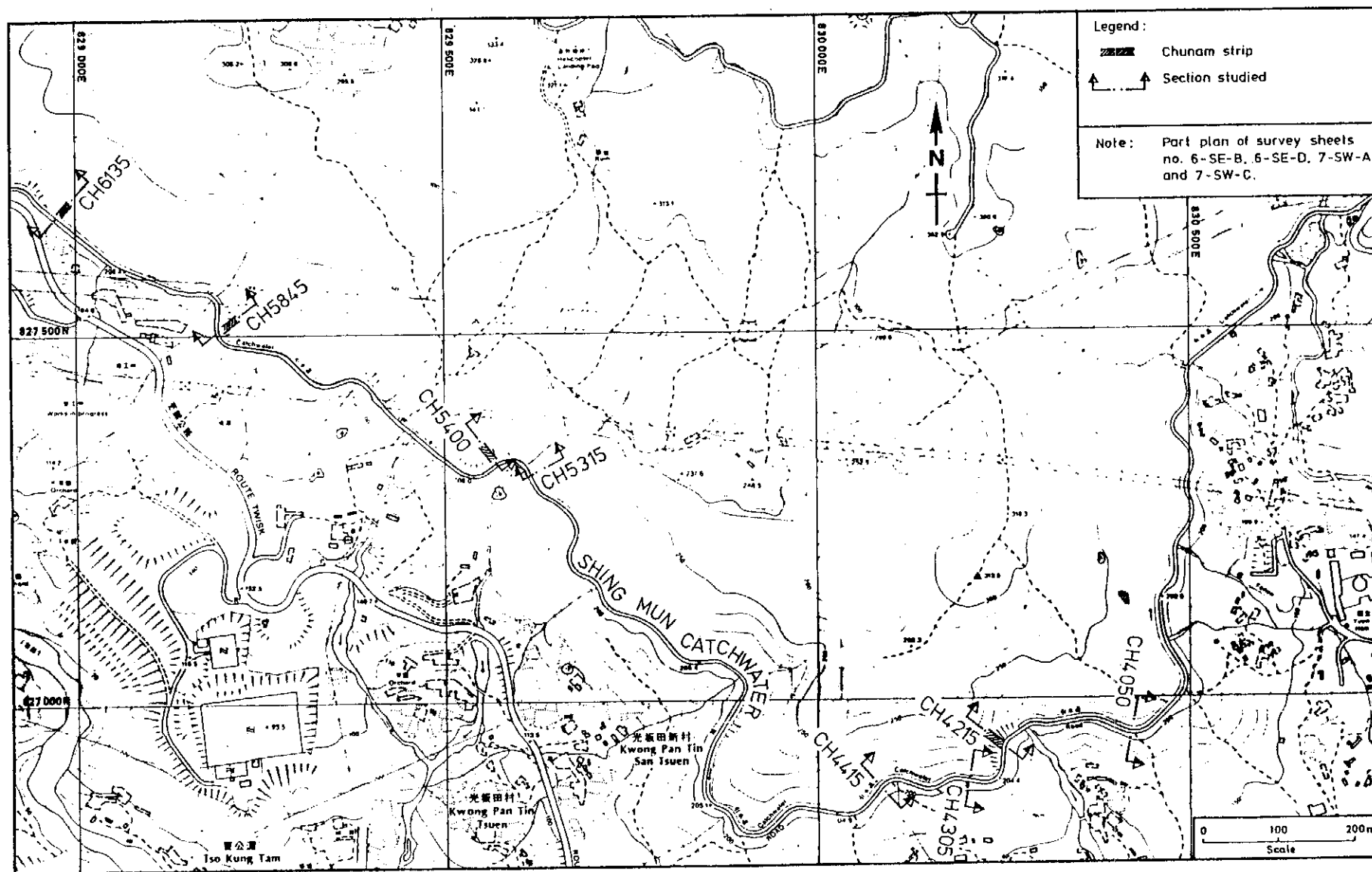


Figure 4.1 - Location Map of Slopes Studied along the Shing Mun Catchwater

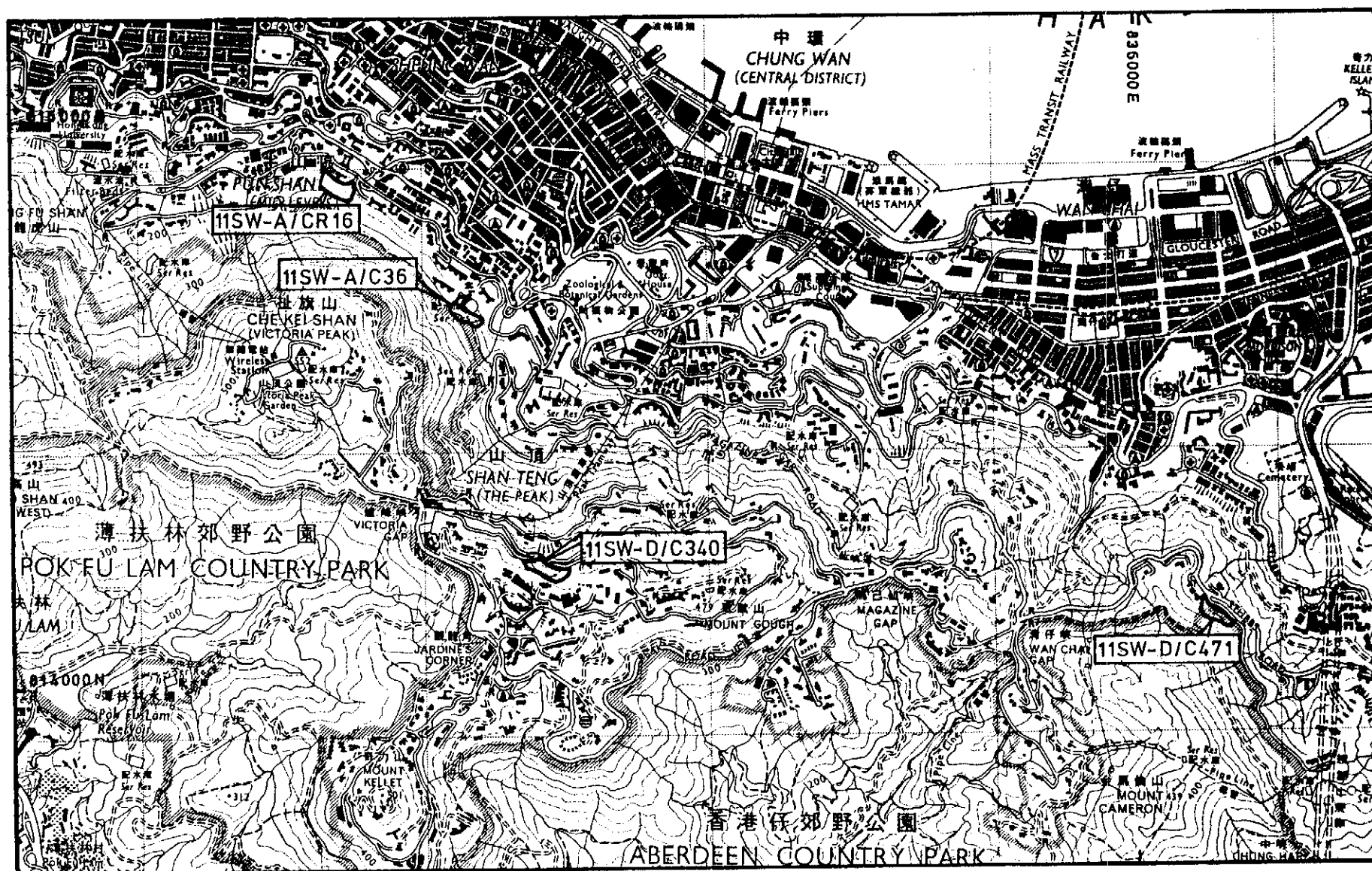


Figure 4.2 - Location Map of Slopes Studied on Hong Kong Island

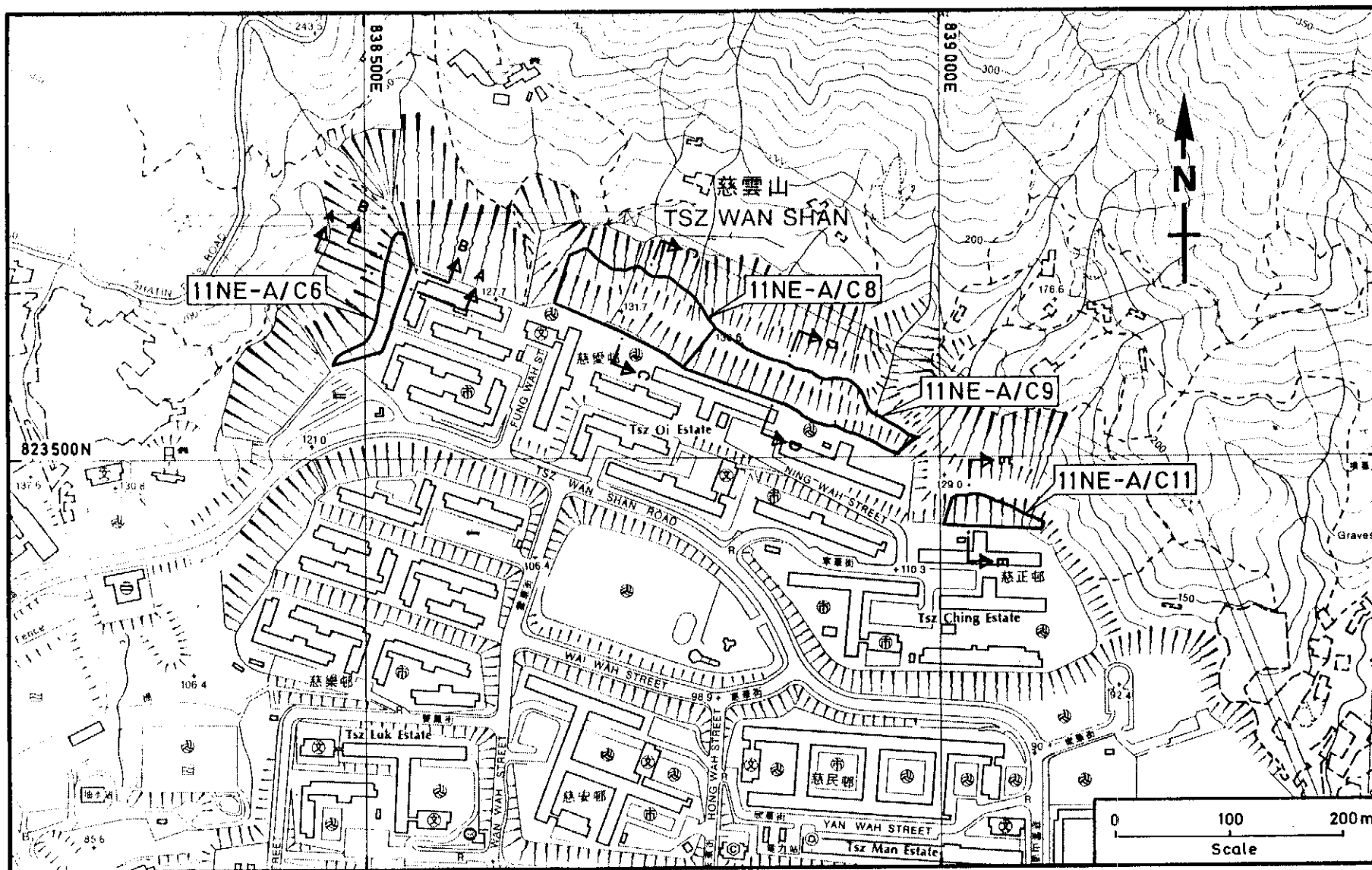


Figure 4.3 - Location Map of Slopes Studied at Tsze Wan Shan

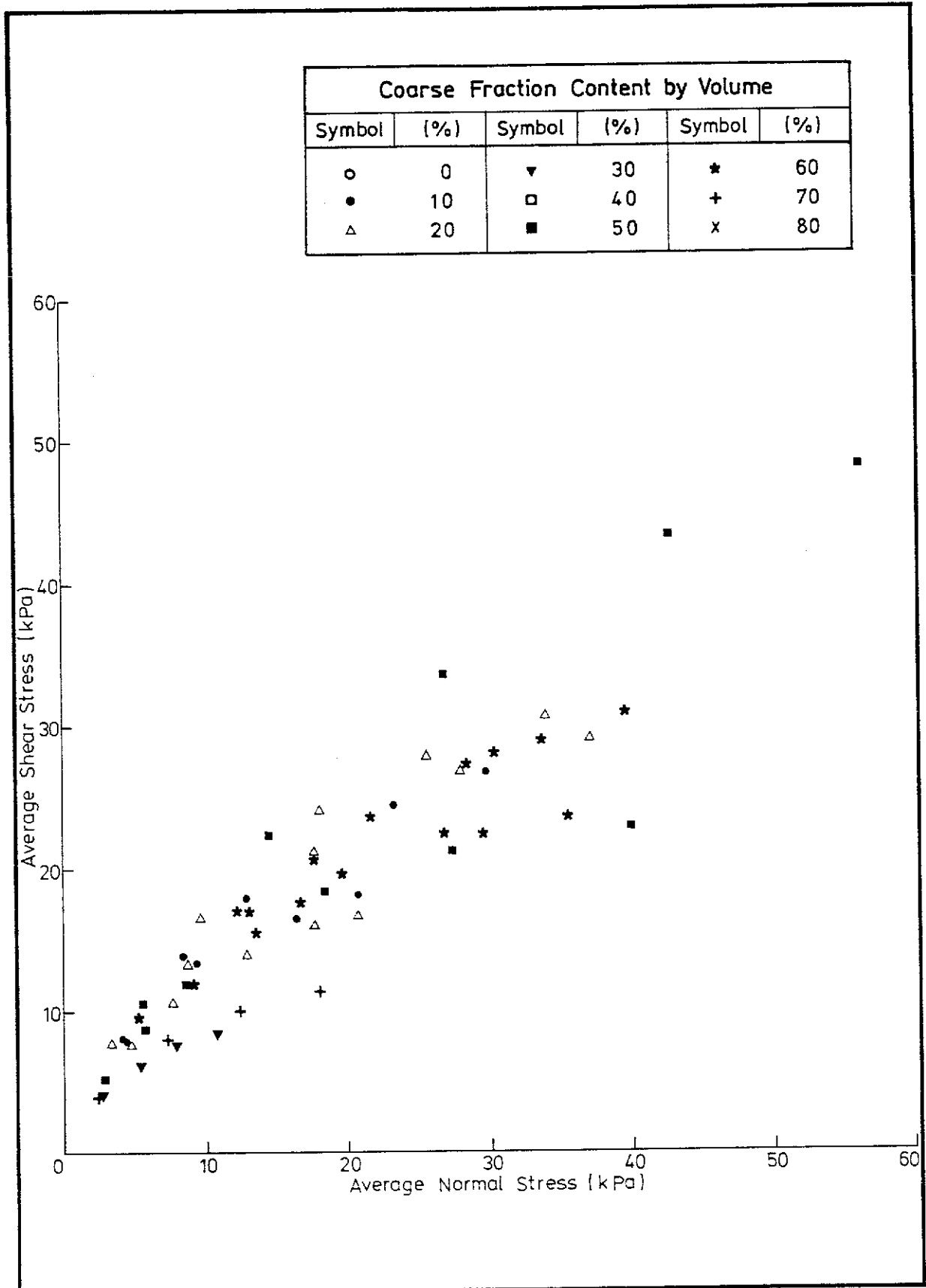


Figure 4.4 - Back-analysed Average Shear and Normal Stresses along Potential Failure Surfaces, Shing Mun Catchwater Slopes

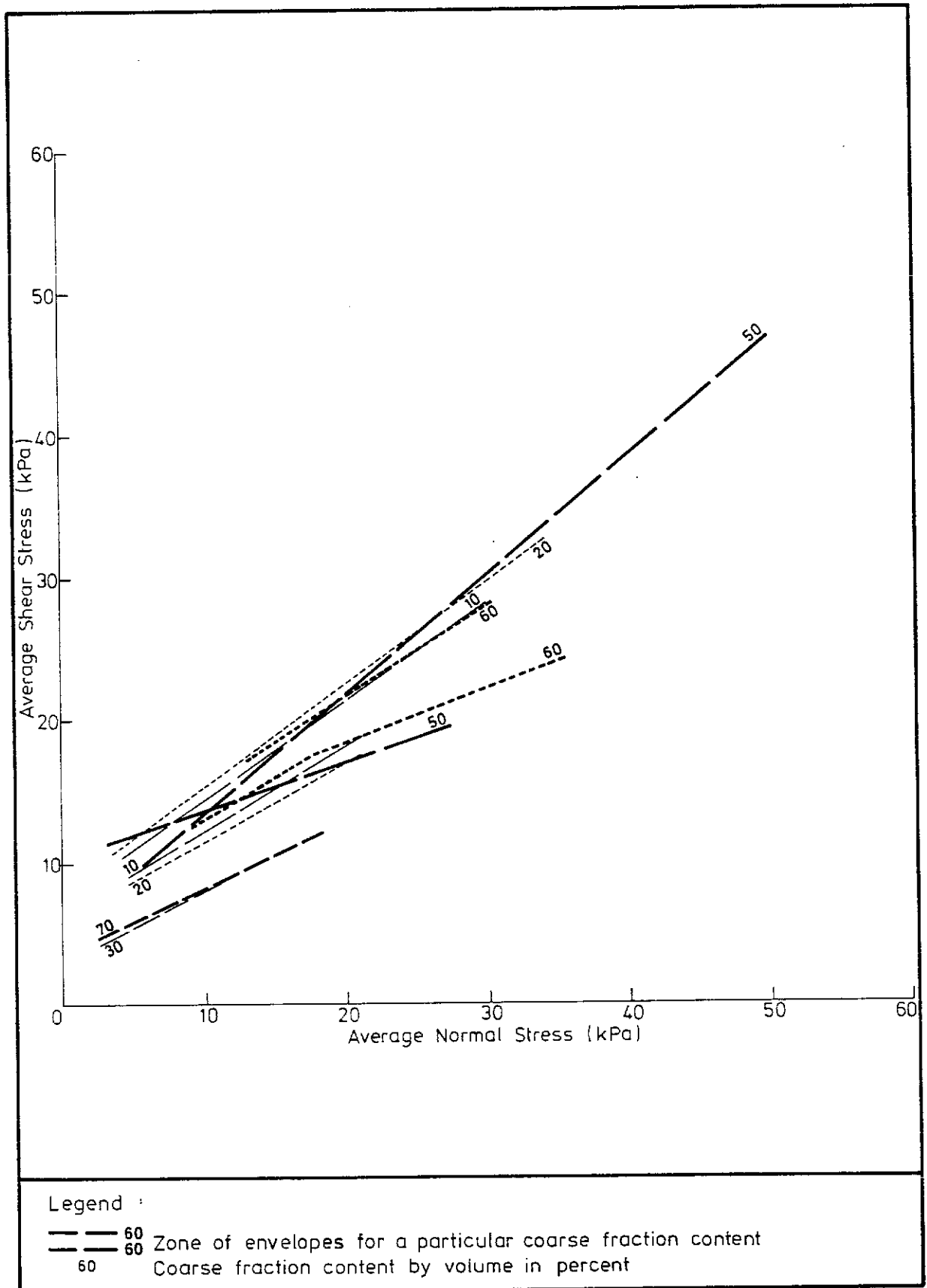


Figure 4.5 - Back-calculated Least-squares Shear Strength Envelopes for Various Coarse Fraction Contents, Shing Mun Catchwater Slopes

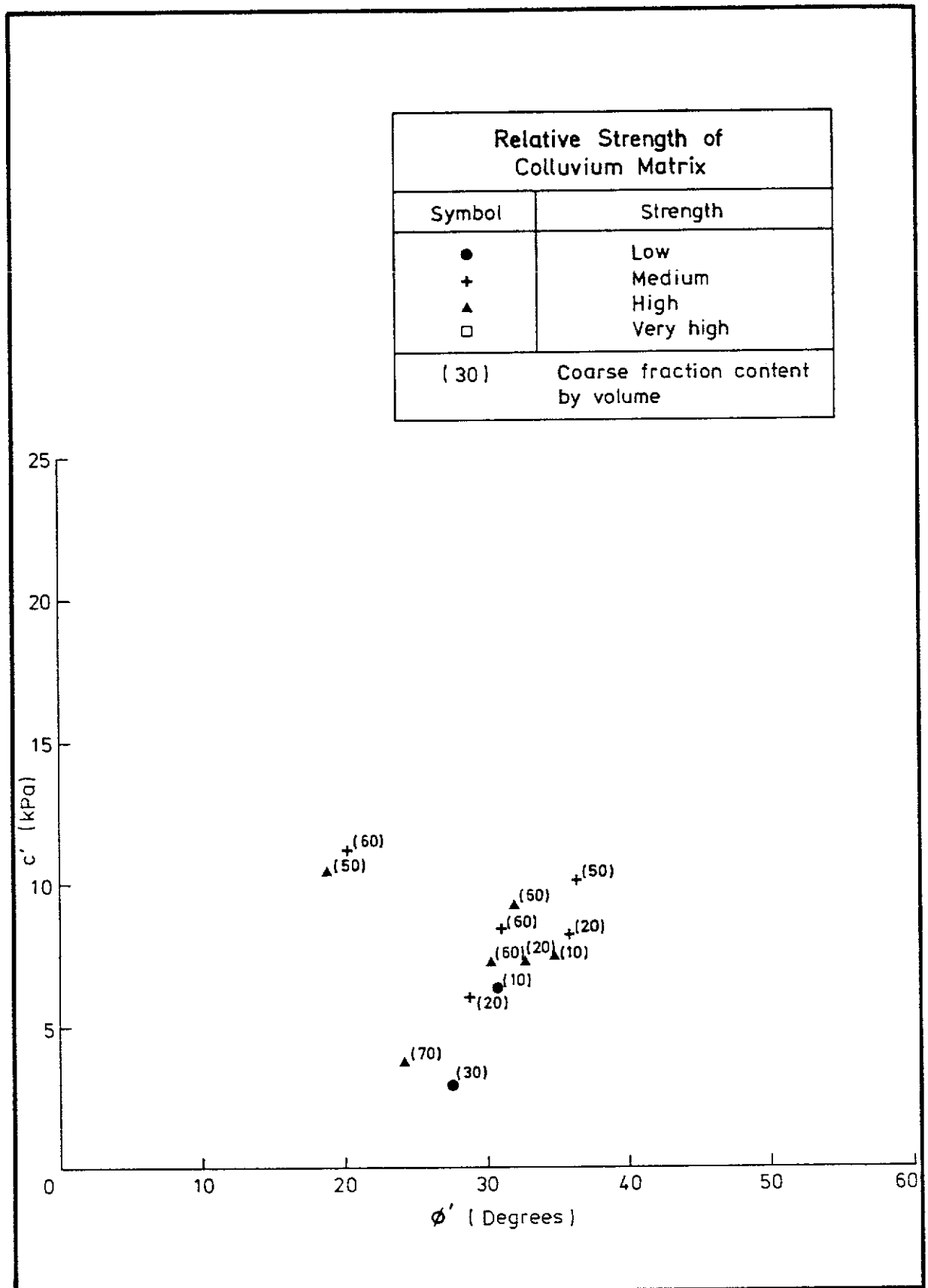


Figure 4.6 - Plot of Back-calculated c' versus ϕ' for Various Coarse Fraction Contents, Shing Mun Catchwater Slopes ($\sigma_n' \leq 50$ kPa)

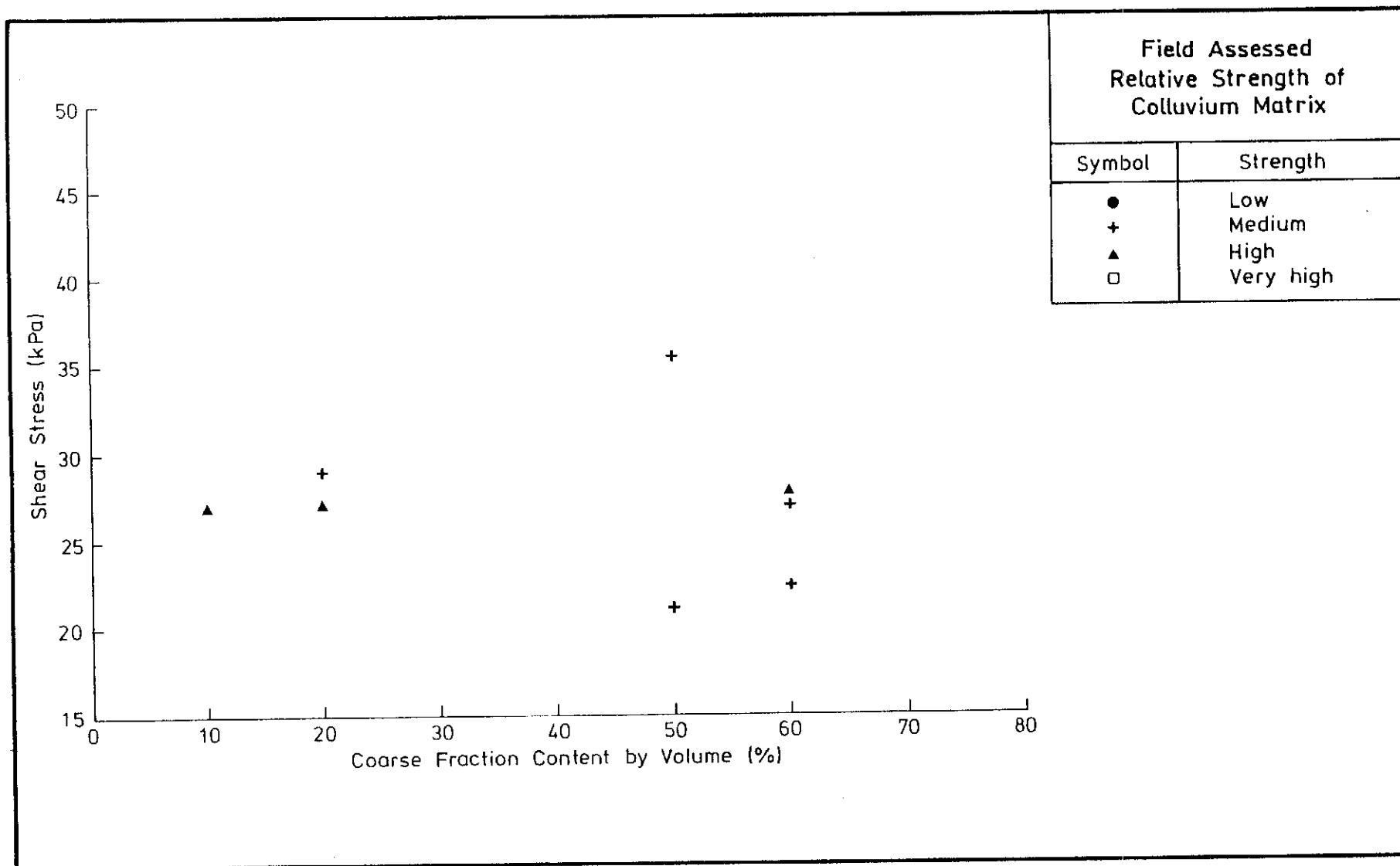


Figure 4.7 - Variation of Back-calculated Shear Stress at $\sigma_n' = 30$ kPa with Coarse Fraction Content, Shing Mun Catchwater Slopes

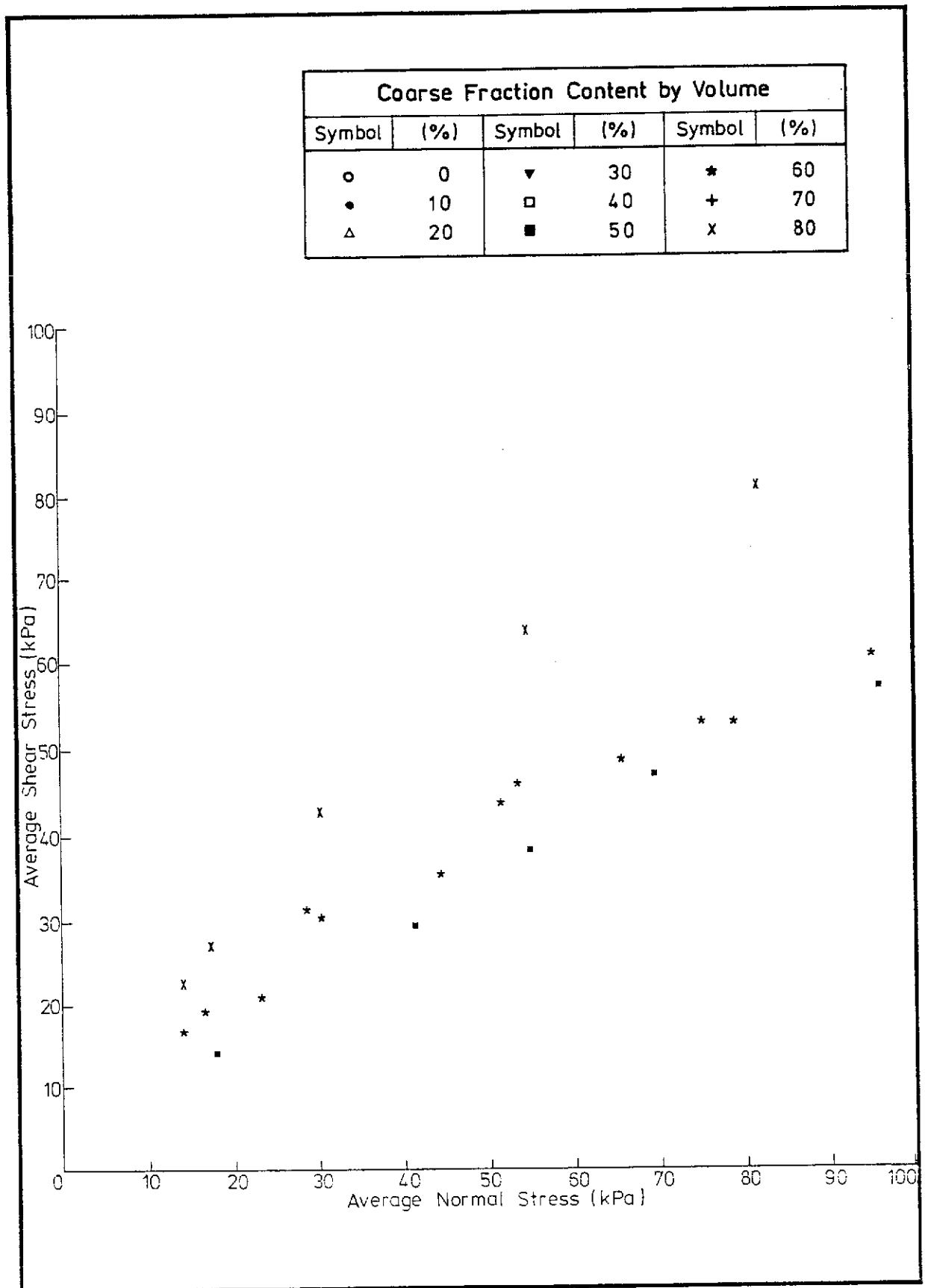


Figure 4.8 - Back-analysed Average Shear and Normal Stresses along Potential Failure Surfaces, Tsz Wan Shan Estate Slopes

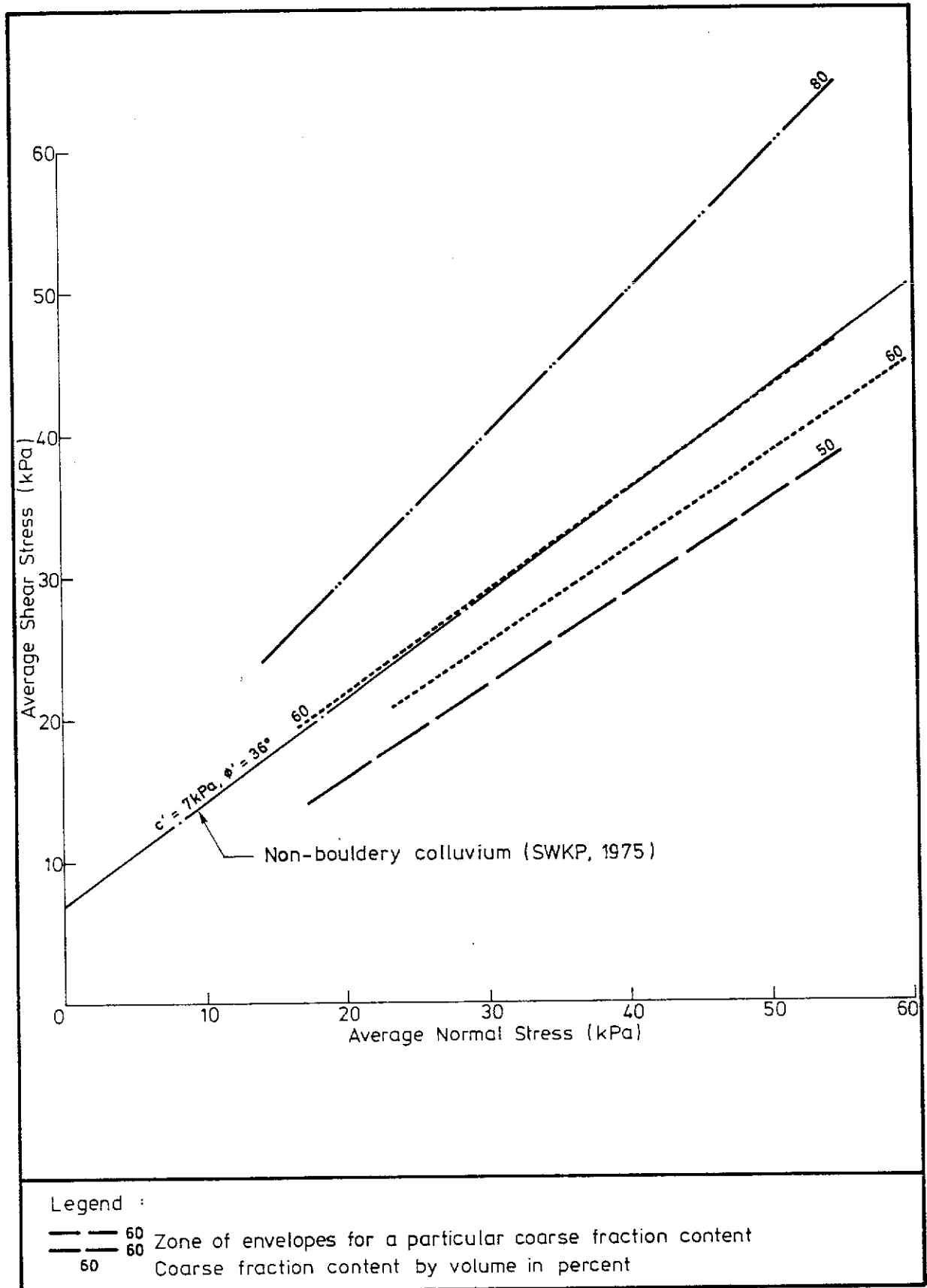


Figure 4.9 - Back-calculated Least-squares Shear Strength Envelopes for Various Coarse Fraction Contents, Tsz Wan Shan Estate Slopes

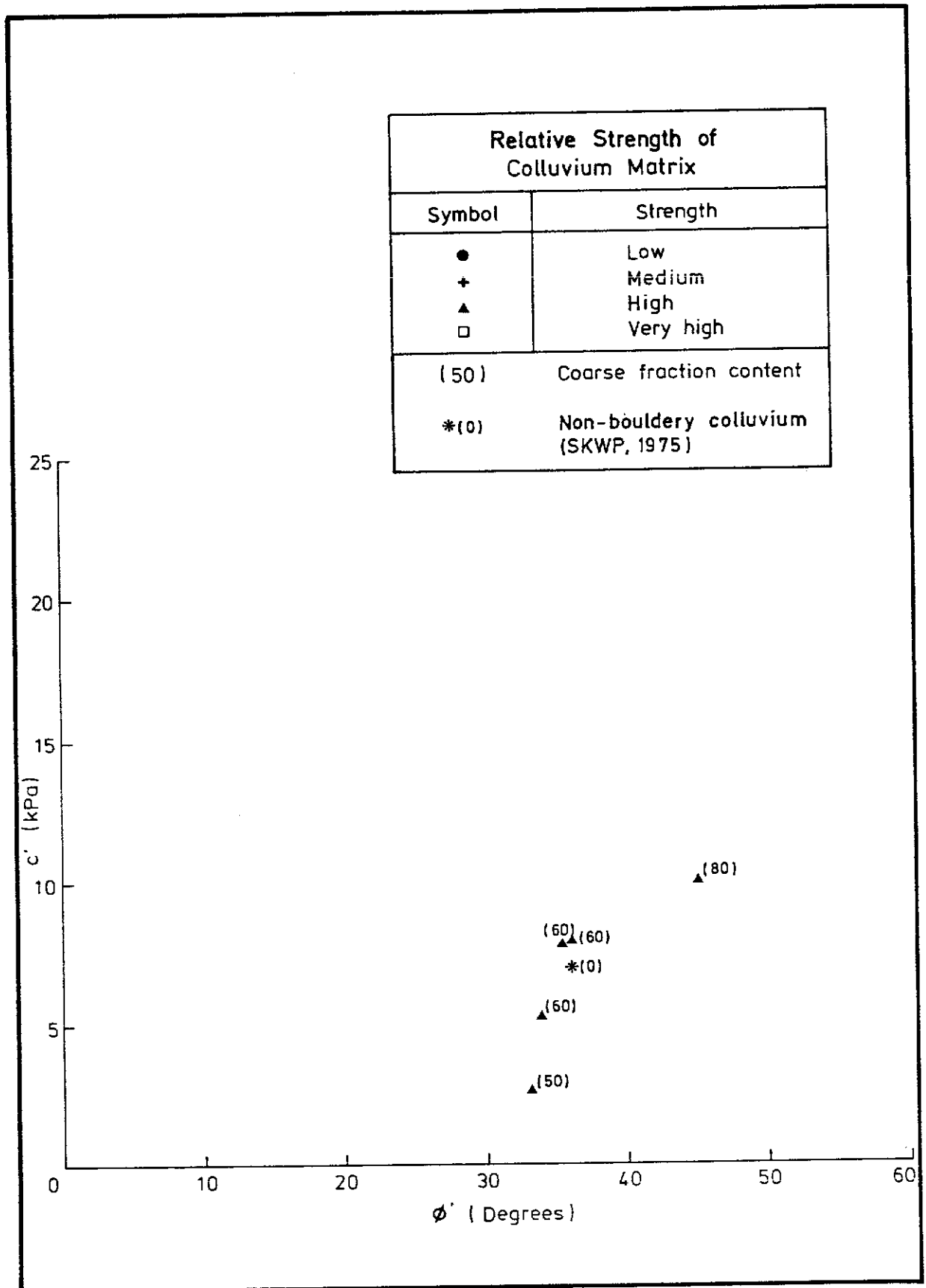


Figure 4.10 - Plot of Back-calculated c' versus ϕ' for Various Coarse Fraction Contents, Tsz Wan Shan Estate Slopes ($\sigma_n' \leq 50$ kPa)

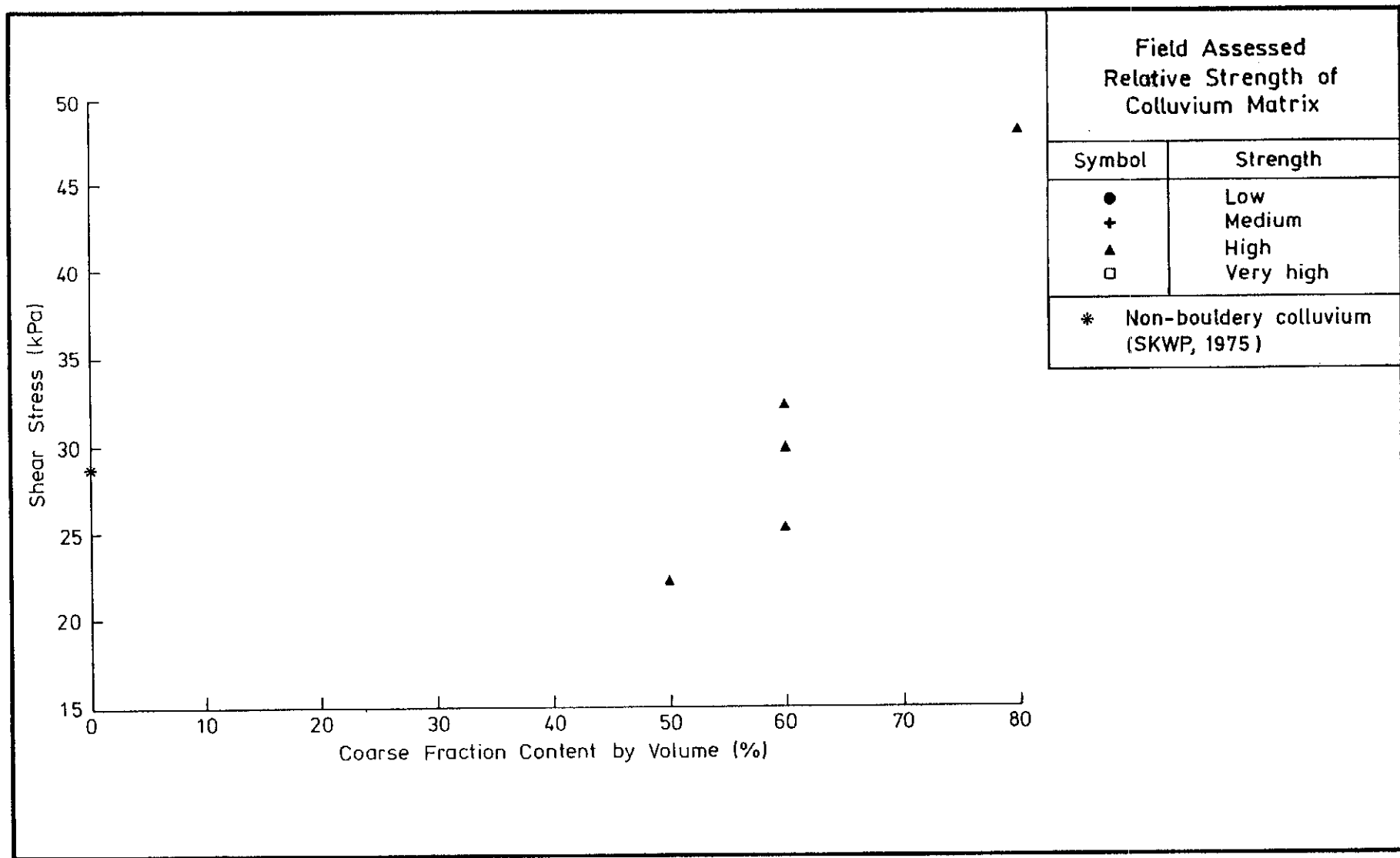


Figure 4.11 - Variation of Back-calculated 'Minimum' Shear Stress at $\sigma_n' = 30$ kPa with Coarse Fraction Content, Tsz Wan Shan Estate Slopes

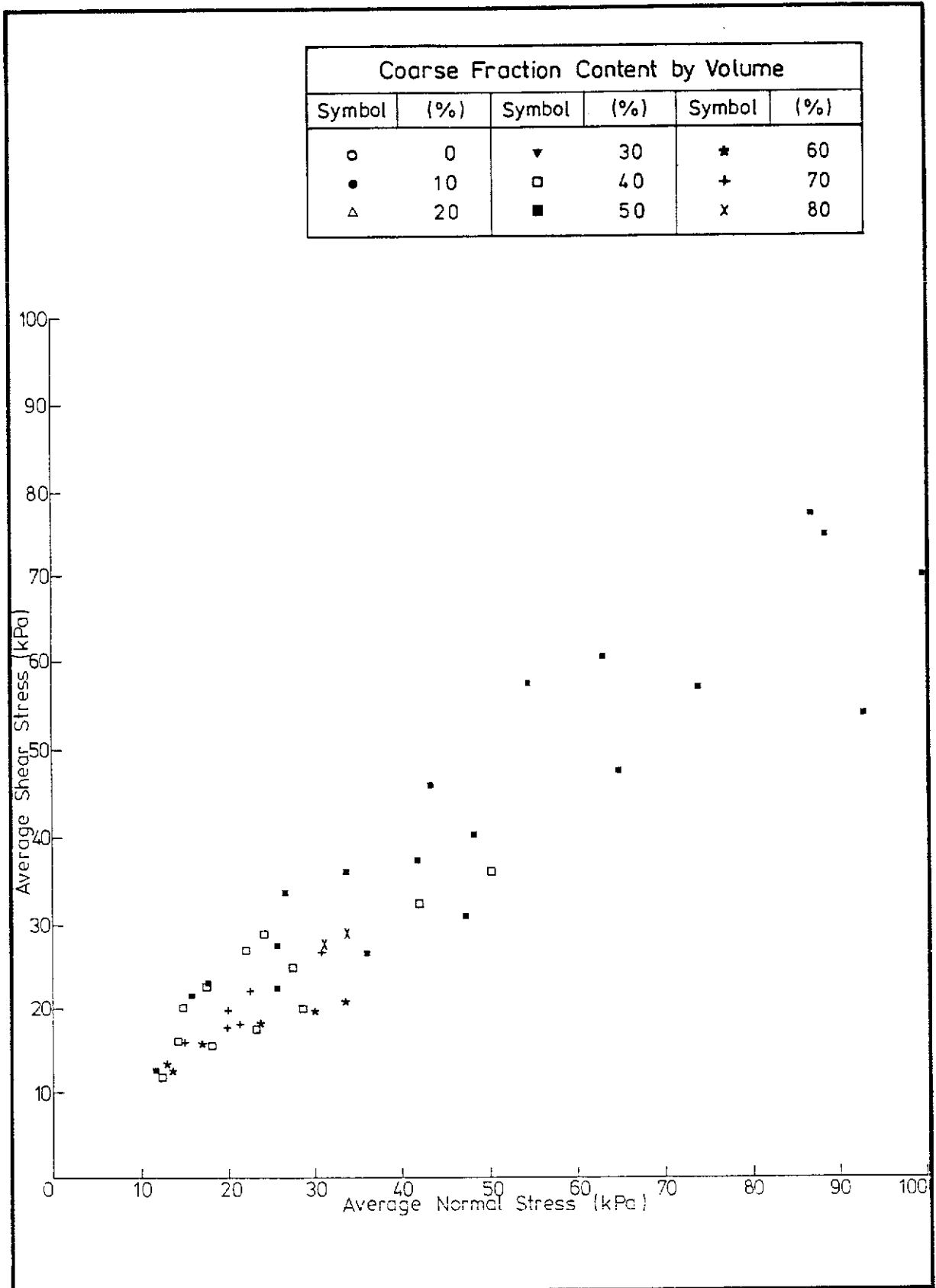


Figure 4.12 - Back-analysed Average Shear and Normal Stresses along Potential Failure Surfaces, Mid-levels and Peak Slopes

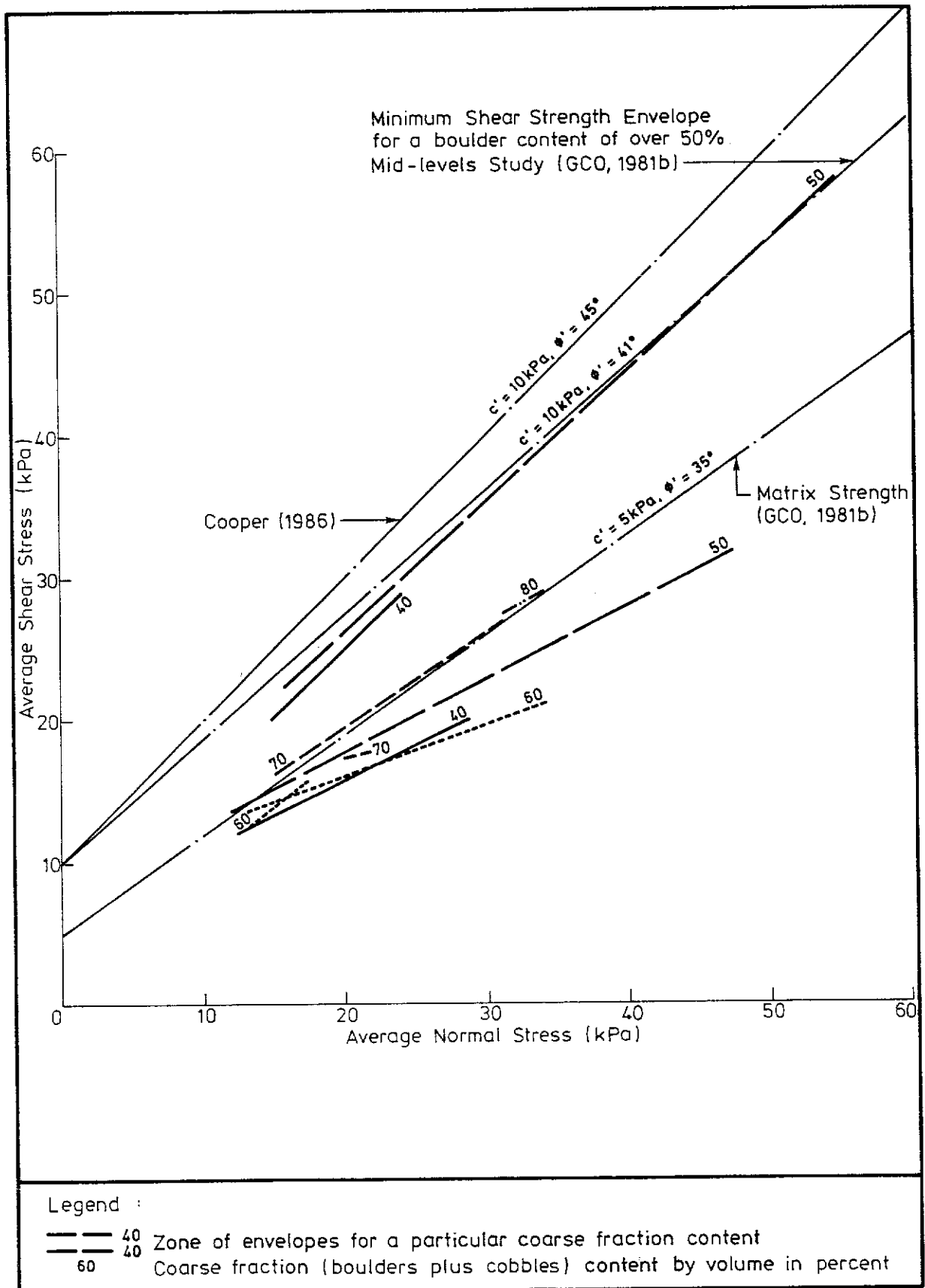


Figure 4.13 - Back-calculated Least-squares Shear Strength Envelopes for Various Coarse Fraction Contents, Mid-levels and Peak Slopes

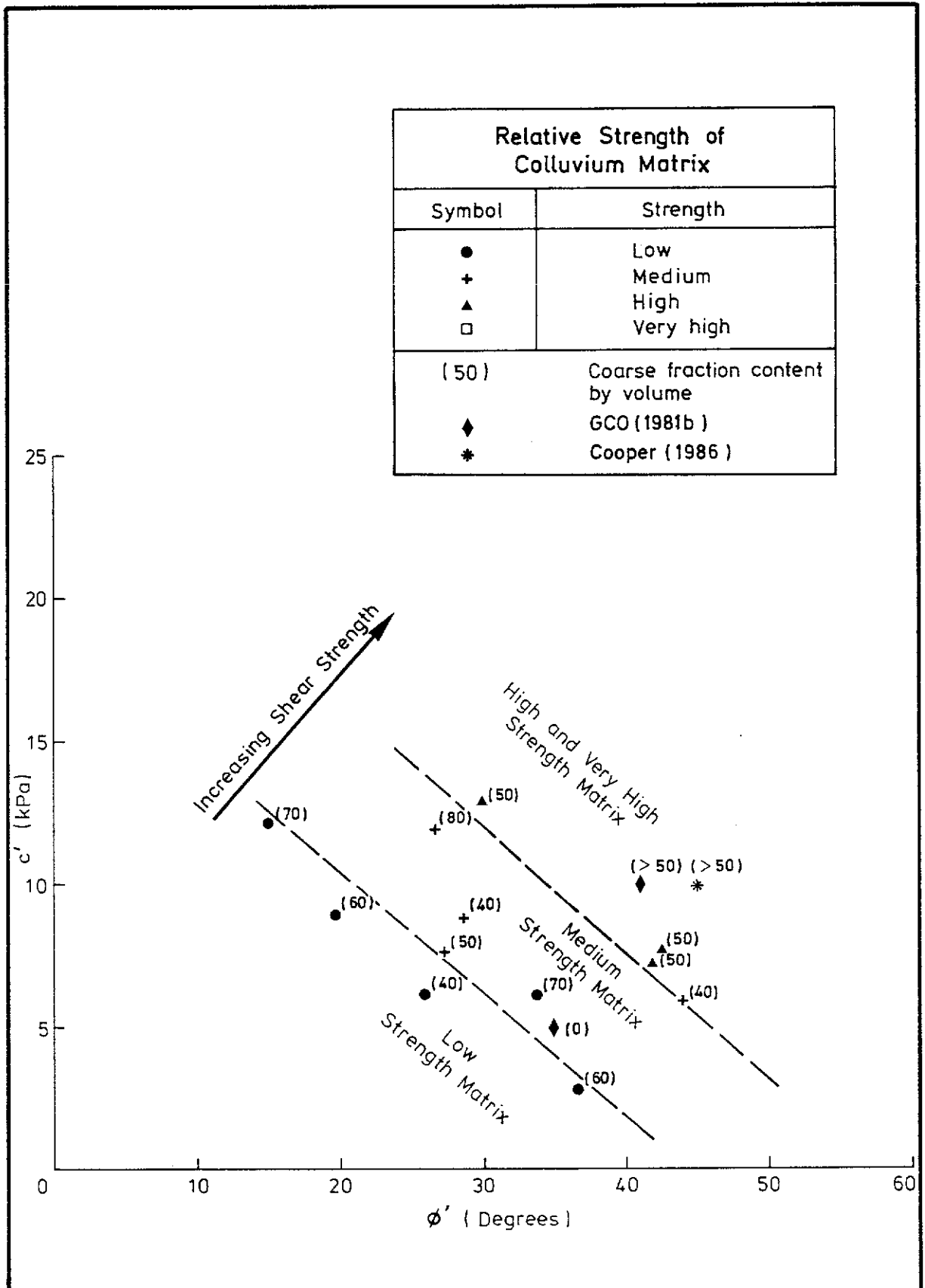


Figure 4.14 - Plot of Back-calculated c' versus ϕ' for Various Total Coarse Fraction Contents, Mid-levels and Peak Slopes ($\sigma_n' \leq 50$ kPa)

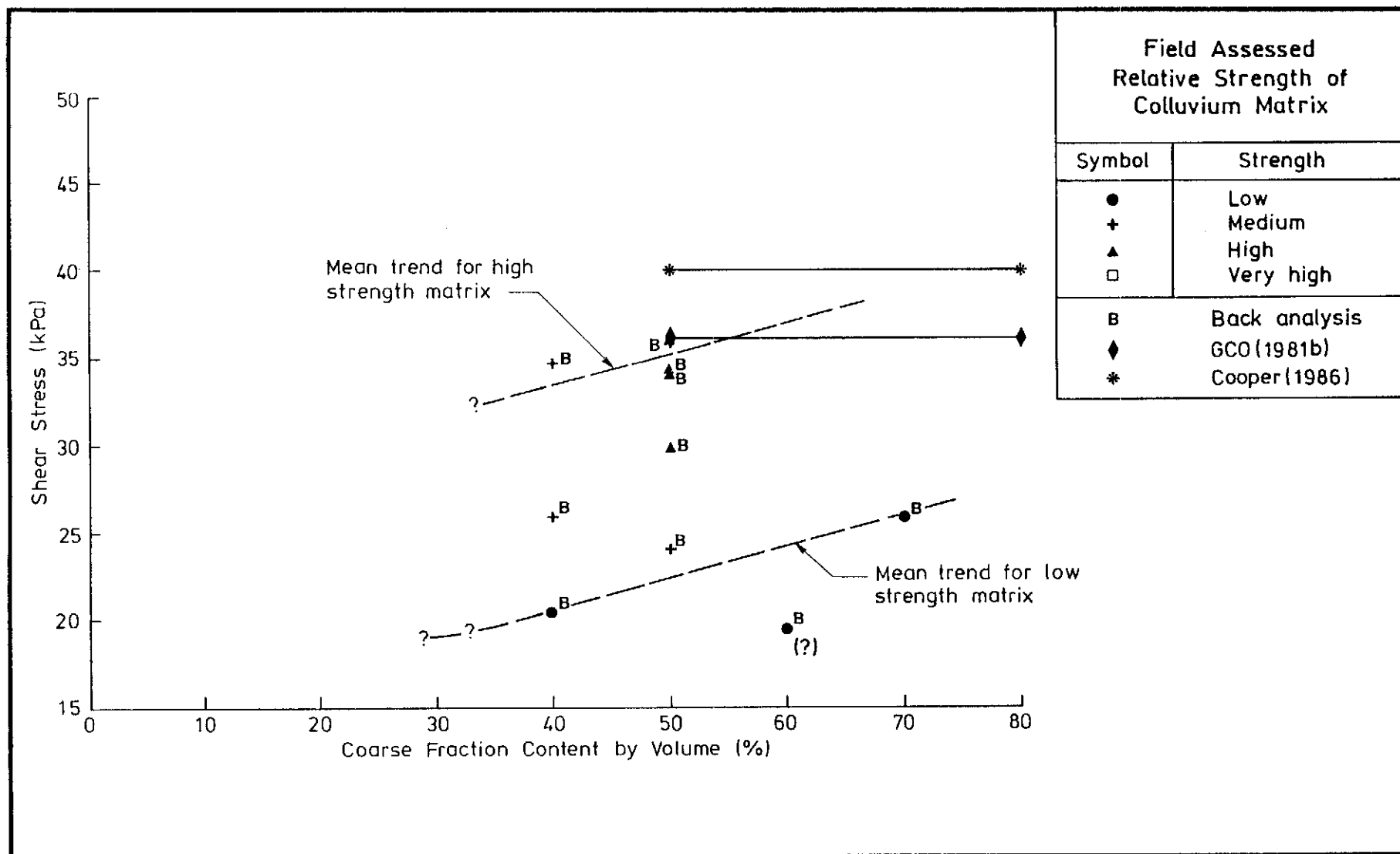


Figure 4.15 - Variation of Back-calculated 'Minimum' Shear Stress at $\sigma'_n = 30$ kPa with Coarse Fraction Content, Mid-Levels and Peak Slopes

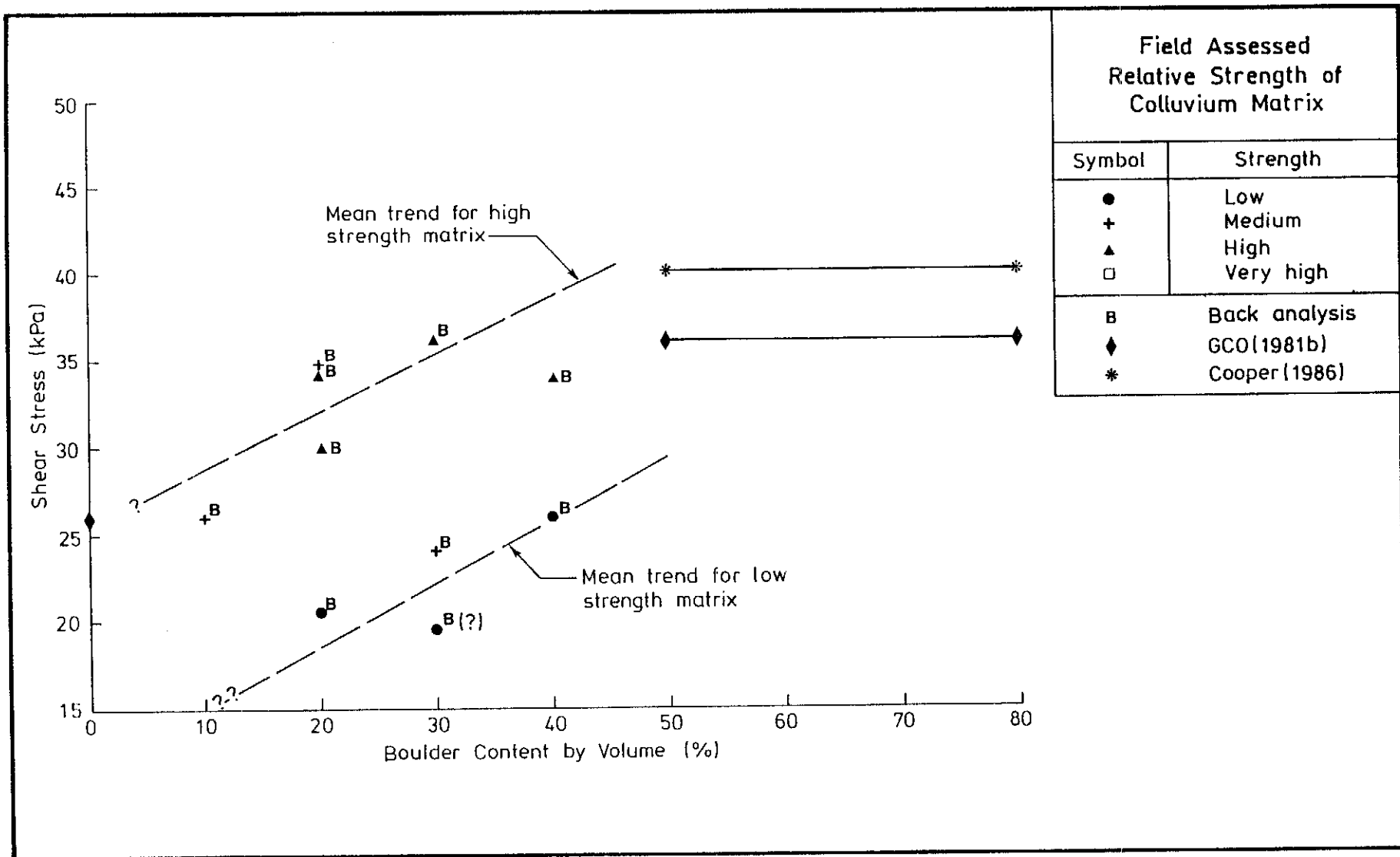


Figure 4.16 - Variation of Back-calculated Shear Stress at $\sigma_n' = 30$ kPa with Boulder Content, Mid-Levels and Peak Slopes

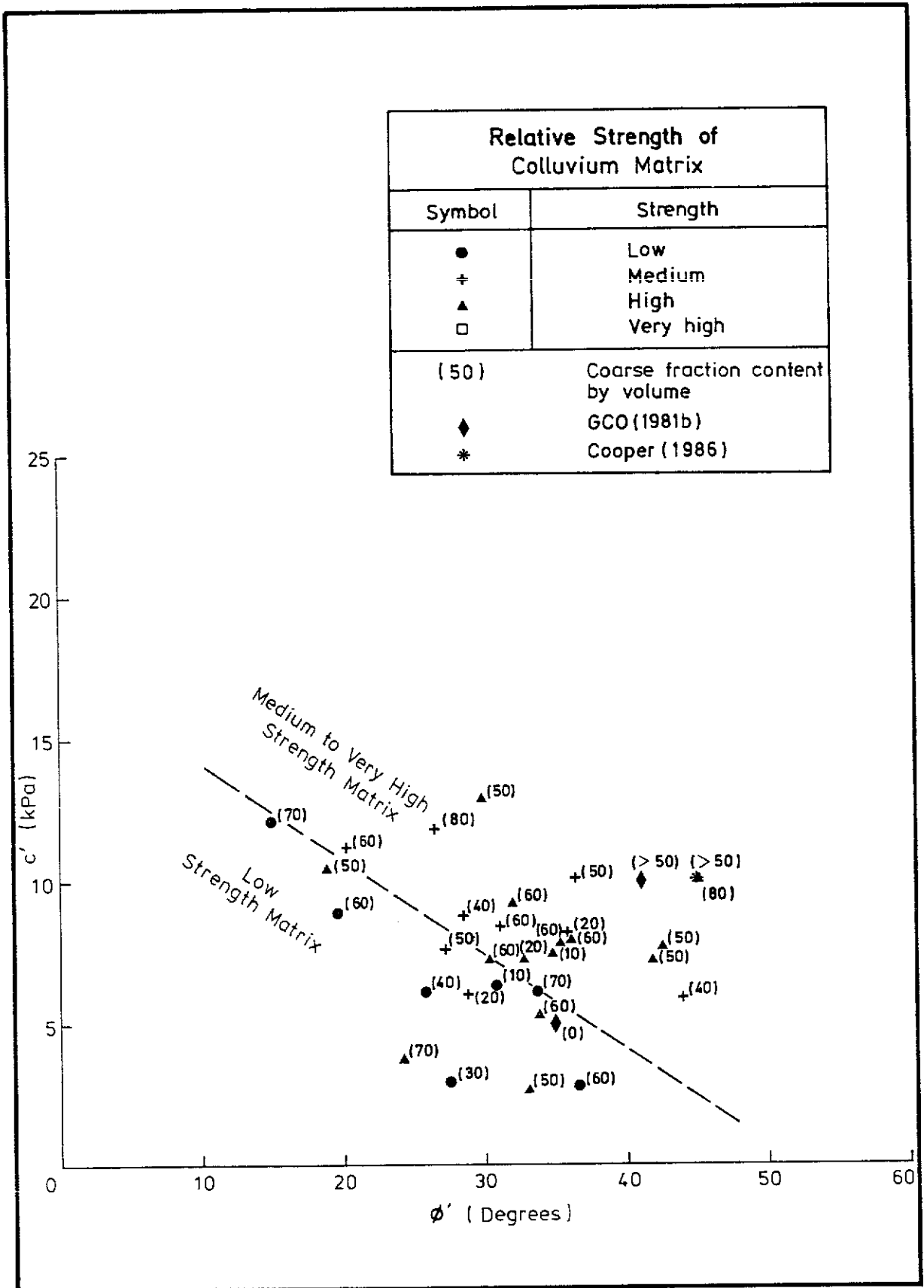


Figure 4.17 - Plot of Back-calculated c' versus ϕ' for Various Coarse Fraction Contents, All Slopes ($\sigma_n' \leq 50$ kPa)

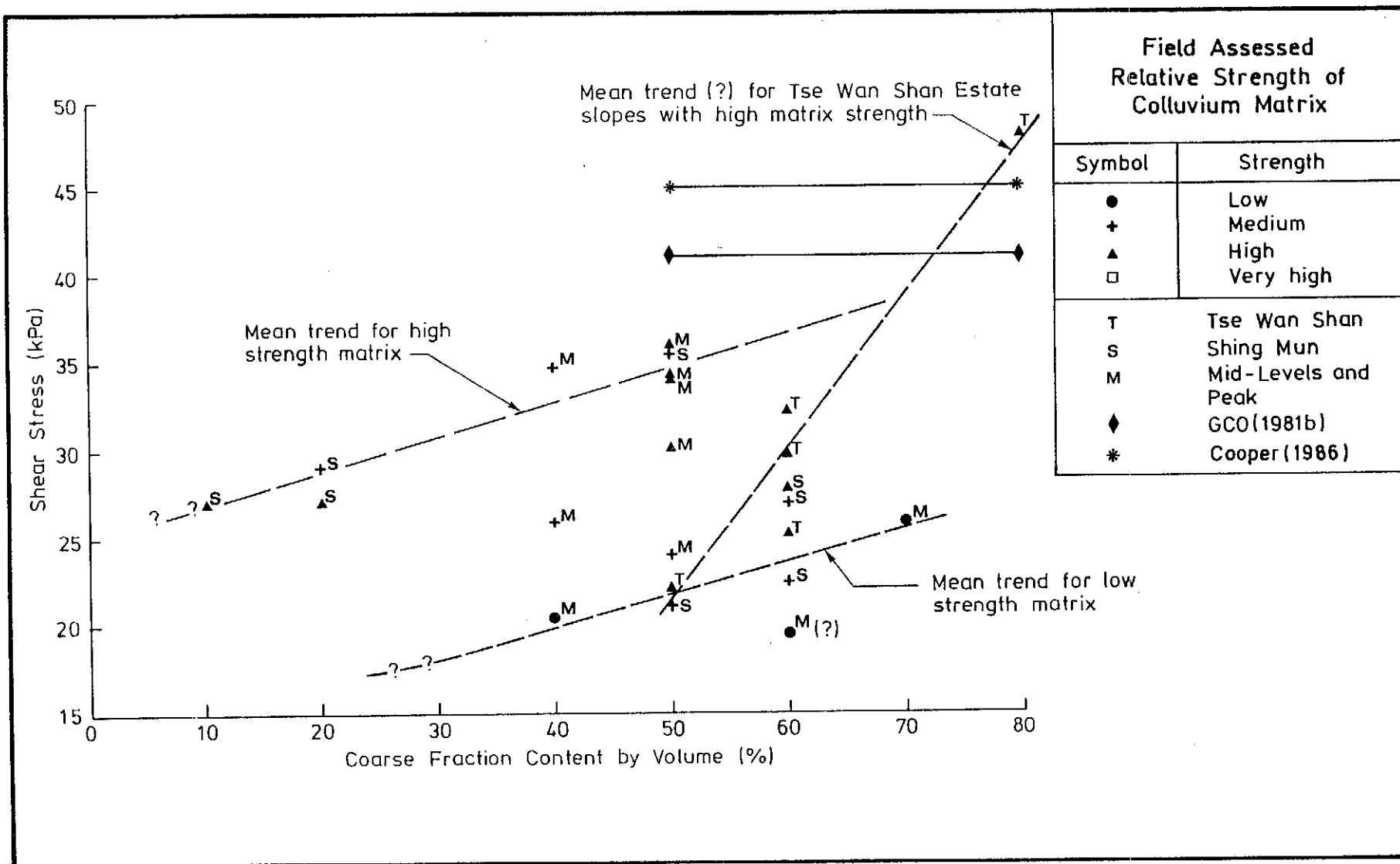


Figure 4.18 - Variation of Back-calculated 'Minimum' Shear Stress at $\sigma'_n = 30$ kPa with Coarse Fraction Content, All Slopes

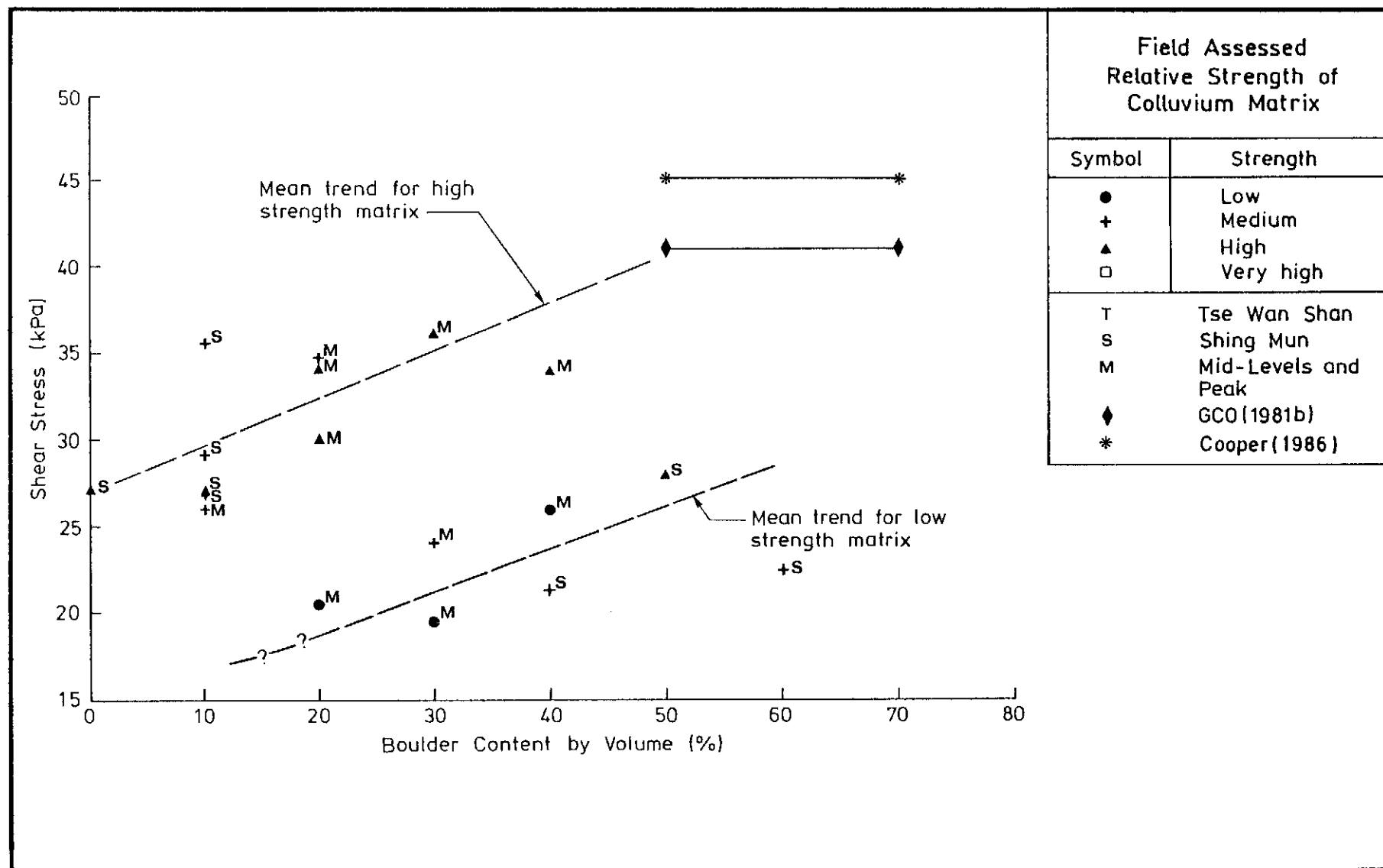


Figure 4.19 - Variation of Back-calculated Shear Stress at $\sigma'_n = 30$ kPa with Boulder Content, All Slopes

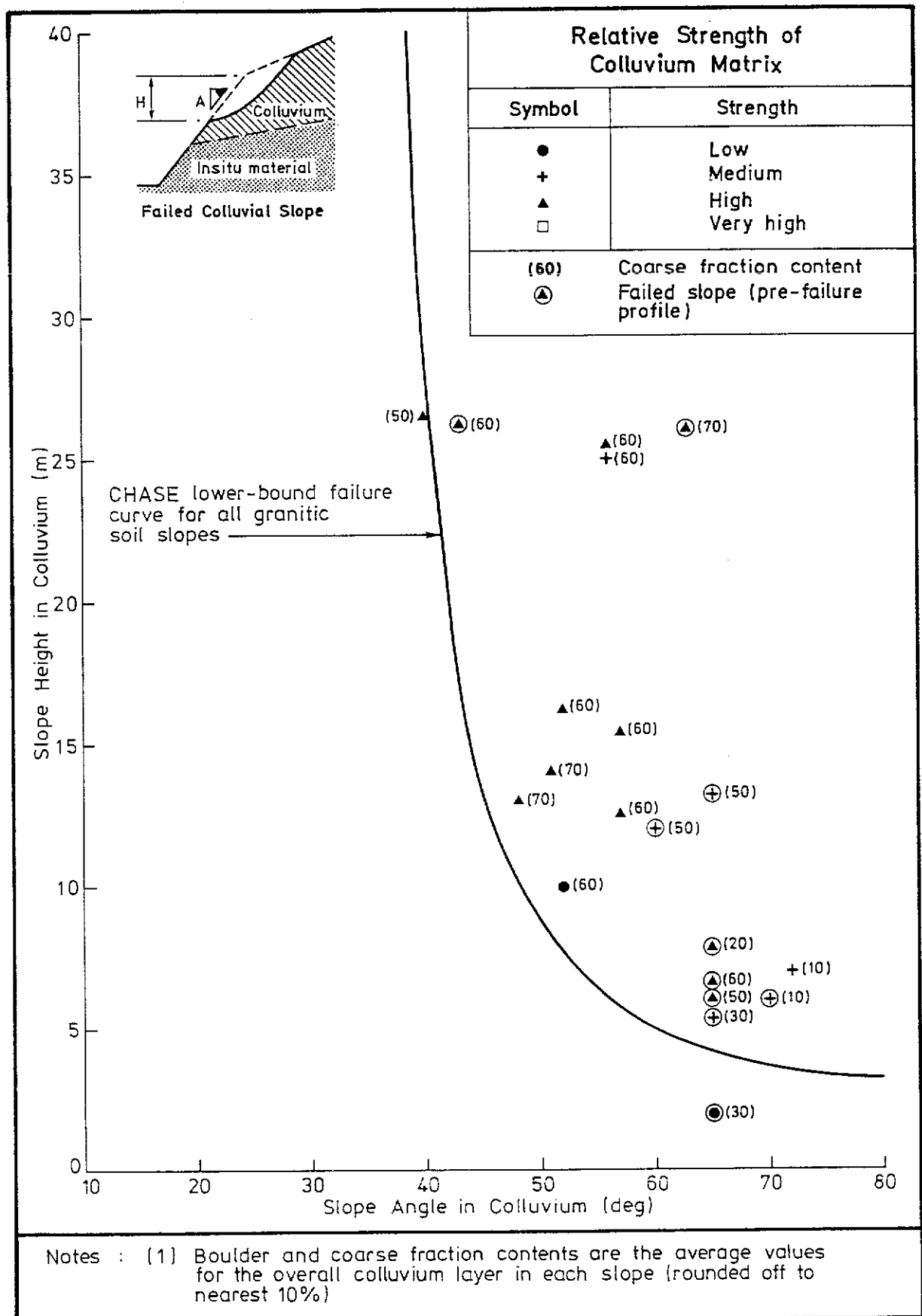


Figure 4.20 - Slope Height versus Slope Angle for Selected Colluvium Slopes in Hong Kong

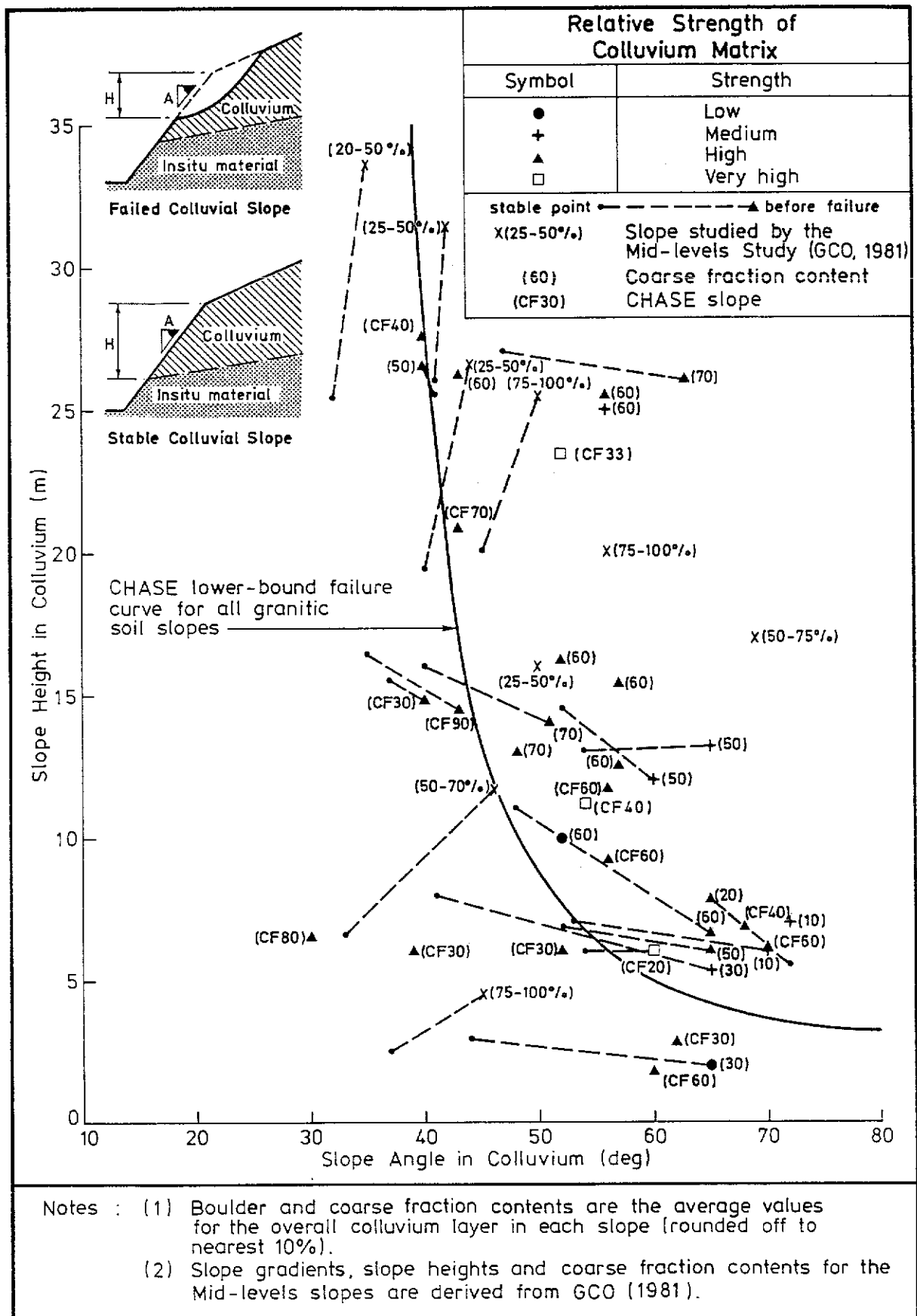


Figure 4.21 - Slope Height versus Slope Angle for Colluvium Slopes in Hong Kong

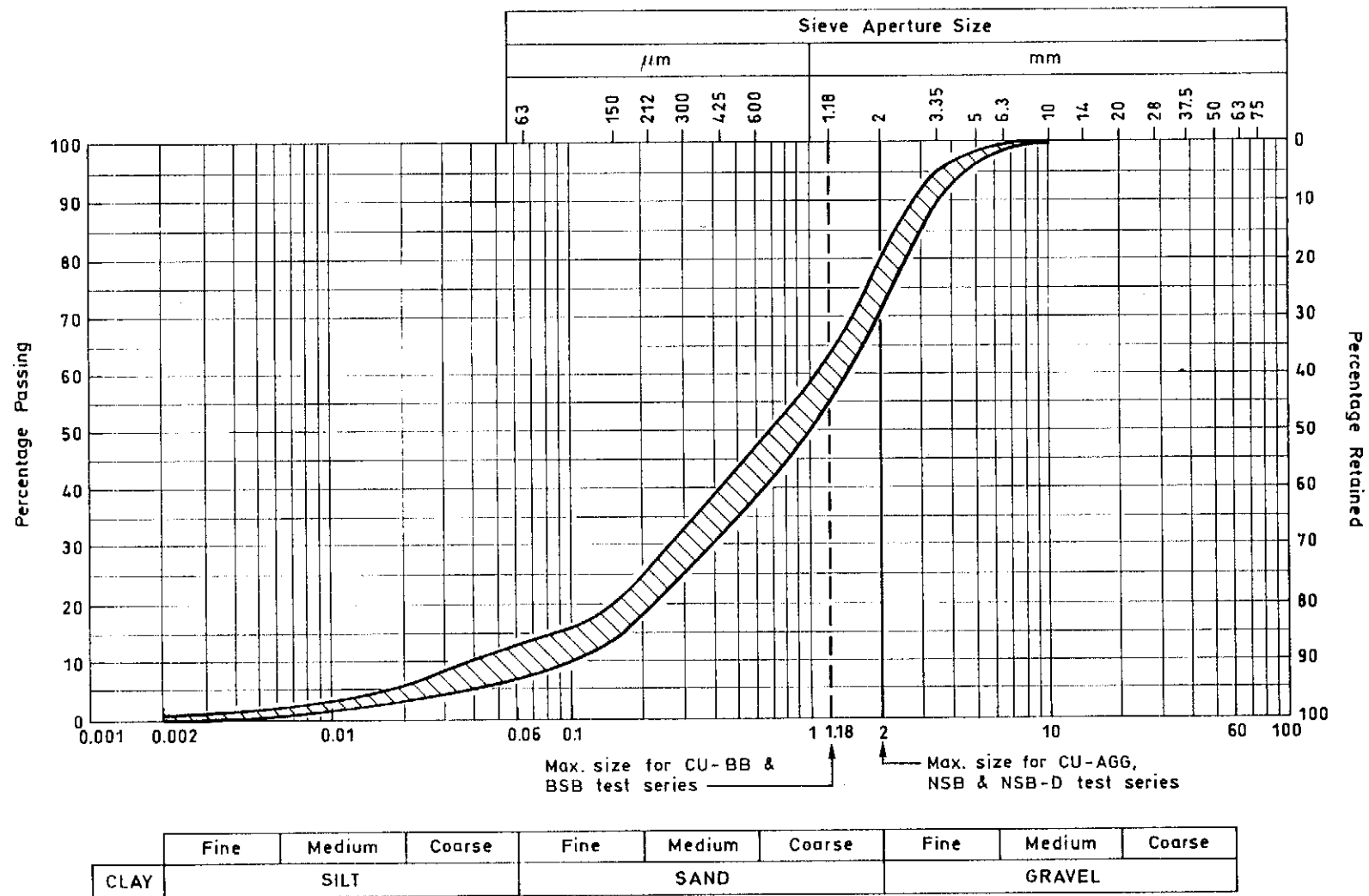


Figure 5.1 - Particle Size Distribution of Completely Decomposed Granite Used as Matrix Material in Laboratory Tests

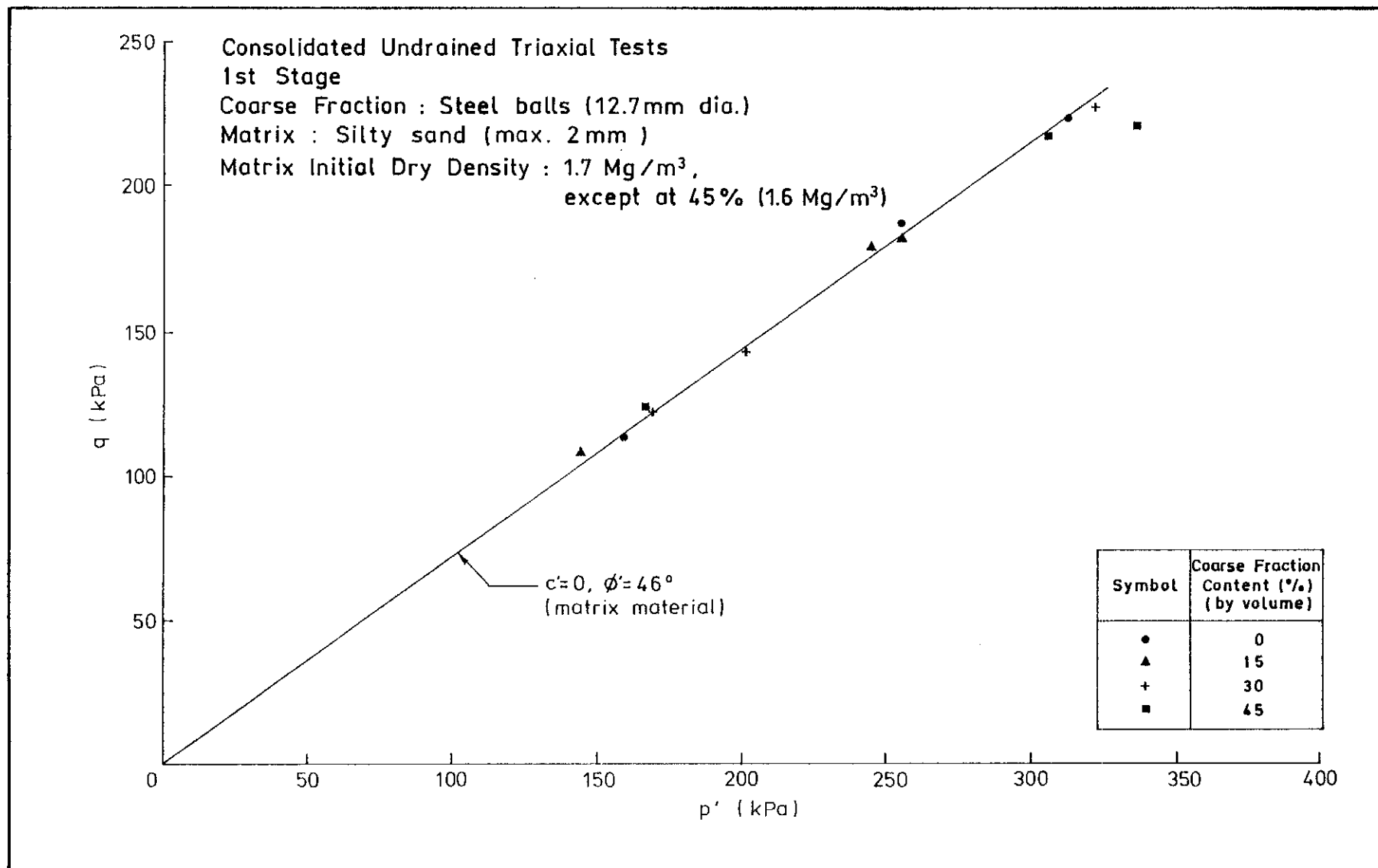


Figure 5.2 - p'-q Plot of Triaxial Test Results on Soil Specimens Containing Steel Balls

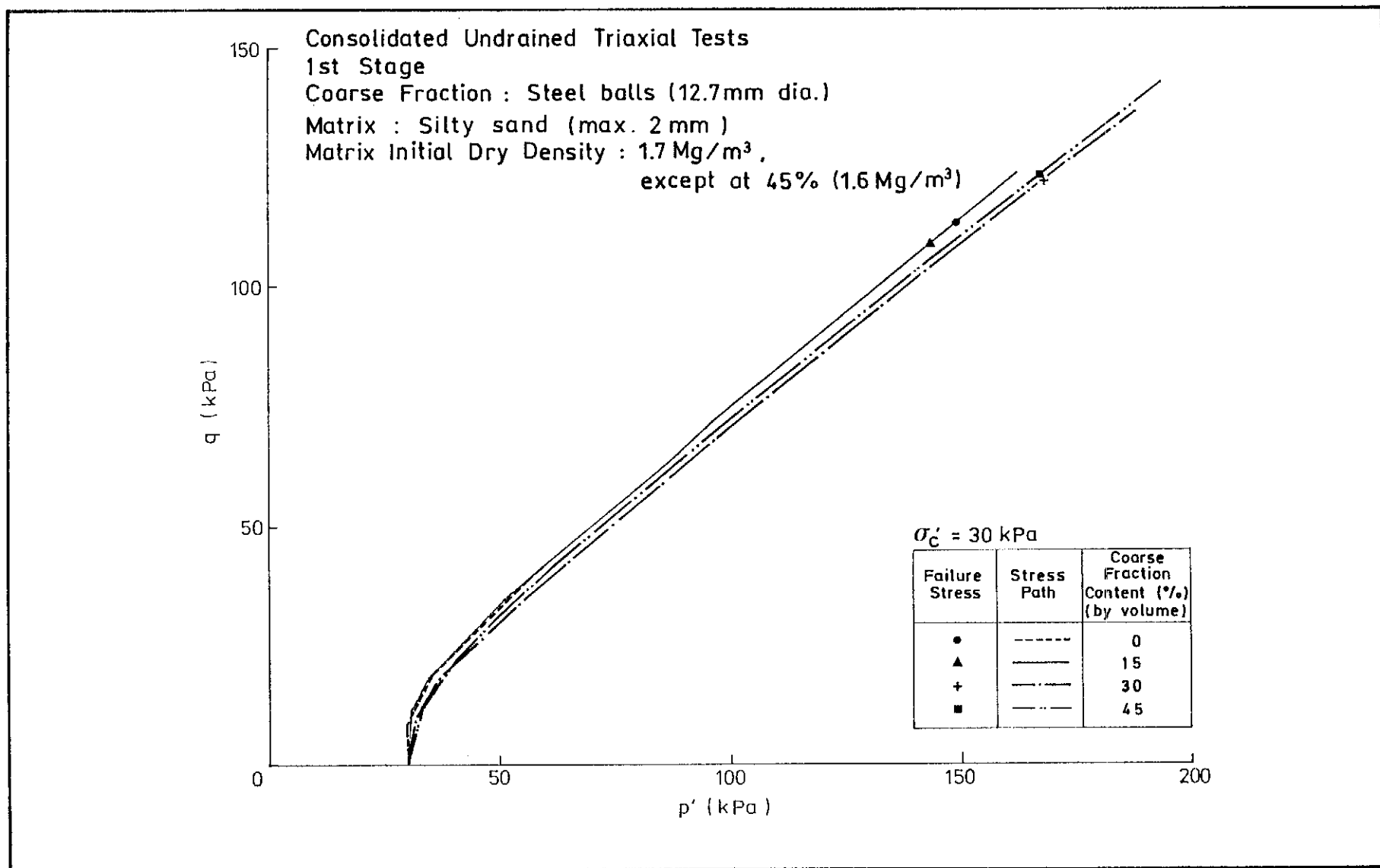


Figure 5.3 - Selected Stress Paths of Triaxial Tests Carried Out on Soil Specimens Containing Steel Balls ($\sigma'_c = 30$ kPa)

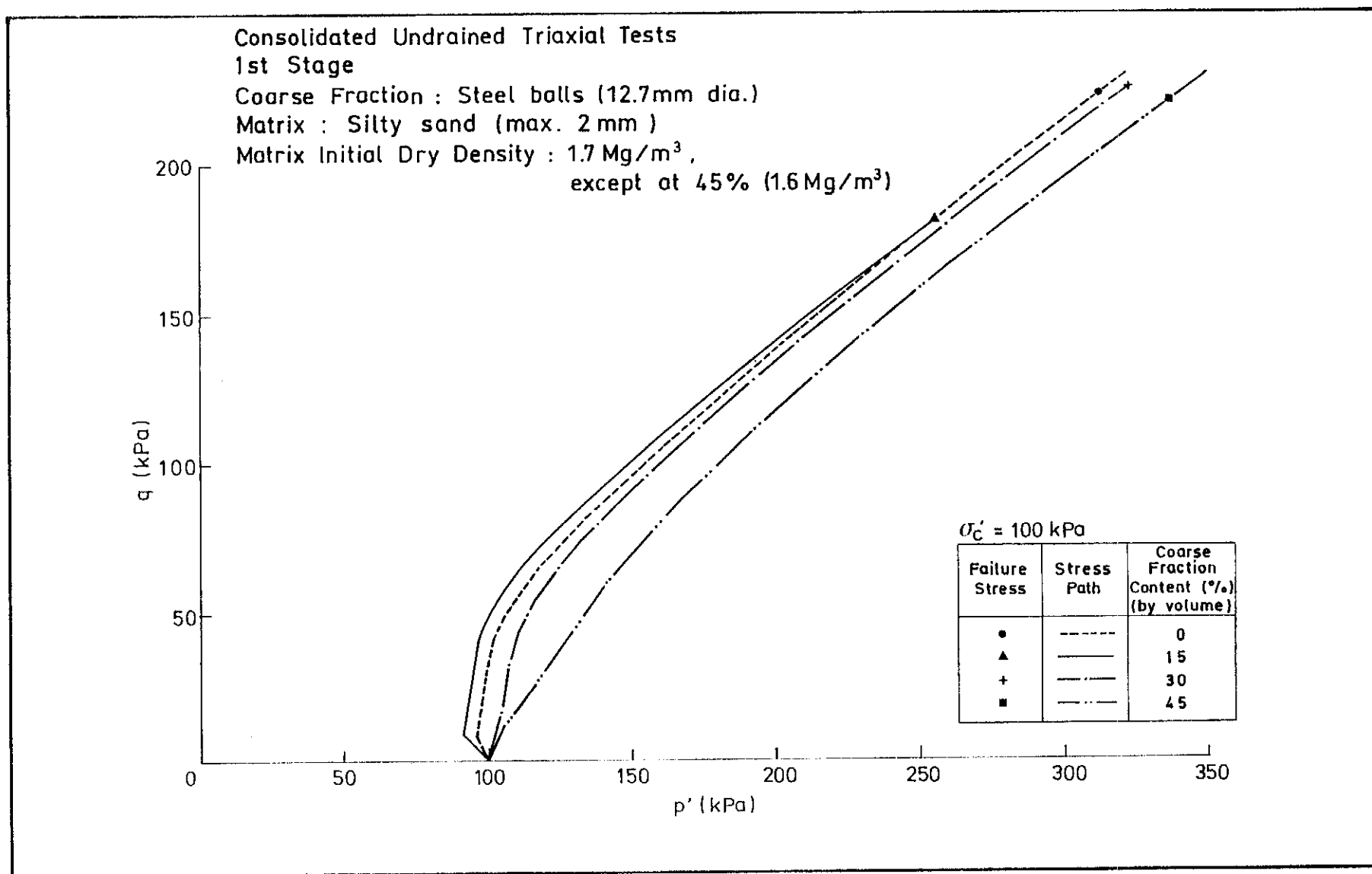


Figure 5.4 - Selected Stress Paths of Triaxial Tests Carried Out on Soil Specimens Containing Steel Balls ($\sigma'_c = 100 \text{ kPa}$)

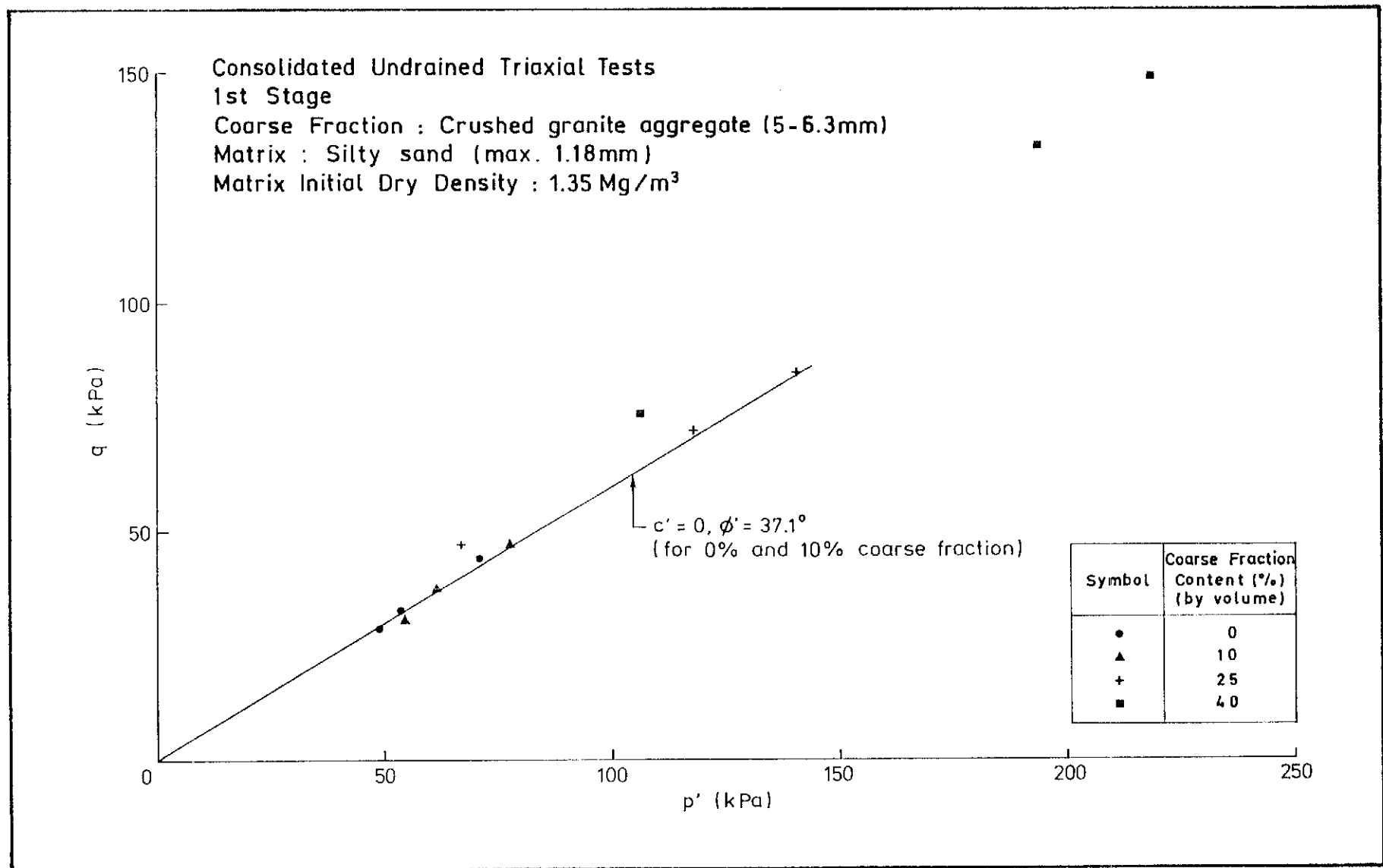


Figure 5.5 - p'-q Plot of Triaxial Test Results on Soil Specimens Containing Aggregates

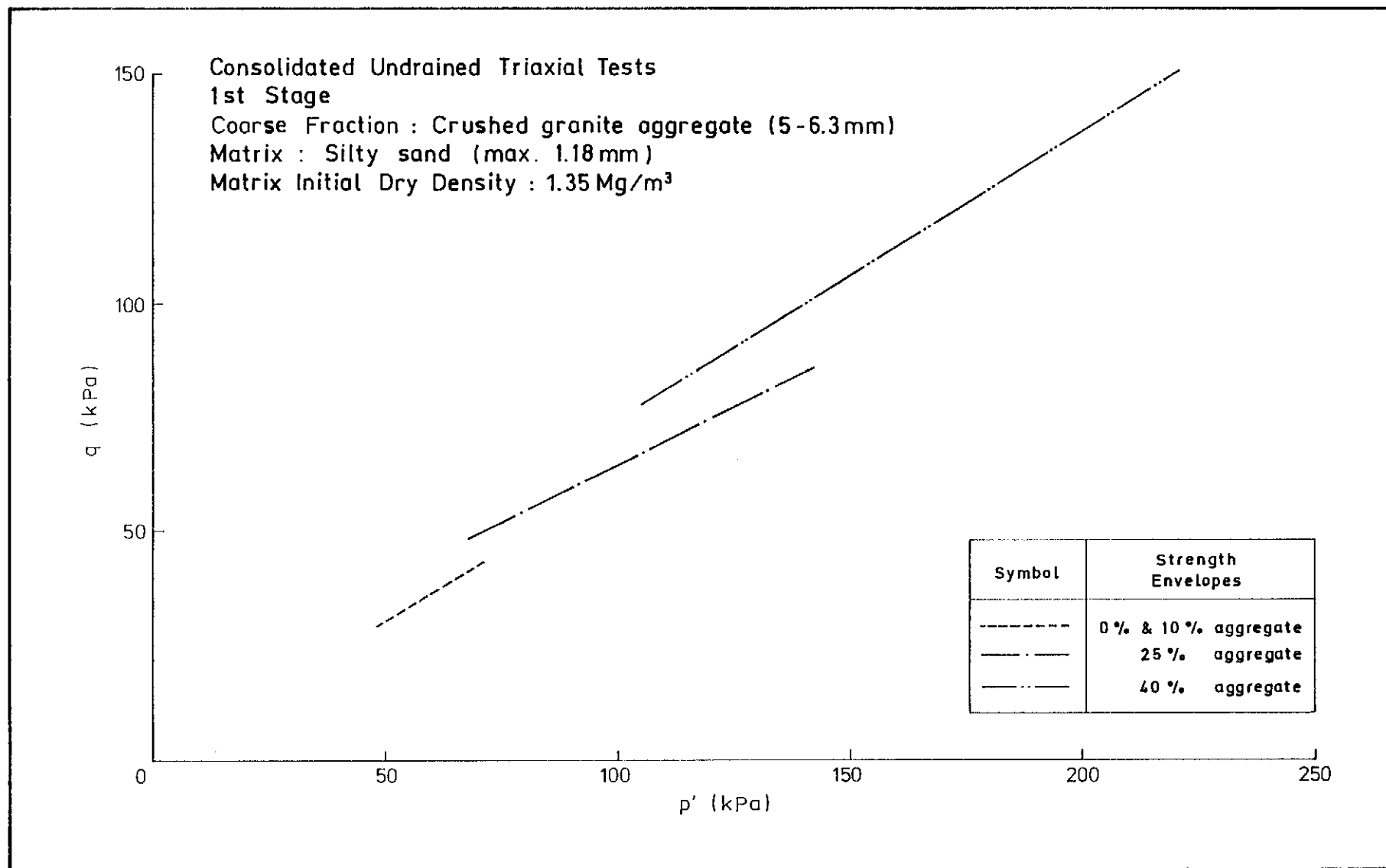


Figure 5.6 - Results of Triaxial Tests on Soil Specimens Containing Aggregates Showing Variation of Shear Strength with Coarse Fraction Content

Consolidated Undrained Triaxial Tests

1st Stage

Coarse Fraction : Crushed granite aggregate (5-6.3 mm)

Matrix : Silty Sand (max. 1.18 mm)

Matrix Initial Dry Density : 1.35 Mg/m³

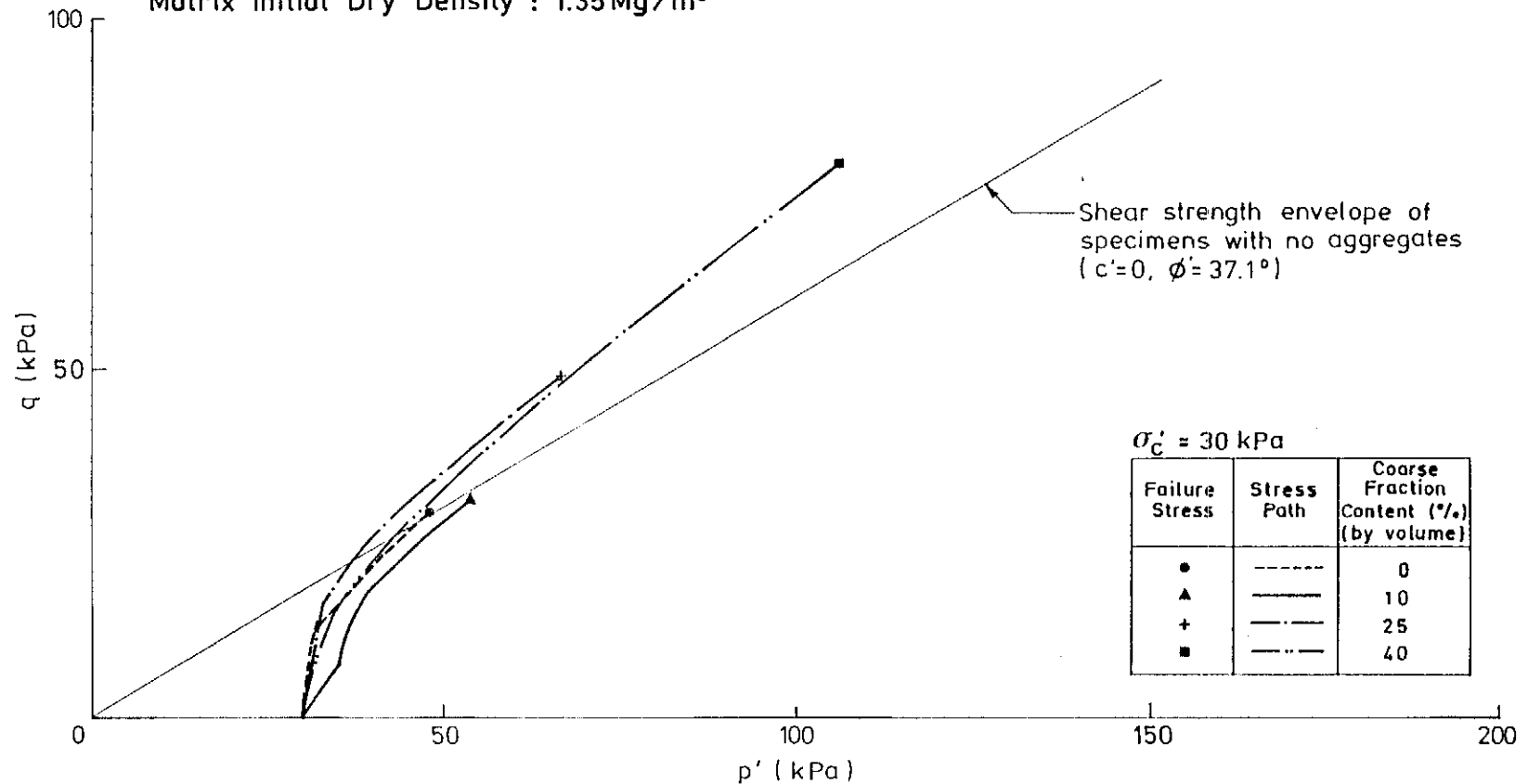


Figure 5.7 - Selected Stress Paths of Triaxial Tests Carried Out on Soil Specimens Containing Aggregates ($\sigma'_c = 30$ kPa)

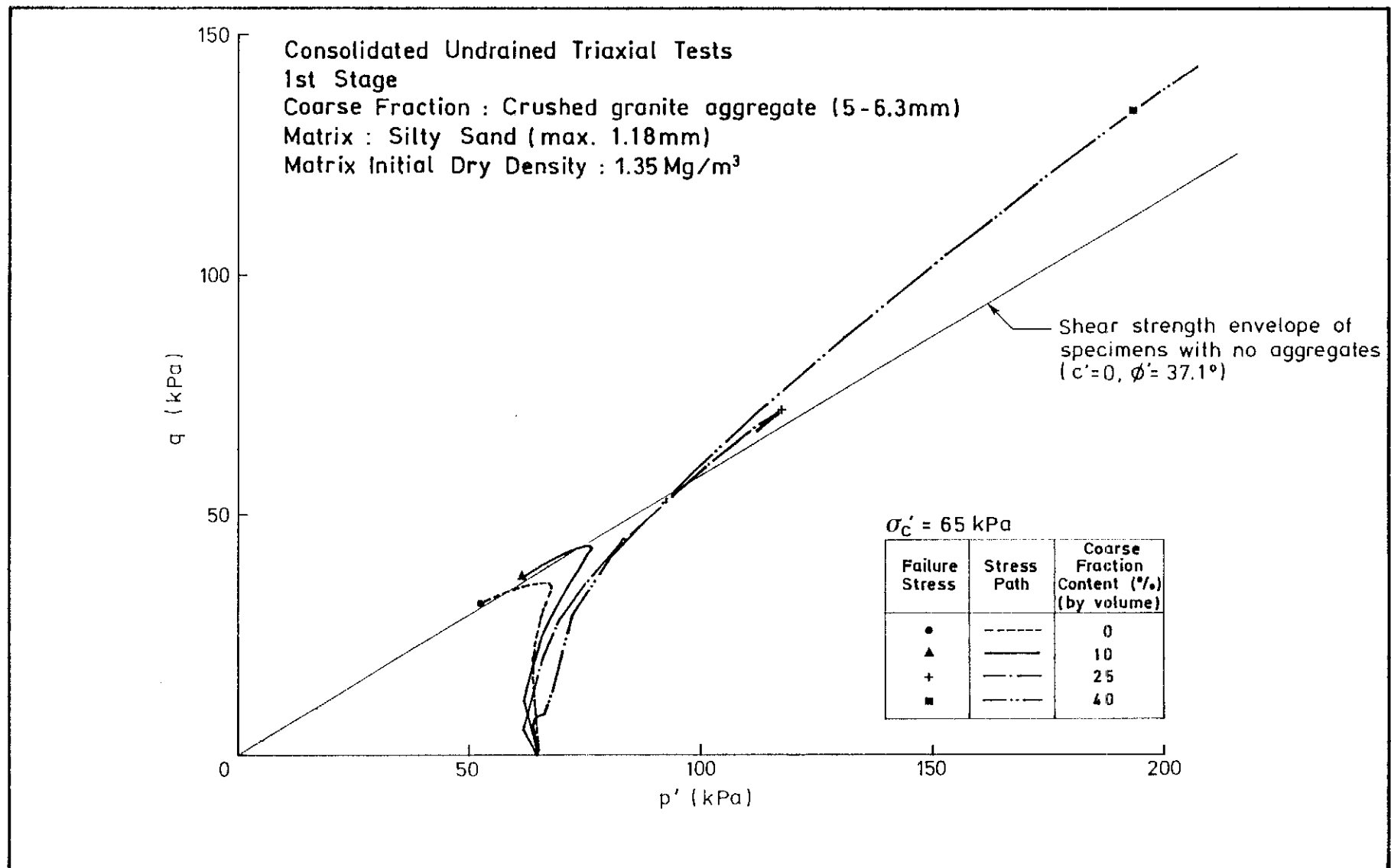


Figure 5.8 - Selected Stress Paths of Triaxial Tests Carried Out on Soil Specimens Containing Aggregates ($\sigma'_c = 65 \text{ kPa}$)

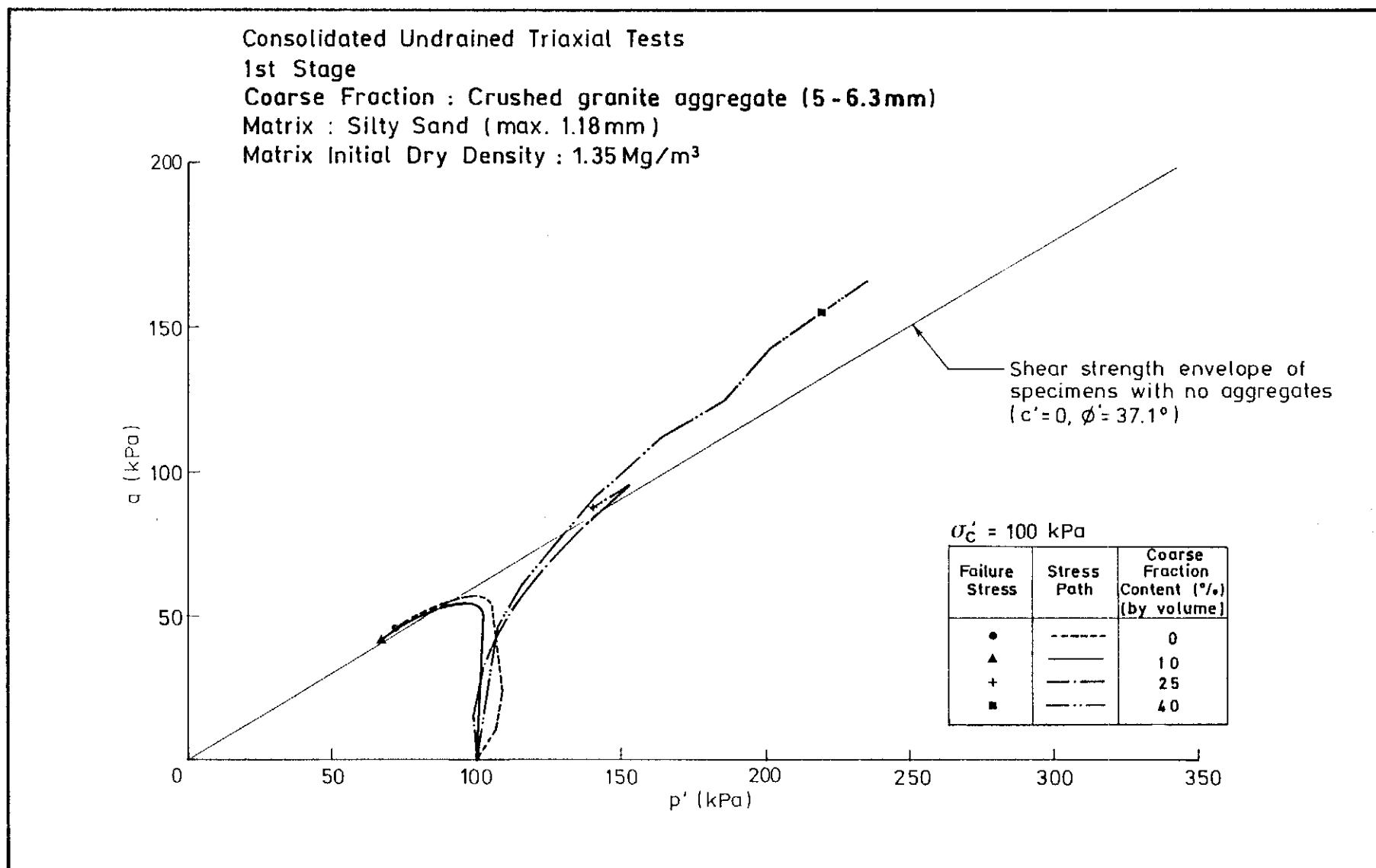


Figure 5.9 - Selected Stress Paths of Triaxial Tests Carried Out on Soil Specimens Containing Aggregates ($\sigma'_c = 100$ kPa)

Direct Shear Tests

Soaked Condition : 2 days

Shear Box : 300 × 300 × 148mm

Coarse Fraction : Crushed granite aggregate (20-28mm)

Matrix : Silty Sand (max. 2mm)

Matrix Initial Dry Density : 1.6 Mg/m³

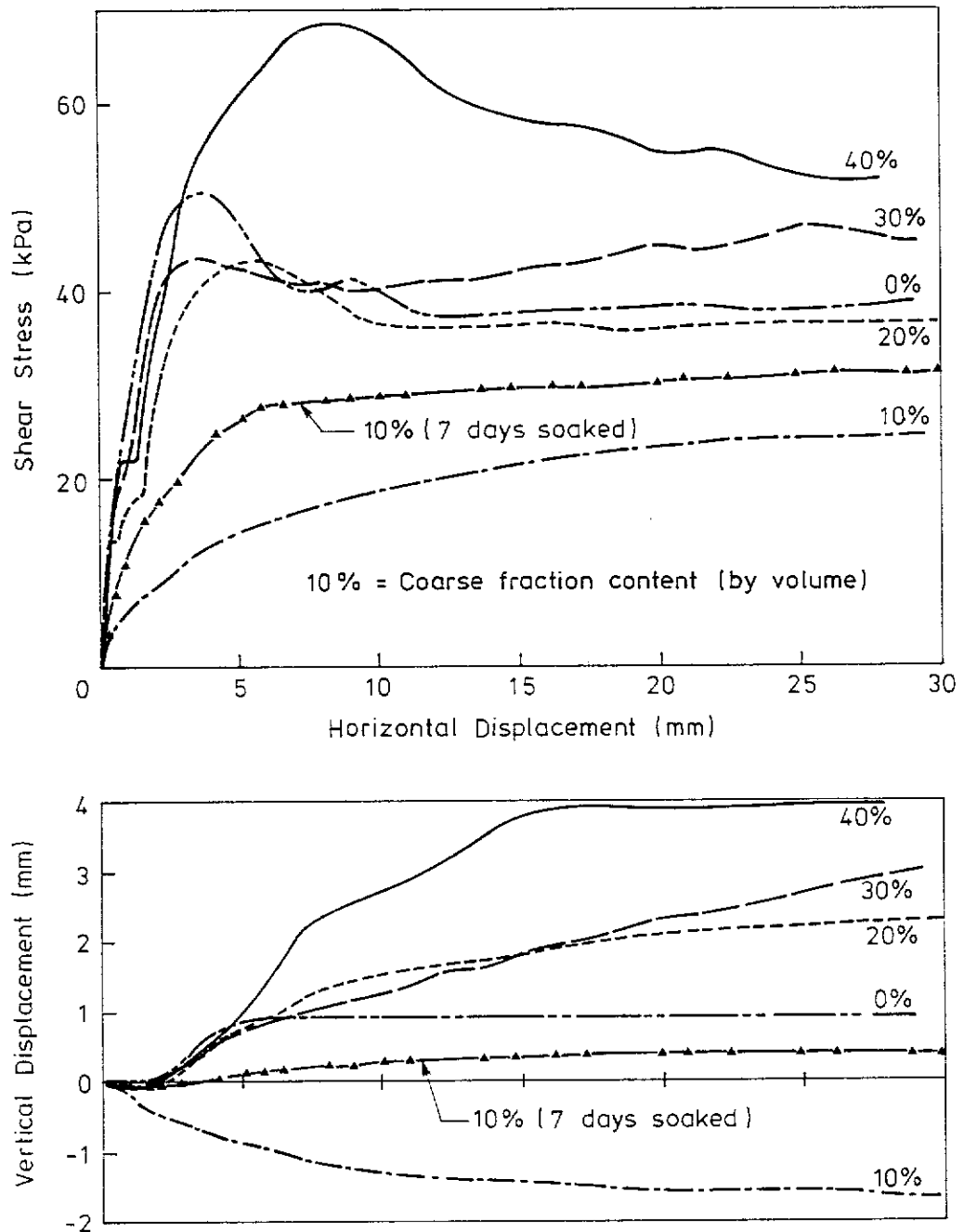


Figure 5.10 - Typical Shear Stress versus Horizontal Displacement Curves for Soil Specimens Containing Aggregates, Tested in 300 mm Shear Box

Direct Shear Tests

Soaked Condition : 2 days except shown

Shear Box : 300 × 300 × 148mm

Coarse Fraction : Crushed granite aggregate (20-28mm)

Matrix : Silty Sand (max. 2mm)

Matrix Initial Dry Density : 1.6 Mg/m³

$\sigma_n = 35 \text{ kPa}$

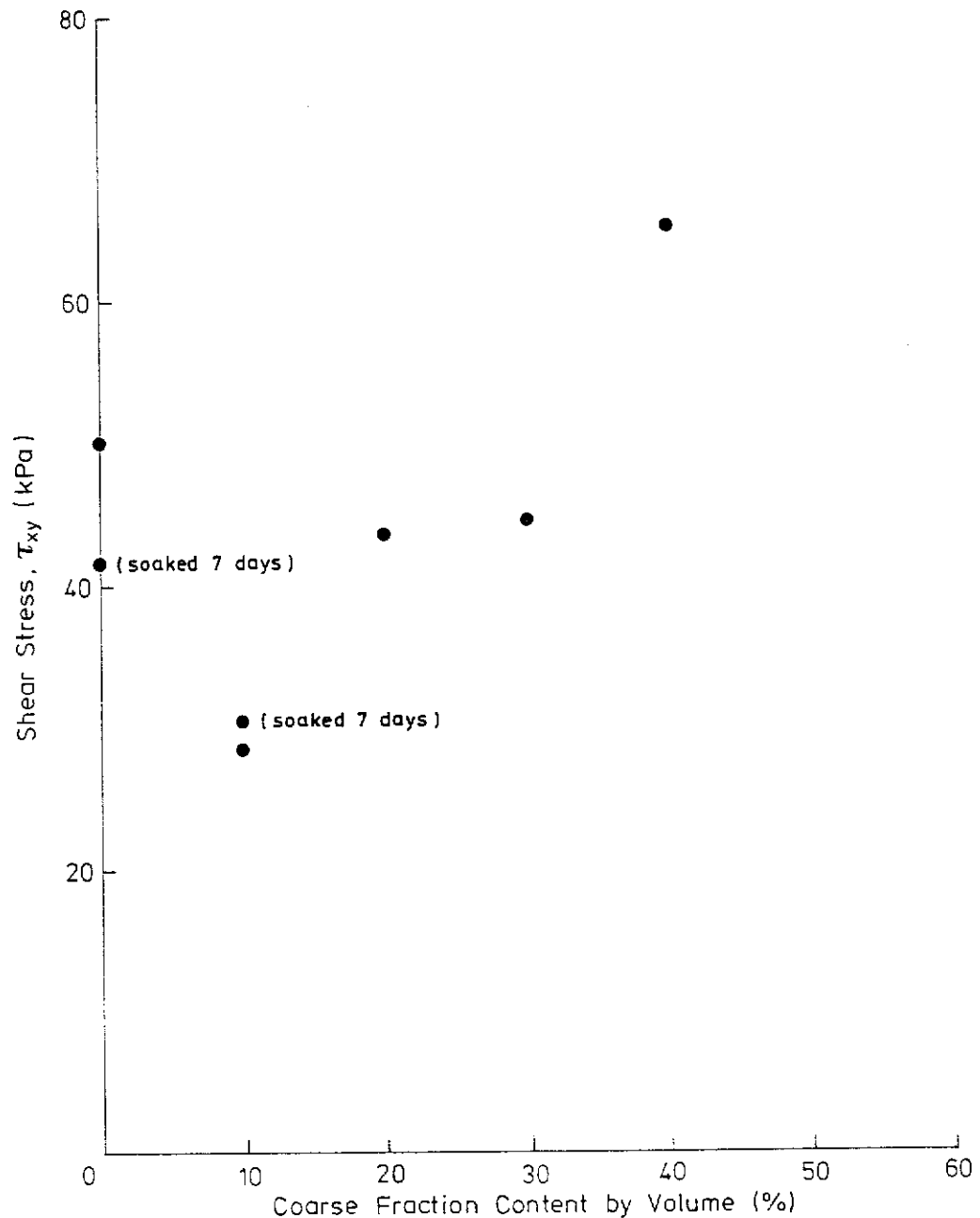


Figure 5.11 - Results of Direct Shear Tests Carried Out on Soil Specimens Containing Aggregates Showing Variation of Shear Strength with Coarse Fraction Contents (300 mm Shear Box)

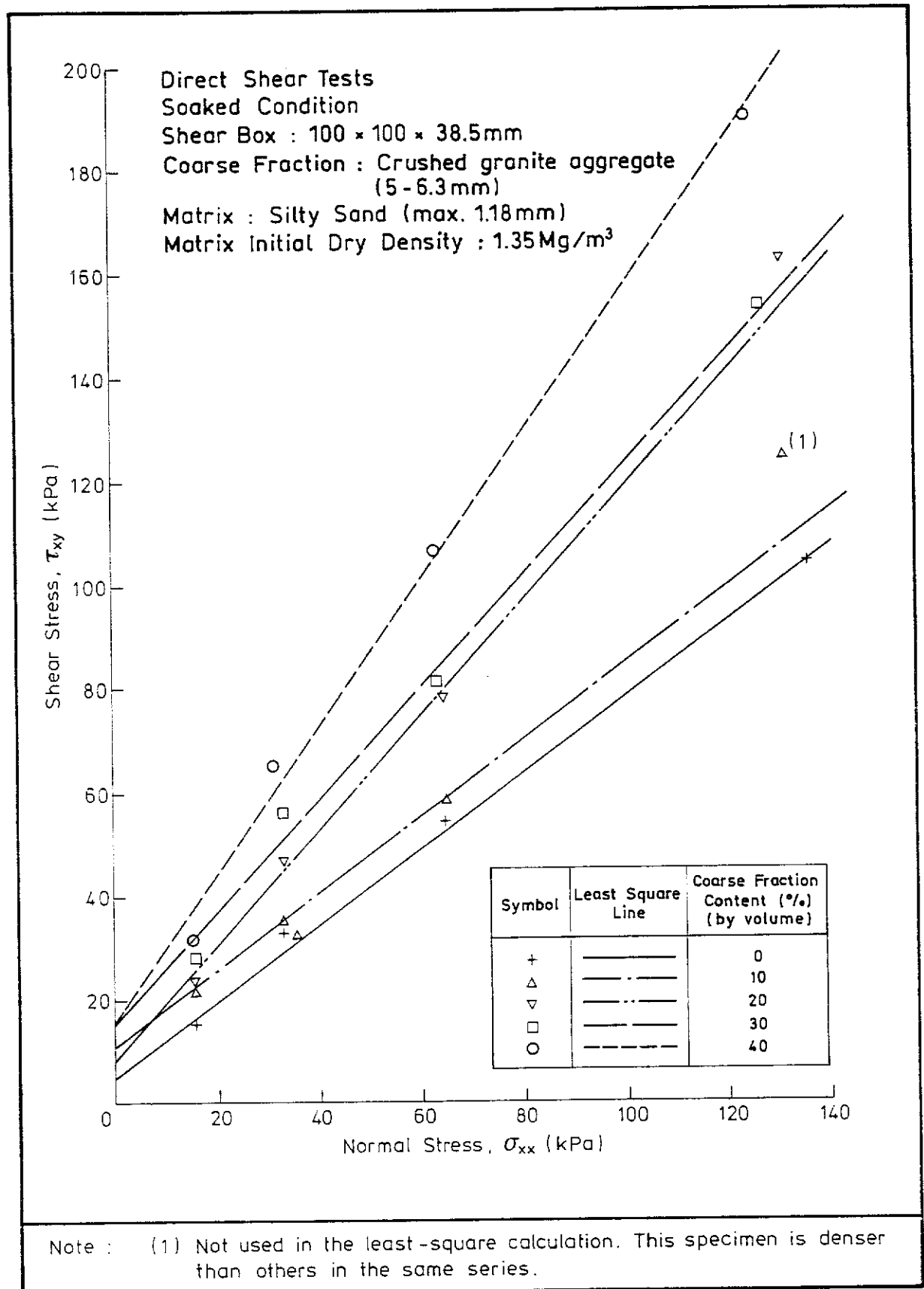


Figure 5.12 - Results of Direct Shear Tests Carried Out on Soil Specimens Containing Aggregates Showing Variation of Shear Strength with Coarse Fraction Content (100 mm Shear Box)

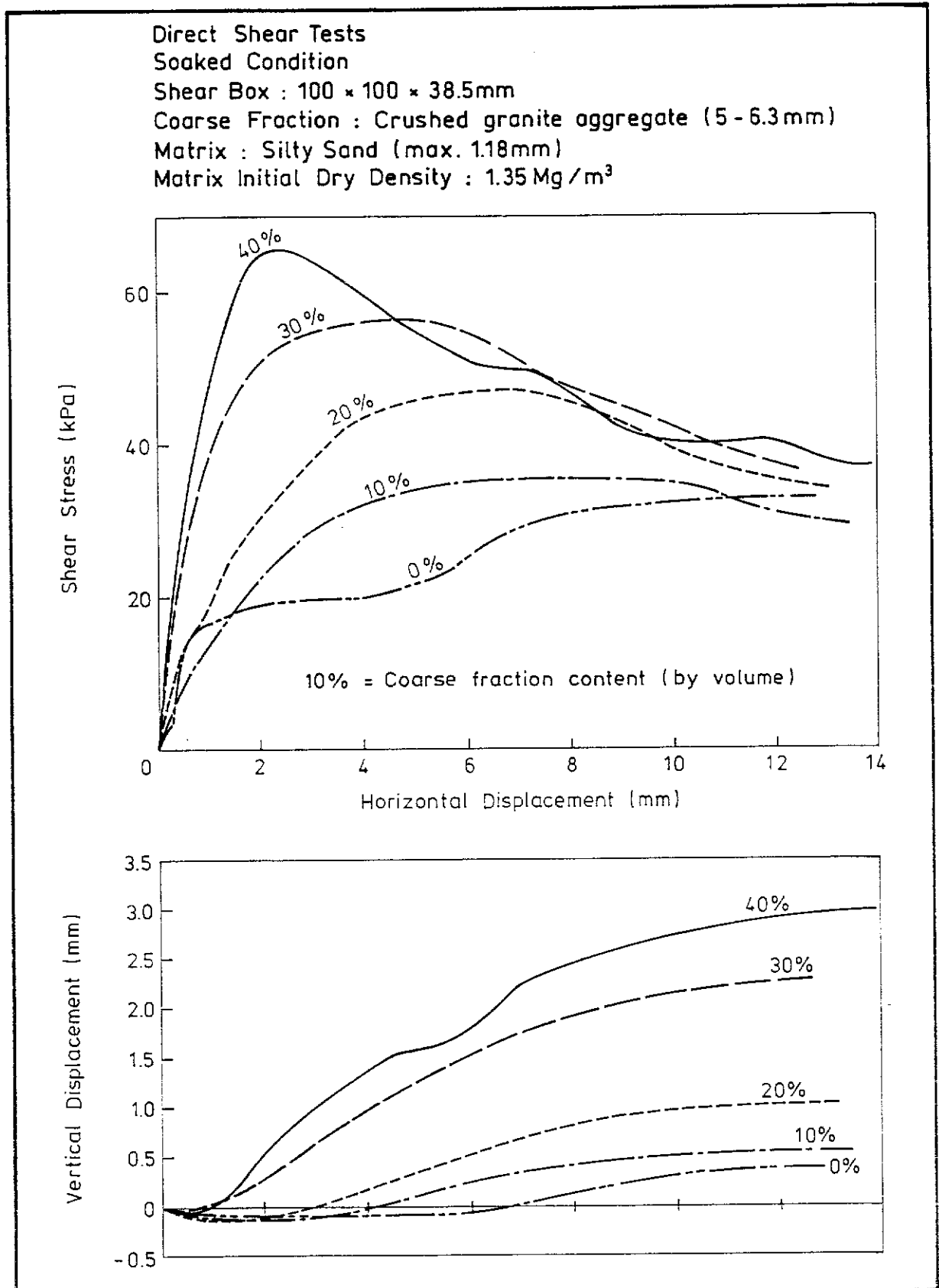


Figure 5.13 - Typical Shear Stress versus Horizontal Displacement Curves for Soil Specimens Containing Aggregates, Tested in 100 mm Direct Shear Box ($\sigma_n = 30$ kPa)

Direct Shear Tests

Soaked Condition

Shear Box : 100 × 100 × 38.5mm

Coarse Fraction : Crushed granite aggregate (5 - 6.3mm)

Matrix : Silty Sand (max. 1.18mm)

Matrix Initial Dry Density : 1.35 Mg/m³

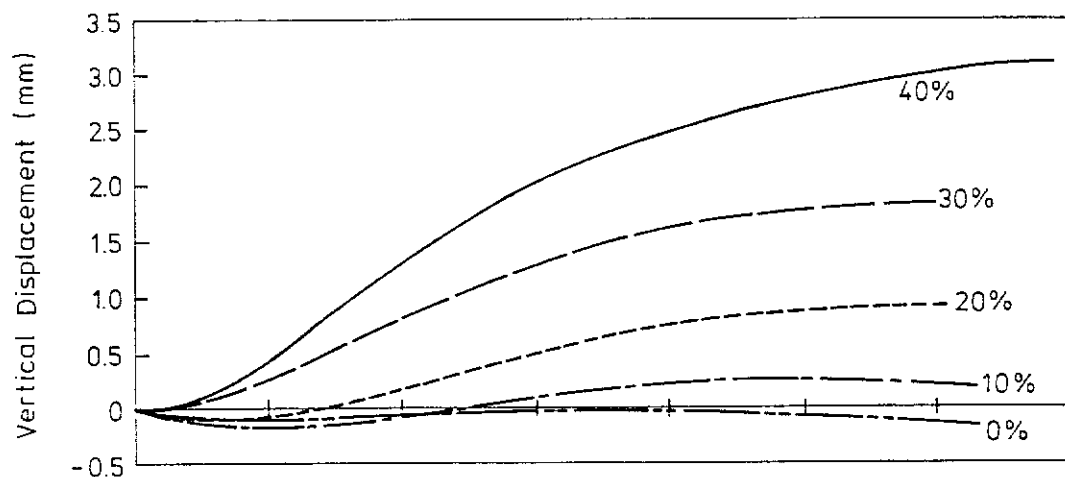
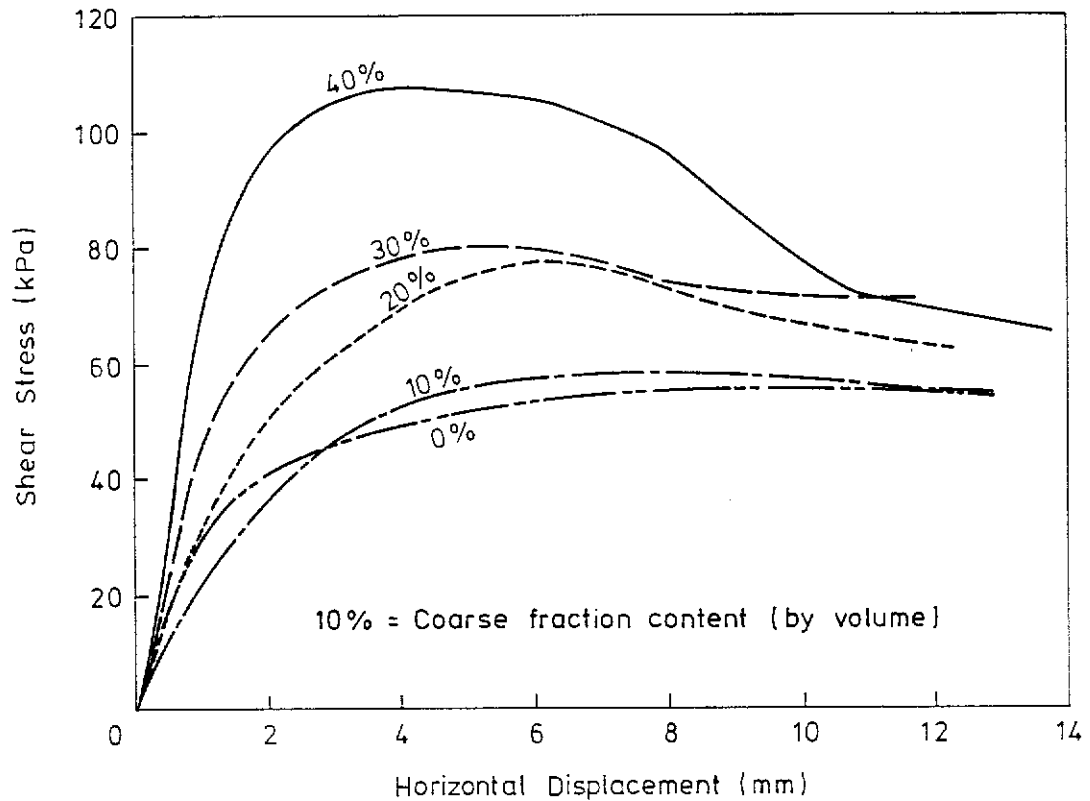


Figure 5.14 - Typical Shear Stress versus Horizontal Displacement Curves for Soil Specimens Containing Aggregates, Tested in 100 mm Direct Shear Box ($\sigma_n = 60$ kPa)

Direct Shear Tests

Soaked Condition

Shear Box : 100 × 100 × 38.5mm

Coarse Fraction : Crushed granite aggregate (5 - 6.3mm)

Matrix : Silty Sand (max. 1.18mm)

Matrix Initial Dry Density : 1.35 Mg/m³

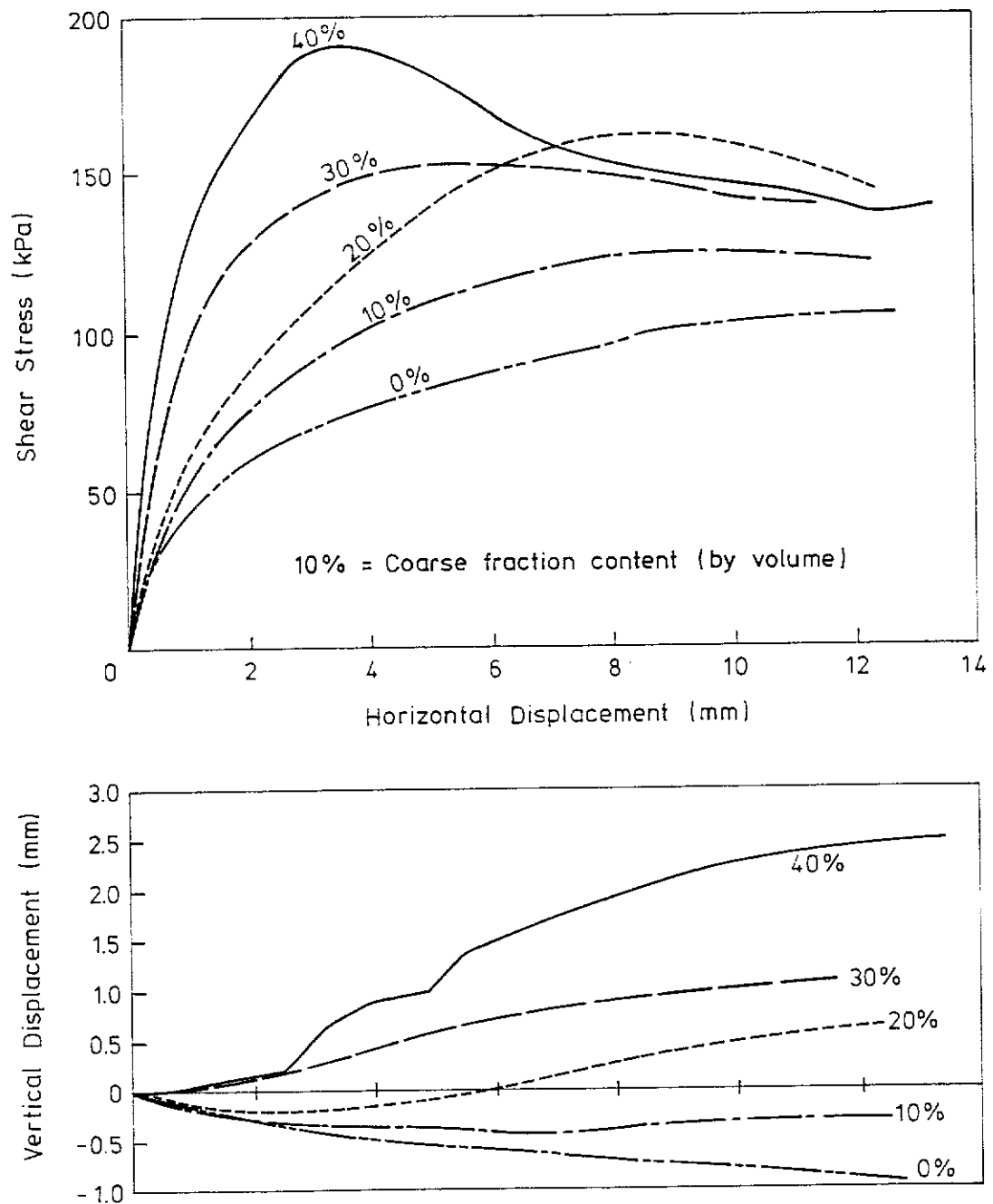


Figure 5.15 - Typical Shear Stress versus Horizontal Displacement Curves for Soil Specimens Containing Aggregates, Tested in 100 mm Direct Shear Box ($\sigma_n = 120$ kPa)

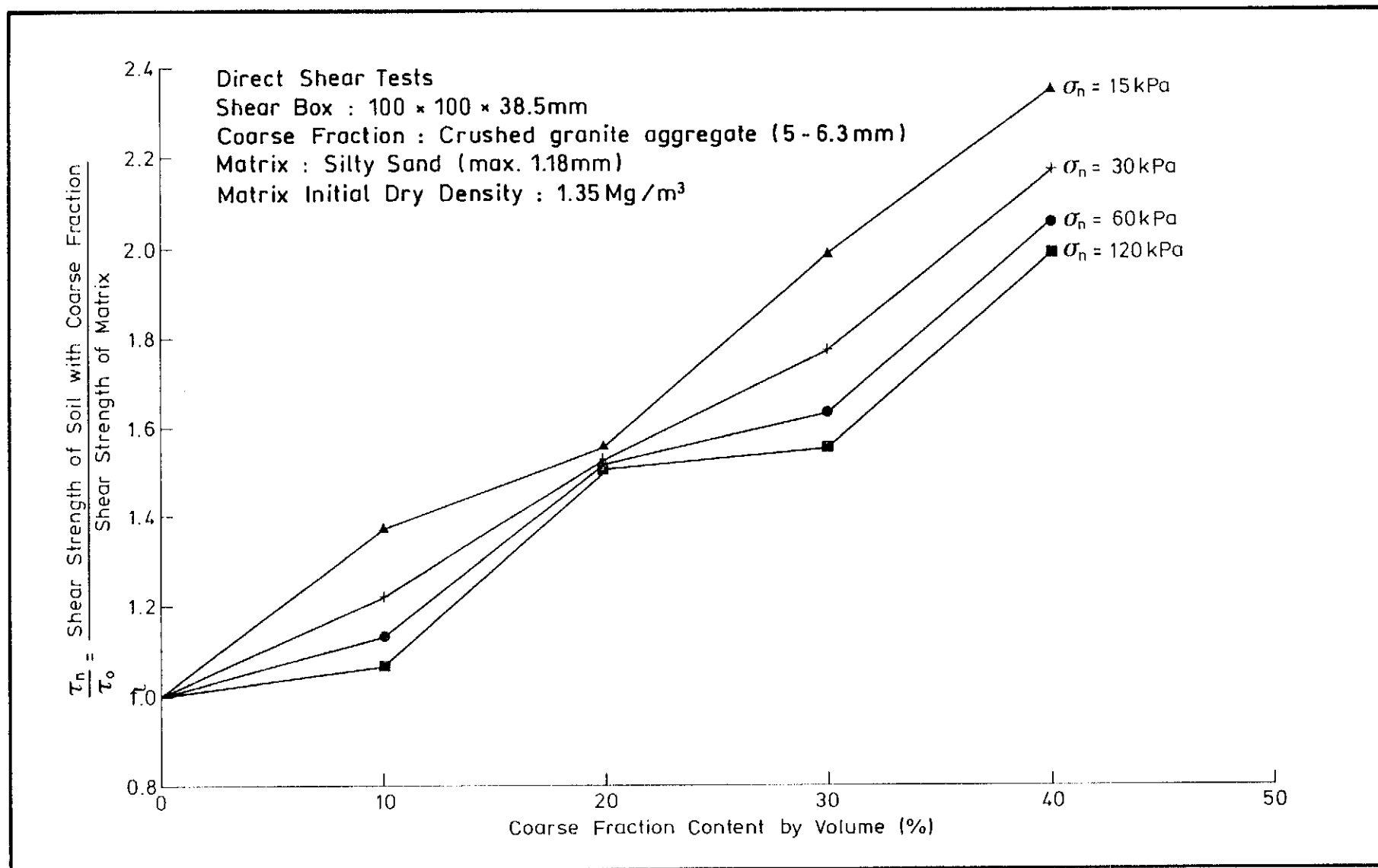


Figure 5.16 - Summary Results of Direct Shear Tests Carried Out on Soil Specimens Containing Aggregates Showing the Effects of Coarse Fraction Content on Normalized Shear Strength (100 mm Shear Box)

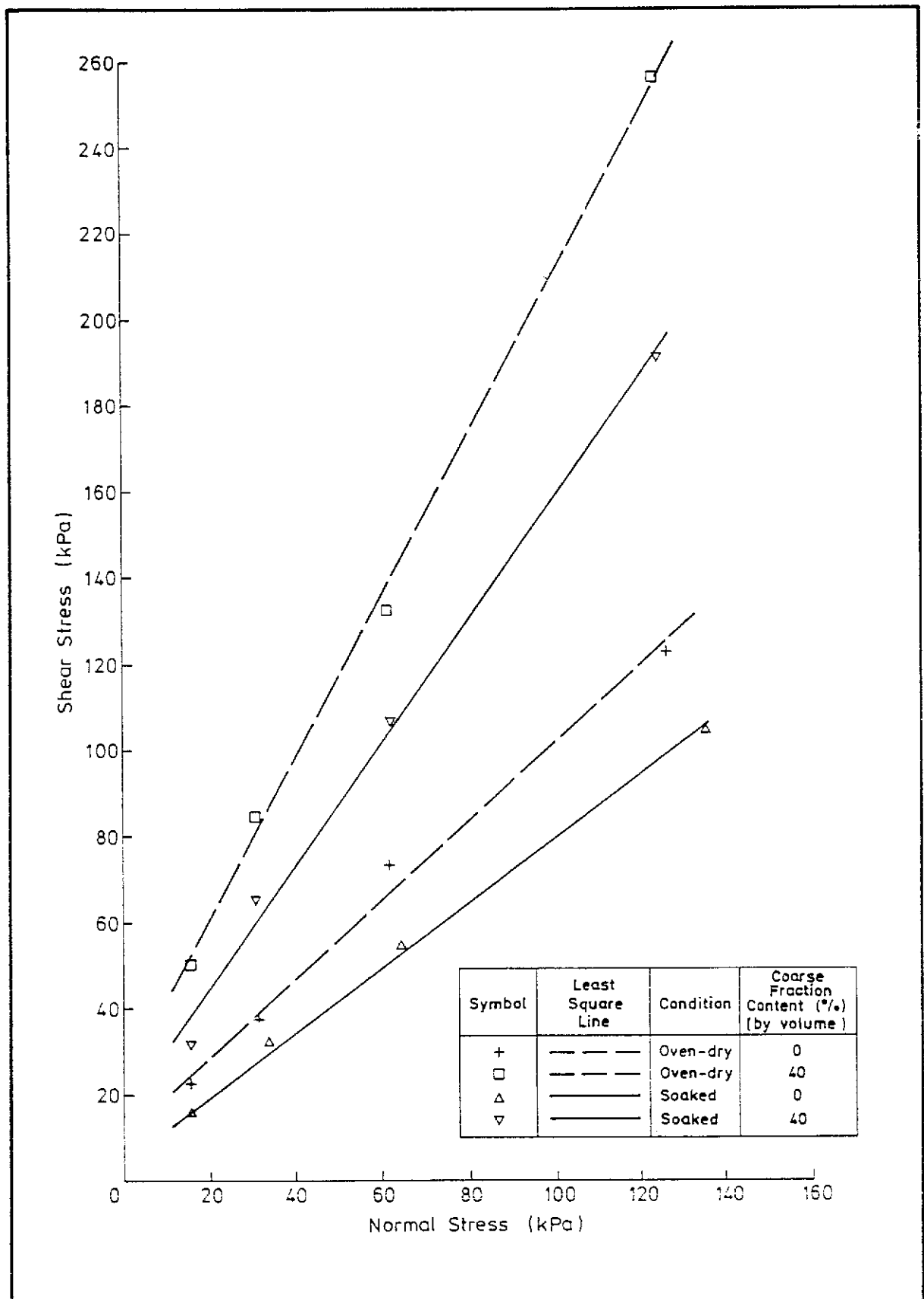
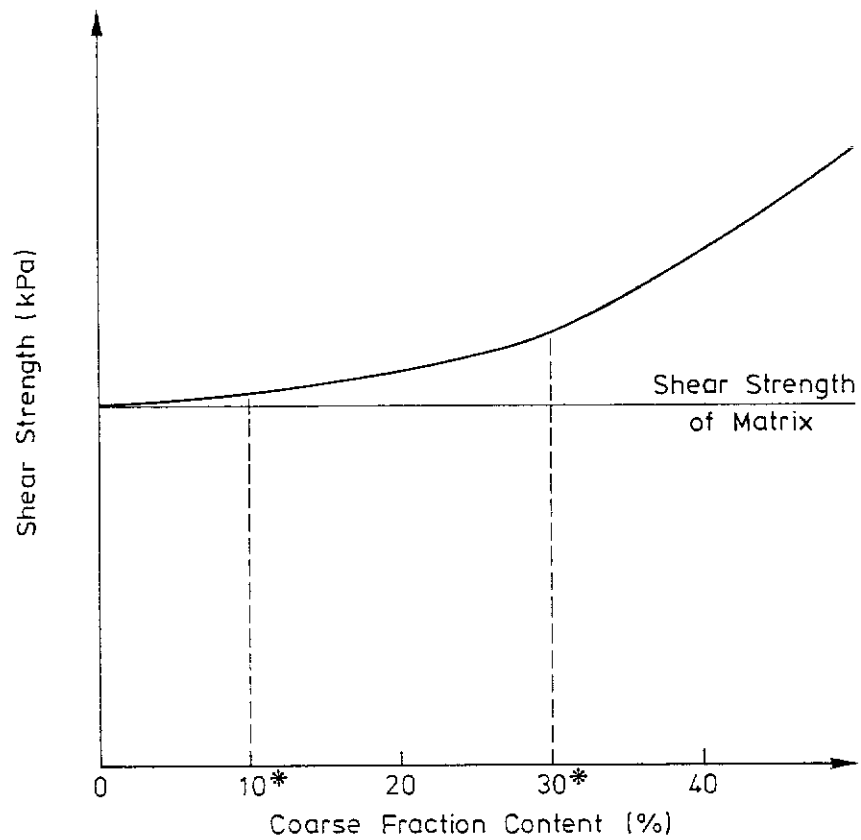


Figure 5.17 - Results of Direct Shear Tests Carried Out on Soil Specimens Containing Aggregates Showing the Effects of Moisture Content on Shear Strength



| | | | | |
|-------------------|--------|-----------------|-----------------|-----------------|
| Primary Control | Matrix | Matrix | Coarse Fraction | Coarse Fraction |
| Secondary Control | — | Coarse Fraction | Matrix | — |

Legend :

* The value depends on a number of factors, e.g. type of test and testing apparatus, shape and size of coarse particles, normal stress, etc.

Figure 5.18 - Schematic Summary of Laboratory Test Results Showing Variation of Shear Strength with Coarse Fraction Content

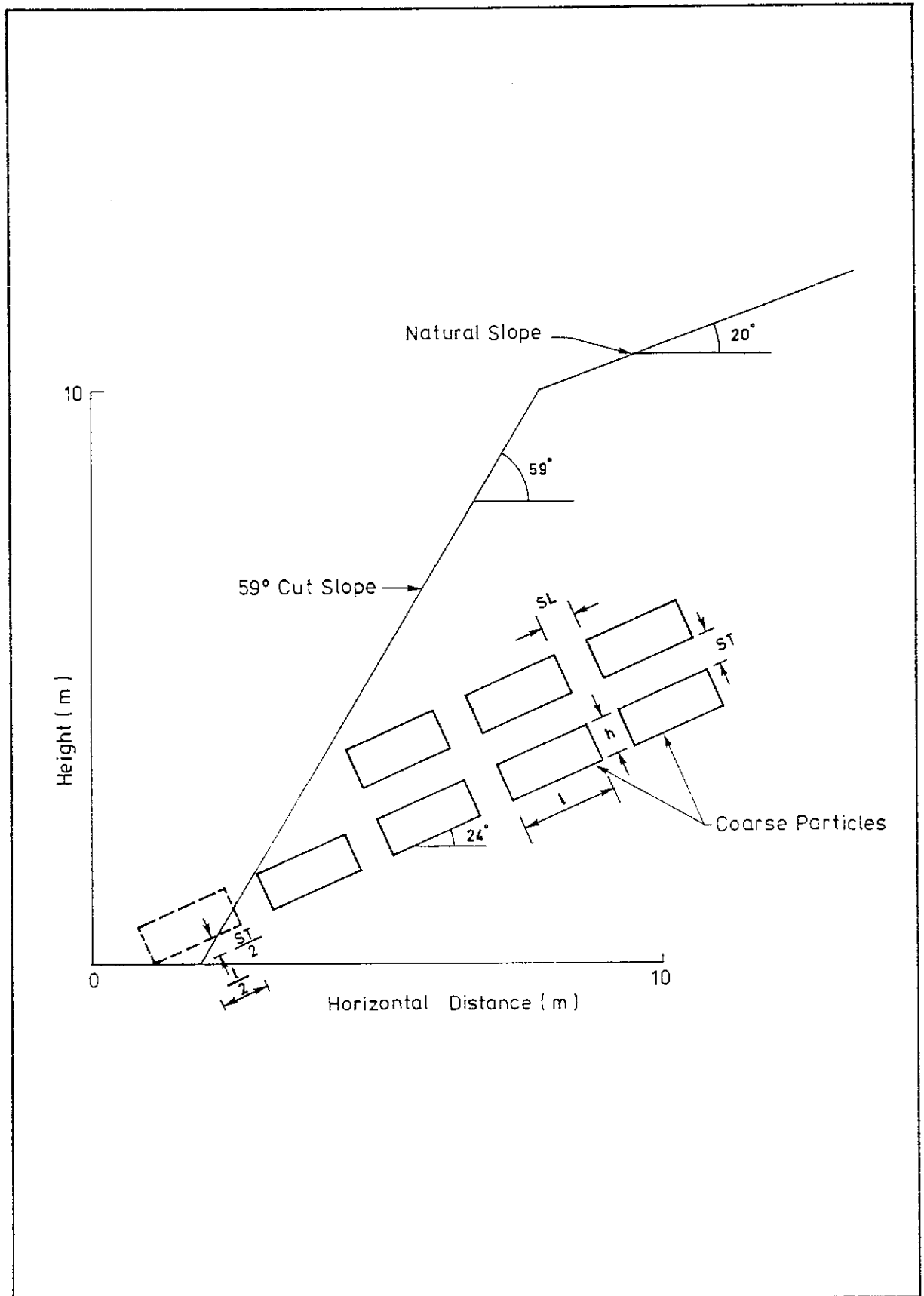


Figure 6.1 - Theoretical Slope Model Adopted to Analyse the Effects of Coarse Fractions on Slope Stability

| Slip No | F.O.S. |
|---------|--------|
| 1 | 1.05 |
| 2 | 1.15 |
| 3 | 1.09 |
| 4 | 1.18 |
| 5 | 1.08 |
| 6 | 1.15 |
| 7 | 1.16 |
| 8 | 1.19 |

| Particle Dimension $h \times l$ (m x m) | Particle Spacing, ST/SL | Matrix Strength | | Slope Height (m) |
|---|----------------------------|-----------------|------------------|---------------------|
| | | c' (kPa) | ϕ' (deg) | |
| 0.8 x 1.6 | 1.0 | 5 | 35 | 10 |

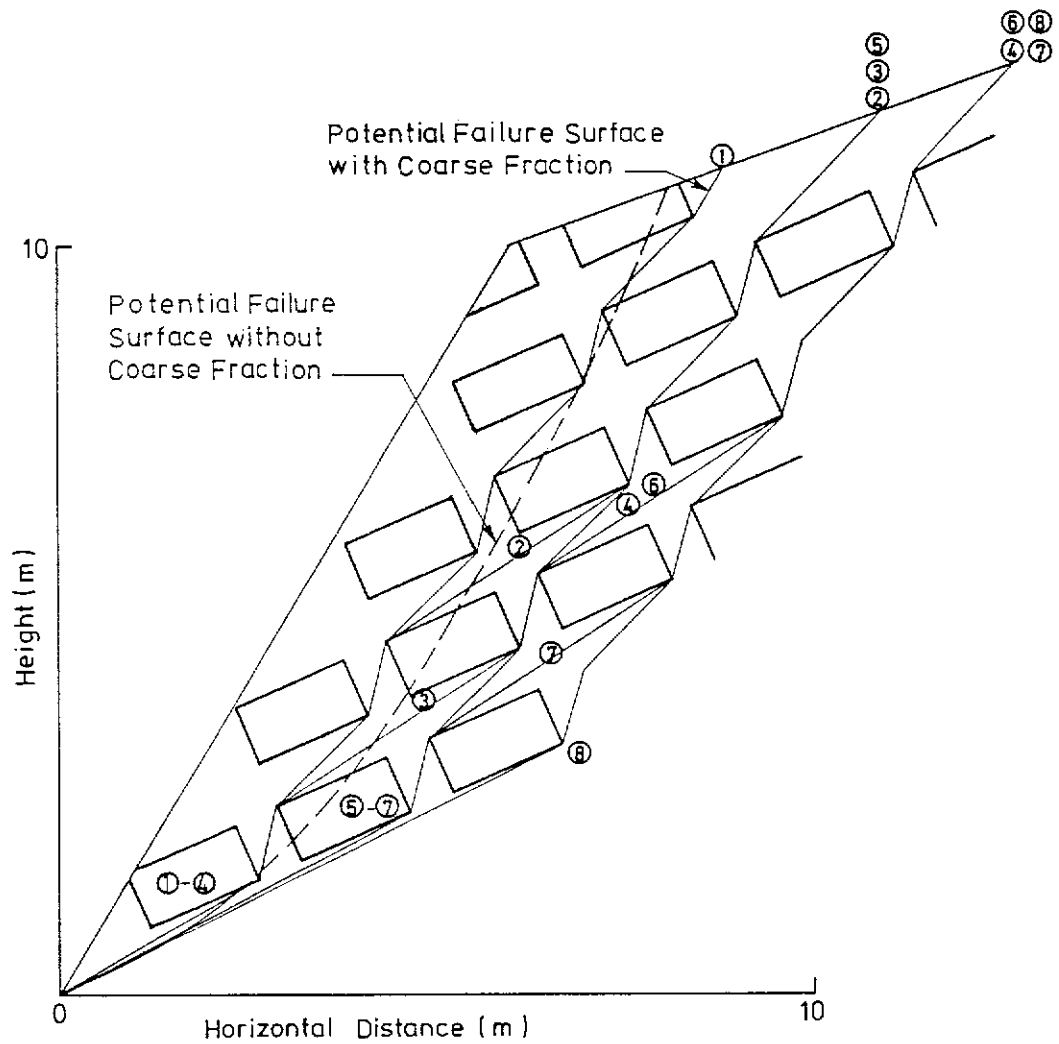


Figure 6.2 - Locations of Typical Potential Failure Surfaces in the Theoretical Slope Model

| Particle Dimension $h \times l$ (m x m) | Particle Spacing, ST/SL | Matrix Strength | | Slope Height (m) |
|---|----------------------------|-----------------------|-----------------------|---------------------|
| | | c' (kPa) | ϕ' (deg) | |
| 0.8x1.6 | 1.0 | 5 | 35 | 10 |
| Factor of Safety:: | | <u>Slip 1</u> 0.88 | <u>Slip 2</u> 1.00 | |

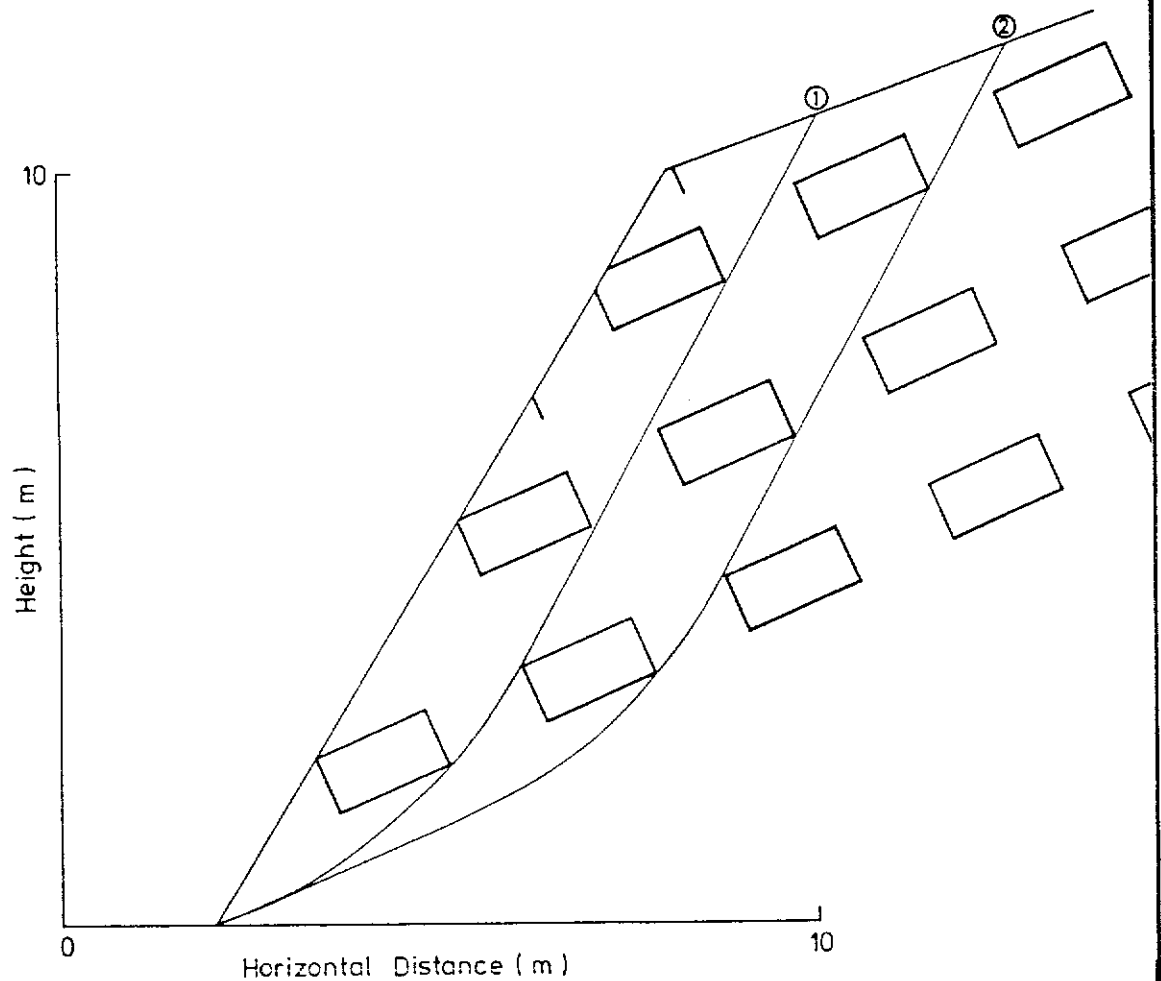


Figure 6.3 - Hand-drawn Potential Failure Surfaces in the Theoretical Slope Model with a Coarse Fraction Content of 20%

| Particle Dimensions, $h \times l$ (m x m) | Particle Spacing, ST/SL | Matrix Strength | | Slope Height (m) |
|---|----------------------------|-----------------|------------------|---------------------|
| | | c' (kPa) | ϕ' (deg) | |
| 0.8 x 1.6 | 1.0 | 5 | 35 | 10 |

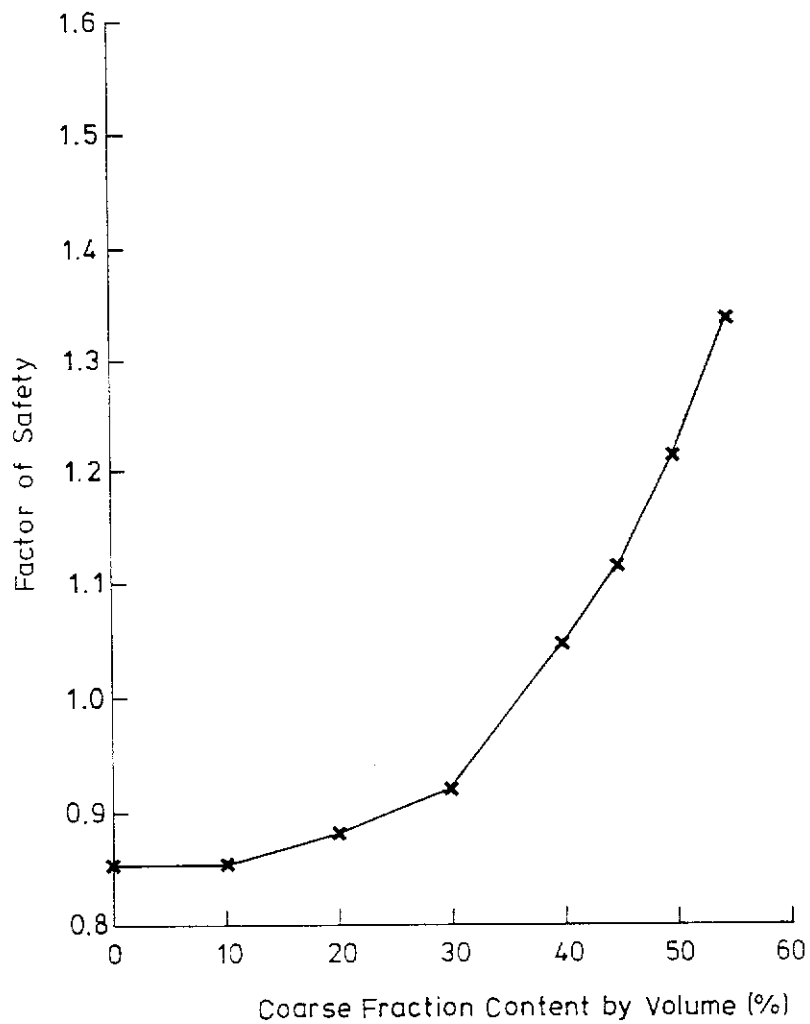


Figure 6.4 - Results of Theoretical Slope Model Analysis Showing the Effects of Coarse Fraction Content on Factor of Safety

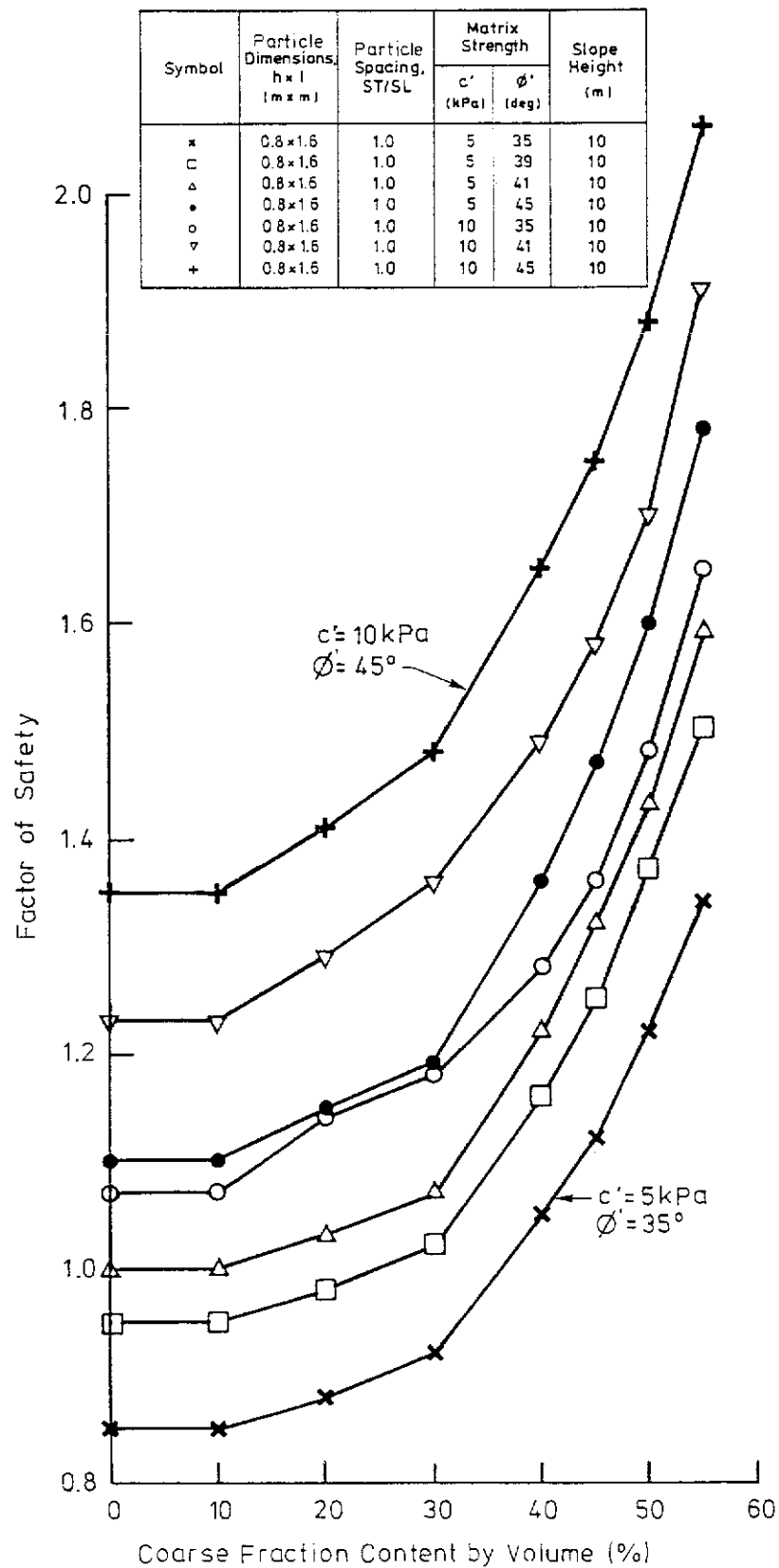


Figure 6.5 - Results of Theoretical Slope Model Analysis Showing the Effects of Matrix Strength and Coarse Fraction Content on Factor of Safety

| Symbol | Particle Dimensions, h x l (m x m) | Particle Spacing, ST/SL | Matrix Strength | | Slope Height (m) |
|--------|--|----------------------------|-----------------|-------------|---------------------|
| | | | c' (kPa) | φ' (deg) | |
| × | 0.8 × 1.6 | 1.0 | 5 | 35 | 10 |
| □ | 0.8 × 1.6 | 1.0 | 5 | 39 | 10 |
| △ | 0.8 × 1.6 | 1.0 | 5 | 41 | 10 |
| • | 0.8 × 1.6 | 1.0 | 5 | 45 | 10 |
| ○ | 0.8 × 1.6 | 1.0 | 10 | 35 | 10 |
| ▽ | 0.8 × 1.6 | 1.0 | 10 | 41 | 10 |
| + | 0.8 × 1.6 | 1.0 | 10 | 45 | 10 |

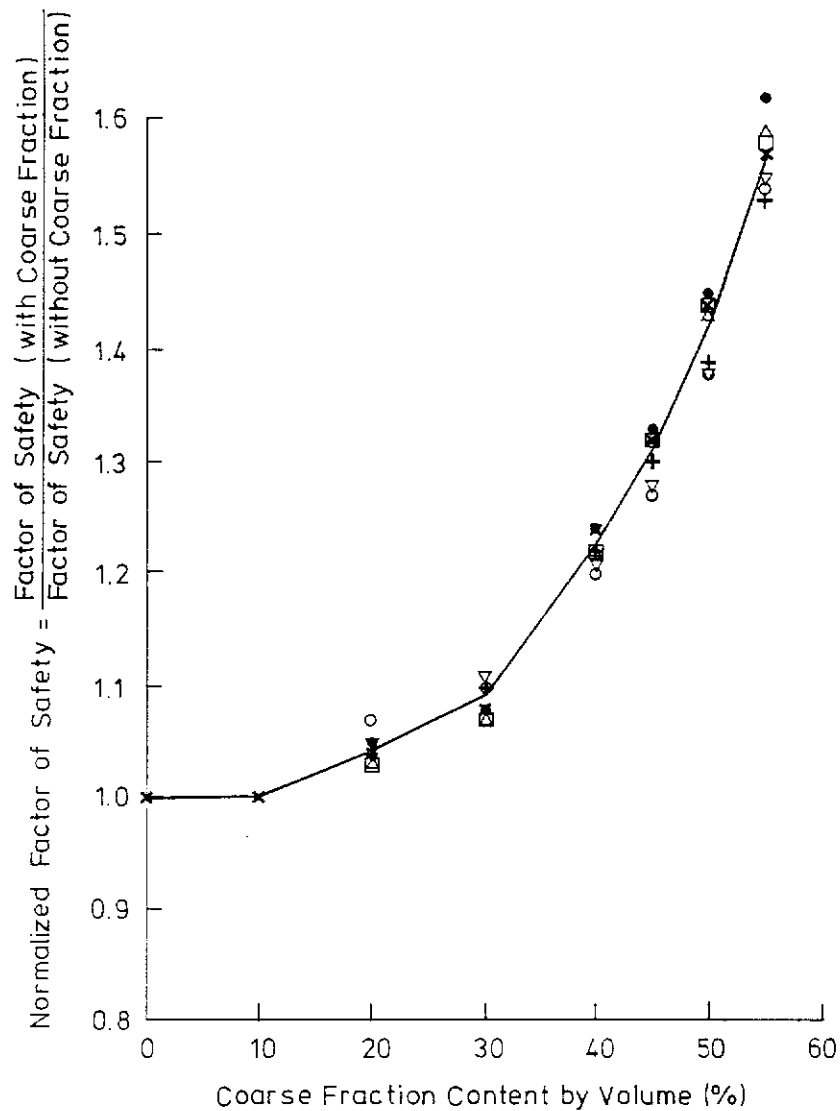


Figure 6.6 - Results of Theoretical Slope Model Analysis Showing the Effects of Coarse Fraction Content on Normalized Factor of Safety for Different Matrix Strengths

| Particle Dimensions, $h \times l$ (mm) | Matrix Strength | | Coarse Fraction Content by Volume (%) | Slope Height (m) |
|---|-----------------|------------------|---------------------------------------|------------------|
| | c' (kPa) | ϕ' (deg) | | |
| 0.8 x 1.6 | 5 | 35 | 40 | 10 |
| <div style="display: flex; align-items: center;"> <div style="margin-right: 10px;"> $\left. \begin{array}{c} (45) \\ (30) \end{array} \right\}$ </div> <div> Range of factor of safety between 30% and 45% coarse fraction content </div> </div> | | | | |

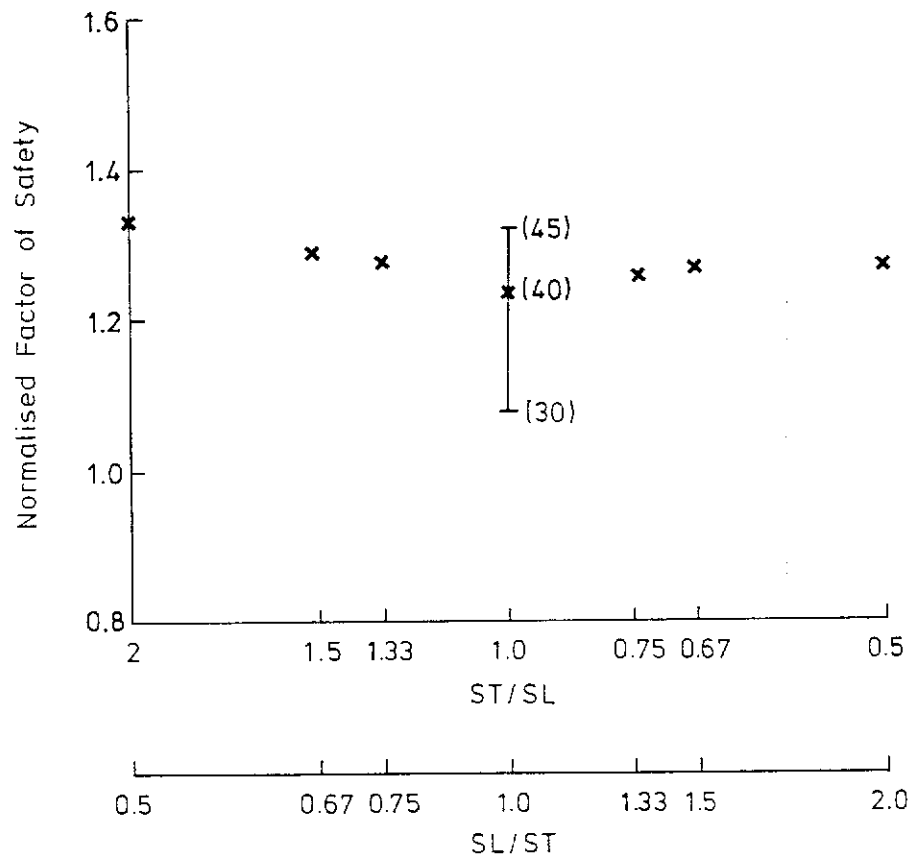


Figure 6.7 - Results of Theoretical Slope Model Analysis Showing the Effects of Particle Spacing and Coarse Fraction Content on Normalized Factor of Safety

| Symbol | Particle Dimensions, $h \times l$ (m x m) | Particle Spacing, ST/SL | Matrix Strength | | Slope Height (m) |
|--------|---|----------------------------|-----------------|------------------|---------------------|
| | | | c' (kPa) | ϕ' (deg) | |
| □ | 1.6 x 1.6 | 1.0 | 5 | 35 | 10 |
| × | 0.8 x 0.8 | 1.0 | 5 | 35 | 10 |

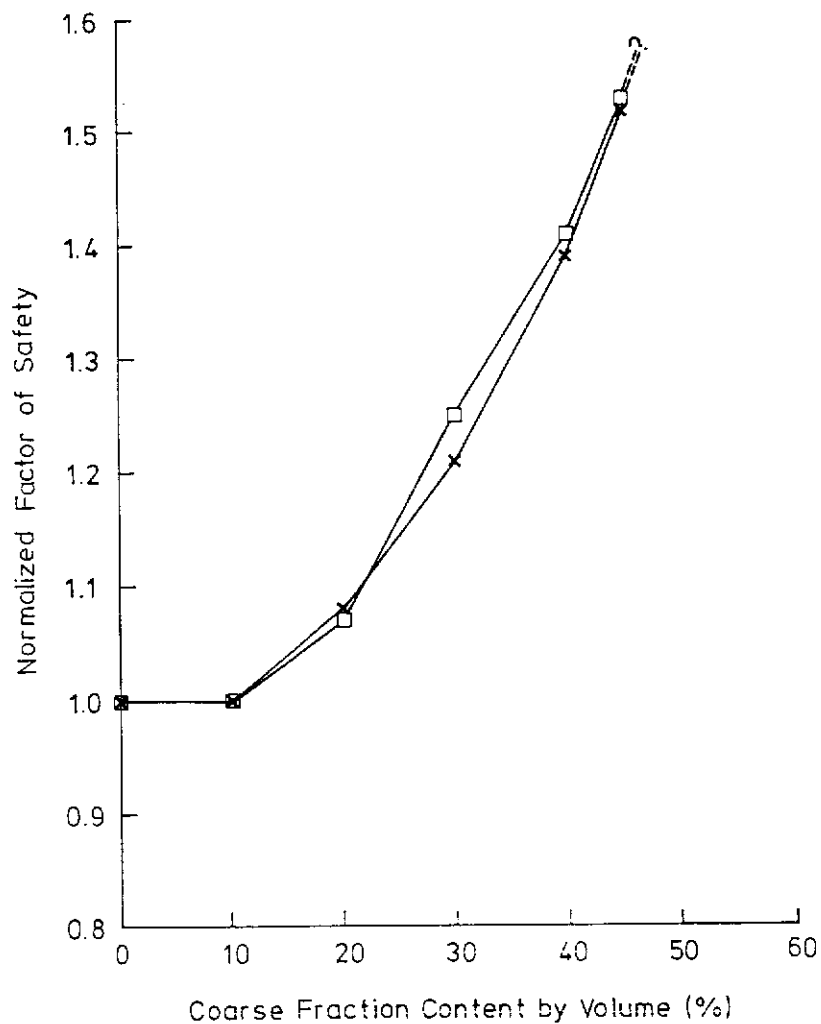


Figure 6.8 - Results of Theoretical Slope Model Analysis Showing the Effects of Particle Size (Constant Shape) on Normalized Factor of Safety

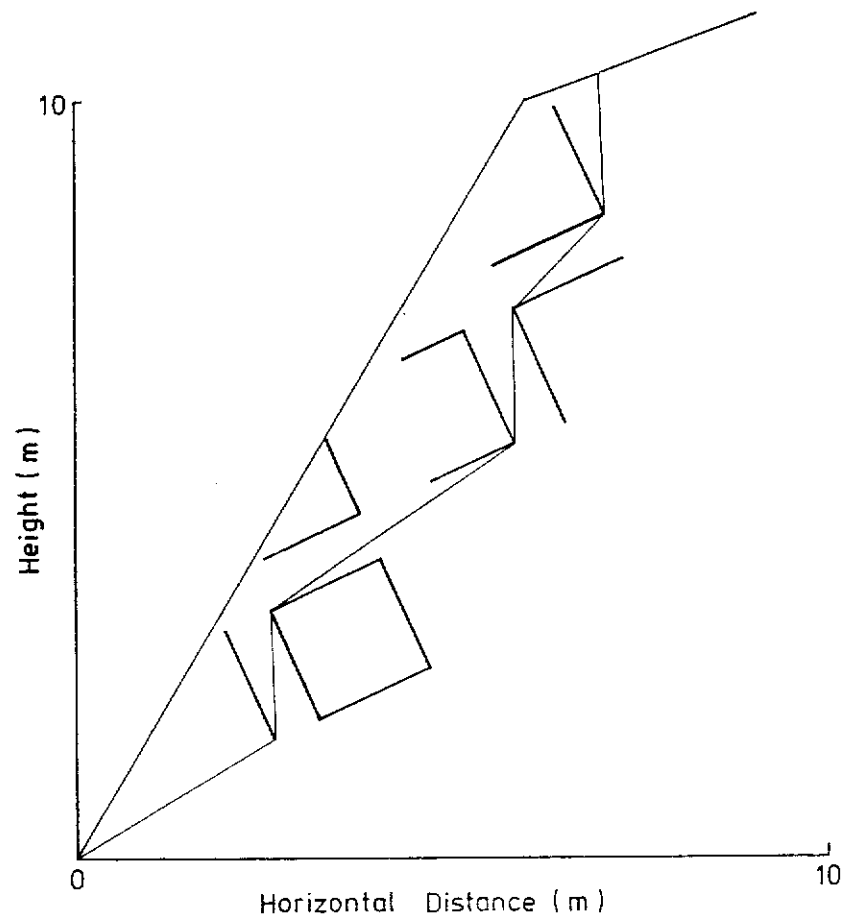


Figure 6.9 - Potential Failure Surface with Vertical-to Forward-Inclined Portions in the Theoretical Slope Model

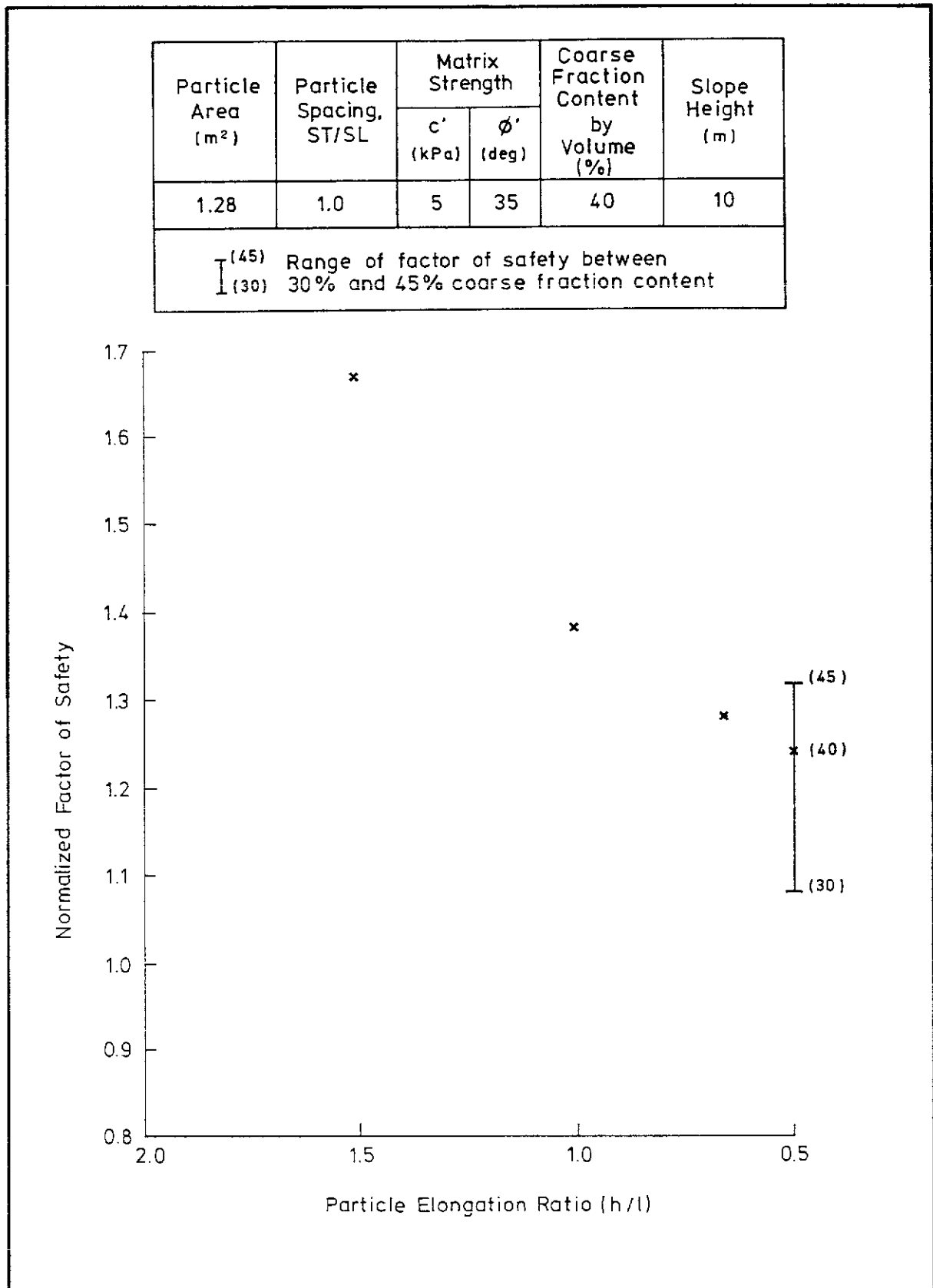


Figure 6.10 - Results of Theoretical Slope Model Analysis Showing the Effects of Particle Elongation Ratio (Constant Area) on Normalized Factor of Safety

| Particle Height (m) | Particle Spacing, ST/SL | Matrix Strength | | Slope Height (m) |
|--|----------------------------|-----------------|------------------|---------------------|
| | | c' (kPa) | ϕ' (deg) | |
| 0.8 | 1.0 | 5 | 35 | 10 |
| <div style="display: flex; align-items: center;"> <div style="margin-right: 10px;"> <div style="border-left: 1px solid black; height: 20px; width: 10px; margin-bottom: 5px;"></div> <div style="border-left: 1px solid black; height: 20px; width: 10px; margin-bottom: 5px;"></div> </div> <div> (45) Range of factor of safety between 30% and 45% coarse fraction content (30) </div> </div> | | | | |

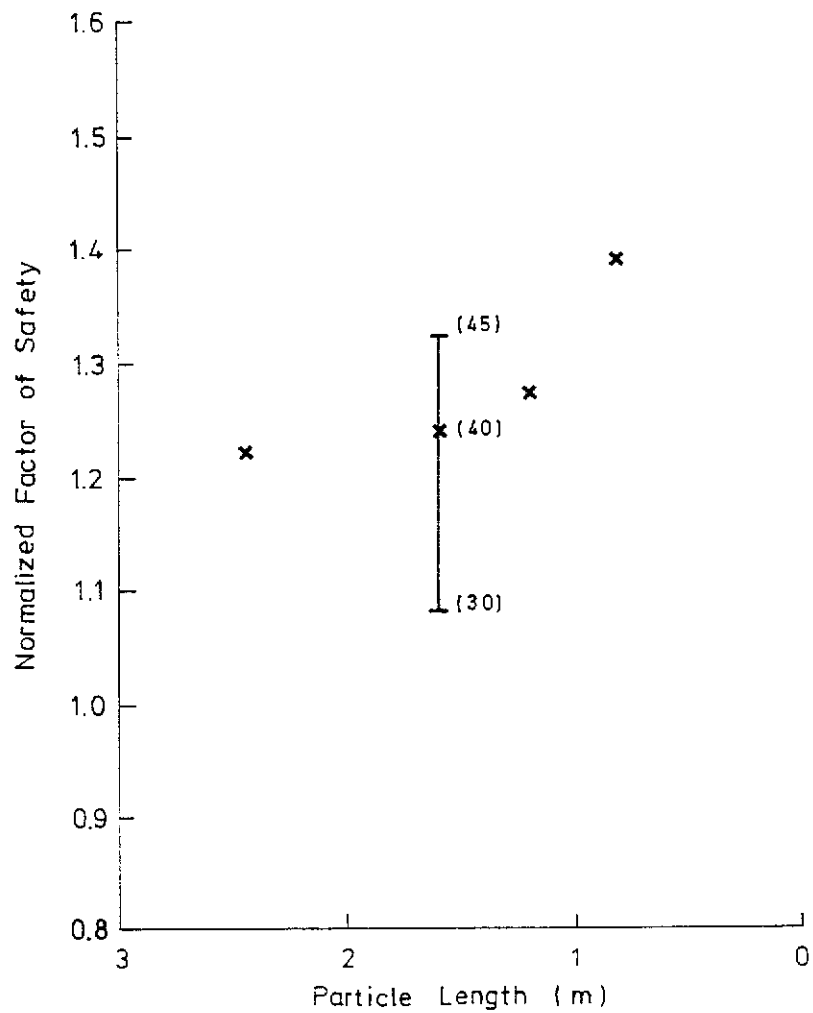


Figure 6.11 - Results of Theoretical Slope Model Analysis Showing the Effects of Particle Length on Normalized Factor of Safety

| Particle Length (m) | Particle Spacing, ST/SL | Matrix Strength | | Slope Height (m) |
|--|----------------------------|-----------------|------------------|---------------------|
| | | c' (kPa) | ϕ' (deg) | |
| 1.6 | 1.0 | 5 | 35 | 10 |
| <div style="display: flex; align-items: center;"> <div style="margin-right: 10px;"> <div style="border-left: 1px solid black; height: 20px; width: 10px; margin-bottom: 5px;"></div> <div style="border-left: 1px solid black; height: 20px; width: 10px; margin-top: 5px;"></div> </div> <div> (45) Range of factor of safety between 30 % and 45% coarse fraction content (30) </div> </div> | | | | |

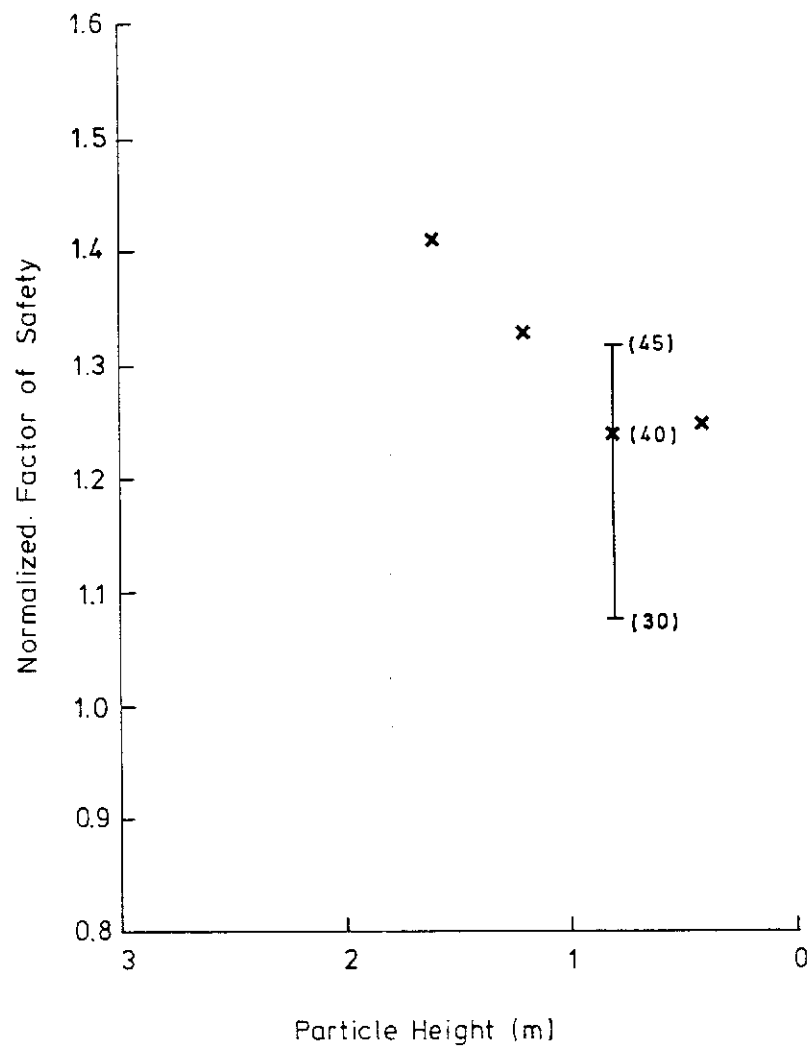
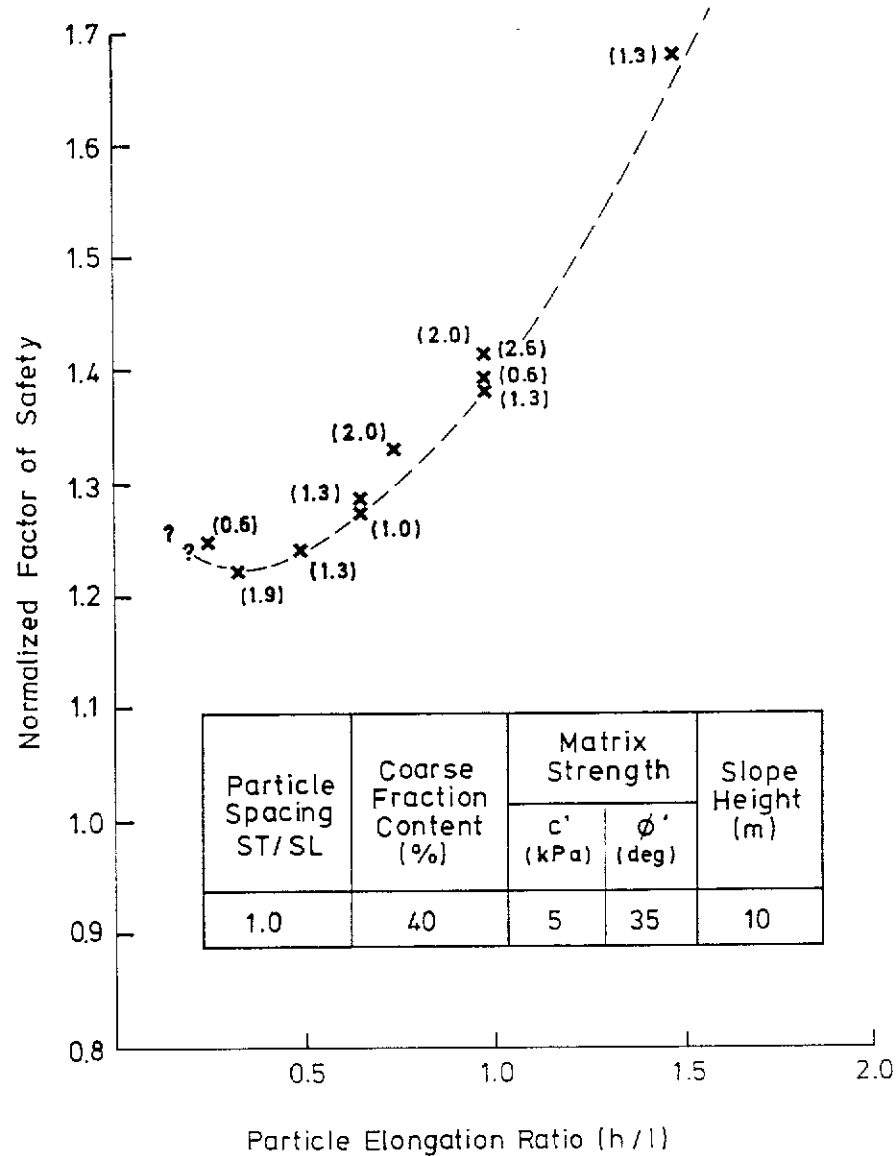


Figure 6.12 - Results of Theoretical Slope Model Analysis Showing the Effects of Particle Height on Normalized Factor of Safety



Legend :

(1.0) Particle area in m^2

Figure 6.13 - Summary of Theoretical Slope Model Analysis Showing the Effects of Particle Elongation Ratio on Normalized Factor of Safety

| Symbol | Particle Shape | Particle Area (m ²) | Particle Spacing, ST/SL | Matrix Strength | | Slope Height (m) |
|--------|------------------|---------------------------------|-------------------------|-----------------|----------|------------------|
| | | | | c' (kPa) | φ' (deg) | |
| x □ | Circle Square | 2.01 | 1.0 | 5 | 35 | 10 |

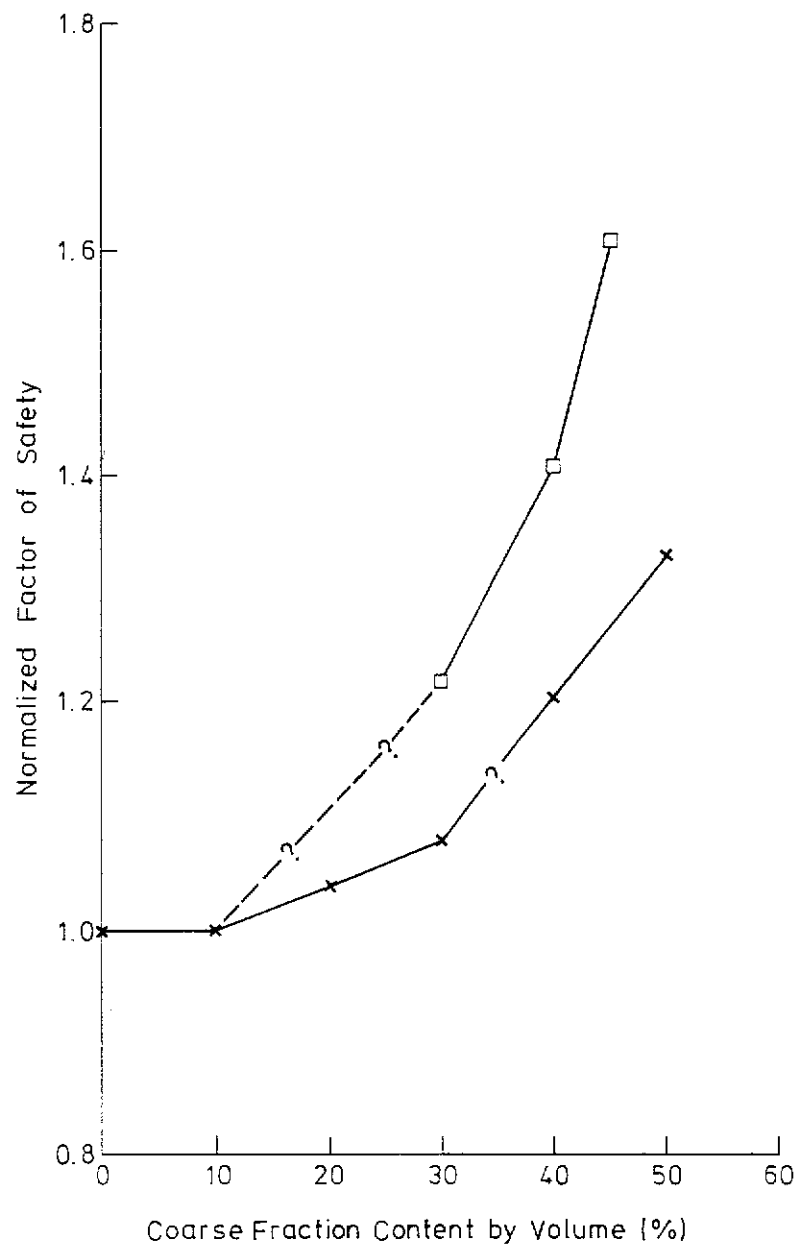


Figure 6.14 - Summary of Theoretical Slope Model Analysis Showing the Effects of Particle Shape (Constant Area) on Normalized Factor of Safety

| Symbol | Particle Dimension, h x l (m x m) | Particle Spacing, ST/SL | Matrix Strength | | Slope Height (m) |
|--------|---|----------------------------|-----------------|------------------|---------------------|
| | | | c' (kPa) | ϕ' (deg) | |
| □ | 0.8 x 1.6 | 1.0 | 5 | 35 | 10 |
| x | 0.8 x 1.6 | 1.0 | 5 | 35 | 15 |

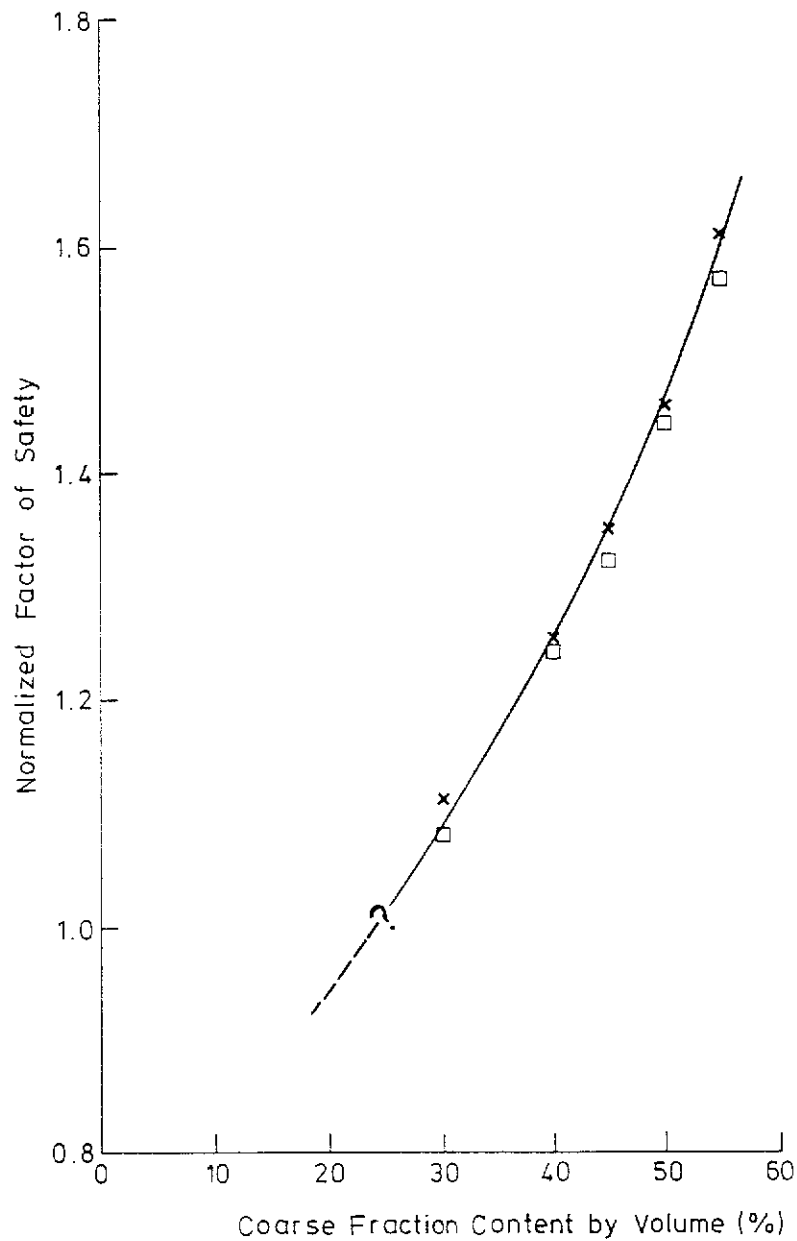


Figure 6.15 - Summary of Theoretical Slope Model Analysis Showing the Effects of Slope Height on Normalized Factor of Safety

| Particle Density (Mg/m ³) | Matrix Density (Mg/m ³) | Particle Dimension, h × l (m × m) | Particle Spacing, ST/SL | Matrix Strength | | Slope Height (m) |
|--|--|---|----------------------------|-----------------|-------------|---------------------|
| | | | | c' (kPa) | φ' (deg) | |
| 2.55 | 1.50 | 0.8 × 1.6 | 1.0 | 5 | 35 | 10 |
| (14.7) Mass Unit Weight in kN/m ³ | | | | | | |

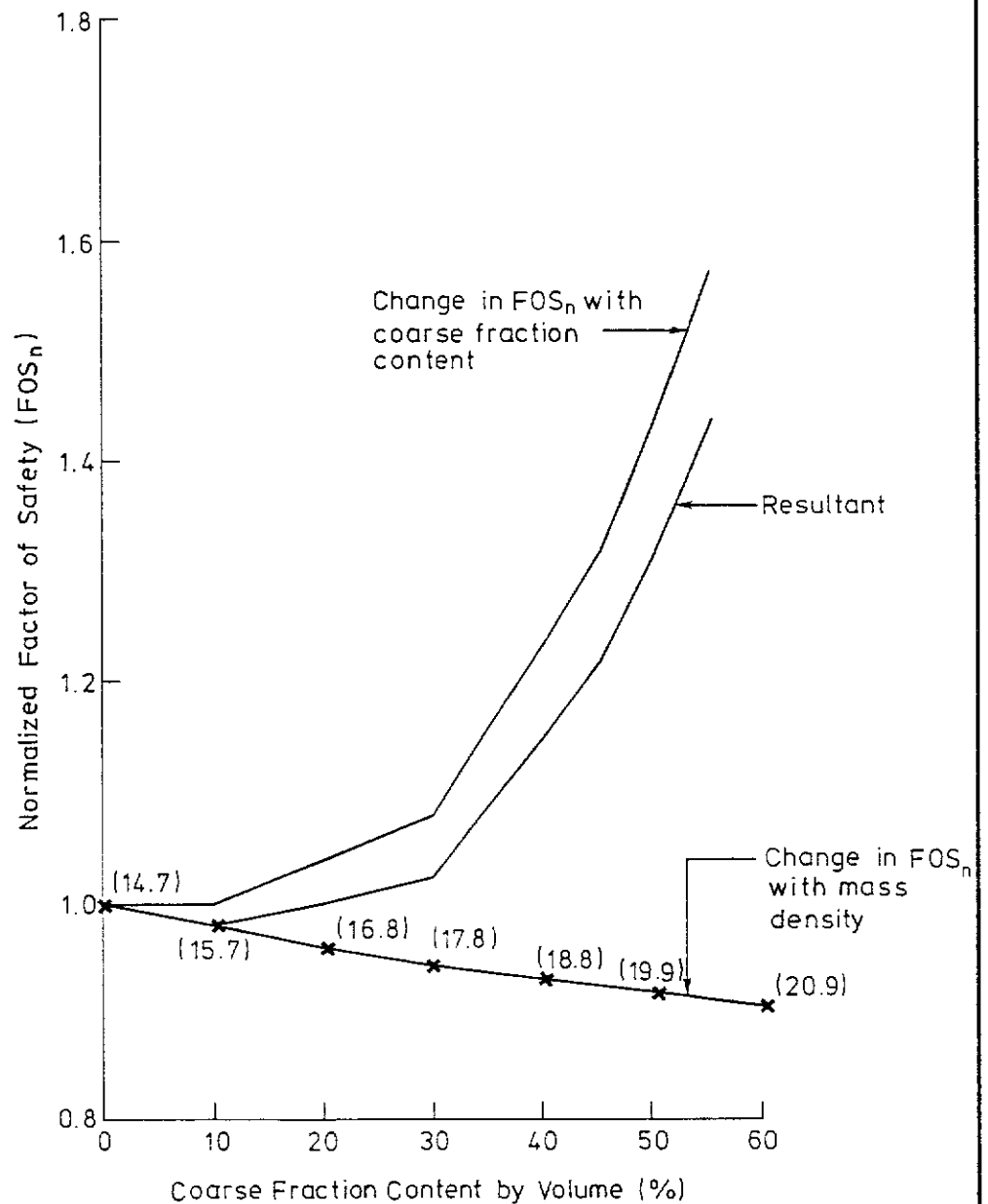


Figure 6.16 - Results of Theoretical Slope Model Analysis Showing Combined Effects of Increasing Coarse Fraction Content and Mass Density on Normalized Factor of Safety

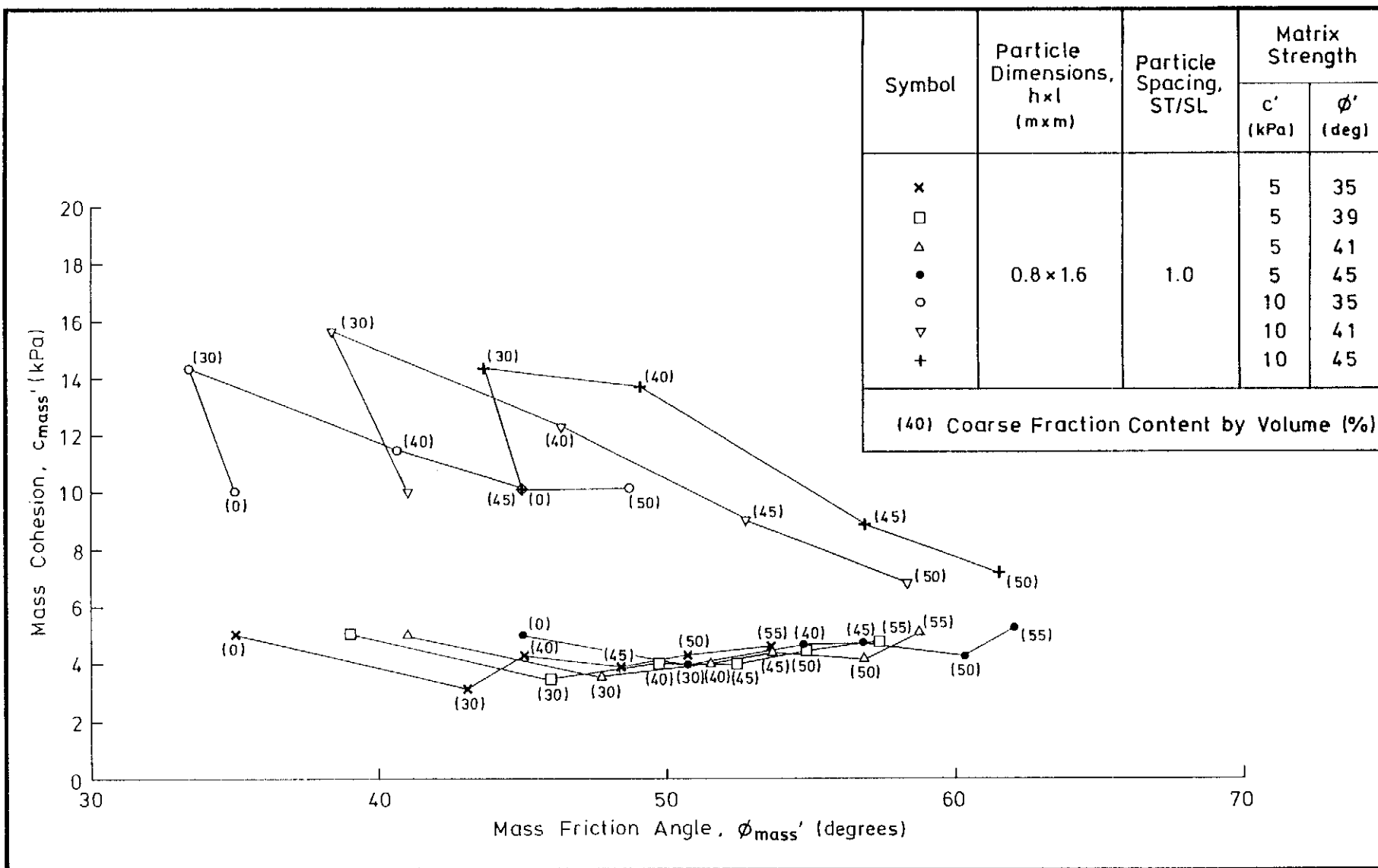


Figure 6.17 - Summary Results of Theoretical Slope Model Analysis Showing the Effects of Coarse Fraction Content on Back-calculated Mass Cohesion and Mass Friction Angle for Different Matrix Strengths

| Symbol | Particle Dimension, h x l (m x m) | Particle Spacing, ST/SL | Matrix Strength | |
|--------|---|----------------------------|-----------------|------------------|
| | | | c' (kPa) | ϕ' (deg) |
| x | 0.8 x 1.6 | 1.0 | 5 | 35 |
| □ | | | | 39 |
| △ | | | | 41 |
| • | | | | 45 |

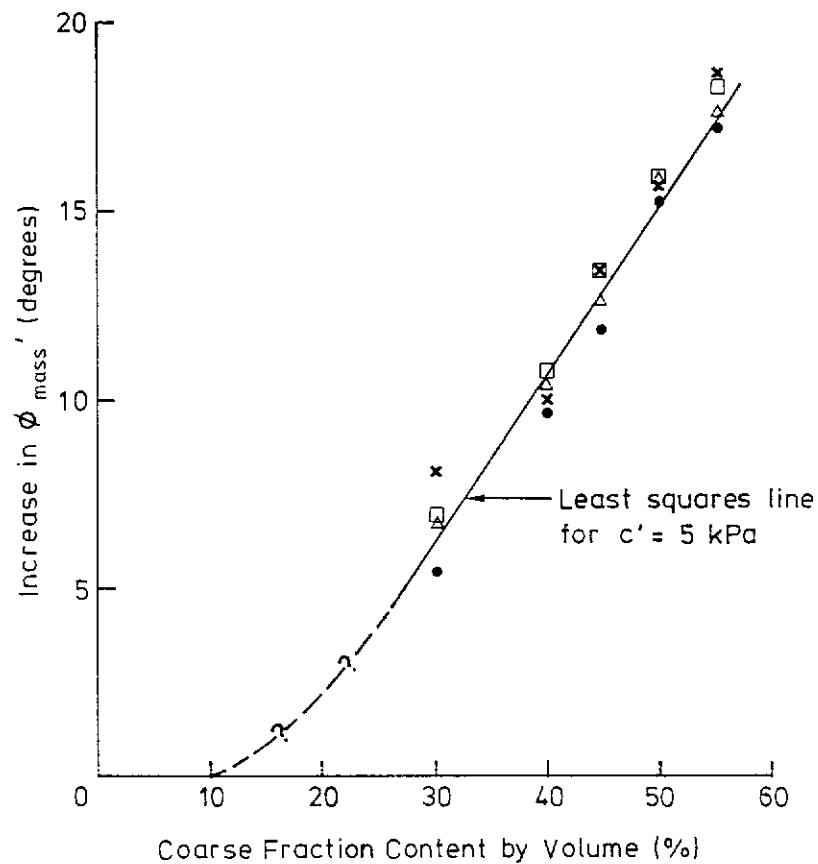


Figure 6.18 - Summary Results of Theoretical Slope Model Analysis Showing the Effects of Coarse Fraction Content Expressed as Increases in Mass Friction Angle

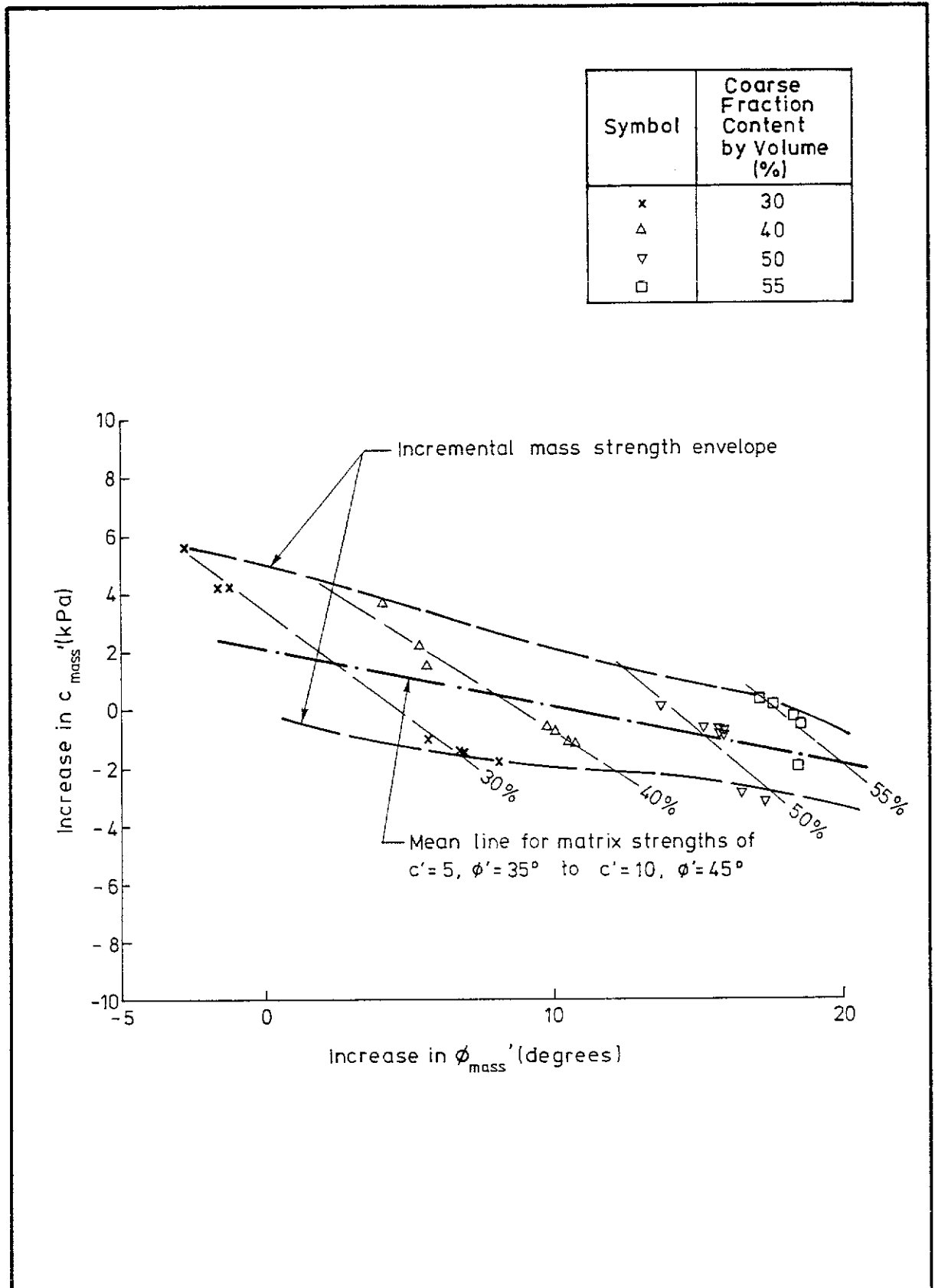


Figure 6.19 - Summary Results of Theoretical Slope Model Analysis Showing the Relationship between Mass Friction Angle, Mass Cohesion and Coarse Fraction Content

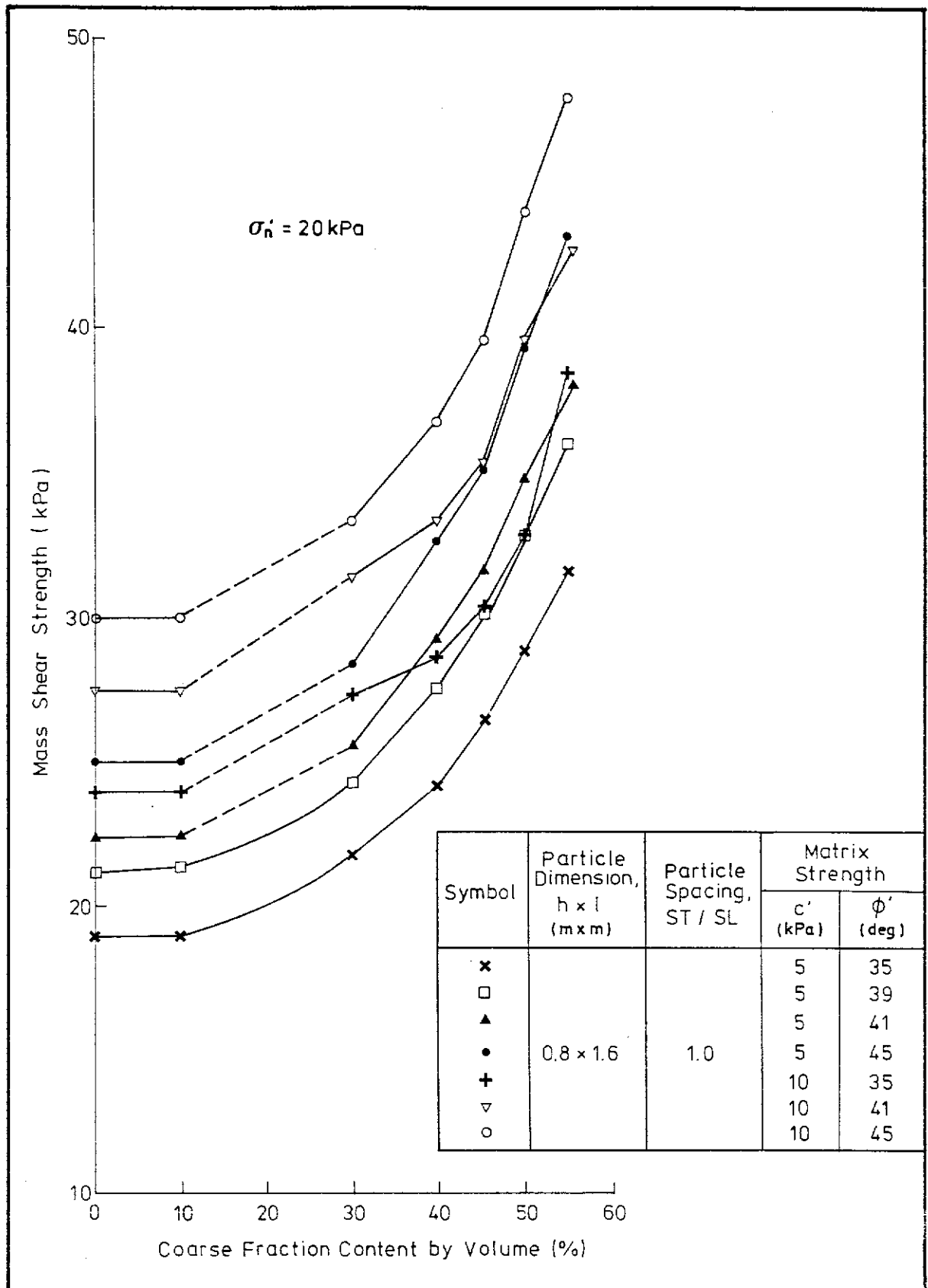


Figure 6.20 - Summary Results of Theoretical Slope Model Analysis Showing the Effects of Coarse Fraction and Matrix Strength on Back-calculated Mass Shear Strength

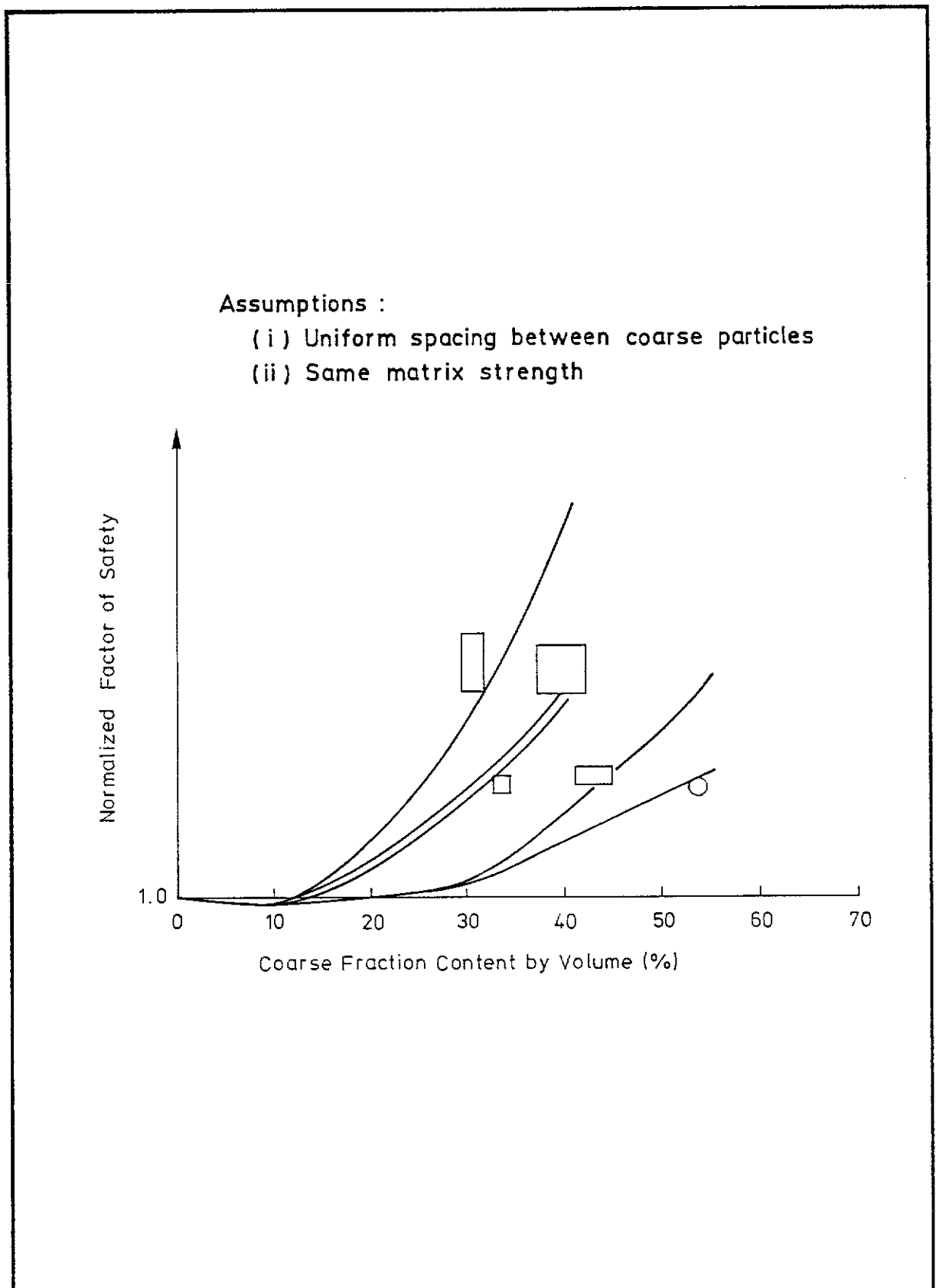


Figure 6.21 - Schematic Diagram Summarizing the Results of Theoretical Slope Model Analysis on the Effects of Coarse Fraction Properties on Normalized Factor of Safety

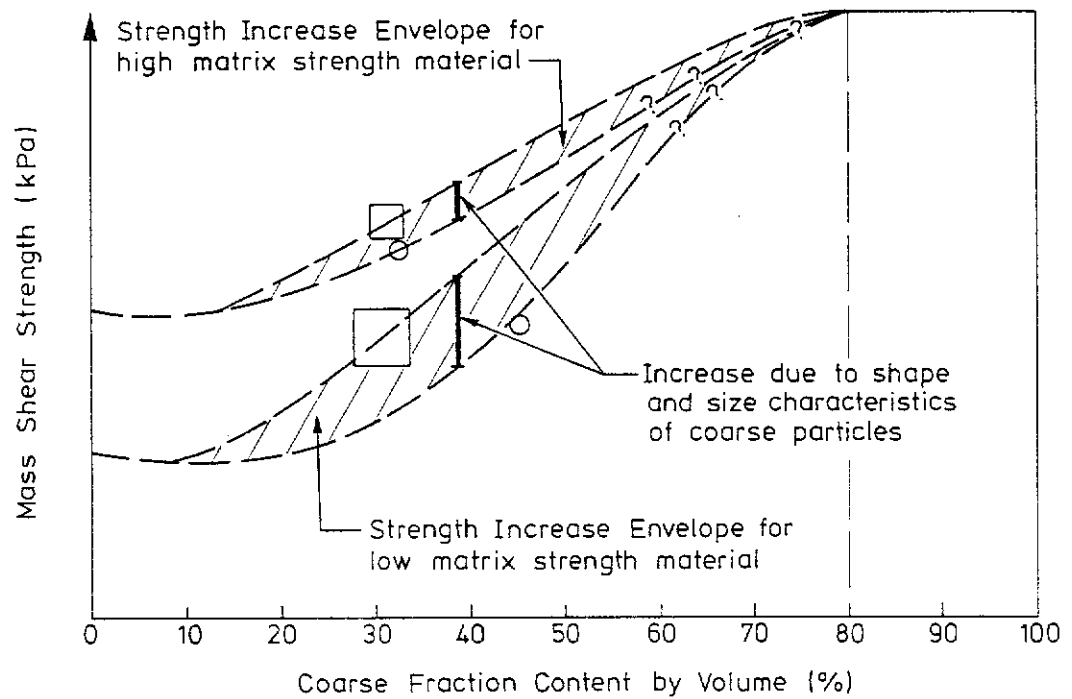


Figure 7.1 - Schematic Diagram Showing the Results of Laboratory Tests, Back Analysis and Theoretical Slope Model Analysis on the Effects of Coarse Fraction and Matrix Strength on Mass Shear Strength of Colluvium

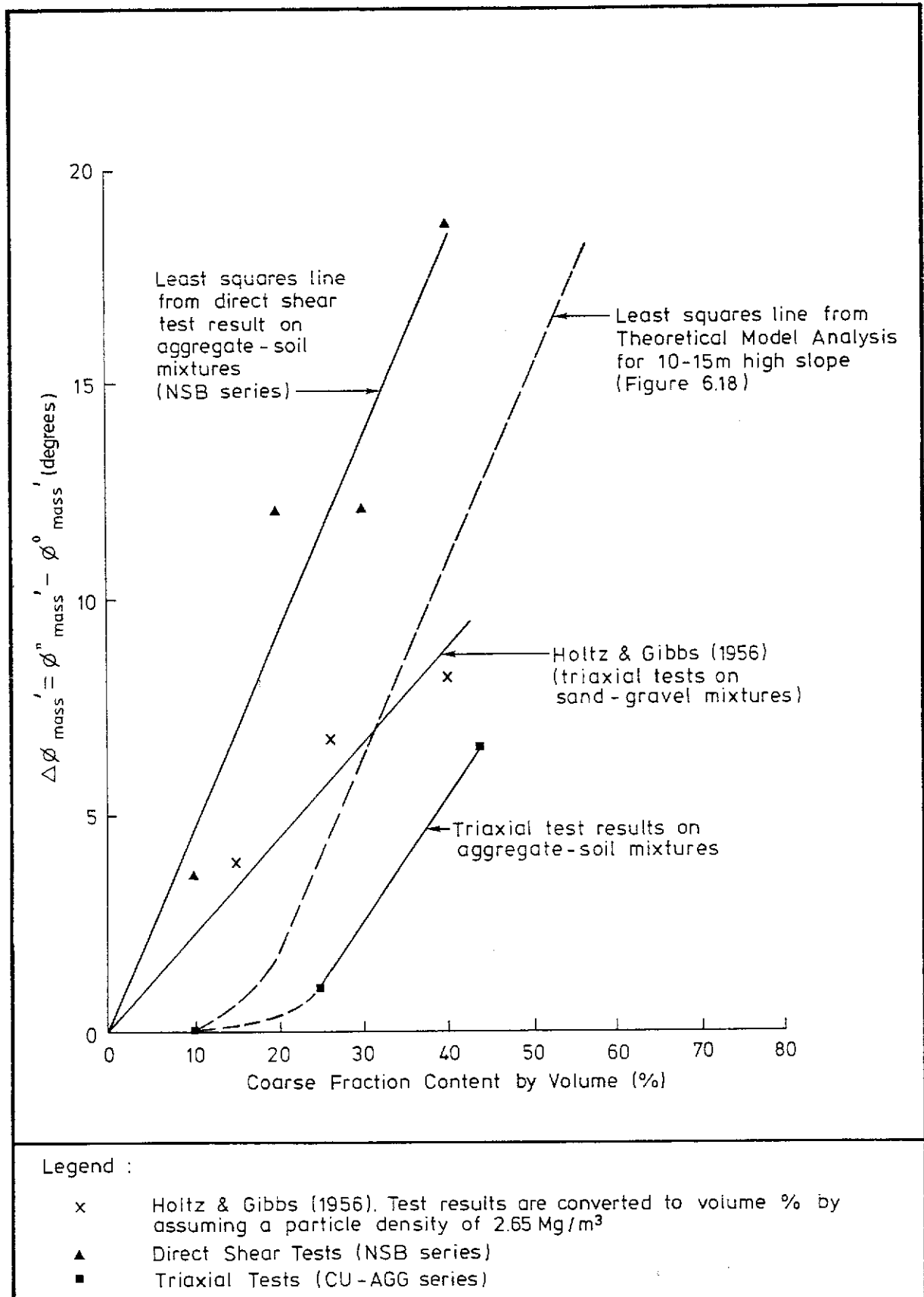


Figure 7.2 - Comparison of Results of Laboratory Study and Theoretical Slope Model Analysis and the Relationship Between Increase in Mass Shear Strength and Coarse Fraction Content

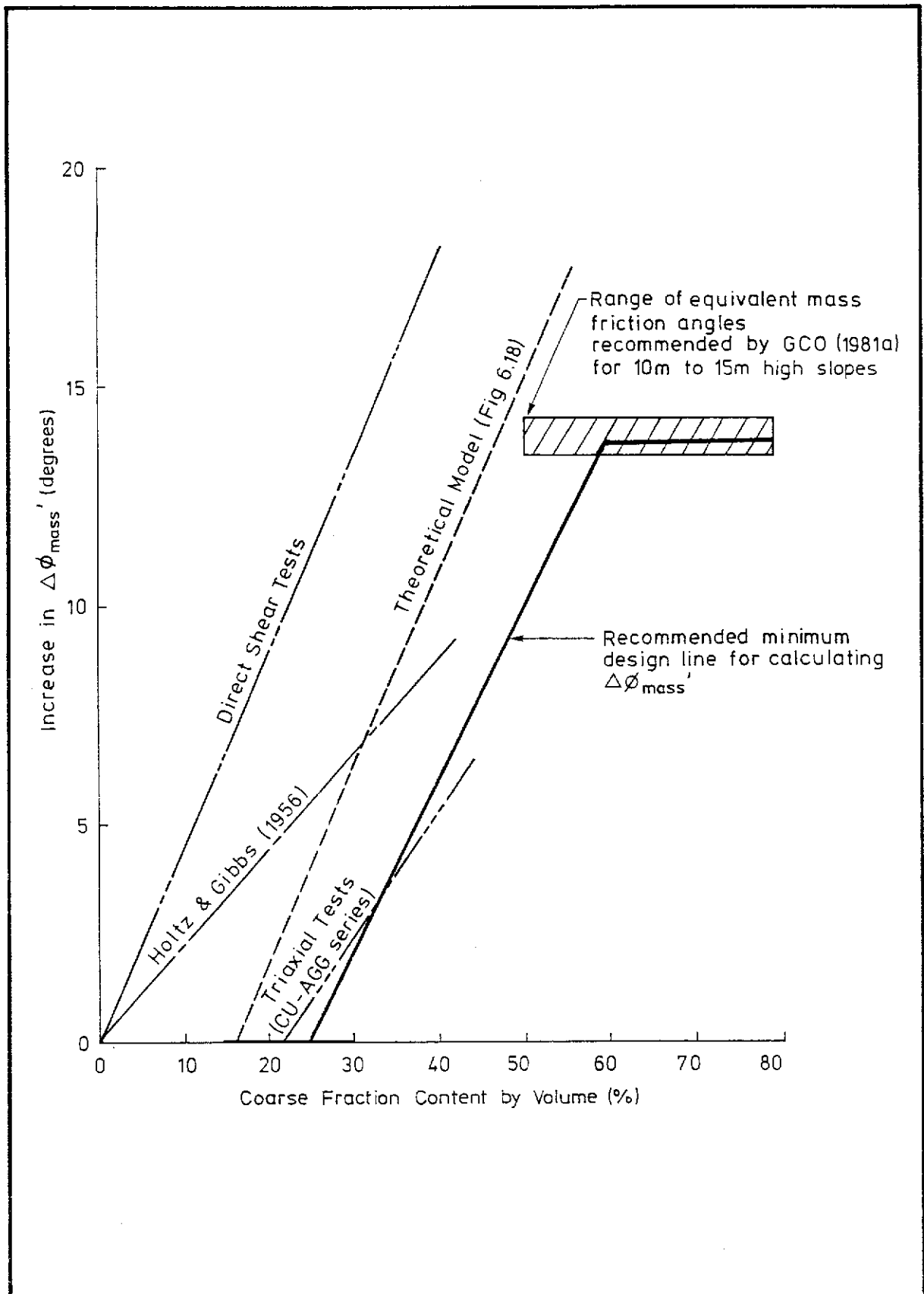


Figure 7.3 - Summary of the Hong Kong Study and the Recommendation for Mass Strength Increases For Slope Analysis in Colluvium

LIST OF PLATES

| Plate No. | | Page No. |
|--------------|---|-------------|
| 4.1 | Slope at CH 4415, Shing Mun Catchwater | 156 |
| 4.2 | Slope at Mount Nicholson Road, the Peak | 157 |
| 4.3 | Slope behind the Chater Hall Service Reservoir, Mid-levels | 158 |
| 4.4 | Slope behind Fairmont Gardens, Mid-levels. Overlay Shows the Boundaries between Various Colluvium Layers | 159 |



Negative No. SP91 10407



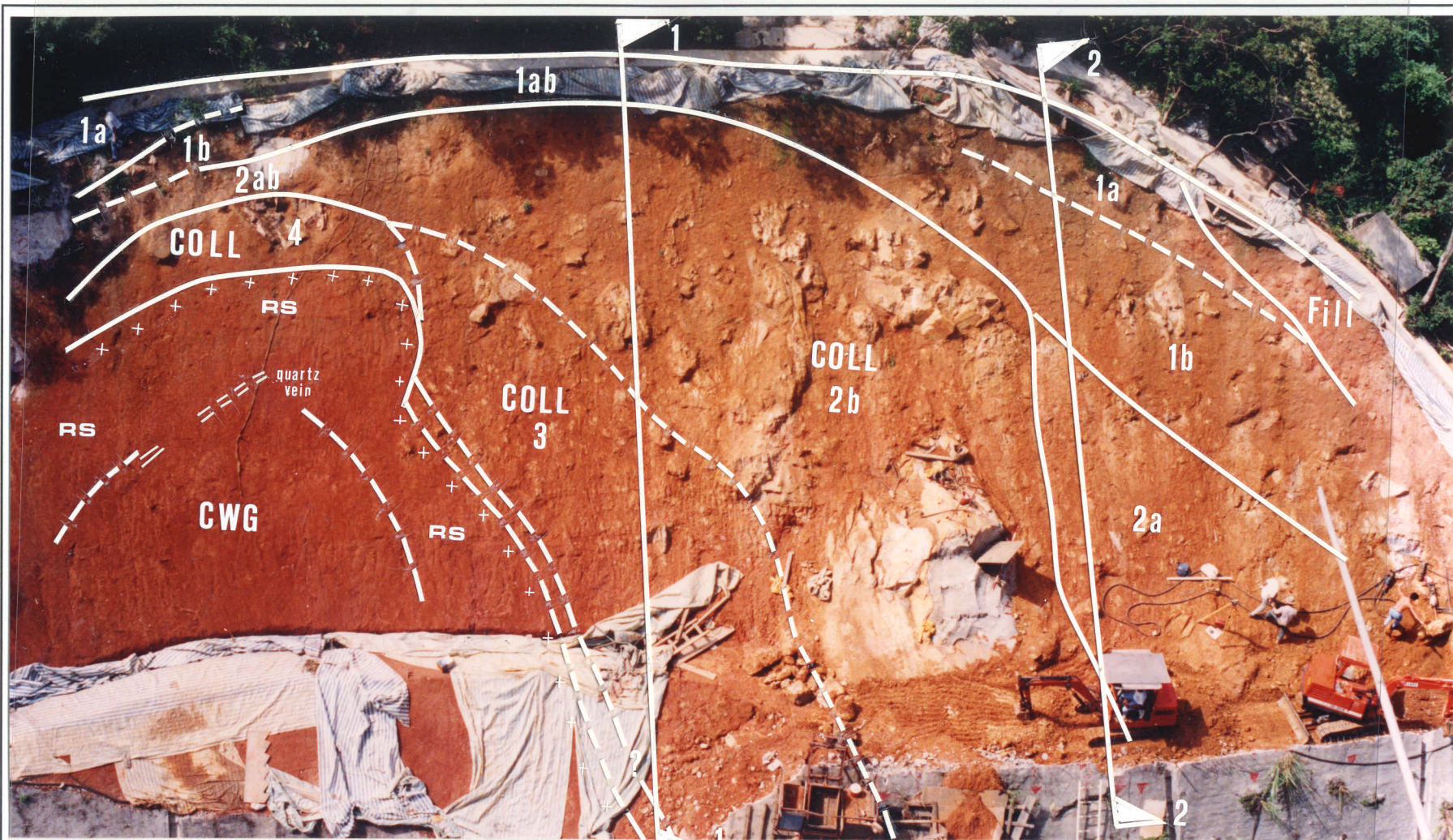
Negative No. SP91 058 07C

Plate 4.2 - Slope at Mount Nicholson Road, the Peak



Negative No. SP91 058 09C

Plate 4.3 - Slope behind the Chater Hall Service Reservoir, Mid-levels



Negative No. SP89 087 01C

Plate 4.4 - Slope behind Fairmont Gardens, Mid-levels. Overlay Shows the Boundaries between Various Colluvium Layers

APPENDIX A

BACK ANALYSIS METHODS OF CALCULATIONS

BACK ANALYSES METHODS OF CALCULATIONS

In this study, the Morgenstern & Price (1965) (M&P) method of analysis was used to determine the factor of safety of a slope both for the back-analysis of natural slopes and the theoretical slope model analysis. This method was chosen over the commonly-used Janbu Rigorous method (Janbu, 1972), because it is more rigorous in its formulation (Fredlund & Krahn, 1977) and it always gives a solution, unlike Janbu's method. The analysis was carried out using the computer program GSLPC (Leung et al, 1989).

The values of average normal stress, σ_{avg}' , and average shear stress, τ_{avg} , along a given potential slip surface cannot be determined from the GSLPC program. Therefore, an indirect approach was used to determine these stresses. The normal and shear stresses along a potential slip surface are a function of slope geometry and the characteristics of the slip surface. Experience with Janbu's method indicates that σ_{avg}' and τ_{avg} are often independent of $\tan \phi'$ and c' . A similar procedure has been suggested by Kenney (1967) to back-calculate the average stresses along a slip surface. The relationship between σ_{avg}' , and τ_{avg} , is given by the following formula in terms of $\tan \phi'$, c' , and factor of safety, F :

$$\tau_{avg} = c'/F + \sigma_{avg}' \tan \phi'/F \quad (A1)$$

Re-arranging equation (A1), the following formula is obtained :

$$c'/F = \tau_{avg} + \sigma_{avg}' \tan \phi'/F \quad (A2)$$

Since σ_{avg}' and τ_{avg} are independent of c' and $\tan \phi'$, equation (A2) represents a linear function. By plotting c'/F against $\tan \phi'/F$, the gradient and the intercept of the line will give σ_{avg}' and τ_{avg} , respectively.

A range of c' - ϕ' values were used in the calculation of factors of safety along the potential slip surfaces. The values of c' ranged from 0 kPa to 12 kPa by an increment of 3 kPa and the values of ϕ' from 25° to 45° by an increment of 5° . An example is given in Figure A.1. The data points generally fall along a straight line, confirming the applicability of the indirect approach. Occasionally, some data points were found to be located significantly outside the mean line. By varying c' or ϕ' by a very small value, it was often found that they also plotted along the mean line. The exact cause of the anomalous data is not known.

A check was also carried out on the accuracy of σ_{avg}' and τ_{avg} determinations by the above method. The program PC-SLOPE was used to calculate the average stresses along the potential slip surfaces in the slope at Plantation Road. The PC-SLOPE program uses a rigorous formulation similar to the M & P method to calculate the factor of safety (Fredlund & Krahn, 1977). Values of $\sigma_{avg}' = 30.1$ kPa and $\tau_{avg} = 25.6$ kPa were calculated from the program. The corresponding values determined from the indirect approach given above were; $\sigma_{avg}' = 31.2$ kPa and $\tau_{avg} = 27.5$ kPa. These were considered to be acceptable in view of the accuracy of the assumptions made in the back analysis approach used in this study. For slip surfaces located in more than one colluvium layer, the coarse fraction and boulder contents, P_{fs} , were calculated by the following equation:

$$P_{fs} = \sum l_i p_i / L \quad (A3)$$

where l_i is the length of the slip surface in layer i , p_i is the coarse fraction or boulder content of layer i , and L is the total length of the slip surface. The coarse fraction or boulder contents calculated from the above formula were rounded off to the nearest 10%.

References

- Fredlund, D. G. & Krahn, J. (1977). Comparison of slope stability methods of analysis. Canadian Geotechnical Journal, vol. 14, pp 429-439.
- Janbu, N. (1972). Slope stability computations. Embankment Dam Engineering : Casagrande Volume, edited by R. C. Hirschfield & S. J. Poulos, John Wiley & Sons, New York, pp 47-89.
- Kenney T. C. (1967). Slide behaviour and shear resistance of a quick clay determined from a study of the landslide at Selnes, Norway. Proceedings of the Geotechnical Conference, Oslo, vol. 1, pp 57-64.
- Leung, Y.C., Lam, H.F. & Cooper, A.J. (1989). User Manual For GCO Program 'GSLPC'. GCO Computer Manual, CM 1/89, Geotechnical Control Office, Hong Kong, 88 p.
- Morgenstern, N. R. & Price, V. E. (1965). The analyses of the stability of general slip surfaces. Geotechnique, vol. 15, pp 79-93.

APPENDIX A

LIST OF FIGURE

| Figure No. | | Page No. |
|---------------|--|-------------|
| A1 | An Example of Average Stress Calculation | 164 |

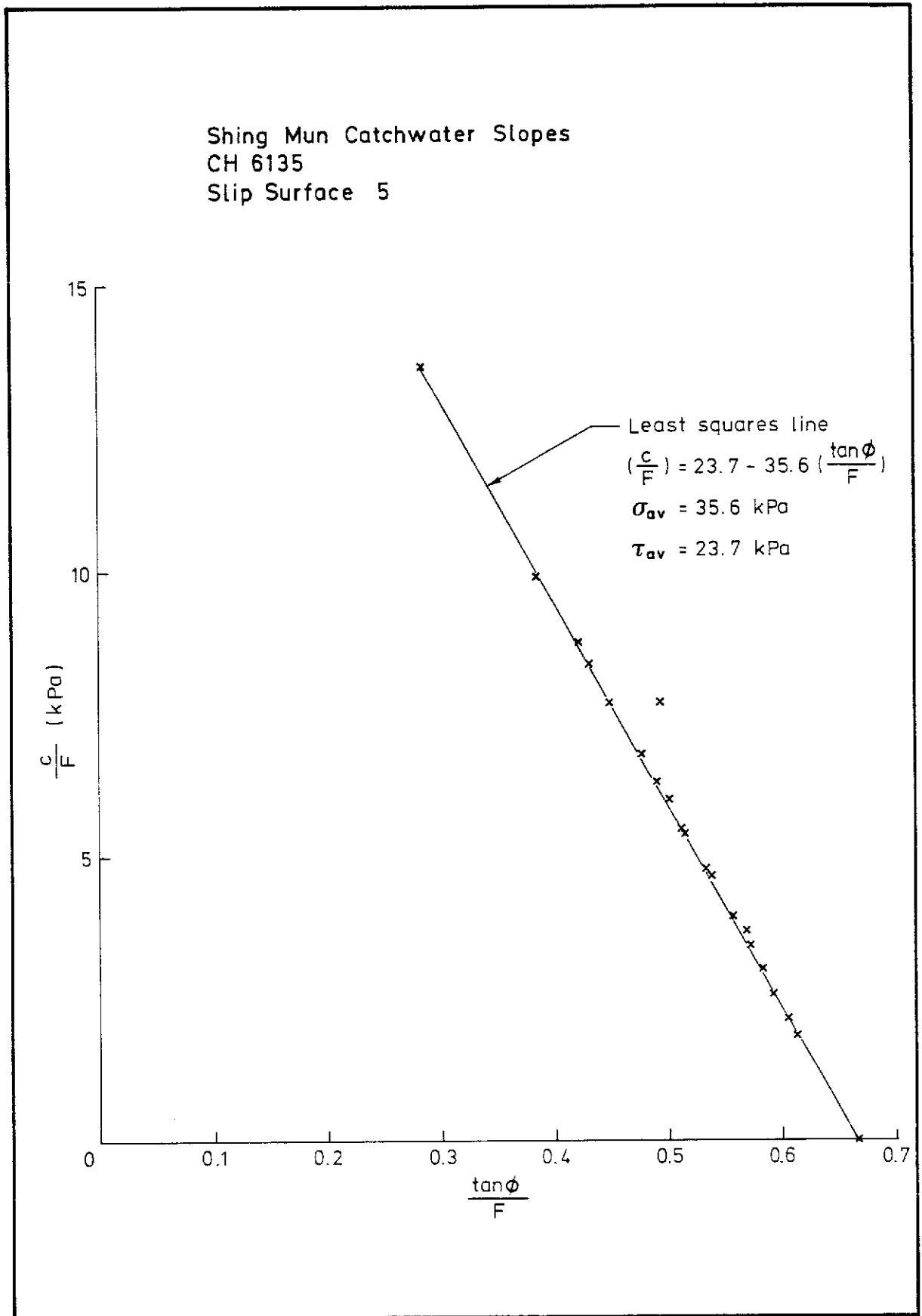


Figure A.1 - An Example of Average Stress Calculation

APPENDIX B
DETAILED RESULTS OF BACK ANALYSES

APPENDIX B

LIST OF TABLES

| Table No. | | Page No. |
|--------------|---|-------------|
| B.1 | Results of Back Analysis, Shing Mun Catchwater Slopes | 167 |
| B.2 | Results of Back Analysis, Tsz Wan Shan Estate Slopes | 168 |
| B.3 | Results of Back Analysis, Slope behind Chater Hall Service Reservoir | 169 |
| B.4 | Results of Back Analysis, Slopes at Mount Nicholson Road and Plantation Road | 170 |

Table B.1 - Results of Back Analysis, Shing Mun Catchwater Slopes

| Slope no. (Chainage) | Slip Surface No. | Normal Stress σ'_{av} (kPa) | Shear Stress τ_{av} (kPa) | Boulder Content ⁽¹⁾ (%) | Cobble & Boulder Content ⁽¹⁾ (%) | Relative Strength of Matrix ⁽²⁾ | Remarks |
|-------------------------|------------------------|---|---|--|--|--|------------|
| 4050 | 1 | 4.5 | 7.7 | 10 | 20 | Medium | Figure B.1 |
| | 2 | 7.8 | 10.7 | 10 | 20 | Medium | |
| | 3 | 13.0 | 14.1 | 10 | 20 | Medium | |
| | 4 | 17.0 | 16.1 | 10 | 20 | Medium | |
| | 5 | 21.0 | 16.9 | 10 | 20 | Medium | |
| | 6 | 4.0 | 8.3 | 0 | 10 | Medium | |
| | 7 | 8.5 | 14.1 | 0 | 10 | Medium | |
| | 8 | 13.0 | 18.2 | 0 | 10 | Medium | |
| | 9 | 23.5 | 24.3 | 0 | 10 | Medium | |
| | 10 | 29.6 | 26.8 | 0 | 10 | Medium | |
| 4215 | 1 | 4.5 | 7.9 | 10 | 20 | High | Figure B.2 |
| | 2 | 8.9 | 13.4 | 10 | 20 | High | |
| | 3 | 17.8 | 21.1 | 10 | 20 | High | |
| | 4 | 28.0 | 26.6 | 10 | 20 | High | |
| | 5 | 37.2 | 29.1 | 10 | 20 | High | |
| 4305 | 1 | 2.7 | 4.0 | 20 | 30 | Low | Figure B.3 |
| | 2 | 5.5 | 6.2 | 20 | 30 | Low | |
| | 3 | 8.2 | 7.5 | 20 | 30 | Low | |
| | 4 | 10.9 | 8.3 | 20 | 30 | Low | |
| 4415 | 1 | 9.1 | 12.1 | 50 | 60 | High | Figure B.4 |
| | 2 | 16.9 | 17.6 | 50 | 60 | High | |
| | 3 | 26.7 | 22.4 | 50 | 60 | High | |
| | 4 | 12.9 | 16.9 | 50 | 60 | High | |
| | 5 | 21.6 | 23.4 | 50 | 60 | High | |
| | 6 | 28.5 | 26.9 | 50 | 60 | High | |
| | 7 | 30.3 | 27.8 | 50 | 60 | High | |
| 5315 | 1 | 4.4 | 8.0 | 10 | 10 | Low | Figure B.5 |
| | 2 | 9.5 | 13.0 | 10 | 10 | Low | |
| | 3 | 16.2 | 16.5 | 10 | 10 | Low | |
| | 4 | 20.8 | 17.9 | 10 | 10 | Low | |
| | 5 | 3.4 | 7.9 | 10 | 20 | Medium | |
| | 6 | 9.7 | 16.8 | 10 | 20 | Medium | |
| | 7 | 18.2 | 23.9 | 10 | 20 | Medium | |
| | 8 | 25.9 | 27.9 | 10 | 20 | Medium | |
| | 9 | 34. | 30.5 | 10 | 20 | Medium | |
| 5400 | 1 | 5.3 | 9.1 | 10 | 60 | Medium | Figure B.6 |
| | 2 | 12.1 | 17.0 | 10 | 60 | Medium | |
| | 3 | 17.8 | 21.1 | 10 | 60 | Medium | |
| | 4 | 33.5 | 28.7 | 10 | 60 | Medium | |
| | 5 | 39.8 | 31.0 | 10 | 60 | Medium | |
| | 6 | 5.6 | 10.4 | 10 | 50 | Medium | |
| | 7 | 14.6 | 22.3 | 10 | 50 | Medium | |
| | 8 | 26.9 | 33.7 | 10 | 50 | Medium | |
| | 9 | 42.8 | 43.3 | 10 | 50 | Medium | |
| | 10 | 56.2 | 48.3 | 10 | 50 | Medium | |
| 5845 | 1 | 2.4 | 3.9 | 70 | 70 | High | Figure B.7 |
| | 2 | 7.5 | 8.0 | 70 | 70 | High | |
| | 3 | 12.4 | 9.9 | 70 | 70 | High | |
| | 4 | 18.3 | 11.2 | 70 | 70 | High | |
| | 5 | 3.0 | 5.4 | 40 | 50 | High | |
| | 6 | 8.7 | 11.9 | 40 | 50 | High | |
| | 7 | 18.5 | 18.3 | 40 | 50 | High | |
| | 8 | 27.4 | 20.8 | 40 | 50 | High | |
| | 9 | 39.9 | 22.9 | 40 | 50 | High | |
| 6135 | 1 | 5.7 | 8.6 | 40 | 50 | Medium | Figure B.8 |
| | 2 | 13.7 | 15.4 | 50 | 60 | Medium | |
| | 3 | 19.8 | 19.3 | 50 | 60 | Medium | |
| | 4 | 29.9 | 22.4 | 60 | 60 | Medium | |
| | 5 | 35.6 | 23.7 | 60 | 60 | Medium | |

Notes : (1) An averaging process based on the relative length of slip surface in each layer was used to calculate a 'coarse fraction content' for slip surfaces affecting more than one colluvium layer. The value such calculated was rounded off to the nearest 10%.

(2) See Table 4.3 for definition of terms. An averaging process, identical to that used for the coarse fraction content, was used for slip surfaces affecting more than one colluvium layer.

Table B.2 - Results of Back Analysis, Tsz Wan Shan Estate Slopes

| Slope no. (Chainage) | Slip Surface No. | Normal Stress σ'_{av} (kPa) | Shear Stress τ_{av} (kPa) | Cobble & Boulder Content ⁽¹⁾ (%) | Relative Strength of Matrix ⁽²⁾ | Remarks |
|-------------------------|------------------------|---|---|--|--|-------------|
| 11NE-A/C6 (CH B80) | 1 | 13.9 | 16.5 | 60 | Very high | Figure B.13 |
| | 2 | 28.7 | 31.3 | 60 | Very high | |
| | 3 | 53.7 | 46.2 | 60 | Very high | |
| | 4 | 78.6 | 52.8 | 60 | Very high | |
| | 5 | 105.7 | 53.6 | 60 | Very high | |
| 11NE-A/C6 (CH B96) | 1 | 16.6 | 18.9 | 60 | Very high | Figure B.14 |
| | 2 | 30.5 | 30.3 | 60 | Very high | |
| | 3 | 51.5 | 43.9 | 60 | Very high | |
| | 4 | 75.0 | 53.0 | 60 | Very high | |
| | 5 | 102.6 | 55.9 | 60 | Very high | |
| 11NE-A/C8 | 1 | 17.8 | 14.2 | 50 | Very high | Figure B.15 |
| | 2 | 41.4 | 29.5 | 50 | Very high | |
| | 3 | 54.7 | 38.3 | 50 | Very high | |
| | 4 | 69.6 | 47.0 | 50 | Very high | |
| | 5 | 95.7 | 57.2 | 50 | Very high | |
| 11NE-A/C9 | 1 | 23.4 | 20.6 | 60 | Very high | Figure B.16 |
| | 2 | 44.4 | 35.7 | 60 | Very high | |
| | 3 | 65.6 | 48.9 | 60 | Very high | |
| | 4 | 94.8 | 60.6 | 60 | Very high | |
| | 5 | 119.2 | 66.1 | 60 | Very high | |
| | 6 | 142.4 | 69.8 | 60 | Very high | |
| 11NE-A/C11 | 1 | 14.1 | 22.6 | 75 | Very high | Figure B.17 |
| | 2 | 17.3 | 27.3 | 75 | Very high | |
| | 3 | 30.3 | 42.6 | 75 | Very high | |
| | 4 | 54.6 | 63.6 | 75 | Very high | |
| | 5 | 51.7 | 80.8 | 75 | Very high | |
| | 6 | 111.7 | 93.5 | 75 | Very high | |
| | 7 | 140.7 | 98.3 | 75 | Very high | |

Notes : (1) Based on CHASE data.
(2) Based on CHASE data. See Table 4.3 for definition of terms.

Table B.3 - Results of Back Analysis, Slope behind Chater Hall Service Reservoir

| Slope no. (Chainage) | Slip Surface No. | Normal Stress σ'_{av} (kPa) | Shear Stress τ_{av} (kPa) | Boulder Content ⁽¹⁾ (%) | Cobble & Boulder Content ⁽¹⁾ (%) | Relative Strength of Matrix ⁽²⁾ | Remarks |
|-------------------------|------------------------|---|---|--|--|--|-------------|
| CS2 | 1 | 25.8 | 27.4 | 30 | 50 | High | Figure B.18 |
| | 2 | 41.8 | 37.1 | 20 | 50 | High | |
| | 3 | 48.5 | 40.2 | 20 | 50 | High | |
| | 4 | 65.0 | 47.7 | 20 | 50 | High | |
| | 5 | 92.9 | 53.8 | 20 | 50 | High | |
| CS3 | 1 | 12.3 | 11.9 | 20 | 40 | Low | Figure B.19 |
| | 2 | 18.1 | 15.2 | 20 | 40 | Low | |
| | 3 | 23.3 | 17.6 | 20 | 40 | Low | |
| | 4 | 28.7 | 19.9 | 20 | 40 | Low | |
| | 5 | 14.4 | 24.8 | 10 | 40 | Medium | |
| | 6 | 27.6 | 32.1 | 10 | 40 | Medium | |
| | 7 | 42.0 | 35.7 | 10 | 40 | Medium | |
| | 8 | 50.4 | 36.0 | 10 | 40 | Medium | |
| | 9 | 33.7 | 57.0 | 30 | 50 | High | |
| | 10 | 74.3 | 69.9 | 40 | 50 | High | |
| | 11 | 100.0 | 80.1 | 40 | 50 | High | |
| | 12 | 133.6 | 21.4 | 40 | 50 | High | |
| | 13 | 15.9 | 33.2 | 30 | 50 | Very High | |
| | 14 | 26.8 | 57.2 | 30 | 50 | High | |
| | 15 | 54.6 | 77.4 | 30 | 50 | High | |
| | 16 | 87.5 | 89.4 | 30 | 50 | High | |
| | 17 | 110.0 | 102.0 | 20 | 50 | High | |
| | 18 | 146.6 | | 20 | 50 | High | |
| CS4 | 1 | 13.1 | 13.3 | 30 | 60 | Low | Figure B.20 |
| | 2 | 23.7 | 18.1 | 30 | 60 | Low | |
| | 3 | 30.0 | 19.5 | 30 | 60 | Low | |
| | 4 | 33.9 | 20.8 | 30 | 60 | Low | |
| | 5 | 11.8 | 12.7 | 30 | 50 | Medium | |
| | 6 | 25.7 | 22.3 | 30 | 50 | Medium | |
| | 7 | 36.2 | 26.7 | 30 | 50 | Medium | |
| | 8 | 47.3 | 31.1 | 30 | 50 | Medium | |
| | 9 | 17.8 | 23.1 | 20 | 50 | High | |
| | 10 | 43.6 | 46.2 | 20 | 50 | High | |
| | 11 | 63.2 | 60.4 | 20 | 50 | High | |
| | 12 | 88.5 | 75.0 | 20 | 50 | High | |
| | 13 | 110.3 | 83.5 | 20 | 50 | High | |

Notes : (1) An averaging process based on the relative length of slip surface in each layer was used to calculate a 'coarse fraction content' for slip surfaces affecting more than one colluvium layer. The value such calculated was rounded off to the nearest 10%.

(2) See Table 4.3 for definition of terms. An averaging process, identical to that used for the coarse fraction content, was used for slip surfaces affecting more than one colluvium layer.

Table B.4 - Results of Back Analysis, Slopes at Mount Nicholson Road and Plantation Road

| Slope no. (Chainage) | Slip Surface No. | Normal Stress σ'_{av} (kPa) | Shear Stress τ_{av} (kPa) | Boulder Content ⁽¹⁾ (%) | Cobble & Boulder Content ⁽¹⁾ (%) | Relative Strength of Matrix ⁽²⁾ | Remarks |
|--------------------------------------|------------------------|---|---|--|--|---|-------------|
| 11SW-D/C471 Plantation Road | P1-1 | 15.2 | 15.9 | 40 | 70 | Low | Figure B.21 |
| | 2 | 20.1 | 19.7 | 40 | 70 | Low | |
| | 3 | 22.7 | 21.8 | 40 | 70 | Low | |
| | 4 | 24.0 | 28.8 | 40 | 70 | Low | |
| | 5 | 31.2 | 27.5 | 40 | 80 | Low | |
| | 6 | 34.0 | 28.9 | 40 | 80 | Low | |
| | P2-1 | 13.3 | 12.7 | 40 | 60 | Low | |
| | 2 | 17.2 | 15.6 | 40 | 60 | Low | |
| | 3 | 19.9 | 17.4 | 50 | 70 | Low | |
| | 4 | 21.4 | 17.8 | 50 | 70 | Low | |
| 11SW-D/C340 Mt. Nicholson Road | 1 | 14.9 | 20.1 | 20 | 40 | Medium | Figure B.22 |
| | 2 | 17.4 | 22.6 | 20 | 40 | Medium | |
| | 3 | 22.1 | 27.2 | 20 | 40 | Medium | |
| | 4 | 24.0 | 29.8 | 20 | 40 | Medium | |

Notes : (1) An averaging process based on the relative length of slip surface in each layer was used to calculate a 'coarse fraction content' for slip surfaces affecting more than one colluvium layer. The value such calculated was rounded off to the nearest 10%.

(2) See Table 4.3 for definition of terms. An averaging process, identical to that used for the coarse fraction content, was used for slip surfaces affecting more than one colluvium layer.

APPENDIX B

LIST OF FIGURES

| Figure No. | | Page No. |
|------------|--|----------|
| B.1 | Back Analysis of Slope at CH 4050, Shing Mun Catchwater | 173 |
| B.2 | Back Analysis of Slope at CH 4215, Shing Mun Catchwater | 174 |
| B.3 | Back Analysis of Slope at CH 4305, Shing Mun Catchwater | 175 |
| B.4 | Back Analysis of Slope at CH 4415, Shing Mun Catchwater | 176 |
| B.5 | Back Analysis of Slope at CH 5330, Shing Mun Catchwater | 177 |
| B.6 | Back Analysis of Slope at CH 5400, Shing Mun Catchwater | 178 |
| B.7 | Back Analysis of Slope at CH 5845, Shing Mun Catchwater | 179 |
| B.8 | Back Analysis of Slope at CH 6135, Shing Mun Catchwater | 180 |
| B.9 | Back-Analysed Average Shear and Normal Stresses along Potential Failure Surfaces, Shing Mun Catchwater Slopes | 181 |
| B.10 | Back-calculated Least-squares Shear Strength Envelopes for Various Boulder Contents, Shing Mun Catchwater Slopes | 182 |
| B.11 | Plot of Back-calculated c' versus ϕ' for Various Boulder Contents, Shing Mun Catchwater Slopes ($\sigma'_n \leq 50$ kPa) | 183 |
| B.12 | Variation of Back-calculated 'Minimum' Shear Stress at $\sigma'_n = 30$ kPa with Boulder Content, Shing Mun Catchwater Slopes | 184 |
| B.13 | Back Analysis of Slope 11NE-A/C6 (CH B80), Tsz Wan Shan Estate | 185 |
| B.14 | Back Analysis of Slope 11NE-A/C6 (CH B96), Tsz Wan Shan Estate | 186 |
| B.15 | Back Analysis of Slope 11NE-A/C8, Tsz Wan Shan Estate | 187 |
| B.16 | Back Analysis of Slope 11NE-A/C9, Tsz Wan Shan Estate | 188 |
| B.17 | Back Analysis of Slope 11NE-A/C11, Tsz Wan Shan Estate | 189 |

| Figure No. | | Page No. |
|------------|---|----------|
| B.18 | Back Analysis of Slope 11SW-A/C36 (Section CS2), Chater Hall Service Reservoir | 190 |
| B.19 | Back Analysis of Slope 11SW-A/C36 (Section CS3), Chater Hall Service Reservoir | 191 |
| B.20 | Back Analysis of Slope 11SW-A/C36 (Section CS4), Chater Hall Service Reservoir | 192 |
| B.21 | Back Analysis of Slope 11SW-D/C471, Plantation Road | 193 |
| B.22 | Back Analysis of Slope 11SW-D/C340, Mount Nicholson Road | 194 |
| B.23 | Back-analysed Average Shear and Normal Stresses along Potential Failure Surface, Mid-levels and Peak Slopes | 195 |
| B.24 | Back-calculated Least-squares Shear Strength Envelopes for Various Boulder Contents, Mid-levels and Peak Slopes | 196 |
| B.25 | Plot of Back-calculated c' versus ϕ' for Various Boulder Contents, Mid-levels and Peak Slopes ($\sigma_n' \leq 50$ kPa) | 197 |
| B.26 | Back-calculated Least-squares Shear Strength Envelopes for Various Boulder Contents, All Slopes | 198 |
| B.27 | Back-calculated Least-squares Shear Strength Envelopes for Various Coarse Fraction Contents, All Slopes | 199 |
| B.28 | Plot of Back-calculated c' versus ϕ' for Various Boulder Contents, All Slopes ($\sigma_n' \leq 50$ kPa) | 200 |

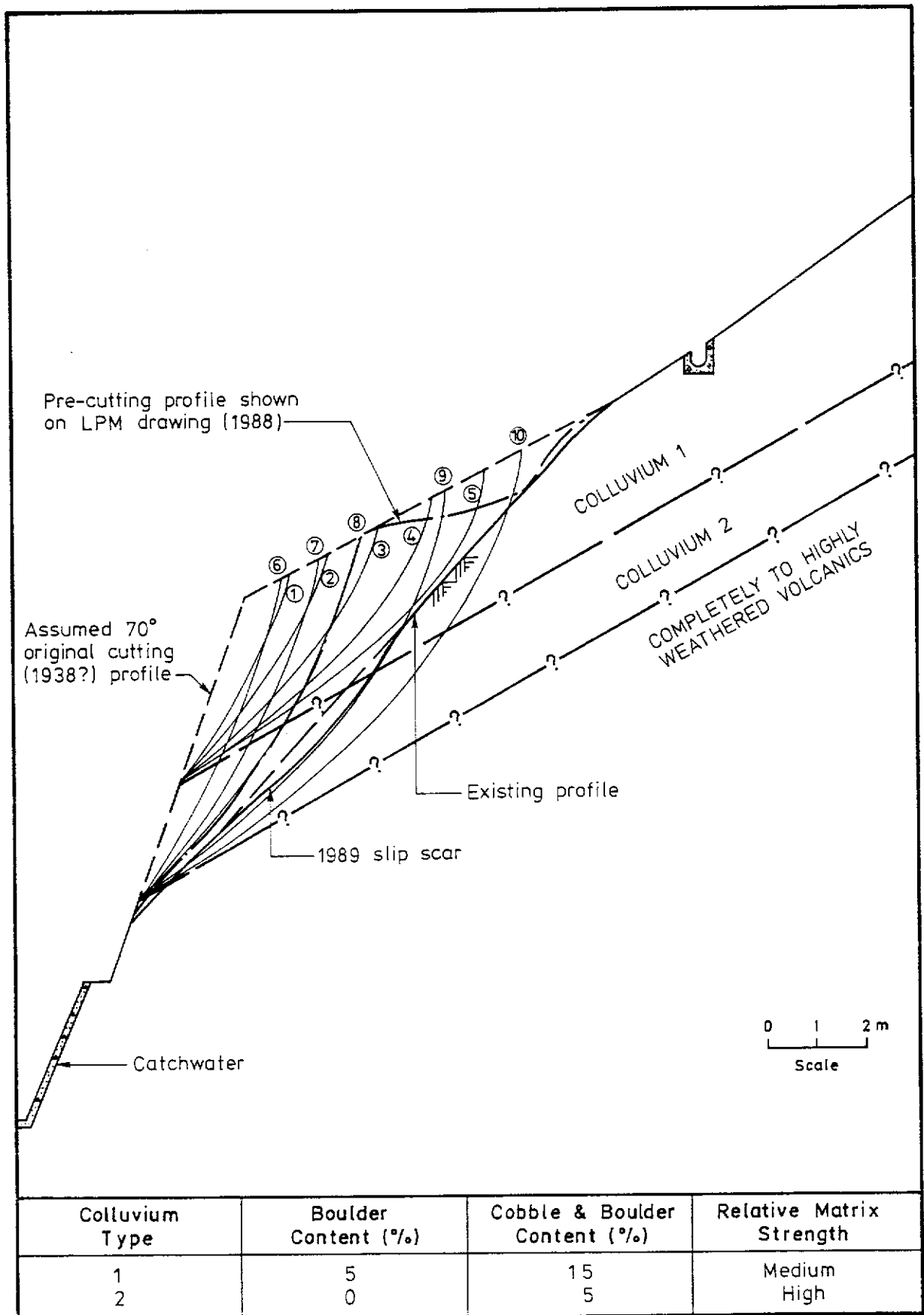


Figure B.1 - Back Analysis of Slope at CH 4050, Shing Mun Catchwater

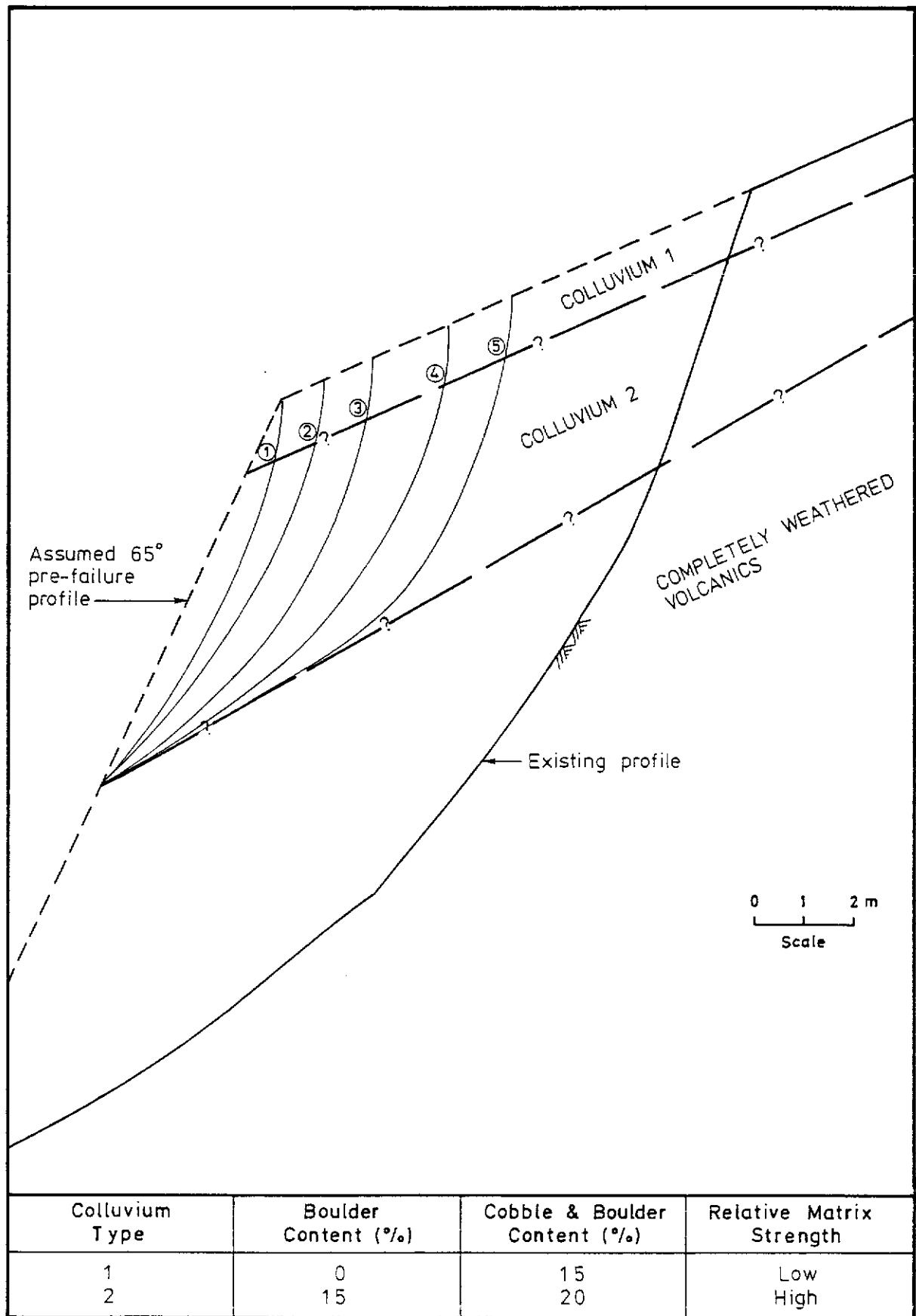


Figure B.2 - Back Analysis of Slope at CH 4215, Shing Mun Catchwater

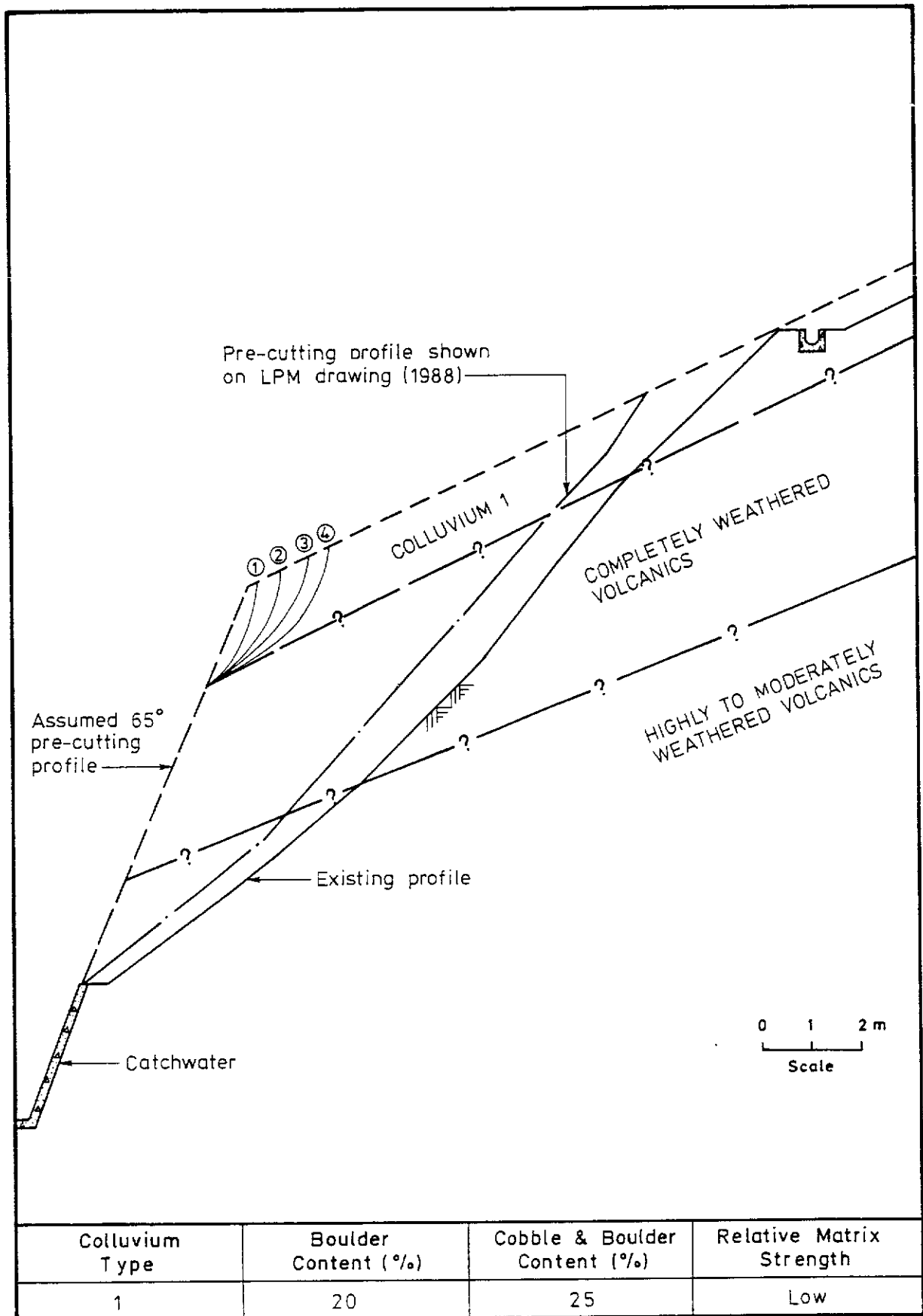


Figure B.3 - Back Analysis of Slope at CH 4305, Shing Mun Catchwater

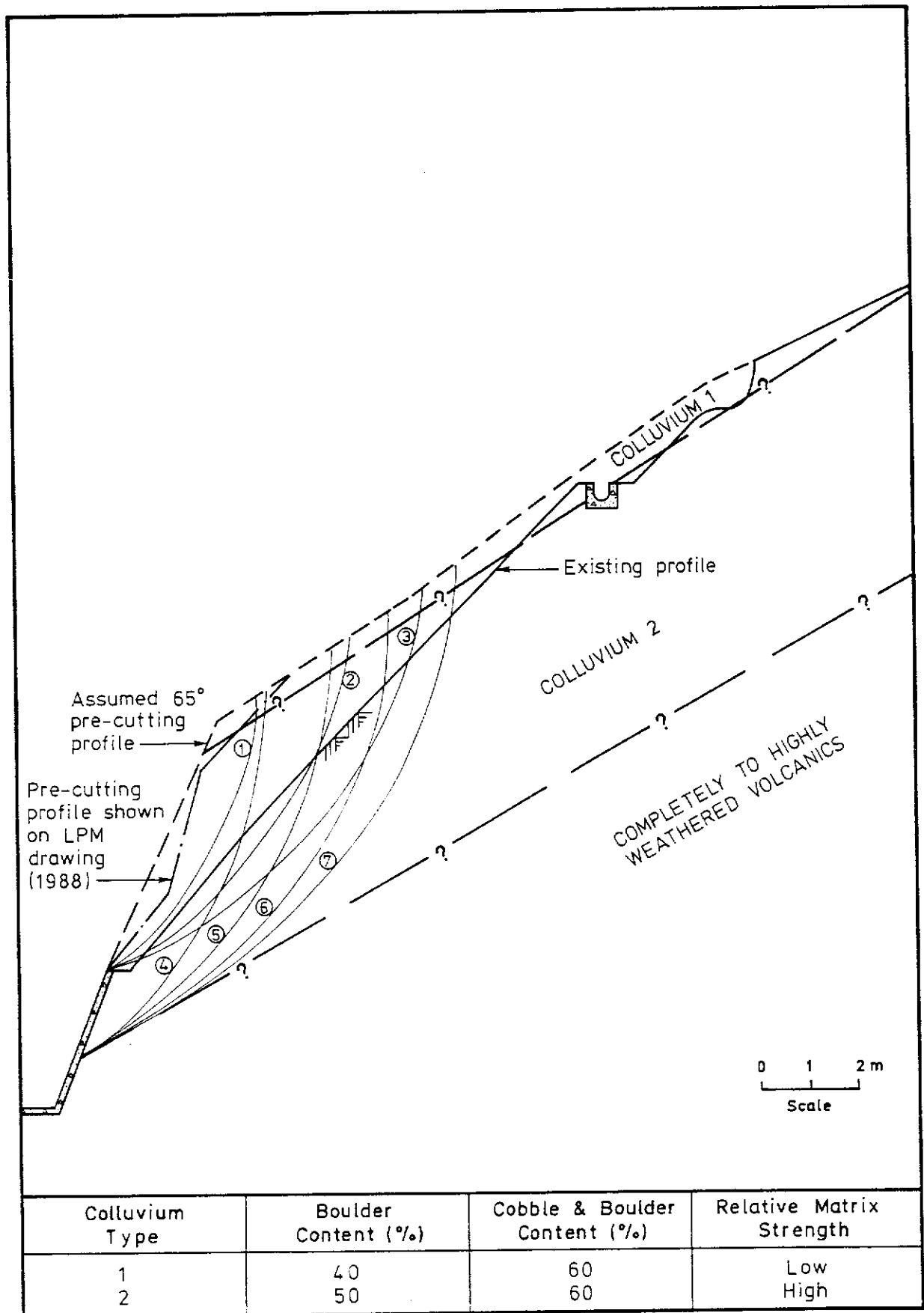


Figure B.4 - Back Analysis of Slope at CH 4415, Shing Mun Catchwater

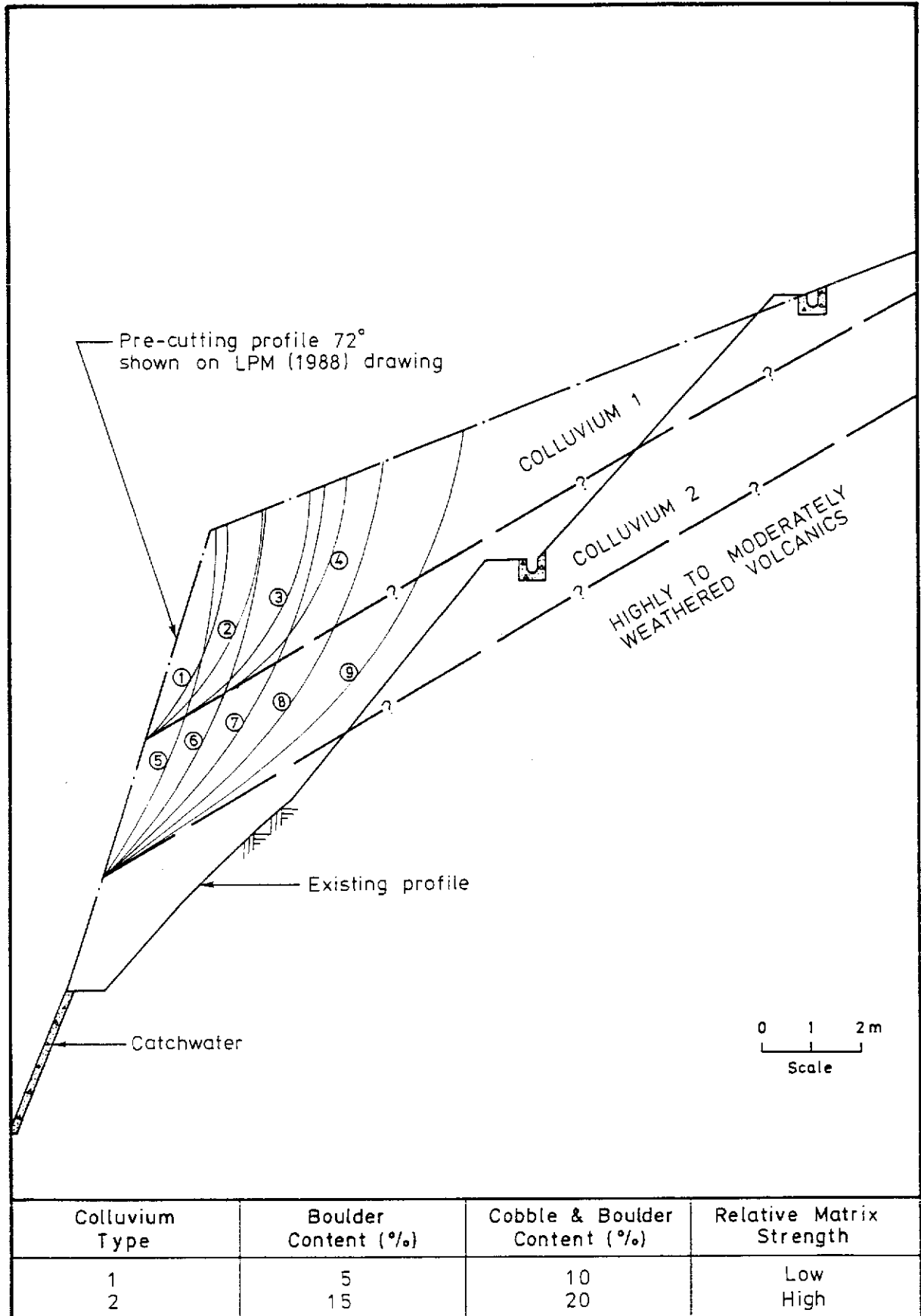


Figure B.5 - Back Analysis of Slope at CH 5330, Shing Mun Catchwater

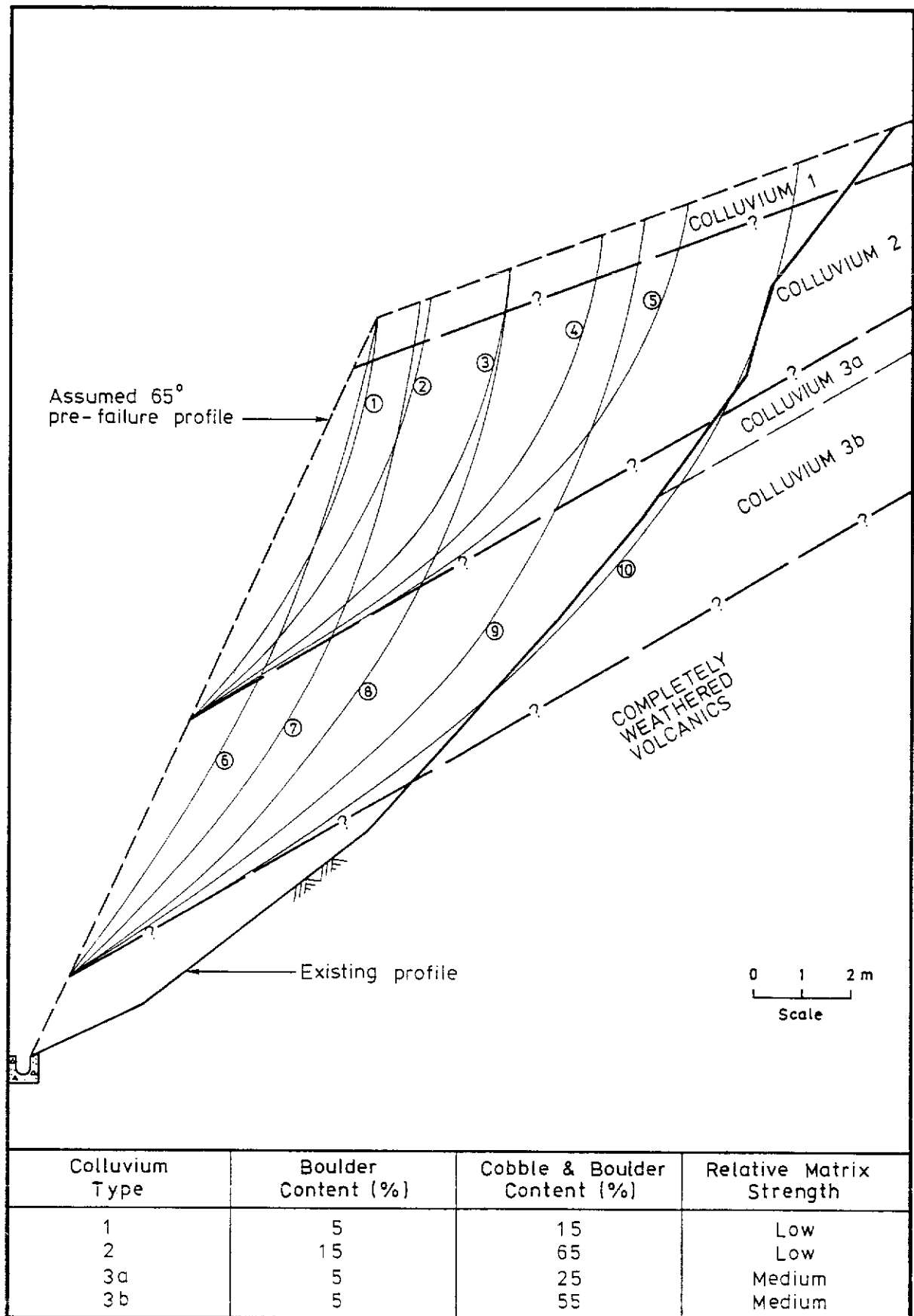


Figure B.6 - Back Analysis of Slope at CH 5400, Shing Mun Catchwater

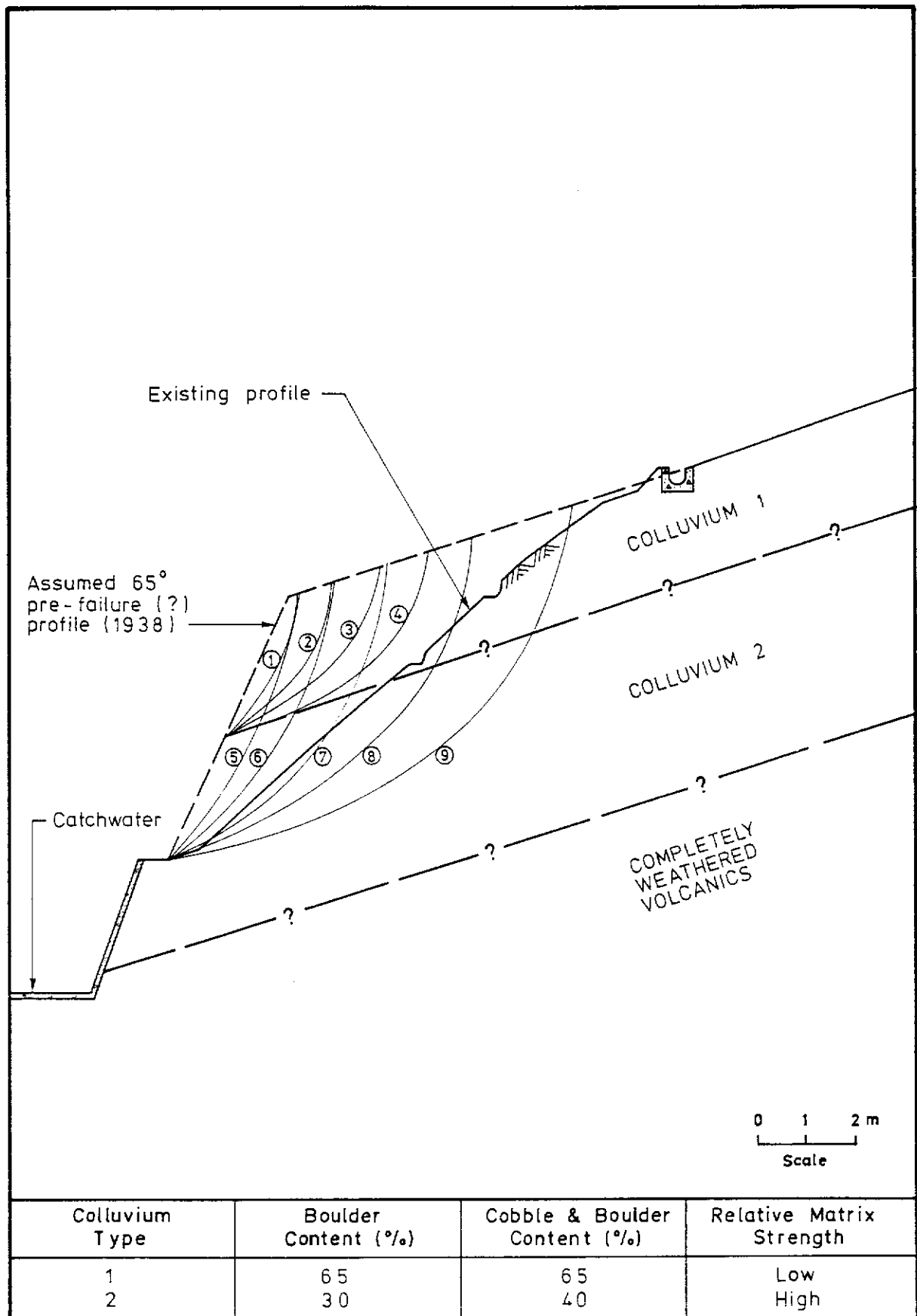


Figure B.7 - Back Analysis of Slope at CH 5845, Shing Mun Catchwater

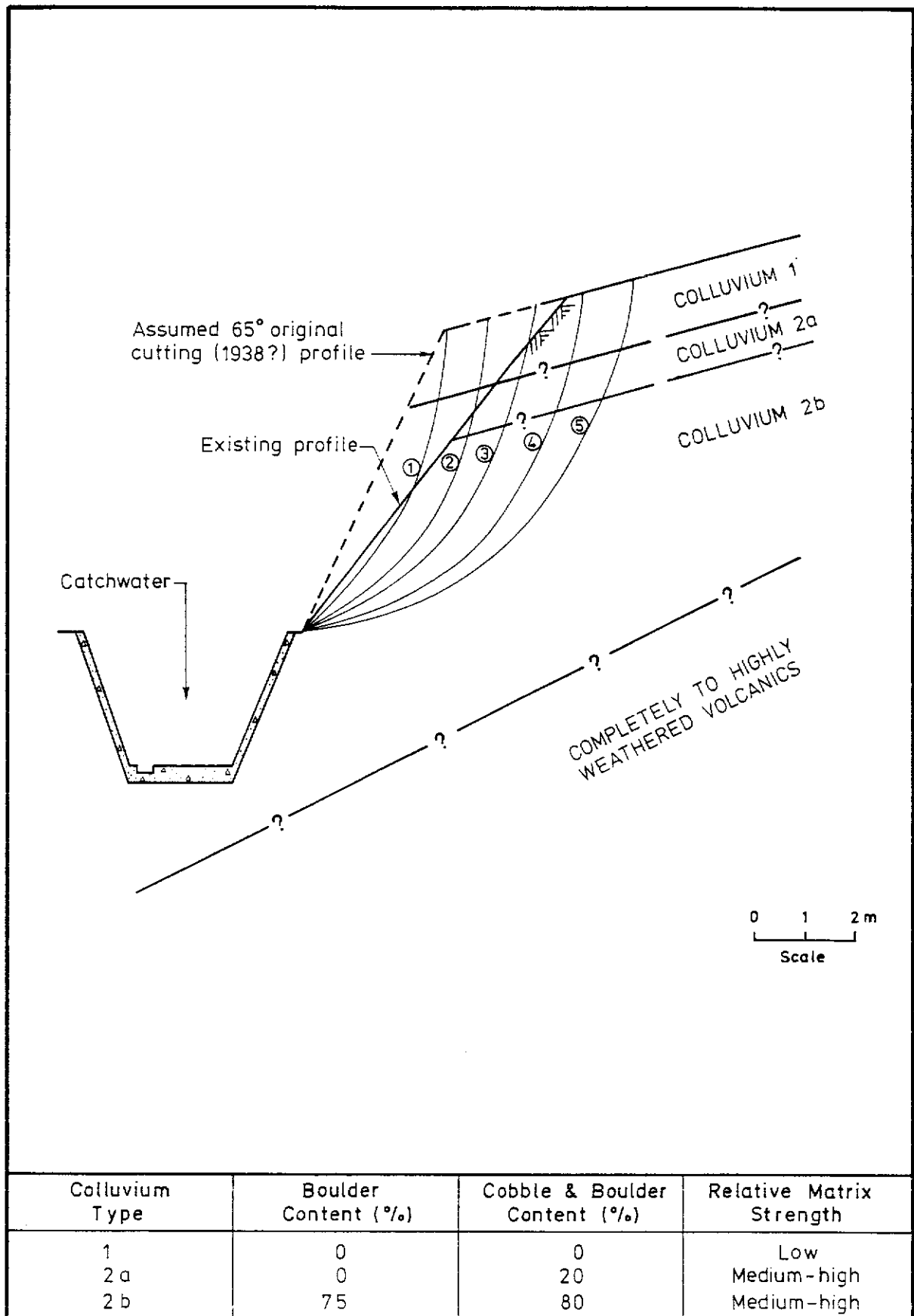


Figure B.8 - Back Analysis of Slope at CH 6135, Shing Mun Catchwater

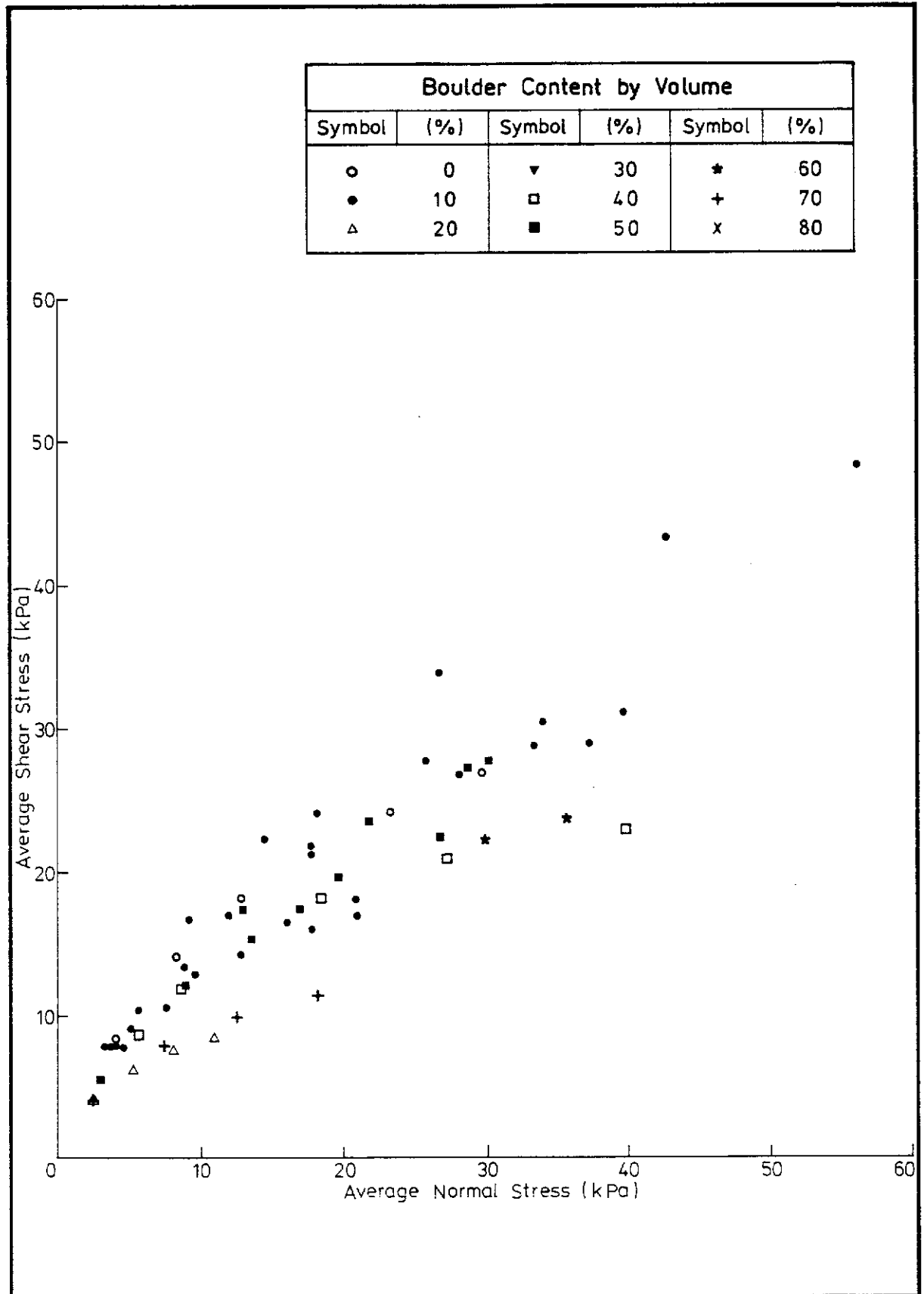


Figure B.9 - Back-Analysed Average Shear and Normal Stresses along Potential Failure Surfaces, Shing Mun Catchwater Slopes

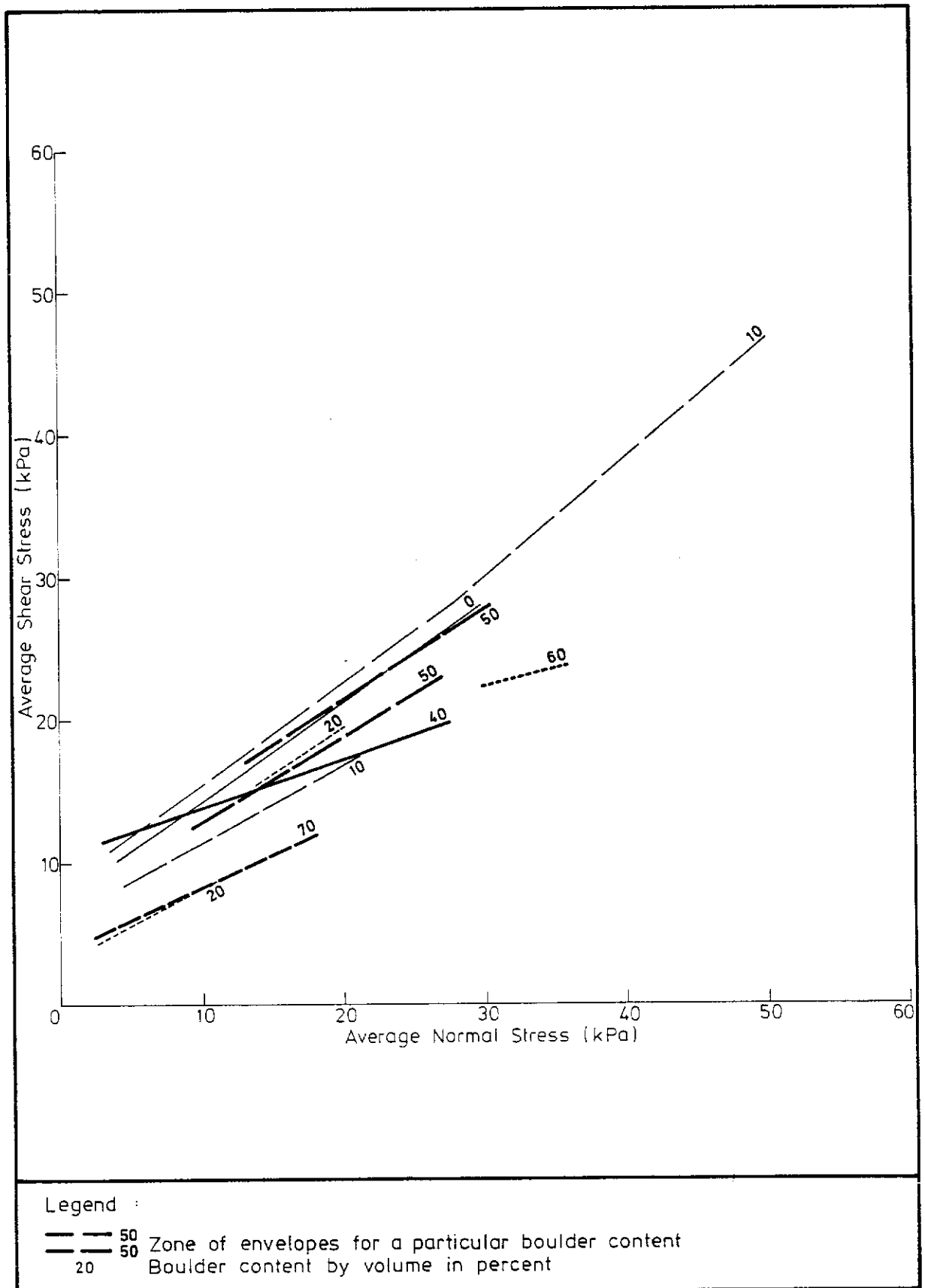


Figure B.10 - Back-calculated Least-squares Shear Strength Envelopes for Various Boulder Contents, Shing Mun Catchwater Slopes

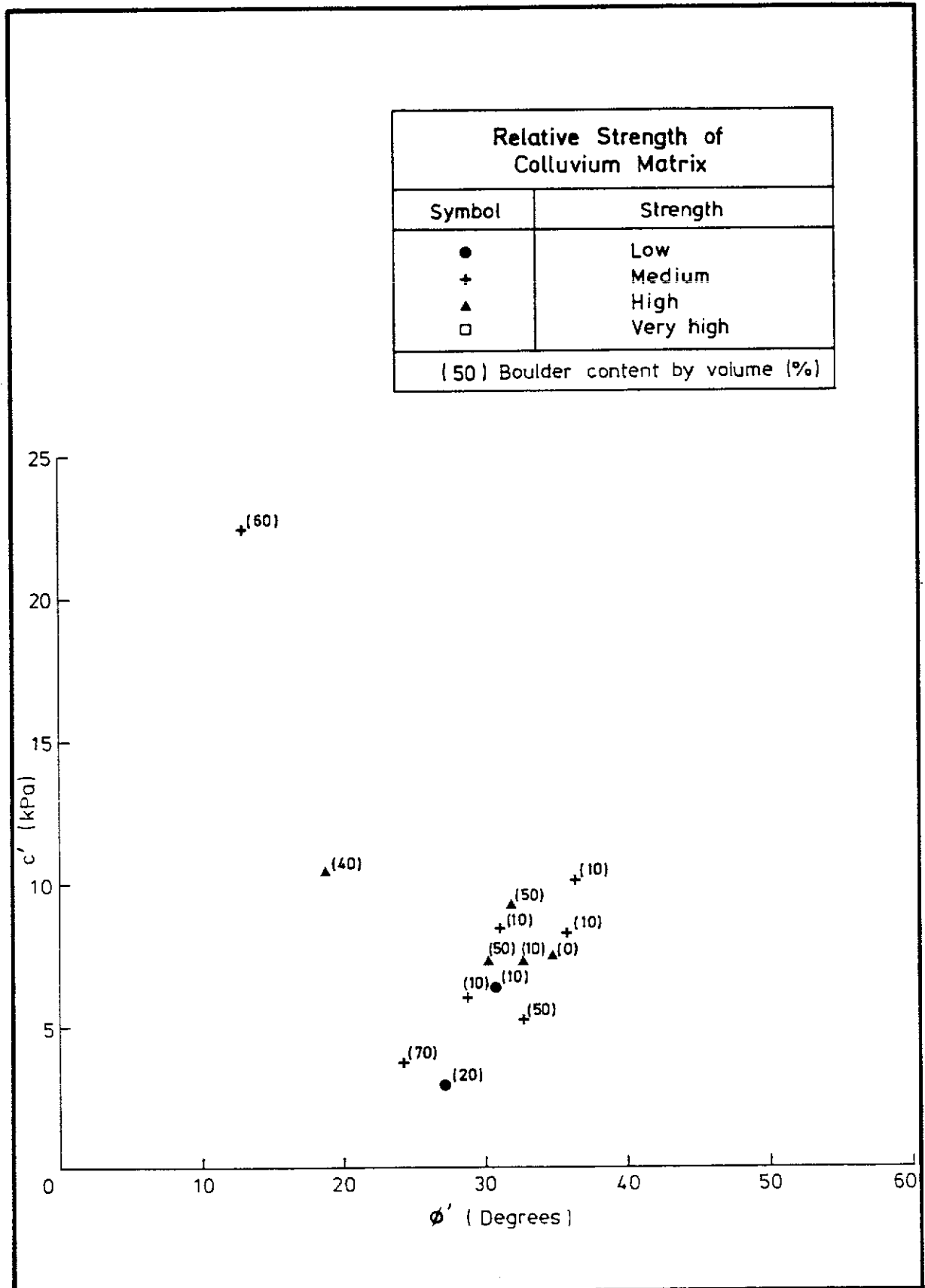


Figure B.11 - Plot of Back-calculated c' versus ϕ' for Various Boulder Contents, Shing Mun Catchwater Slopes ($\sigma_n' \leq 50$ kPa)

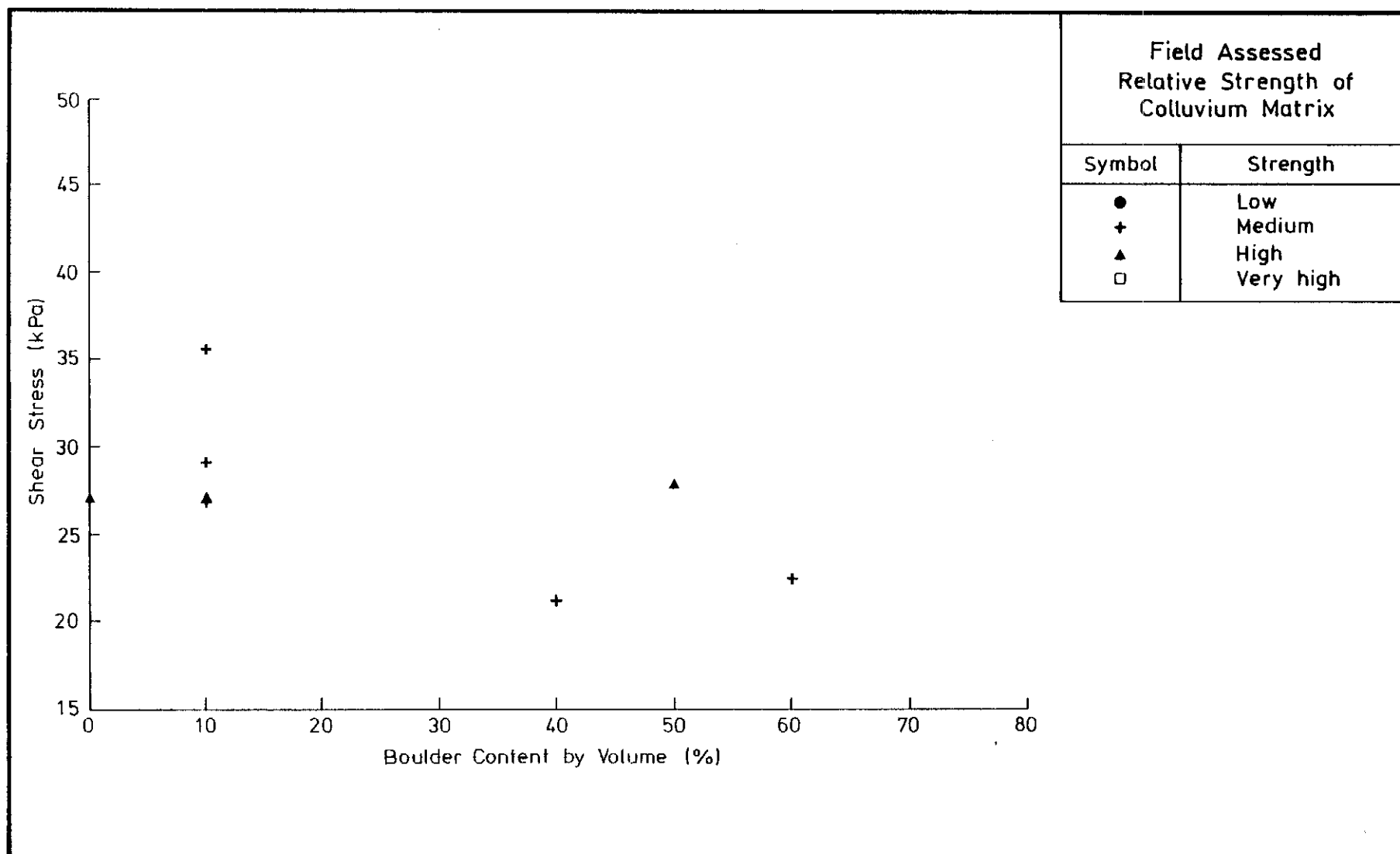


Figure B.12 - Variation of Back-calculated 'Minimum' Shear Stress at $\sigma_n' = 30$ kPa with Boulder Content, Shing Mun Catchwater Slopes

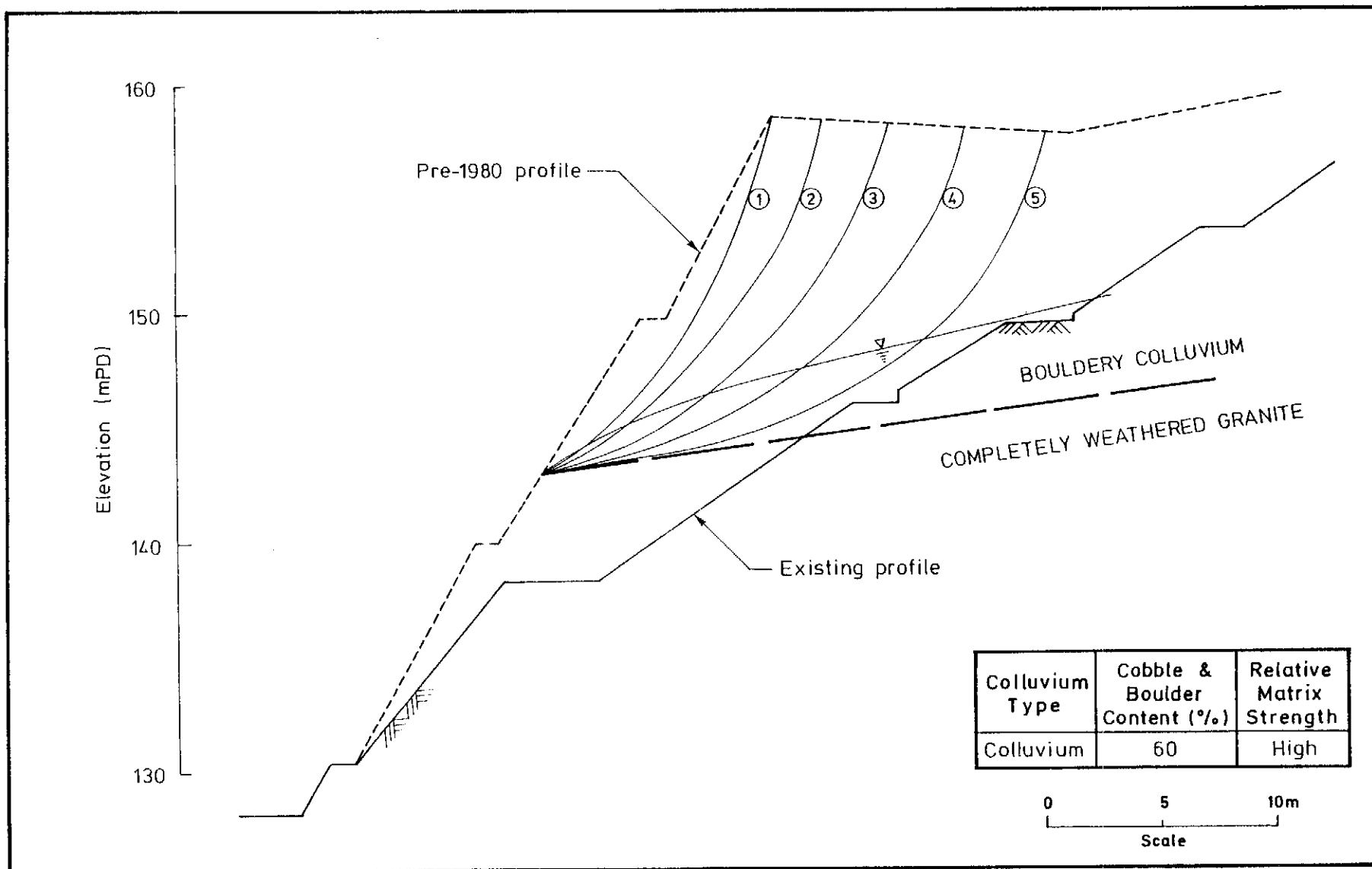


Figure B.13 - Back Analysis of Slope 11NE-A/C6 (CH B80), Tsz Wan Shan Estate

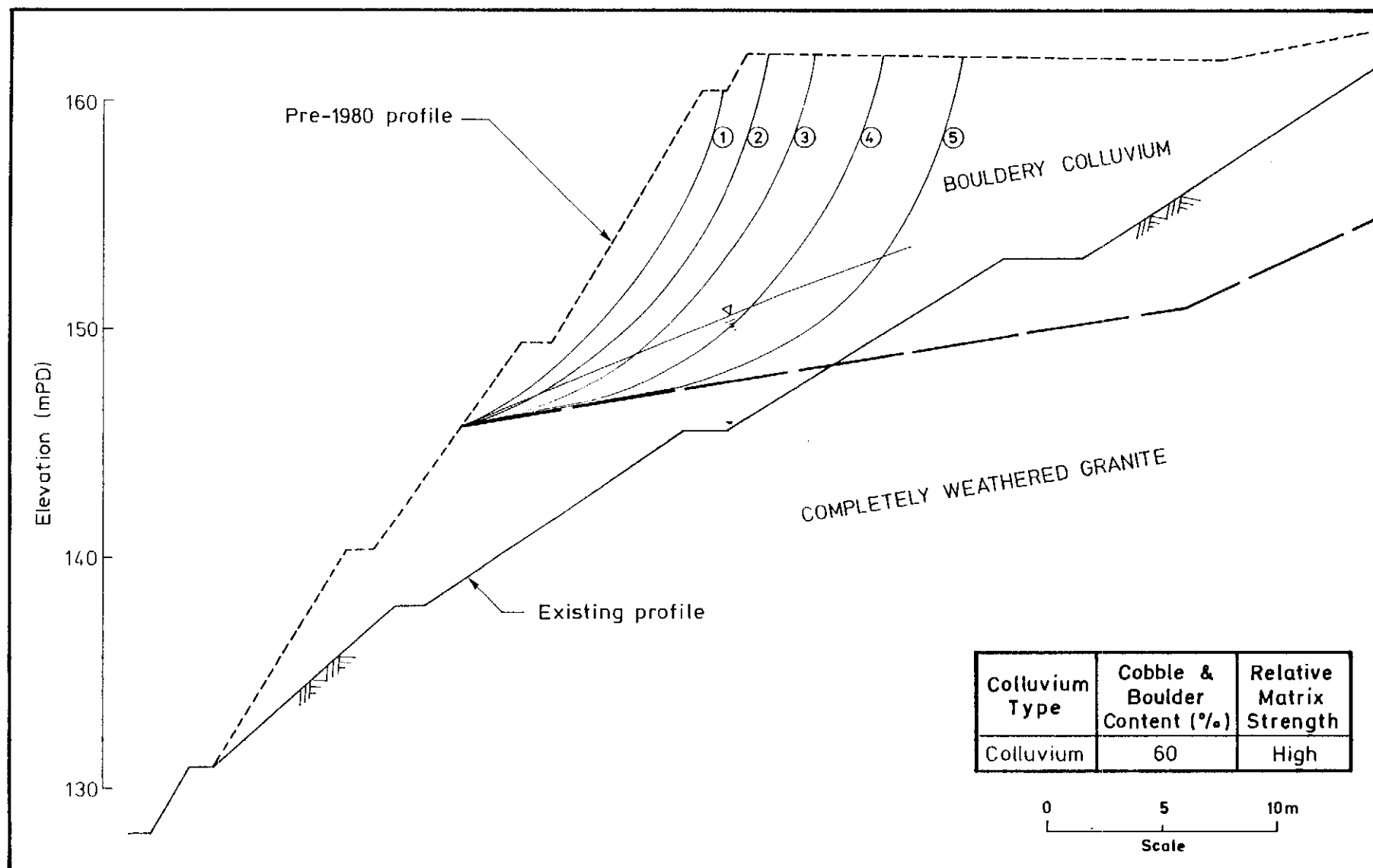


Figure B.14 - Back Analysis of Slope 11NE-A/C6 (CH B80), Tsz Wan Shan Estate

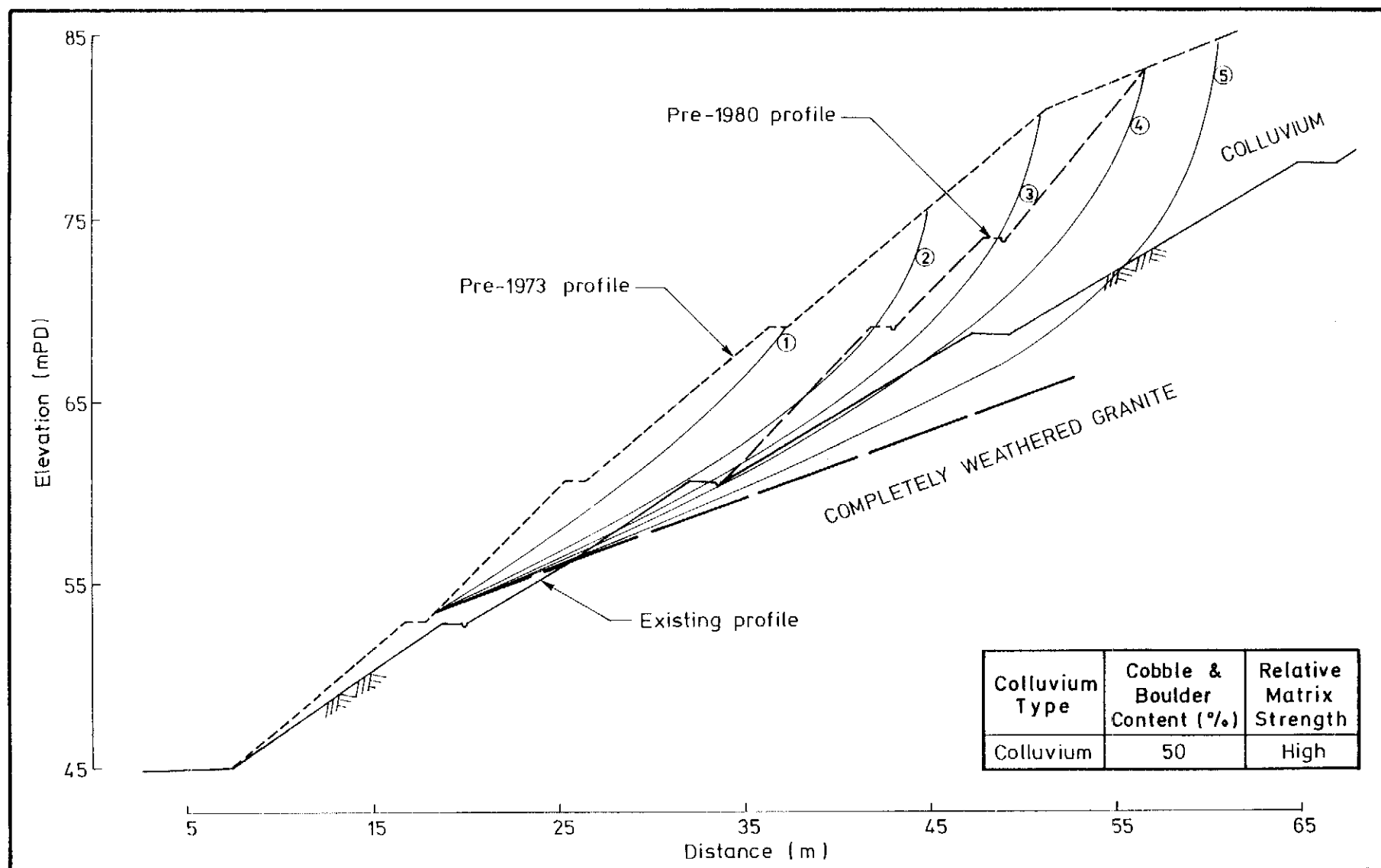


Figure B.15 - Back Analysis of Slope 11NE-A/C8, Tsz Wan Shan Estate

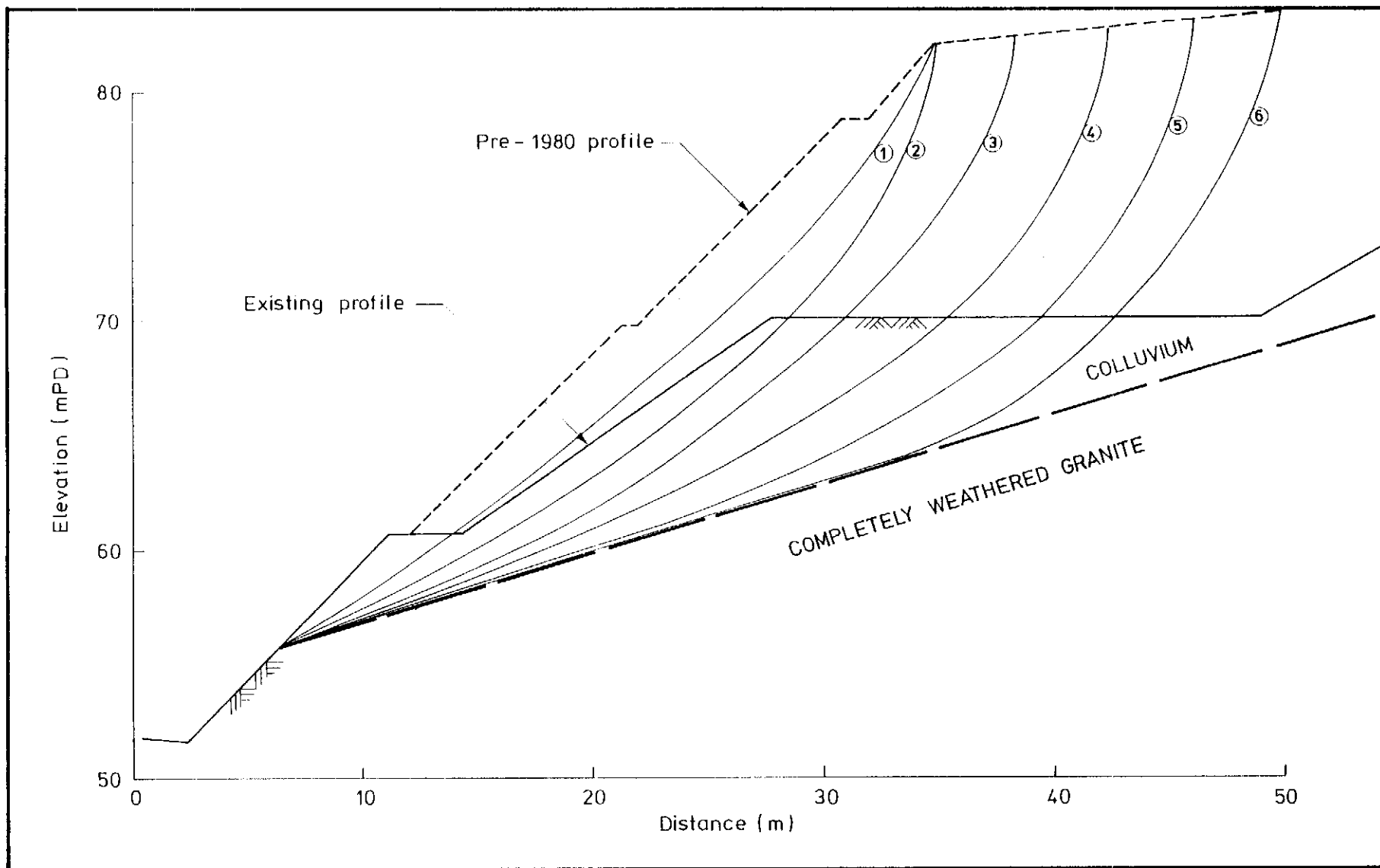


Figure B.16 - Back Analysis of Slope 11NE-A/C9, Tsz Wan Shan Estate

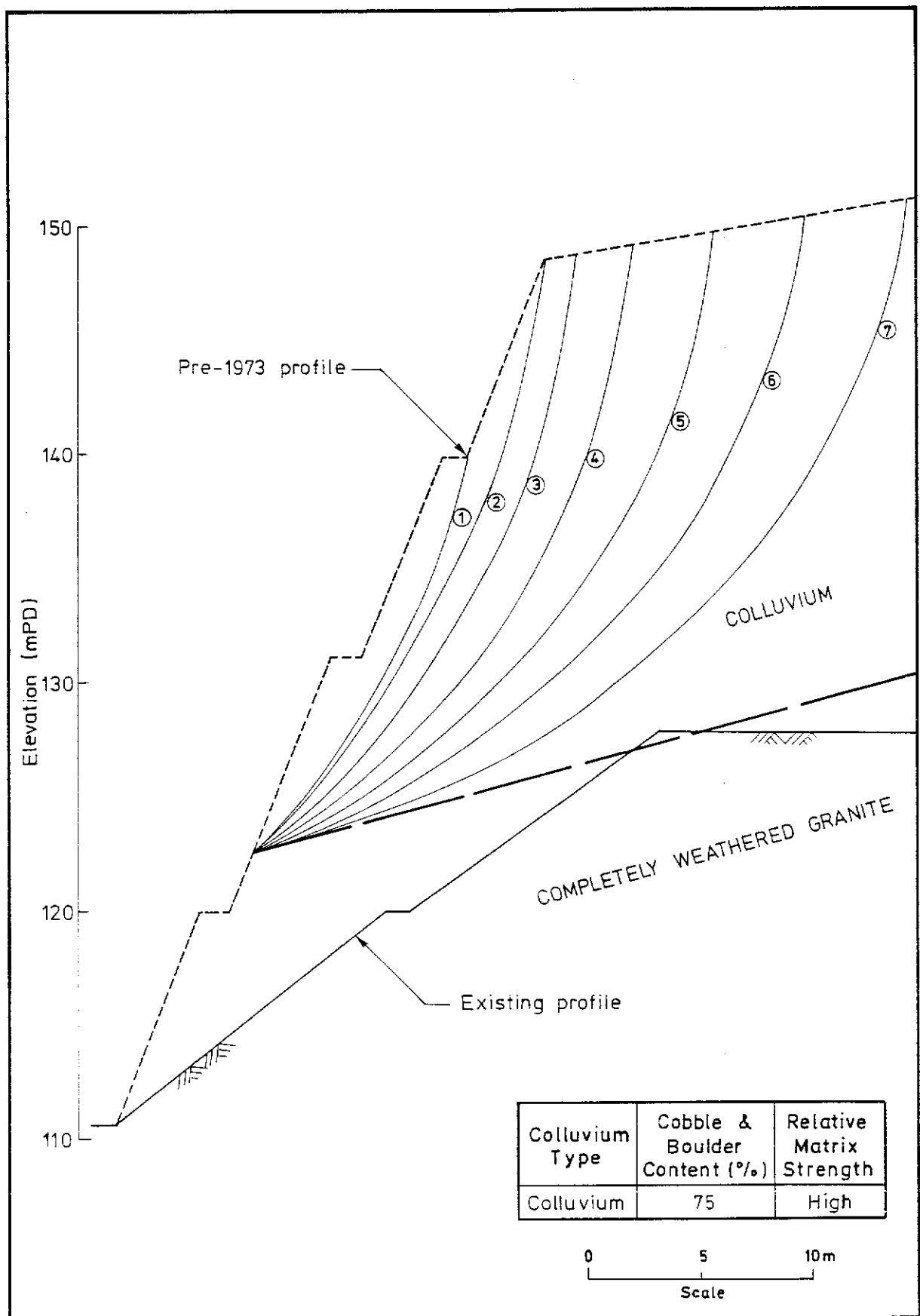


Figure B.17 - Back Analysis of Slope 11NE-A/C11, Tsz Wan Shan Estate

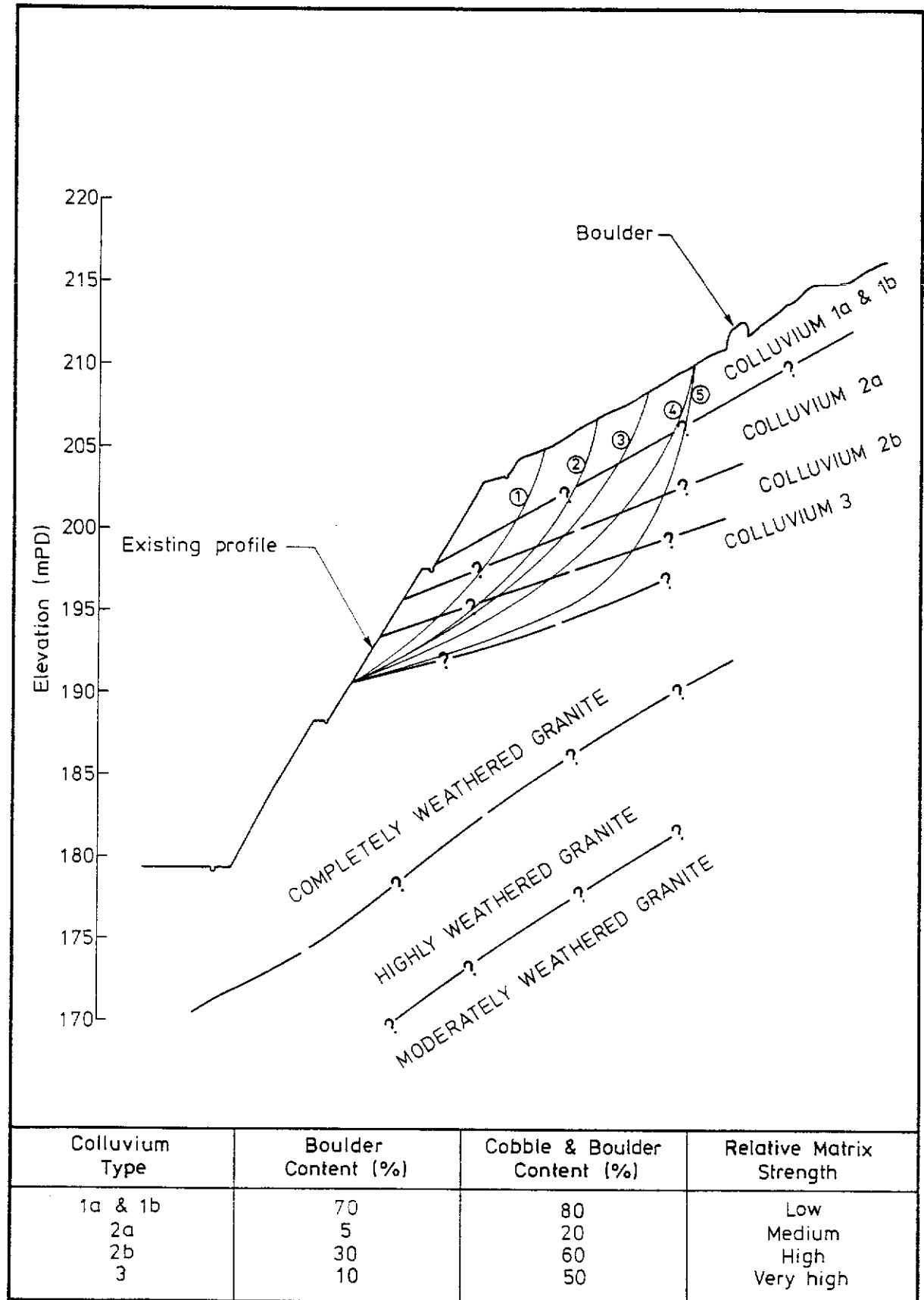


Figure B.18 - Back Analysis of Slope 11SW-A/C36 (Section CS2), Chater Hall Service Reservoir

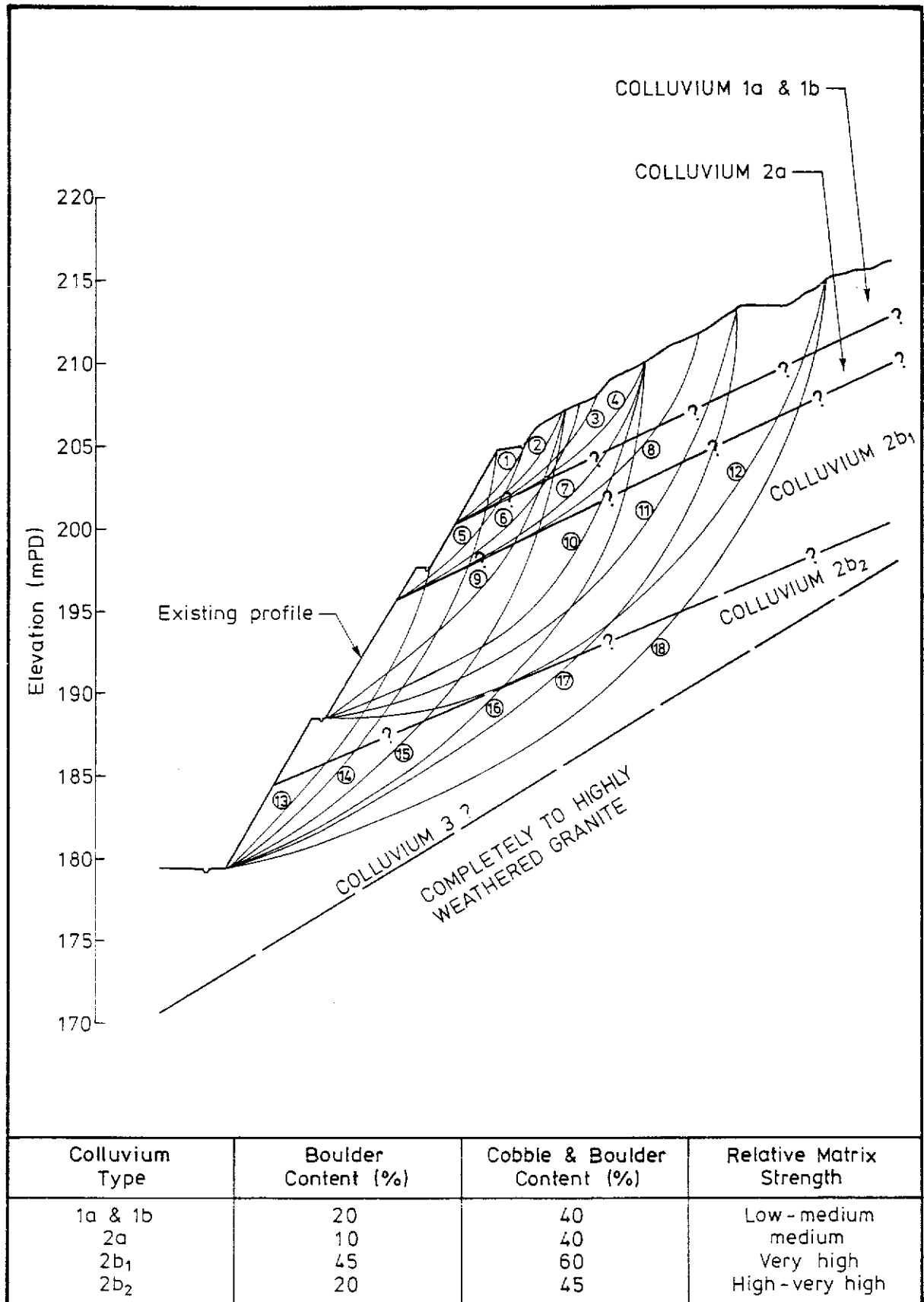


Figure B.19 - Back Analysis of Slope 11SW-A/C36 (Section CS3), Chater Hall Service Reservoir

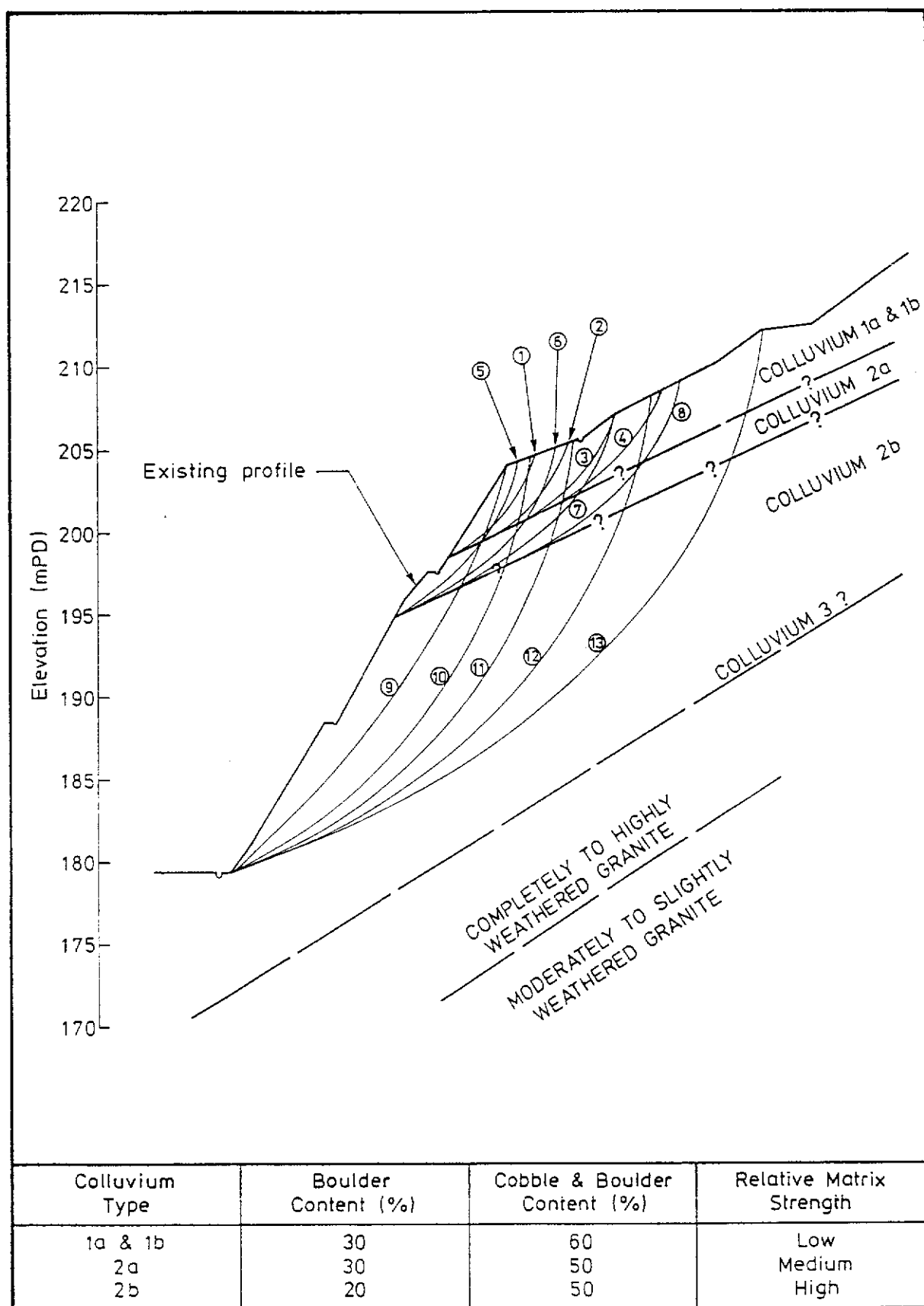


Figure B.20 - Back Analysis of Slope 11SW-A/C36 (Section CS4), Chater Hall Service Reservoir

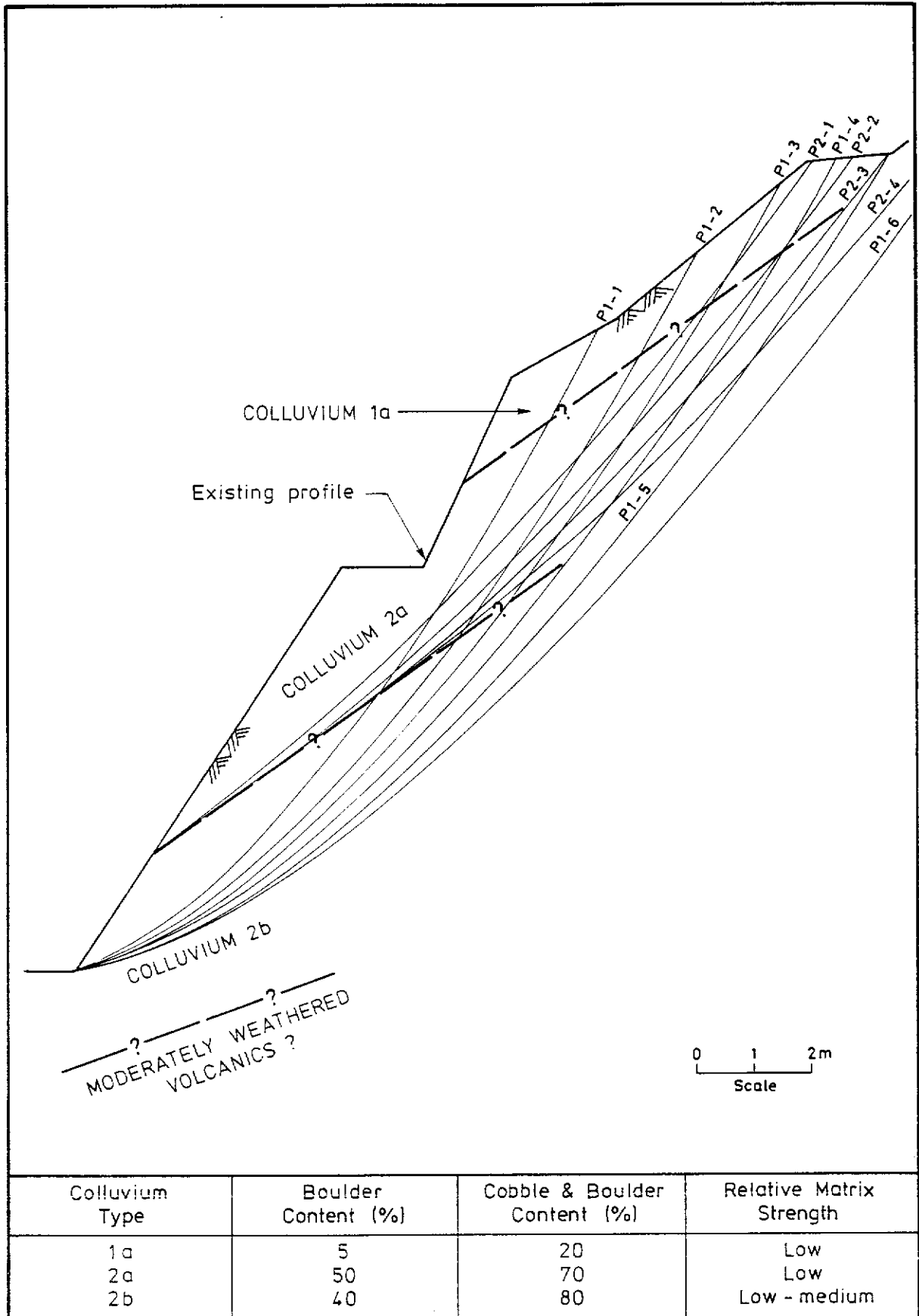


Figure B.21 - Back Analysis of Slope 11SW-D/C471, Plantation Road

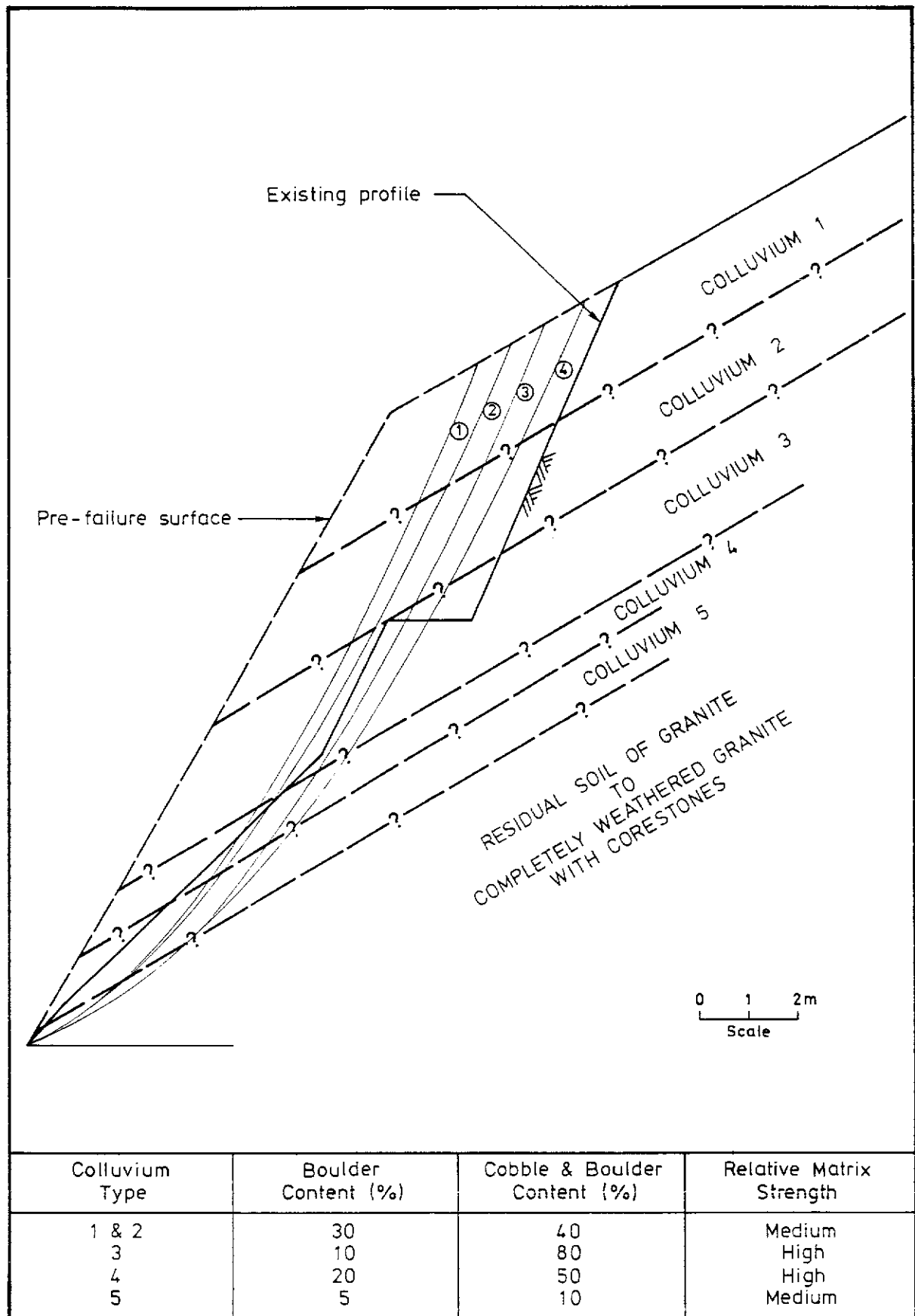


Figure B.22 - Back Analysis of Slope 11SW-D/C340, Mount Nicholson Road

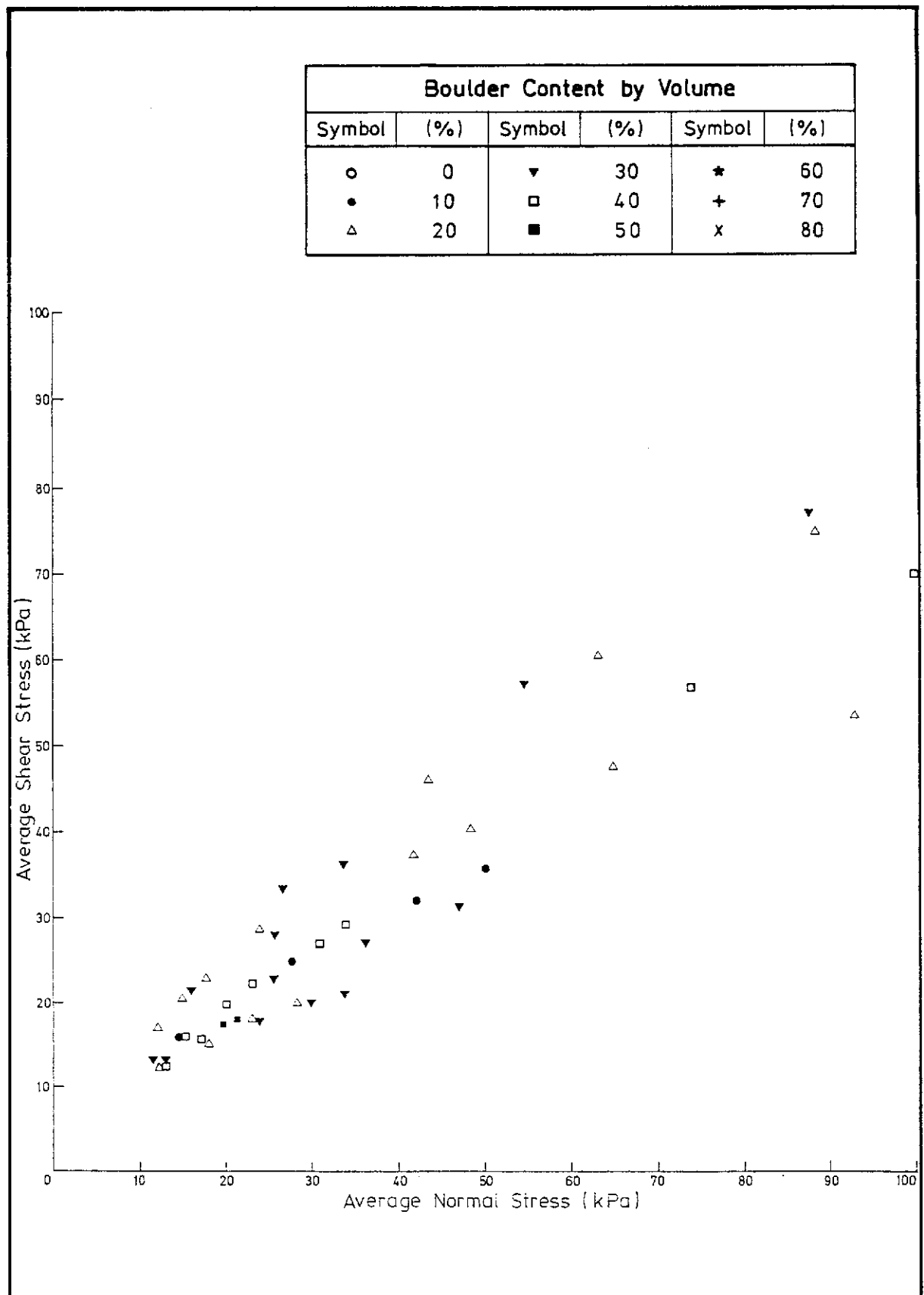


Figure B.23 - Back-analysed Average Shear and Normal Stresses along Potential Failure Surface, Mid-levels and Peak Slopes

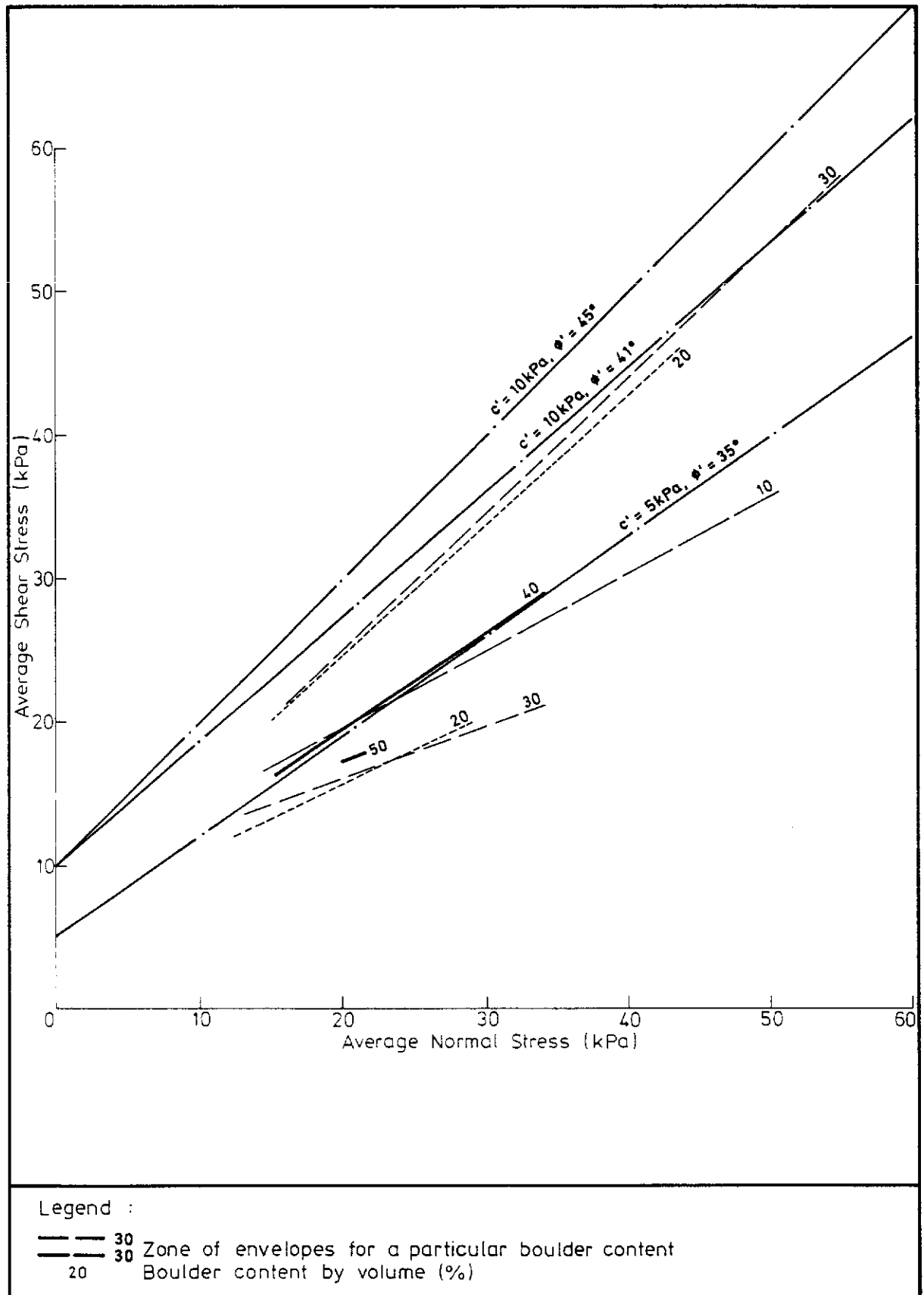


Figure B.24 - Back-calculated Least-squares Shear Strength Envelopes for Various Boulder Contents, Mid-levels and Peak Slopes

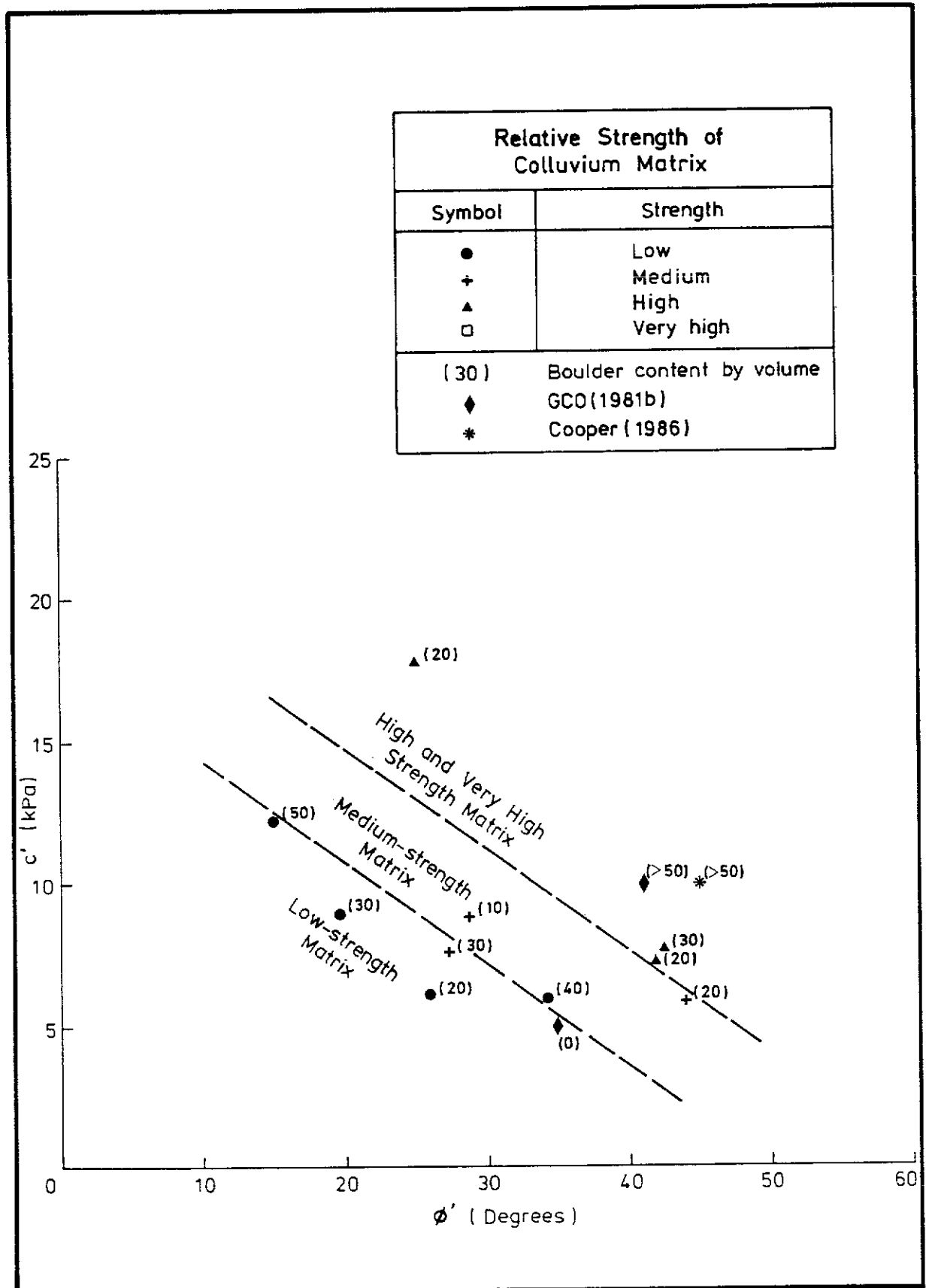


Figure B.25 - Plot of Back-calculated c' versus ϕ' for Various Boulder Contents, Mid-levels and Peak Slopes ($\sigma_n' \leq 50$ kPa)

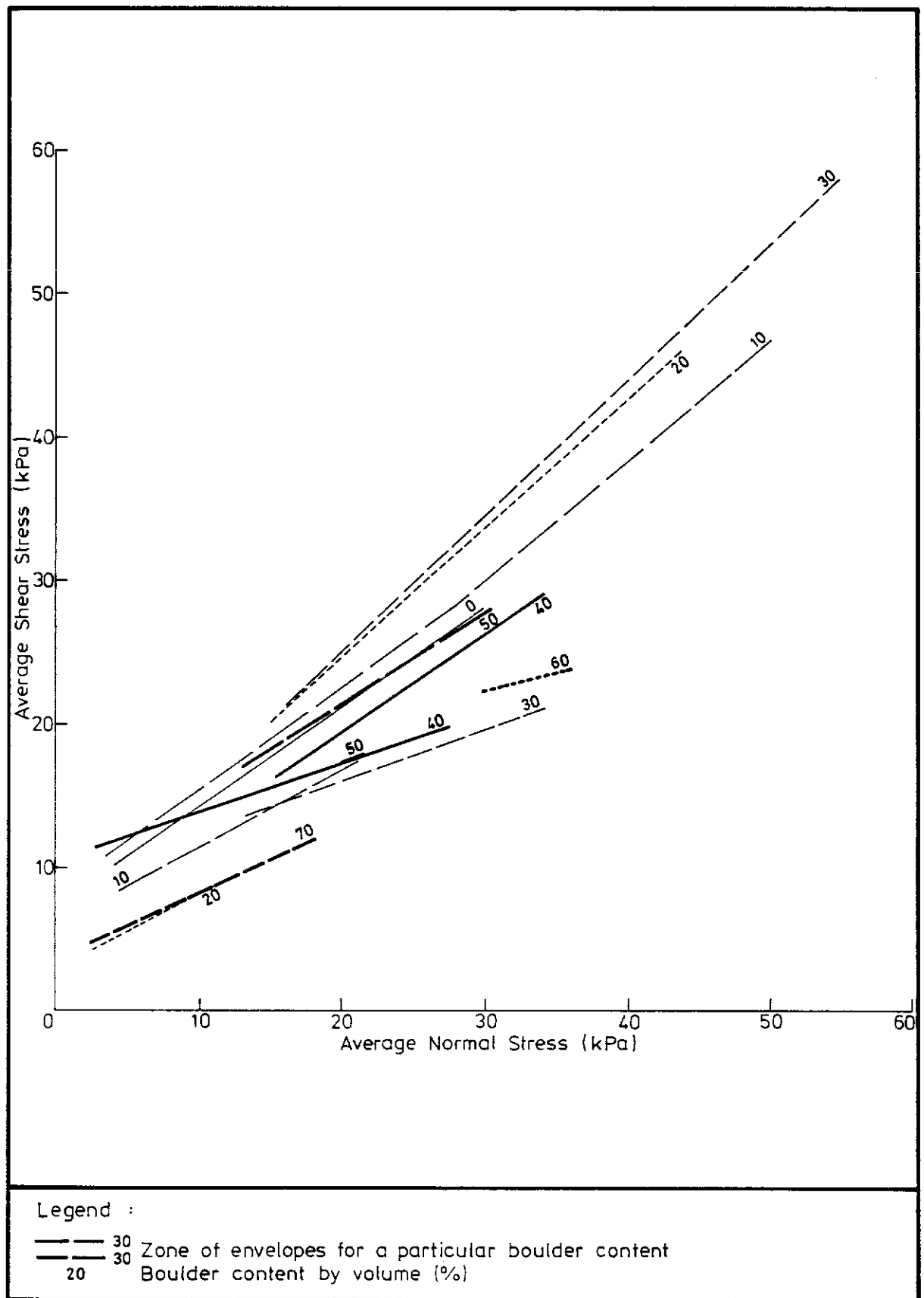


Figure B.26 - Back-calculated Least-squares Shear Strength Envelopes for Various Boulder Contents, All Slopes

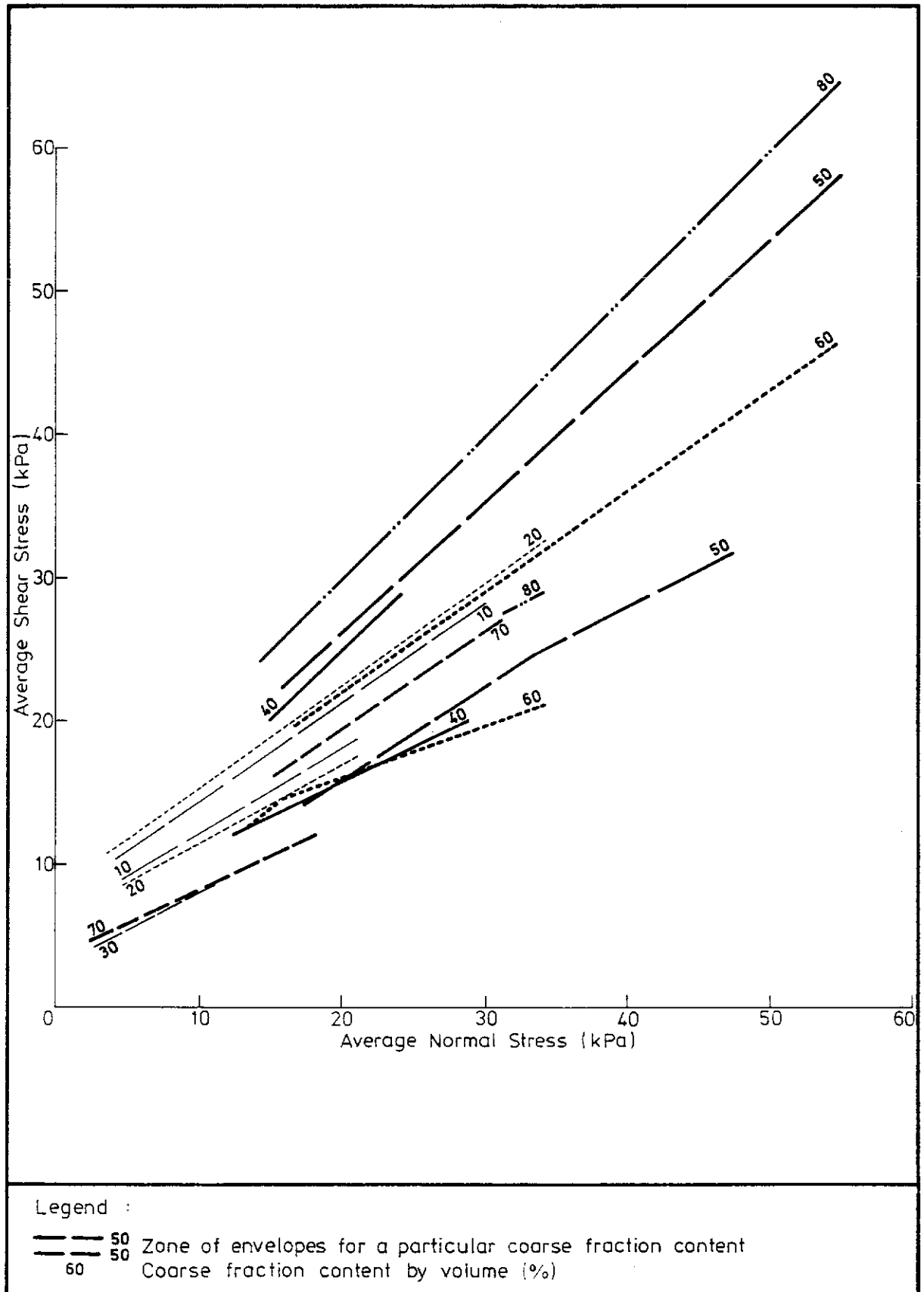


Figure B.27 - Back-calculated Least-squares Shear Strength Envelopes for Various Coarse Fraction Contents, All Slopes

APPENDIX C
SAMPLE PREPARATION TECHNIQUES

SAMPLE PREPARATION TECHNIQUES

1. Triaxial Tests On Specimens Containing Steel Balls (CU - BB Series)

The steel balls used as the coarse fraction in the triaxial tests came with a surrounding layer of protective oil. This layer was removed prior to sample preparation. The matrix material was prepared from a completely decomposed granitic soil obtained from the Mount Butler Quarry. Particles larger than 2 mm were removed by dry sieving.

The matrix material and the steel balls were placed in a 100 mm inner diameter sample mould in 18 equal layers. The inside wall of the mould was greased to minimize side friction. For each layer, the matrix material was first poured into the mould and levelled gently with a spatula. Trial runs had shown that the soil must be placed wet for better compaction performance. A water content of about 14% was found to be satisfactory. Steel balls were placed by hand over the matrix layer as uniformly as possible. A second layer of matrix material was then added. After placing six layers of matrix material and steel balls, the sample was compressed to a thickness equal to one-third of its height, by using a tight-fitted ram. After the compression, the ram was removed. The surface of the compacted soil was scarified or broken up to a depth equal to one ball diameter. The process was repeated two more times before the sample was extruded from the mould.

The samples were saturated by back pressure to achieve a B value of over 0.97 before consolidation.

2. Triaxial Tests on Specimens Containing Aggregates (CU-AGG Series)

The sample preparation technique was similar to that used in CU-BB series except that a mould of 76 mm diameter and an aggregate size of 5-6.3 mm were used. Flaky aggregates with a maximum-to-minimum-dimension ratio larger than 4 were removed.

After testing, the amount of aggregate retained by 5 mm sieve was weighed. The same sample of aggregate was used in as many test specimens as possible.

3. Large Direct Shear Box Tests on Specimens Containing Aggregates (BSB Series)

A mixture of oven-dried matrix material and aggregate was placed in four layers in a direct shear box. Each layer was spread out evenly to obtain a uniform distribution of particles. After the placement of first two layers, the sample was compressed to a thickness of 70 mm. The surface of the compacted layer was scarified or broken up to a depth equivalent to the mean diameter of the particles. The next 2 layers were then placed. The sample was compressed to give a final thickness of 148 mm. The weight of the matrix material and aggregate in each layer was adjusted for the differences in layer thickness. The sample was soaked for at least 2 days under a normal stress of 5 kPa before shearing.

The same sample of aggregate was used in as many test specimens as possible.

4. Small Direct Shear Box Tests on Specimens Containing Aggregates (NSB and NSB-D Series)

The matrix material and aggregate were oven-dried, mixed thoroughly and poured as one layer in a small direct shear box. The sample was compressed to a thickness of 38.5 mm. The samples were then soaked overnight under a normal pressure of 5 kPa before shearing.

APPENDIX D
PROGRAM 'INCL.BAS'

PROGRAM 'INCL.BAS'

```

DECLARE FUNCTION NormBk% (SlipBlock%)
'Purpose : to generate slip surface for rectangular inclusion bearing method
' Valid possible for inclusion content > 30%
DECLARE SUB GrBlocks (PreBlock AS ANY, x%, y%, Gr AS ANY)
DECLARE SUB RunGslp (DataFile$, FOS!)
DECLARE SUB Genslip (SlipBk%(), SlipBkNo%(), AllowCases%)
DECLARE FUNCTION yslip! (x!)
DECLARE SUB Block (corner AS ANY, nx%, ny%, position%)
DECLARE FUNCTION yground! (x!)
DECLARE SUB HorBlocks (PreSlip AS ANY, Tryx%, Tryy%, Ground%, Dif!)
DECLARE SUB GrLast (pt1 AS ANY, pt2 AS ANY, LastPt AS ANY)
DECLARE SUB GenChoice (LastBkx%, LastBky%, InitDif!, Firstx%, HitGround%(), Dif!())
COMMON SHARED h!, l!, sl!, st!, Incl!
COMMON SHARED An2Ra#
COMMON SHARED SlopeH!, BatterA!, UpperA!
COMMON SHARED MaxSlipPt%
COMMON SHARED Trials%, CritSlip%
TYPE xy
  x AS SINGLE
  y AS SINGLE
END TYPE

CONST false = 0, true = NOT false
An2Ra# = ATN(1) / 45

Trials% = 4
'Trials% = no of trials
CLS

'Inclusion percentage
INPUT "Inclusion percentage (%) = ", ic%
PRINT

'Height of the slope
INPUT "Vertical Height of the batter = ", SlopeH!

'Block dimension
PRINT "Input block information"
INPUT "Height = ", h!
INPUT "Length = ", l!
INPUT "Lateral Spacing = ", sl!
INPUT "Transverse Spacing = ", st!
INPUT "Transverse Spacing/Lateral Spacing = ", srl!
sl! = ((h! + srl * l!) + SQR((h! + srl * l!) ^ 2 + 4 * (l! * h! / ic% * 100 - l! * h!) * srl)) / 2 / srl
st! = srl * sl!
PRINT "Lateral Spacing = "; sl!
PRINT "Transverse Spacing = "; st!

INPUT "Block Inclination Angle = ", Incl!
PRINT

'OutPut file master
INPUT "Output GSLPC Data File Master (without extension) = ", Master$

'slope configuration
BatterA! = 59
UpperA! = 20

DIM corner AS xy

'Estimate the number of slip data points
MaxSlipPt% = 2 + INT((SlopeH! * (COS(Incl! * An2Ra#) + 2 * ABS(TAN((UpperA! - Incl!) * An2Ra#)))) / (h! + sl!)) * 2

DIM SlipBk%(1 TO Trials%, 1 TO MaxSlipPt%, 0 TO 2)
' record the slip block no.
' the first field records the number of slip paths chosen, i.e. Trials%
' the second field records the block
' the third field records the x and y number of the slip and the corner position
DIM SlipInf%(1 TO Trials%, 0 TO 1)
' record actual number of slip blocks and the ending condition
' with the following convention for the ending condition
' 1 if the ground surface is between two blocks at the same level
' 2 if the ground surface is at the bottom corner (3) of a block
' 3 if the ground surface is above the last block
DIM SlipPt%(1 TO Trials% * 3, 1 TO MaxSlipPt%) AS xy

'Store all trial slip surface - to eliminate duplicate
DIM AllSlipInf%(1 TO Trials% * 3, 0 TO 1)
DIM AllSlipBk%(1 TO Trials% * 3, 1 TO MaxSlipPt%, 0 TO 2)
DIM FOS!(1 TO Trials% * 3)

SlipNo% = 0
CLS
'Try three sets of critical slips
'CritSlip% = critical slip number
FOR CritSlip% = 2 TO 4
  PRINT "Based on Slip No "; CritSlip%; " ("; ic%; "% inclusion)"
  CALL Genslip(SlipBk%(), SlipInf%(), AllowCases%)
  FOR i = 1 TO AllowCases%
    'Compare slip with those previously obtained
    duplicate% = false
    FOR j = 1 TO SlipNo%
      'Check the slip surface information
      duplicate% = true
      IF (AllSlipInf%(j, 0) = SlipInf%(i, 0)) AND (AllSlipInf%(j, 1) = SlipInf%(i, 1)) THEN
        FOR k = 1 TO SlipInf%(i, 0)
          FOR ll = 0 TO 2
            IF AllSlipBk%(j, k, ll) <> SlipBk%(i, k, ll) THEN
              duplicate% = false
              EXIT FOR
            END IF
          NEXT
        NEXT
        IF NOT duplicate% THEN EXIT FOR
      ELSE
        duplicate% = false
      END IF
      IF duplicate% THEN EXIT FOR
    NEXT
  NEXT
  SlipNo% = SlipNo% + 1
NEXT

```

```
'If the slip surface is not duplicate, record down the information
IF NOT duplicate THEN
  SlipNo% = SlipNo% + 1
  AllslipInf$(SlipNo%, 0) = SlipInf$(i, 0)
  AllslipInf$(SlipNo%, 1) = SlipInf$(i, 1)
  FOR j = 1 TO SlipInf$(i, 0)
    FOR k = 0 TO 2
      AllslipBk$(SlipNo%, j, k) = SlipBk$(i, j, k)
    NEXT
  NEXT
END IF
NEXT
NEXT
NEXT

CLS
TotalslipNo% = SlipNo%
'Display the slip information
FOR SlipNo% = 1 TO TotalslipNo%
  'Print out block no of the slips
  PRINT "**** L="; LTRIM$(STR$(l)); ".H="; LTRIM$(STR$(h)); ". ST/SL="; LTRIM$(STR$(st / sl));
  PRINT ". IC="; LTRIM$(STR$(ic)); ". Incl. angle = "; LTRIM$(STR$(Incl));
  PRINT "0. Slip No "; LTRIM$(STR$(SlipNo%)); "*****";
  FOR j = 1 TO AllslipInf$(SlipNo%, 0)
    IF j MOD 5 = 1 THEN PRINT
    FOR k = 0 TO 2
      PRINT AllslipBk$(SlipNo%, j, k); " ";
    NEXT
    PRINT " ";
  NEXT
  PRINT
NEXT

'Generate the slip surface
SELECT CASE AllslipInf$(SlipNo%, 1)
CASE 1
  'Ground surface terminated between two adjacent blocks
  FOR j = 1 TO AllslipInf$(SlipNo%, 0) - 1
    CALL Block(SlipPt(SlipNo%, j), AllslipBk$(SlipNo%, j, 0), AllslipBk$(SlipNo%, j, 1), AllslipBk$(SlipNo%, j, 2))
  NEXT
  CALL GrBlocks(SlipPt(SlipNo%, AllslipInf$(SlipNo%, 0) - 2), AllslipBk$(SlipNo%, AllslipInf$(SlipNo%, 0) - 1, 0),
  AllslipBk$(SlipNo%, AllslipInf$(SlipNo%, 0) - 1, 1), SlipPt(SlipNo%, AllslipInf$(SlipNo%, 0)))
CASE 2
  'Ground surface terminated at one bottom corner
  FOR j = 1 TO AllslipInf$(SlipNo%, 0)
    CALL Block(SlipPt(SlipNo%, j), AllslipBk$(SlipNo%, j, 0), AllslipBk$(SlipNo%, j, 1), AllslipBk$(SlipNo%, j, 2))
  NEXT
CASE 3
  'Ground surface terminated between two block levels
  FOR j = 1 TO AllslipInf$(SlipNo%, 0)
    CALL Block(SlipPt(SlipNo%, j), AllslipBk$(SlipNo%, j, 0), AllslipBk$(SlipNo%, j, 1), AllslipBk$(SlipNo%, j, 2))
  NEXT
  CALL GrLast(SlipPt(SlipNo%, AllslipInf$(SlipNo%, 0) - 1), SlipPt(SlipNo%, AllslipInf$(SlipNo%, 0)), SlipPt(SlipNo%,
  AllslipInf$(SlipNo%, 0) + 1))
  AllslipInf$(SlipNo%, 0) = AllslipInf$(SlipNo%, 0) + 1
END SELECT

'Generate the GSLP file
Filename$ = LTRIM$(LTRIM$(Master$)) + "." + STRING$(2 - INT(SlipNo% / 10), "0") + LTRIM$(STR$(SlipNo%))
OPEN Filename$ FOR OUTPUT AS #1
PRINT #1, "ACOL 3- L="; LTRIM$(STR$(l)); ".H="; LTRIM$(STR$(h)); ". ST/SL=";
PRINT #1, LTRIM$(STR$(st / sl)); ". IC="; LTRIM$(STR$(ic)); ". Incl. angle = "; LTRIM$(STR$(Incl));
'Ground information
IF SlipPt(SlipNo%, AllslipInf$(SlipNo%, 0)).x > SlopeH1 / TAN(BatterA1 * An2Ra#) THEN
  PRINT #1, "GROUND3"
  PRINT #1, "0.0 0.0 ";
  PRINT #1, USING "###.## ###.## "; SlopeH1 / TAN(BatterA1 * An2Ra#); SlopeH1;
  PRINT #1, USING "###.## ###.## "; SlipPt(SlipNo%, AllslipInf$(SlipNo%, 0)).x; SlipPt(SlipNo%, AllslipInf$(SlipNo%, 0)).y
ELSE
  PRINT #1, "GROUND2"
  PRINT #1, "0.0 0.0 ";
  PRINT #1, USING "###.## ###.## "; SlipPt(SlipNo%, AllslipInf$(SlipNo%, 0)).x; SlipPt(SlipNo%, AllslipInf$(SlipNo%, 0)).y
END IF
'lip information
PRINT #1, "SLIP"; LTRIM$(STR$(AllslipInf$(SlipNo%, 0)));
FOR j = 1 TO AllslipInf$(SlipNo%, 0)
  IF j MOD 5 = 1 THEN PRINT #1,
  PRINT #1, USING "###.## ###.## "; SlipPt(SlipNo%, j).x; SlipPt(SlipNo%, j).y;
NEXT
PRINT #1,
'Strata information
PRINT #1, "STRATA1"
PRINT #1, "18 5 35 1 0.0"
'Interstice force information
PRINT #1, "IFORCES"; LTRIM$(STR$(AllslipInf$(SlipNo%, 0) + 3));
FOR j = 1 TO AllslipInf$(SlipNo%, 0) + 3
  IF j MOD 10 = 1 THEN PRINT #1,
  PRINT #1, "0 1 ";
NEXT
CLOSE #1

'Run Gslp
CALL RunGslp1(Filename$, FOS$(SlipNo%))
PRINT

' IF SlipNo% = TotalslipNo% THEN EXIT FOR
' PRINT "Press any key to run the next case"
dummy$ = INPUT$(1)
NEXT
PRINT
PRINT "Press any key to display the FOS in order"
dummy$ = INPUT$(1)
'Sort the FOS
'Initialization
DIM Order$(1 TO TotalslipNo%)
FOR i = 1 TO TotalslipNo%
  Order$(i) = i
NEXT

'Selection method
FOR i = 1 TO TotalslipNo% - 1
  FOR j = i + 1 TO TotalslipNo%
    IF FOS$(Order$(j)) < FOS$(Order$(i)) THEN
      SWAP Order$(i), Order$(j)
    END IF
  NEXT
NEXT
```

```

NEXT
NEXT
'Display the sorted FOS
PRINT "FOS", "Slip No"
FOR i = 1 TO TotalSlipNo%
  PRINT FOS!(Order%(i)), Order%(i)
NEXT

'arrange the slip number in sorted file order
PRINT "Do you want the slip number arranged in FOS order (Y/n)";
key$ = INPUT$(1)
PRINT key$
IF (key$ = "y") OR (key$ = "Y") THEN
  'Rename the files to have a temp master name, incl_ten
  'Note ■ is ASCII code 220
  FOR i = 1 TO TotalSlipNo%
    OldFilename$ = LTRIM$(RTRIM$(Master$)) + "." + STRING$(2 - INT(i / 10), "0") + LTRIM$(STR$(i))
    NewFilename$ = "incl" + "." + STRING$(2 - INT(i / 10), "0") + LTRIM$(STR$(i))
    NAME OldFilename$ AS NewFilename$
  NEXT
  'Rename the files in sorted order
  FOR i = 1 TO TotalSlipNo%
    NewFilename$ = LTRIM$(RTRIM$(Master$)) + "." + STRING$(2 - INT(i / 10), "0") + LTRIM$(STR$(i))
    OldFilename$ = "incl" + "." + STRING$(2 - INT(Order%(i) / 10), "0") + LTRIM$(STR$(Order%(i)))
    NAME OldFilename$ AS NewFilename$
  NEXT
END IF
END
```

```
SUB Block (corner AS xy, nx%, ny%, position%)
'Return co-ordinate of the a block (nx%, ny%) for corner, position
'corner position
'      1      2
'      3      4

DIM cg, cornera AS xy
IF (nx% = 0) OR (ny% = 0) THEN
  cornera.x = 0
  cornera.y = 0
ELSE
  'cg = cg of the block
  cg.x = (nx% - 1) * (l1 + sl1)
  cg.y = (h1 + st1) * (ny% - .5)

  SELECT CASE position%
    CASE 1
      cornera.x = cg.x - l1 / 2
      cornera.y = cg.y + h1 / 2
    CASE 2
      cornera.x = cg.x + l1 / 2
      cornera.y = cg.y + h1 / 2
    CASE 3
      cornera.x = cg.x - l1 / 2
      cornera.y = cg.y - h1 / 2
    CASE 4
      cornera.x = cg.x + l1 / 2
      cornera.y = cg.y - h1 / 2
  END SELECT
END IF

'To transform back to the common x,y
rad1 = Incl1 * An2Ra#
corner.x = cornera.x * COS(rad1) - cornera.y * SIN(rad1)
corner.y = cornera.x * SIN(rad1) + cornera.y * COS(rad1)

END SUB
```

```
SUB GenChoice (LastBkx%, LastBky%, InitDif!, Firstx%, HitGround%(), Dif!())
'Generate a number of possible slip points continued from a slip surface
' as given by global variable Trials%
'LastBkx%, LastBky% = x,y of block touched by the slip (at corner 1)
'InitDif! = Initial difference
'return the Firstx% number of the first block touched by the first possible slip
' at corner 3
'dif!() keeps the cumulative difference

'Calculate the last point
DIM PreSlip AS xy, corner AS xy
CALL Block(PreSlip, LastBkx%, LastBky%, 1)

'Try the first one
IF LastBkx% = 0 THEN
  Tryx% = 1
ELSE
  Tryx% = LastBkx%
END IF
Tryy% = LastBky% + 1
Initx% = Tryx%

'Calculate the slip points
Dif! = InitDif!
CALL HorBlocks(PreSlip, Tryx%, Tryy%, dummy%, Dif!)

CALL Block(corner, Tryx%, Tryy%, 4)
IF corner.y > yslip(corner.x) THEN
  'search for the min
  DO WHILE true
    Tryx% = Tryx% + 1
    'Check if this is the min
    'check the cross over the slip surface
    CALL Block(corner, Tryx%, Tryy%, 4)
    IF corner.y < yslip(corner.x) THEN EXIT DO
  LOOP
END IF

'Inspect the one that give the min
IF Tryx% - Initx% > INT(Trials% / 2) THEN
  Firstx% = Tryx% - INT(Trials% / 2)
ELSE
  Firstx% = Initx%
END IF

'Make the first one has a value in Dif!
Temp% = Firstx%
DO
  FOR i = 1 TO Trials%
    Dif!(i) = InitDif!
    CALL HorBlocks(PreSlip, Temp% + i - 1, Tryy%, HitGround%(i), Dif!(i))
  NEXT
  Temp% = Firstx% + 1
LOOP UNTIL Dif!(1) > 0

END SUB
```

```

SUB GenSlip (SlipBk{()}, SlipInf{()}, AllowCases{})
' to generate Trials{ } different slips
' with the minimized least square difference between slip surface
' and the critical surface with normalized by no of data point and
' the length of the slip surface
' DIM SlipBk{1 TO Trials{ }, 1 TO MaxSlipPt{ }, 0 TO 2)
' record the slip block no.
' the first field records the number of slip paths chosen, i.e. 5
' the second field records the block
' the third field records the x and y number of the slip and the corner position
' DIM SlipInf{1 TO Trials{ }, 0 TO 1)
' record actual number of slip blocks and the ending condition
' with the following convention
' 1 if the ground surface is between two blocks at the same level
' 2 if the ground surface is at the bottom corner {3} of a block
' 3 if the ground surface is above the last block

Sqt{ } = Trials{ } ^ 2
DIM Dif{1 TO Trials{ }}
DIM TempSlipBk{1 TO Trials{ }, 1 TO MaxSlipPt{ }, 0 TO 2)
DIM TempSlipInf{1 TO Trials{ }, 0 TO 1)
DIM TempHit{1 TO Trials{ }}, TempDif{1 TO Trials{ }}
' total alternates available
DIM HitGr{1 TO SqT{ }}, NextBk{1 TO SqT{ }, 1), NormDif{1 TO SqT{ }}, Order{1 TO SqT{ }}
DIM SlipCase{1 TO SqT{ }}, CaseDif{1 TO SqT{ }}
' HitGr{ } convention
' Convention to be used in recording whether ground has been hit or not
' 0 not hit
' 1 hit at the first level below the top face of the block
' 2 hit at the first level above the top face of the block
' 3 hit below the first block
' -1 hit at the second level below the top face of the block
' -2 hit at the second level above the second face of the block
' -3 hit between the first level and the second level

'NextBk{ } record the next level of block
'SlipCase{ } records the slip case no

'Initialization
'Generate the first layer
AllowCases{ } = Trials{ }
MaxLevel{ } = 1
PRINT "Generating slip surfaces at block level "; MaxLevel{ }

CALL GenChoice(0, 0, 0, Firstx{ }, TempHit{ }, Dif{ })
FOR i = 1 TO Trials{ }
' Set the first point, origin
SlipBk{ } (i, 1, 0) = 0
SlipBk{ } (i, 1, 1) = 0
SlipBk{ } (i, 1, 2) = 1
SlipInf{ } (i, 1) = TempHit{ } (i)
IF TempHit{ } (i) < 3 THEN
SlipInf{ } (i, 0) = 3
SlipBk{ } (i, 2, 0) = Firstx{ } + i - 1
SlipBk{ } (i, 2, 1) = 1
SlipBk{ } (i, 2, 2) = 4
SlipBk{ } (i, 3, 0) = Firstx{ } + i
SlipBk{ } (i, 3, 1) = 1
SlipBk{ } (i, 3, 2) = 1
ELSE
SlipInf{ } (i, 0) = 1
END IF
NEXT

'Execute a do loop until all the examined surfaces hit the ground surface
DO

' initialization
FOR i = 1 TO AllowCases{ }
TempSlipInf{ } (i, 0) = SlipInf{ } (i, 0)
TempSlipInf{ } (i, 1) = SlipInf{ } (i, 1)
FOR j = 1 TO SlipInf{ } (i, 0)
FOR k = 0 TO 2
TempSlipBk{ } (i, j, k) = SlipBk{ } (i, j, k)
NEXT
NEXT
NEXT
MaxLevel{ } = MaxLevel{ } + 1

' Message
PRINT "Generating slip surfaces at block level "; MaxLevel{ }
FOR i = 1 TO SqT{ }
Order{ } (i) = i
NEXT

complete = true
count{ } = 0

FOR i = 1 TO AllowCases{ }
IF SlipInf{ } (i, 1) = 0 THEN
' next level of slip can be generated

CALL GenChoice(SlipBk{ } (i, SlipInf{ } (i, 0), 0), SlipBk{ } (i, SlipInf{ } (i, 0), 1), Dif{ } (i), Start{ }, TempHit{ }, TempDif{ })

FOR j = 1 TO Trials{ }
count{ } = count{ } + 1
CaseDif{ } (count{ }) = TempDif{ } (j)
HitGr{ } (count{ }) = TempHit{ } (j)
SlipCase{ } (count{ }) = i

SELECT CASE TempHit{ } (j)
CASE 0
' 0. No hit
complete = false
NextBk{ } (count{ }, 0) = Start{ } + j - 1
NextBk{ } (count{ }, 1) = SlipBk{ } (i, SlipInf{ } (i, 0), 1) + 1
NormDif{ } (count{ }) = TempDif{ } (j) / NormBk{ } (NextBk{ } (count{ }, 1)) ^ 2 / NextBk{ } (count{ }, 1) / 2
CASE 1, 2
' 1. hit the ground between two block
NextBk{ } (count{ }, 0) = Start{ } + j - 1
NextBk{ } (count{ }, 1) = SlipBk{ } (i, SlipInf{ } (i, 0), 1) + 1
NormDif{ } (count{ }) = TempDif{ } (j) / NormBk{ } (NextBk{ } (count{ }, 1)) ^ 2 / NextBk{ } (count{ }, 1) / 2

```

```

CASE 2
  '2. hit the ground at a bottom corner
  NextBk%(count%, 0) = Start% + j - 1
  NextBk%(count%, 1) = SlipBk%(i, SlipInf%(i, 0), 1) + 1
  NormDif%(count%) = TempDif%(j) / NormBk%(NextBk%(count%, 1)) ^ 2 / (2 * NextBk%(count%, 1) - 1)
CASE 3
  '3. the ground surface is below the blocks
  NormDif%(count%) = TempDif%(j) / NormBk%(NextBk%(count%, 1) - 1) ^ 2 / (NextBk%(count%, 1) - 1) / 2
EXIT FOR
END SELECT
NEXT

ELSE
  'Do not have to go to the next level
  'Check if the no of levels attained is greater than half of the MaxLevel%
  IF SlipBk%(i, SlipInf%(i, 0), 1) > NormBk%(MaxLevel%) / 2 THEN
    'considered it
    count% = count% + 1
    CaseDif%(count%) = Dif%(i)
    HitGr%(count%) = -SlipInf%(i, 1)
    SlipCase%(count%) = i
    SELECT CASE SlipInf%(i, 1)
      CASE 1
        NormDif%(count%) = Dif%(i) / NormBk%(SlipBk%(i, SlipInf%(i, 0), 1)) ^ 2 / SlipBk%(i, SlipInf%(i, 0), 1) / 2
      CASE 2
        NormDif%(count%) = Dif%(i) / (SlipBk%(i, SlipInf%(i, 0), 1) * 2 - 1) / NormBk%(SlipBk%(i, SlipInf%(i, 0), 1)) ^ 2
      CASE 3
        NormDif%(count%) = Dif%(i) / SlipBk%(i, SlipInf%(i, 0), 1) / NormBk%(SlipBk%(i, SlipInf%(i, 0), 1)) ^ 2
    END SELECT
  END IF
END IF
NEXT

'Locate the five that give the min normalized difference
'Check if the maximum no of cases is less than trials%
IF count% < Trials% THEN AllowCases% = count% ELSE AllowCases% = Trials%

'Sort all the cases by selection method
FOR i = 1 TO count% - 1
  FOR j = i + 1 TO count%
    IF NormDif%(Order%(j)) < NormDif%(Order%(i)) THEN
      'swapping
      SWAP Order%(i), Order%(j)
    END IF
  NEXT
NEXT

'Reset the Initial parameter for next case
FOR i = 1 TO AllowCases%
  FOR j = 1 TO TempSlipInf%(SlipCase%(Order%(i)), 0)
    FOR k = 0 TO 2
      SlipBk%(i, j, k) = TempSlipBk%(SlipCase%(Order%(i)), j, k)
    NEXT
  NEXT
  'Check new members
  SELECT CASE HitGr%(Order%(i))
    CASE 0, 1
      'not yet hit the ground, or hit between two blocks
      SlipInf%(i, 0) = TempSlipInf%(SlipCase%(Order%(i)), 0) + 2
      SlipInf%(i, 1) = HitGr%(Order%(i))
      SlipBk%(i, SlipInf%(i, 0) - 1, 0) = NextBk%(Order%(i), 0)
      SlipBk%(i, SlipInf%(i, 0) - 1, 1) = NextBk%(Order%(i), 1)
      SlipBk%(i, SlipInf%(i, 0) - 1, 2) = 4
      SlipBk%(i, SlipInf%(i, 0), 0) = NextBk%(Order%(i), 0) + 1
      SlipBk%(i, SlipInf%(i, 0), 1) = NextBk%(Order%(i), 1)
      SlipBk%(i, SlipInf%(i, 0), 2) = 1
    CASE 2
      'hit at the bottom corner
      SlipInf%(i, 0) = TempSlipInf%(SlipCase%(Order%(i)), 0) + 1
      SlipInf%(i, 1) = HitGr%(Order%(i))
      SlipBk%(i, SlipInf%(i, 0), 0) = NextBk%(Order%(i), 0)
      SlipBk%(i, SlipInf%(i, 0), 1) = NextBk%(Order%(i), 1)
      SlipBk%(i, SlipInf%(i, 0), 2) = 4
    CASE ELSE
      'hit ground
      SlipInf%(i, 0) = TempSlipInf%(SlipCase%(Order%(i)), 0)
      SlipInf%(i, 1) = ABS(HitGr%(Order%(i)))
    END SELECT
    Dif%(i) = CaseDif%(Order%(i))
  NEXT
NEXT

LOOP UNTIL complete
END SUB

```



```
SUB GrBlocks (PreBlock AS xy, x%, y%, Gr AS xy)
'Calculate the ground surface between two adjacent
'The first block one is x%, y%
'The point before touching the first block is preblock
'The intersection point is gr

DIM corner1 AS xy, corner2 AS xy, corner3 AS xy
DIM lastpt1 AS xy, lastpt2 AS xy

CALL Block(corner1, x%, y%, 4)
CALL Block(corner2, x% + 1, y%, 1)

'Check where is the ground surface
'Two possible cases for the last point
' 1: at the block interface

CALL Block(corner3, x% + 1, y%, 3)
CALL GrLast(corner2, corner3, lastpt1)

' 2: Extrapolated from the last slip point
CALL GrLast(corner1, PreBlock, lastpt2)

IF lastpt2.x > lastpt1.x THEN
'the slip point could not be extended into the block
  Gr = lastpt1
ELSE
  Gr = lastpt2
END IF

END SUB
```

```
SUB GrLast (pt1 AS xy, pt2 AS xy, LastPt AS xy)
'Calculate the intersection point, lastpt, between a line defined by points
' pt1 and pt2 with the ground surface

'The break in slope profile
DIM SlopeBreak AS xy
SlopeBreak.x = SlopeH1 / TAN(BatterA1 * An2Ra#)
SlopeBreak.y = SlopeH1

'consider the exception case where pt1 and pt2 form a vertical line
IF pt1.x = pt2.x THEN
  LastPt.x = pt1.x
  IF pt1.x > SlopeBreak.x THEN
    LastPt.y = SlopeBreak.y + (pt1.x - SlopeBreak.x) * TAN(UpperA1 * An2Ra#)
  ELSE
    LastPt.y = pt1.y * TAN(BatterA1 * An2Ra#)
  END IF
ELSE
  'calculate the gradient of the line joining pt1 and pt2
  m1 = (pt1.y - pt2.y) / (pt1.x - pt2.x)
  c1 = pt1.y - m1 * pt1.x
  'check whether if the upper slope intersection with the line

  'gradient of the upper slope
  slm1 = TAN(UpperA1 * An2Ra#)
  slc1 = SlopeBreak.y - SlopeBreak.x * slm1
  'calculate the intersection line
  lastptx1 = (slc1 - c1) / (m1 - slm1)
  IF lastptx1 >= SlopeBreak.x THEN
    'the upper slope profile intersect with the line surface
    LastPt.x = lastptx1
    LastPt.y = c1 + m1 * LastPt.x
  ELSE
    'the line intersection with the lower ground profile
    LastPt.x = c1 / (TAN(BatterA1 * An2Ra#) - m1)
    LastPt.y = LastPt.x * m1 + c1
  END IF
END IF
END SUB
```

```
SUB HorBlocks (Preslip AS xy, Tryx%, Tryy%, Ground%, Dif!)
'Determine two slip points, slip1 and slip2, between 2 adjacent block,
'Tryx%, and Tryx% + 1, at level Tryy%
'ground% = 0 if the slip2 is below the ground
'      1 if the ground surface is between slip1 and slip2
'      2 if the ground surface is at slip1
'      3 if the ground surface is below the block, Tryx% and Tryy%
'Preslip = the immediate previous slip point
'dif! = square differences between slip surface and the critical slip
'The height of the last point ,ground% < 3

DIM corner1 AS xy, corner2 AS xy, corner3 AS xy, slip1 AS xy, slip2 AS xy
DIM pt1 AS xy, pt2 AS xy, lastpt1 AS xy, lastpt2 AS xy

CALL Block(corner1, Tryx%, Tryy%, 4)
CALL Block(corner2, Tryx% + 1, Tryy%, 1)
slip1 = corner1

'Check where is the ground surface
Ground% = 0
IF yground(corner2.x) > corner2.y THEN
'The ground surface is above the block
Ground% = 0
slip2 = corner2
ELSE
SELECT CASE yground(corner1.x)
CASE IS > corner1.y
'The ground surface is between two points
Ground% = 1
'Two possible cases for the last point
' 1: at the block interface

CALL Block(corner3, Tryx% + 1, Tryy%, 3)
CALL GrLast(corner2, corner3, lastpt1)

' 2: Extrapolated from the last slip point
CALL GrLast(corner1, Preslip, lastpt2)

IF lastpt2.x > lastpt1.x THEN
'the slip point could not be extended into the block
slip2 = lastpt1
ELSE
slip2 = lastpt2
END IF
CASE IS = corner1.y
'the slip surface end at the first corner
Ground% = 2
CASE IS < corner1.y
Ground% = 3
END SELECT

END IF

'calculate the cumulative squares of difference between the slip points and the gen. pts
SELECT CASE Ground%
CASE 0, 1
Dif! = Dif! + (slip1.y - yslip(slip1.x)) ^ 2 + (slip2.y - yslip(slip2.x)) ^ 2
CASE 2
Dif! = Dif! + (slip1.y - yslip(slip1.x)) ^ 2
END SELECT

END SUB
```

```
FUNCTION NormBk% (SlipBlock%)
'Procedure to evaluate the equivalent height of the slip in term of block
'Limited to the max. number of blocks as defined by the critical slip under considered

DIM LastPt AS xy
'Slip surfaces 2 to 4 of family E1
SELECT CASE CritSlip%
CASE 2
    LastPt.x = 7.13
    LastPt.y = 10.36
CASE 3
    LastPt.x = 8.1
    LastPt.y = 10.75
CASE 4
    LastPt.x = 9.06
    LastPt.y = 11.09
END SELECT

MaxBlock% = INT((LastPt.y * COS(Incl% * An2Ra%) - LastPt.x * SIN(Incl% * An2Ra%) - st% / 2) / (st% + h%)) + 1
IF MaxBlock% < SlipBlock% THEN NormBk% = SlipBlock% ELSE NormBk% = MaxBlock%
END FUNCTION
```

```
SUB RunGslp1 (DataFile$, FOS!)
' Run GSLP directly
DataFile$ = name of the GSLP data file
FOS! = FOS calculated

NextChannel = FREEFILE
OPEN "GSOUT.DAT" FOR OUTPUT AS #NextChannel
CLOSE #NextChannel
KILL "GSOUT.DAT"

NextChannel = FREEFILE
OPEN "GPLOT.SCR" FOR OUTPUT AS #NextChannel
CLOSE #NextChannel
KILL "GPLOT.SCR"

DosCommand$ = "COPY " + DataFile$ + " GSLPIN.DAT > NUL"
SHELL DosCommand$

SHELL "COPY C:\SLOPE\GSLP\GCONW.DAT GCON.DAT > NUL"

'Run GSLP and store the result in a temporary file gslp.tem
' is ASCII char 220
SHELL "C:\slope\gslp\gslpc > gslp.tem "

'Get the FOS from the file gslp.tem and type the result
OPEN "gslp.tem" FOR INPUT AS #NextChannel

'Check if GSLP has been executed
IF EOF(#NextChannel) THEN
  PRINT ("Could not run GSLPC")
  FOS! = 9999
ELSE
  LINE INPUT #NextChannel, Answer$
  PRINT Answer$
  'Check if there is an answer
  Equal% = INSTR(Answer$, "=")
  IF Equal% > 0 THEN
    'there is an answer
    FOS! = VAL(RTRIM$(LTRIM$(MID$(Answer$, Equal% + 1))))
  ELSE
    'No FOS, set FOS! = 9999
    FOS! = 9999
  END IF
END IF
CLOSE #NextChannel

'Kill temporary files
KILL "GCON.DAT"
KILL "gslp.tem"

END SUB
```

```
FUNCTION yground (x)
  'return y of the ground surface
  IF x < SlopeH1 / TAN(BatterA1 * An2Ra#) THEN
    yground = x * TAN(BatterA1 * An2Ra#)
  ELSE
    yground = (x - SlopeH1 / TAN(BatterA1 * An2Ra#)) * TAN(UpperA * An2Ra#) + SlopeH1
  END IF
END FUNCTION
```

```

FUNCTION yslip( x!)
' Return the y co-ordinate of the slip surface for a given x
' The critical slips are based on a slope height of 10 m
SELECT CASE CritSlip%
CASE 2
    TotalPts% = 6
CASE 3
    TotalPts% = 8
CASE 4
    TotalPts% = 8
END SELECT

DIM slip(0 TO TotalPts%) AS xy

'Initialization
' Slip surface E1-3
SELECT CASE CritSlip%
CASE 2
    slip(0).x = 0
    slip(1).x = .68
    slip(2).x = 2.04
    slip(3).x = 3.41
    slip(4).x = 5.26
    slip(5).x = 6.4
    slip(6).x = 7.15
    slip(0).y = 0
    slip(1).y = .4
    slip(2).y = 1.67
    slip(3).y = 3.3
    slip(4).y = 6.36
    slip(5).y = 8.79
    slip(6).y = 10.42
CASE 3
    slip(0).x = 0
    slip(1).x = .85
    slip(2).x = 1.9
    slip(3).x = 2.82
    slip(4).x = 4.04
    slip(5).x = 4.99
    slip(6).x = 6.14
    slip(7).x = 7.2
    slip(8).x = 8.16
    slip(0).y = 0
    slip(1).y = .36
    slip(2).y = .98
    slip(3).y = 1.79
    slip(4).y = 3.15
    slip(5).y = 4.59
    slip(6).y = 6.63
    slip(7).y = 8.66
    slip(8).y = 10.78
CASE 4
    slip(0).x = 0
    slip(1).x = .72
    slip(2).x = 1.77
    slip(3).x = 3.17
    slip(4).x = 4.72
    slip(5).x = 6
    slip(6).x = 7.22
    slip(7).x = 8.32
    slip(8).x = 9.08
    slip(0).y = 0
    slip(1).y = .24
    slip(2).y = .75
    slip(3).y = 1.76
    slip(4).y = 3.41
    slip(5).y = 5.21
    slip(6).y = 7.39
    slip(7).y = 9.52
    slip(8).y = 11.12
END SELECT

Temp! = 0
normx! = x / SlopeH! * 10
' the slip surface should be represented by a polynomial
' fixed by the data points between the range
IF normx! <= Slip(TotalPts%).x THEN
    FOR i = 0 TO TotalPts%
        term! = Slip(i).y
        FOR j = 1 TO TotalPts%
            term! = term! * (normx! - Slip((i + j) MOD (TotalPts% + 1)).x) / (Slip(i).x - Slip((i + j) MOD (TotalPts% + 1)).x)
        NEXT
        Temp! = Temp! + term!
    NEXT
ELSE
    ' by a straight line defined by the last 3 points
    last% = 3
    sumx! = 0
    sumxy! = 0
    sumy! = 0
    sumxsq! = 0
    FOR i = (TotalPts% - last% + 1) TO TotalPts%
        sumx! = sumx! + Slip(i).x
        sumy! = sumy! + Slip(i).y
        sumxsq! = sumxsq! + Slip(i).x ^ 2
        sumxy! = sumxy! + Slip(i).x * Slip(i).y
    NEXT
    grad! = (last% * sumxy! - sumx! * sumy!) / (last% * sumxsq! - sumx! ^ 2)
    inci! = (sumy! - grad! * sumx!) / last%
    Temp! = inci! + grad! * normx!
END IF
yslip = Temp! / 10 * SlopeH!
END FUNCTION

```

APPENDIX E

METHOD OF CALCULATION OF
MASS SHEAR STRENGTH PARAMETERS FROM
THEORETICAL ANALYSIS

METHOD OF CALCULATION OF MASS SHEAR STRENGTH PARAMETERS FROM THEORETICAL ANALYSIS

The factor of safety of a soil slope, F , is a function of the shear strength (represented by c' and ϕ') and density of the soil (γ), and the slope height (H). This relationship may be expressed by a dimensionless curve in terms of $c'/(H\gamma F)$ vs $\tan \phi'/F$. Such a curve is plotted in Figure E.1 for the typical cut slope geometry used in the theoretical study (Section 6). This curve was used to back calculate the mass shear strength parameters from the results of the theoretical slope analysis as explained below.

The factor of safety for a 10 m high slope is calculated from the theoretical model (Section 6.2). Figure E.1 is used to calculate the values of c' and ϕ' that gives the same factor of safety as that calculated from the theoretical model. These values are then plotted in the c' - ϕ' space (Figure E.2). Another curve for the same slope but with a height of 15 m is also derived in the same way. The intersection point of the two curves gives the mass shear strength parameters, c_{mass}' and ϕ_{mass}' for a slope of a particular coarse fraction content and properties.

APPENDIX E
LIST OF FIGURES

| Figure No. | | Page No. |
|---------------|--|-------------|
| E.1 | Dimensionless Curve Relating Factor of Safety of a Slope to Soil Strength and Slope Height | 222 |
| E.2 | Method of Calculation of c_{mass}' and ϕ_{mass}' from the Results of Theoretical Slope Model Analysis for 10 m and 15 m High Slopes | 223 |

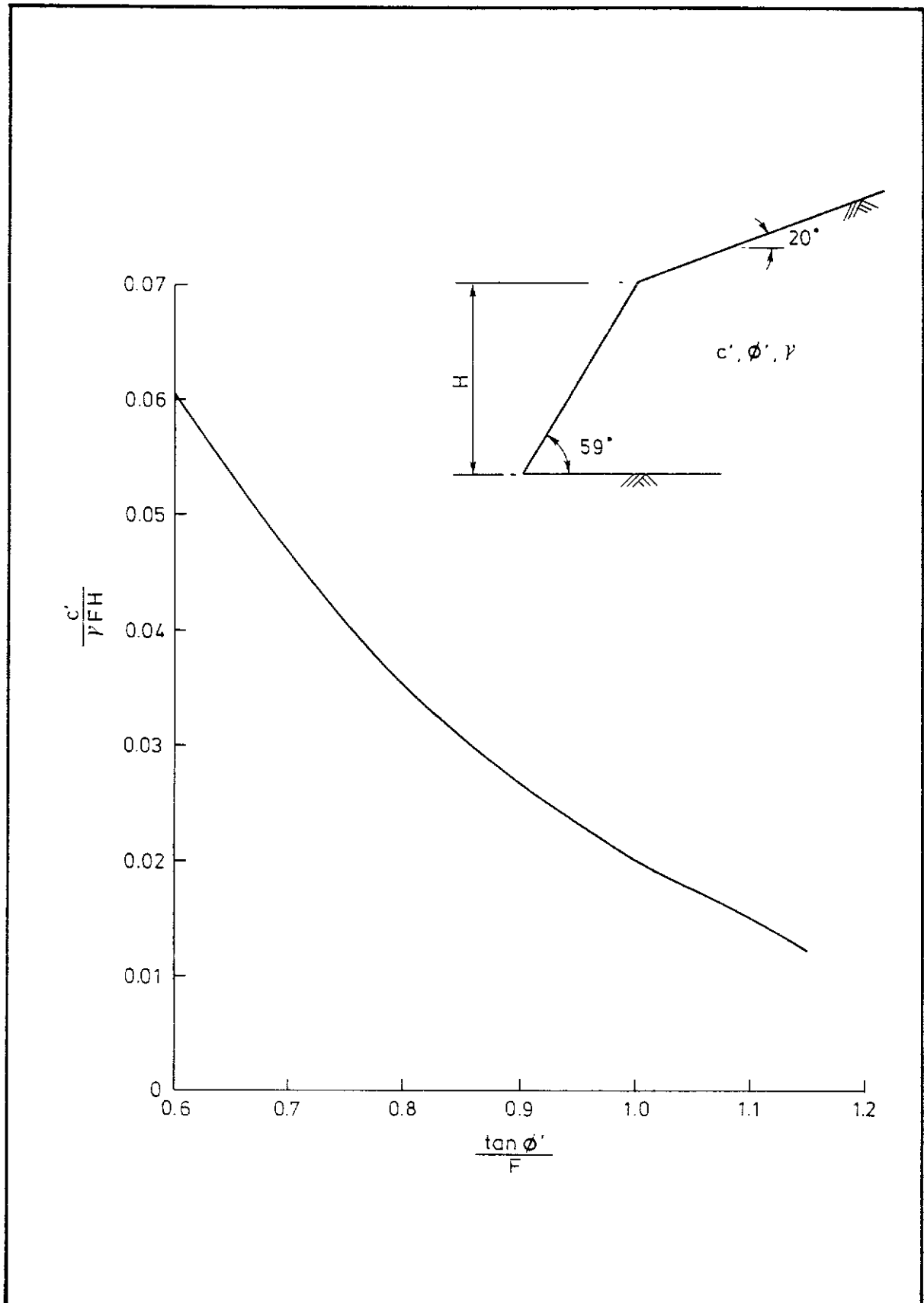


Figure E.1 - Dimensionless Curve Relating Factor of Safety of a Slope to Soil Strength and Slope Height

| Slope Height (m) | Particle Dimensions, $h \times l$ (m x m) | Particle Spacing, ST/SL | Matrix Strength | | Coarse Fraction Content by Volume (%) | FOS |
|---------------------|---|----------------------------|-----------------|------------------|--|--------------|
| | | | c' (kPa) | ϕ' (deg) | | |
| 10 15 | 0.8 x 1.6 | 1.0 | 5 | 39 | 40 | 1.16 1.06 |

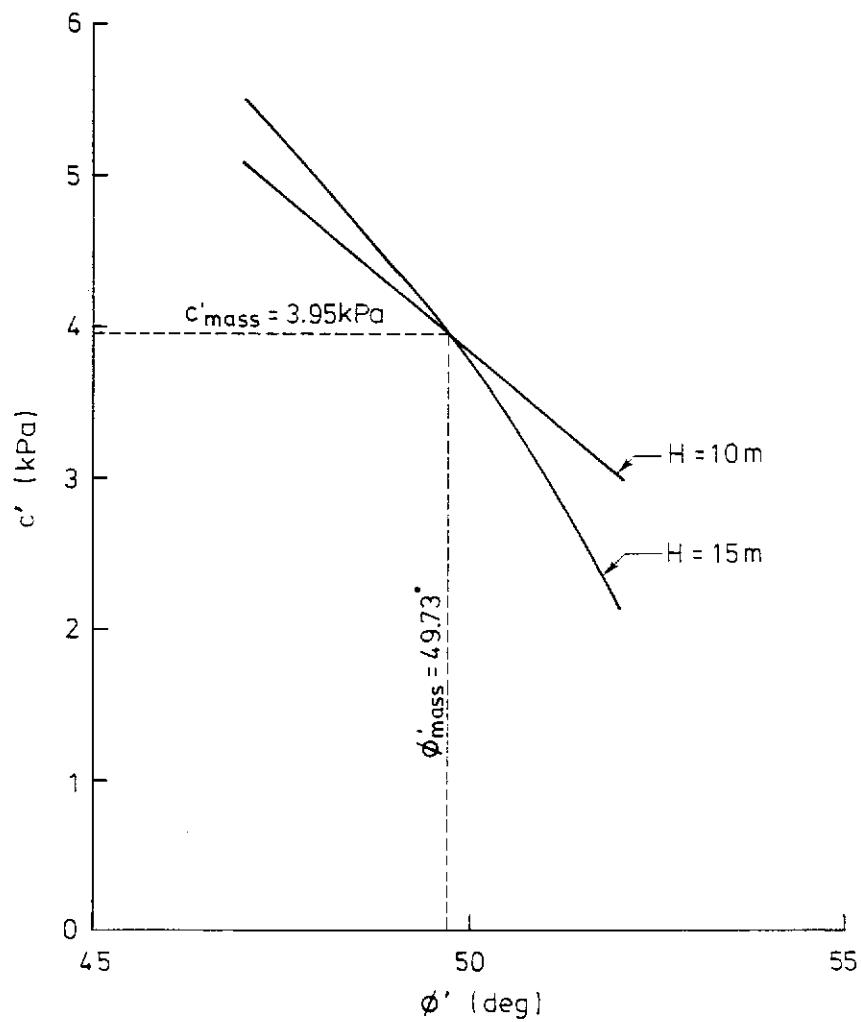


Figure E.2 - Method of Calculation of c'_{mass} and ϕ'_{mass} from the Results of Theoretical Slope Model Analysis for 10 m and 15 m High Slopes